# Equations à Retard et Modèles de Dynamiques de Populations Cellulaires

Fabien Crauste

Institut Camille Jordan
UMR 5208 du CNRS

# Équations à Retard et Modèles de Dynamiques de Populations Cellulaires

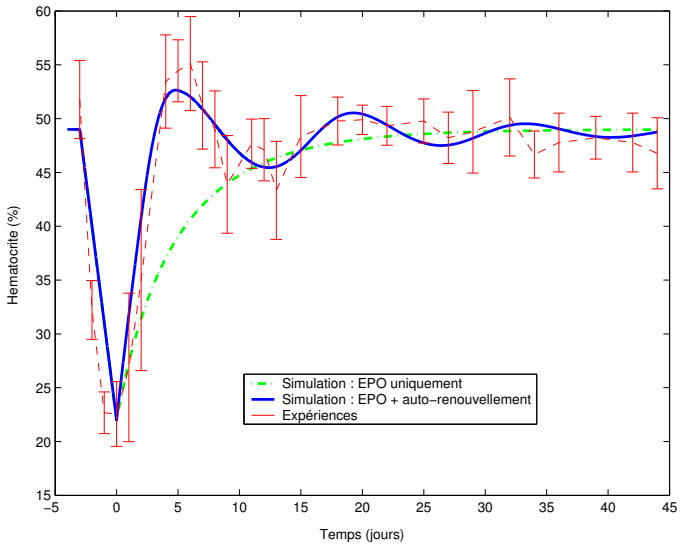


**Fabien Crauste**

Habilitation à Diriger des Recherches

Université Claude Bernard Lyon 1

Université Claude Bernard Lyon 1

École doctorale **InfoMath**, ED 512

Spécialité : **Mathématiques Appliquées**

N. d'ordre 0542014

# Équations à Retard et Modèles de Dynamiques de Populations Cellulaires

## Habilitation à Diriger des Recherches

Soutenue publiquement le 1 décembre 2014 par

**Fabien Crauste**

devant le Jury composé de :

| | | |
|---|---|---|
| M. Mostafa ADIMY | DR Inria, Lyon | Examinateur |
| Mme. Sylvie BENZONI-GAVAGE | PU, UCB Lyon 1 | Présidente |
| M. Olivier GANDRILLON | DR CNRS, Lyon | Examinateur |
| Mme. Béatrice LAROCHE | DR INRA, Jouy-en-Josas | Rapporteur |
| Mme. Angélique STEPHANOU | CR CNRS, Grenoble | Examinatrice |
| M. Jianhong WU | PU, York University (Canada) | Rapporteur |

*À Sandra, présente depuis le début*
*dans les bons comme les mauvais moments*
*qui sut m'insuffler énergie et motivation*
*quand j'en eus besoin*

# Table des matières

# Table des figures

# Rappels

J'ai réalisé ma thèse de doctorat au Laboratoire de Mathématiques Appliquées de l'Université de Pau et des Pays de l'Adour, thèse soutenue le 21 juin 2005 et intitulée "Étude mathématique d'équations aux dérivées partielles hyperboliques modélisant les processus de régulation des cellules sanguines - Applications aux maladies hématologiques cycliques".

Les résultats obtenus durant cette période ont été publiés dans plusieurs revues internationales de mathématiques appliquées [1, 2, 3, 4, 9, 12, 13, 14]. Tous ces travaux concernent l'étude de la stabilité asymptotique d'équations aux dérivées partielles non-linéaires structurées en âge et/ou en maturité [1, 2, 4, 12], ou bien d'équations différentielles à retard non-linéaires [3, 9, 13, 14]. Il s'agit également de travaux de biomathématiques, l'essentiel des réponses apportées ayant eu pour but d'éclairer une ou plusieurs questions biologiques liées à la dynamique de populations de cellules souches hématopoïétiques (prolifération, survie, extinction). Les cellules souches hématopoïétiques sont des cellules indifférenciées à la base de la production de toutes les cellules du sang, au sens large : les cellules myéloïdes, telles que les globules rouges, les plaquettes, les macrophages, les neutrophiles, etc., et les cellules lymphoïdes, impliquées dans la réponse immunitaire spécifique.

J'ai été recruté au CNRS en 2006, par la commission inter-disciplinaire 44 (devenue successivement la CID 43 puis la CID 51), et affecté à l'Institut Camille Jordan, Université Lyon 1. En 2009 j'ai obtenu un financement de l'ANR (programme Jeunes Chercheuses Jeunes Chercheurs) pour coordonner un projet dédié à la modélisation multi-échelles de l'érythropoïèse (projet ProCell, terminé en février 2014). En 2011, j'ai intégré l'équipe Inria Dracula, nouvellement créée et associée à l'Institut Camille Jordan et au Centre de Génétique et Physiologie Moléculaire et Cellulaire de l'Université Lyon 1, dont le thème est "Multi-Scale Modeling of Cell Dynamics : Application to Hematopoiesis". Je présente ici les travaux réalisés depuis mon recrutement au CNRS, en m'appuyant volontairement sur un nombre limité de publications [10, 51, 53, 54, 55, 56, 69], disponibles au Chapitre 5. La liste complète de mes publications est mentionnée au

Chapitre 4.

Depuis 2006, mes travaux de recherche se sont concentrés d'une part sur l'étude qualitative d'équations à retard et d'équations aux dérivées partielles structurées en âge, et d'autre part sur la modélisation en biologie. Mon attention s'est portée sur la stabilité asymptotique d'équations à retard dans les cas où le retard est discret, distribué, ou dépendant de l'état. Concernant les applications en biologie, j'ai poursuivi l'étude de la dynamique des cellules souches hématopoïétiques, débutée lors de ma thèse, et commencé à m'intéresser à la modélisation de l'érythropoïèse (le processus de production des globules rouges) et de la réponse immunitaire, en collaboration avec des collègues biologistes lyonnais. J'ai choisi de présenter séparément mes travaux théoriques (Chapitre 1) et les applications en biologie (Chapitre 2), bien qu'en pratique les deux aspects soient la plupart du temps traités simultanément. Cette présentation a pour but de souligner les apports tant théoriques qu'applicatifs.

Les questions scientifiques auxquelles je consacre actuellement mon activité de recherche concernent la modélisation et l'étude mathématique de processus biologiques liés à des dynamiques cellulaires et impliquant des régulations des mécanismes considérés. Tant les processus que les mécanismes de régulation font intervenir des échelles physiques et temporelles différentes, et je me suis naturellement intéressé, ces dernières années, à des problèmes multi-échelles en biologie, en particulier lors de l'encadrement de la thèse d'Emmanuelle Terry (co-encadrée par Olivier Gandrillon) et de ma participation à la thèse d'Ivan Demin (encadrée par Vitaly Volpert et Charles Dumontet). Ces aspects seront évoqués au Chapitre 2.

# Chapitre 1

# Équations à Retard en Biologie

Les équations à retard, différentielles ou aux dérivées partielles, décrivent l'évolution d'une variable en fonction d'une ou plusieurs valeurs prises par cette variable dans le passé. Il peut s'agir de valeurs ponctuelles, on parlera alors de retard discret (qu'il y ait un ou plusieurs retards), ou d'un ensemble de valeurs prises dans un intervalle, borné ou non, on parlera alors de retard continu (noyau de distribution). L'utilisation d'un retard dans la description d'une dynamique souligne l'importance d'une certaine échelle de temps dans le processus considéré. Souvent, l'apparition d'un retard résulte de l'utilisation d'une structuration, implicite, de la variable considérée : par exemple, une structuration en âge [88]. En conséquence un lien est souvent fait entre équations à retard et équations structurées en âge, tendant à assimiler les deux. La section suivante présentera brièvement le lien entre équations à retard et équations structurées en âge.

La théorie des équations à retard a été développée par J. Hale [73]. Les équations différentielles ordinaires à retard – les termes "équations à retard" seront utilisés dans la suite – sont de dimension infinie, contrairement aux équations différentielles ordinaires sans retard. La condition initiale d'une équation à retard est définie sur un intervalle, de longueur égale au retard (ou, dans certains cas, égale au retard maximum). Les équations à retard interviennent dans de nombreux domaines d'applications des mathématiques, et en particulier en biologie où de nombreux phénomènes sont non-locaux, en la variable de temps mais parfois également en la variable d'espace ou ce qui tient lieu de variable "d'espace" (la maturité, l'âge, la taille, etc.).

Considérons à titre d'exemple l'évolution d'une population animale ne tenant compte que de la natalité et de la mortalité naturelles. En supposant que la mortalité est instantanée dans la population, par rapport à l'échelle de temps considérée (typiquement, la semaine ou le mois), la description de l'évolution de cette population nécessite de connaître le nombre d'individus à l'instant $t$, que l'on peut noter $N(t)$, mais également le nombre d'individus à l'instant $t - \tau$, où $\tau$ est la durée de gestation moyenne de la

population. On peut alors écrire l'équation linéaire à retard discret suivante,

$$\begin{cases} \dfrac{d}{dt}N(t) &= -dN(t) + bN(t-\tau), & t > 0, \\ N(t) &= \varphi(t), & t \in [-\tau, 0], \end{cases} \tag{1.1}$$

où $d$ et $b$ sont respectivement les taux de mortalité et de naissance de la population, et $\varphi$ une condition initiale, définie sur l'intervalle $[-\tau, 0]$.

Je présenterai, à travers ce chapitre, des résultats liés à la stabilité des équations à retard, obtenus dans le cadre de la modélisation de la dynamique des cellules souches hématopoïétiques (voir Section 2.1), de l'érythropoïèse (voir Section 2.2), et de la réponse immunitaire (voir paragraphe 2.3.2). Les questions abordées concernent la stabilité locale asymptotique, la stabilité globale asymptotique, et l'existence de bifurcations, pour des équations à retard discret (cf. 1.2.1), continu distribué (cf. 1.2.2), et dépendant de l'état (cf. 1.2.3). Je profiterai de cette présentation pour discuter des questions liées à l'étude de la stabilité des équations à retard, et aborder quelques questions ouvertes. Les résultats mentionnés dans ce chapitre s'appuient sur les manuscrits présentés aux Sections 5.1, 5.2, 5.3, et 5.4.

## 1.1 Équations structurées en âge et équations à retard

Depuis le début de ma thèse, en 2002, je me suis intéressé à l'étude des équations de transport structurées en âge. Il s'agit d'une classe de modèles basée sur des équations aux dérivées partielles hyperboliques. Ces équations interviennent dans de nombreux modèles de dynamique des populations [20, 42, 43, 59, 88, 102, 124], en particulier lorsque les cellules considérées prolifèrent. La forme générale de telles équations est

$$\partial_t n(t,a) + \partial_a[\psi(a)n(t,a)] = f(t,a,n(t,a)),$$

où $a$ désigne la variable d'âge, positive ou nulle, éventuellement non-bornée, $n$ est une densité de population, et dans toute la suite $\partial_y$ désigne la dérivée partielle par rapport à la variable $y$. La fonction $\psi(a)$ est une vitesse de vieillissement. Typiquement, $\psi(a) = 1$ si la variable d'âge représente un âge chronologique. Dans certains cas, la variable d'âge $a$ peut représenter un marqueur cellulaire, par exemple un marqueur de différenciation, et la vitesse $\psi(a)$ peut ne pas être unitaire.

Dans des cas généraux, les différentes fonctions impliquées dans la description de la dynamique d'une population (taux de mortalité, de prolifération, etc.) peuvent dépendre de la variable d'âge, de la densité de population $n$, de la densité totale $\int n$, etc. En pratique, dans de nombreuses applications il est très difficile de quantifier la dépendance en âge de ces fonctions : les données expérimentales ou cliniques sont rares. Ainsi, il

est commun de ne pas faire dépendre les fonctions décrivant des processus cellulaires de l'âge. On aboutit alors à une équation de la forme

$$\partial_t n(t,a) + \partial_a n(t,a) = f(t, n(t,a)), \quad a \in (0, A), \tag{1.2}$$

où $A \leq +\infty$. Considérons le cas classique où

$$f(t, n(t,a)) = -\alpha(t) n(t,a),$$

et les conditions au bord et initiale sont données par

$$\left\{ \begin{array}{rcl} n(t,0) & = & g(N(t)), \\ n(0,a) & = & n_0(a), \quad a \in (0, A), \end{array} \right. \tag{1.3}$$

où

$$N(t) := \int_0^A n(t,a) da,$$

et $n_0$ est une donnée initiale suffisamment régulière vérifiant $\lim_{a \to A} n_0(a) = 0$ si $A = +\infty$ (on suppose qu'aucune cellule ne peut être immortelle).

L'intégration de (1.2) par rapport à la variable d'âge aboutit à l'équation

$$\frac{d}{dt} N(t) = -\alpha(t) N(t) + g(N(t)) - n(t, A), \quad t > 0. \tag{1.4}$$

En utilisant l'expression de $n(t,a)$ le long des droites caractéristiques $a(t) = t + a_0$, $a_0 \in \mathbb{R}$, le terme $n(t, A)$ peut s'écrire

$$n(t, A) = \left\{ \begin{array}{ll} \exp\left( - \displaystyle\int_0^t \alpha(\theta) d\theta \right) n_0(A - t), & \text{si } t < A, \\ \exp\left( - \displaystyle\int_{t-A}^t \alpha(\theta) d\theta \right) g(N(t - A)), & \text{si } A \leq t. \end{array} \right.$$

On obtient ainsi deux expressions pour l'équation (1.4), une équation différentielle ordinaire non-autonome

$$\left\{ \begin{array}{rcl} \dfrac{d}{dt} N(t) & = & -\alpha(t) N(t) + g(N(t)) - \beta(t), \quad \text{pour } t \in (0, A), \\ N(0) & = & N_0 := \displaystyle\int_0^A n_0(a) da, \end{array} \right. \tag{1.5}$$

où

$$\beta(t) = \exp\left( - \int_0^t \alpha(\theta) d\theta \right) n_0(A - t),$$

et une équation différentielle à retard, pour $t \geq A$,

$$\frac{d}{dt} N(t) = -\alpha(t) N(t) + g(N(t)) - \exp\left( - \int_{t-A}^t \alpha(\theta) d\theta \right) g(N(t - A)). \tag{1.6}$$

Ce résultat est assez général : contrairement à une idée répandue considérant qu'une équation à retard est systématiquement associée à une équation de transport structurée en âge, il convient de préciser que la structuration en âge peut faire apparaître assez naturellement un retard dans une dynamique, mais l'équivalence entre les deux équations n'est exacte que si l'équation à retard est munie d'une condition initiale adéquate, donnée par l'intégration de l'équation structurée sur l'intervalle $[0, A]$. En d'autres termes, le système (1.2)–(1.3) est équivalent à l'équation à retard (1.6) munie d'une condition initiale $\varphi(t)$ solution du système différentiel non-autonome (1.5).

En s'appuyant sur cette propriété, on peut toutefois réduire assez facilement une équation structurée en âge en une équation à retard. L'intérêt peut être double : premièrement les données expérimentales décrivent souvent le comportement d'une population totale au cours du temps, et ne permettent pas souvent d'obtenir le comportement en fonction de l'âge, et deuxièmement la théorie des équations à retard fournit un cadre de travail largement développé pour l'étude des propriétés de ces équations.

Avant de m'intéresser, dans la section suivante, aux résultats obtenus sur la stabilité d'équations à retard, je mentionnerai ici deux modèles structurés en âge auxquels je me suis intéressé, en lien avec la modélisation de la production des globules rouges (cf. Section 2.2). Les résultats obtenus par l'étude de ces modèles seront développés en partie dans la Section 2.2.

Le premier modèle est le résultat d'une collaboration avec Stéphane Génieys et Laurent Pujo-Menjouet (Université Lyon 1) et Olivier Gandrillon (biologiste, Université Lyon 1). Nous avons étudié [56] un nouveau modèle d'érythropoïèse de stress (cf. Section 2.2) : il s'agit de la production de globules rouges dans une situation de stress (une anémie par exemple).

Le modèle que nous avons proposé décrit la dynamique de progéniteurs érythrocytaires, des cellules immatures de la lignée des globules rouges, qui sont soit en état d'auto-renouvellement soit de différenciation, et la dynamique des érythrocytes (globules rouges). Le système d'équations décrivant la dynamique des populations de cellules s'écrit :

$$\begin{cases} \partial_t p(t,a) + \partial_a p(t,a) = -\left[\alpha(E(t)) + \sigma(E(t))\right] p(t,a), & a \in (0, \tau_p), \\ \partial_t s(t,a) + \partial_a s(t,a) = -\alpha(E(t)) s(t,a), & a \in (0, \tau_c), \\ \partial_t e(t,a) + \partial_a e(t,a) = -\gamma e(t,a), & a > 0, \end{cases}$$

avec les conditions aux bords

$$\begin{cases} p(t,0) &= HSC + 2s(t,\tau_c), \\ s(t,0) &= \displaystyle\int_0^{\tau_p} \sigma(E(t))p(t,a)da, \\ e(t,0) &= Ap(t,\tau_p), \end{cases}$$

où $p$ désigne la densité de progéniteurs érythrocytaires, $s$ celle de progéniteurs en état d'auto-renouvellement, et $e$ la densité de globules rouges. Le taux de mort des progéniteurs, noté $\alpha$, est régulé positivement par le nombre total $E(t)$ de globules rouges, et le taux d'auto-renouvellement, noté $\sigma$, est régulé négativement par $E(t)$.

Récemment, en collaboration avec Oscar Angulo (Université de Valladolid, Espagne), je me suis intéressé à une généralisation de ce modèle. Nous avons considéré une dépendance explicite des taux d'auto-renouvellement et de différenciation des cellules progénitrices en la variable d'âge. Le modèle s'écrit :

$$\begin{cases} \partial_t p(t,a) + \partial_a p(t,a) = -\left[\alpha(E(t)) + \sigma(a,E(t)) + \kappa(a,E(t))\right] p(t,a), & a \in (0,\tau_p), \\ \partial_t s(t,a) + \partial_a s(t,a) = -\alpha(E(t))s(t,a), & a \in (0,\tau_c), \\ \partial_t e(t,a) + \partial_a e(t,a) = -\gamma e(t,a), & a > 0, \end{cases}$$

avec les conditions aux bords

$$\begin{cases} p(t,0) &= HSC + 2s(t,\tau_c), \\ q(t,0) &= \displaystyle\int_0^{\tau_p} \sigma(a,E(t))p(t,a)da, \\ e(t,0) &= A\displaystyle\int_0^{\tau_p} \kappa(a,E(t))p(t,a)da, \end{cases}$$

où le taux de différenciation est noté $\kappa$.

J'ai également étudié d'autres modèles structurés en âge, dans le cadre de la dynamique des cellules souches hématopoïétiques [7, 11, 58], mais ces modèles peuvent être considérés, en quelque sorte, comme des versions simplifiées du modèle présenté ci-dessus.

## 1.2 Équations à retard

La stabilité asymptotique locale d'une équation à retard non-linéaire s'obtient par linéarisation et étude de l'équation caractéristique. De façon analogue à un problème d'équations différentielles ordinaires, une équation à retard linéaire est asymptotiquement stable si toutes les valeurs propres sont à parties réelles négatives. D'après Cooke et Grossmann [49], on sait même que la stabilité ne peut être perdue qu'à travers

l'apparition de valeurs propres imaginaires pures. Mais contrairement aux équations différentielles ordinaires, l'équation caractéristique d'une équation différentielle à retard n'est pas un polynôme, mais un polynôme exponentiel. Il possède donc une infinité de racines. Par exemple, l'équation caractéristique de l'équation (1.1) à retard discret $\tau$ est

$$\lambda + d - be^{-\lambda\tau} = 0, \qquad \lambda \in \mathbb{C}. \tag{1.7}$$

Hayes [80] a prouvé en 1957 le résultat suivant, établissant des conditions nécessaires et suffisantes pour la stabilité asymptotique de l'équation linéaire à retard (1.1).

**Lemme 1.2.1.** *Les racines de l'équation (1.7) sont toutes à parties réelles négatives si et seulement si*

$$d\tau > -1, \quad d - b > 0, \qquad -b\tau < \zeta \sin(\zeta) - d\tau \cos(\zeta),$$

*où $\zeta$ est solution de l'équation $\zeta = -d\tau \tan(\zeta)$.*

Dans le cas général, l'équation caractéristique d'un système d'équations différentielles avec un seul retard discret $\tau$ s'écrit

$$P_n(\lambda) + P_{n-1}(\lambda)e^{-\lambda\tau} = 0, \qquad \lambda \in \mathbb{C},$$

où $P_i$ est un polynôme de degré au plus $i$. Le critère de Hayes concernant le signe des parties réelles des racines de cette équation n'est alors plus valable, seules des conditions suffisantes ont à ce jour été obtenues, pour des degrés peu élevés (par exemple, Ruan et Wei [110] pour l'équation $P_3(\lambda) + P_2(\lambda)e^{-\lambda\tau} = 0$).

Dans certains cas, la linéarisation d'une équation ou d'un système à retard discret mène à une équation caractéristique dont les coefficients ne sont pas constants, mais dépendent du retard (de façon explicite ou non). C'est le cas avec les modèles de dynamique des cellules souches (Section 2.1), par exemple. Les équations caractéristiques s'écrivent alors

$$P_n(\lambda, \tau) + P_{n-1}(\lambda, \tau)e^{-\lambda\tau} = 0. \tag{1.8}$$

Lorsqu'on essaye d'identifier les racines imaginaires pures d'une telle équation, on est rapidement confronté à la détermination de points fixes.

Dans les trois sections suivantes, je présenterai des résultats obtenus concernant la stabilité d'équations à retard lorsque le retard est discret, continu, ou dépendant de l'état. Dans le cas d'un retard discret, je ne discuterai que le cas d'un seul retard.

### 1.2.1 Retard discret

J'ai traité dans [51] (cf. Section 5.1) le cas de l'équation

$$P_1(\lambda, \tau) + P_0(\lambda, \tau)e^{-\lambda\tau} = 0, \qquad \tau \in [0, \overline{\tau}]. \tag{1.9}$$

Il s'agit d'une situation illustrant simplement les difficultés rencontrées lorsque les coefficients de l'équation caractéristique (et par extension les coefficients de l'équation linéaire ou linéarisée) ne sont plus indépendants du retard. Dans la suite, on considèrera que

$$P_1(\lambda,\tau) = \lambda + d(\tau), \qquad \text{et} \qquad P_0(\lambda,\tau) = -b(\tau), \tag{1.10}$$

pour conserver les notations introduites dans (1.1) et (1.7).

Plusieurs situations peuvent être observées :

— pour toute valeur de $\tau \in [0,\overline{\tau}]$, les racines de (1.9) sont toutes à parties réelles négatives ;

— pour toute valeur de $\tau \in [0,\overline{\tau}]$, (1.9) possède au moins une racine à partie réelle positive ;

— il existe au moins une valeur $\tau^* \in (0,\overline{\tau})$ telle que les racines de (1.9) sont à parties réelles négatives pour $\tau < \tau^*$, et pour $\tau > \tau^*$, $\tau$ proche de $\tau^*$, (1.9) possède des racines à parties réelles positives.

La première situation implique la stabilité asymptotique de l'équation, ou du système d'équations, à retard associé. Le résultat établi par Hayes [80] (cf. Lemme 1.2.1) montre que cette situation existe dans le cas où les coefficients ne dépendent pas du retard. Contrairement à une idée répandue, le retard n'est donc pas nécessairement source d'instabilité.

La deuxième situation est de loin la plus difficile à obtenir mathématiquement. Mis à part dans le cas où une racine réelle positive peut être déterminée, il est souvent impossible de prouver que pour toute valeur du retard il existe une racine à partie réelle positive.

La troisième situation est la plus "classique", dans le sens où on s'attend à ce qu'une augmentation du retard induise une instabilité. Dans le cas mentionné ci-dessus, et contrairement au cas d'une équation à coefficients indépendants du retard, on peut observer des changements de stabilité (*stability switch*) : une augmentation du retard $\tau$ induit une perte de stabilité, puis permet de nouveau de stabiliser l'équation. On peut dans certains cas observer plusieurs changements de stabilité successifs. Ce résultat a été mis en évidence, théoriquement, par Beretta et Kuang [29]. Plusieurs conditions doivent être satisfaites pour mettre en évidence des changements de stabilité :

1/ les racines de (1.8) doivent être à parties réelles négatives lorsque $\tau = 0$,

2/ $P_n(0,\tau) + P_{n-1}(0,\tau) \neq 0$,

3/ le polynôme $P_n(\lambda,\tau) + P_{n-1}(\lambda,\tau)$ ne doit pas posséder de racine imaginaire pure,

4/ les polynômes $P_n$ et $P_{n-1}$ doivent vérifier

$$\limsup\left\{\left|\frac{P_{n-1}(\lambda,\tau)}{P_n(\lambda,\tau)}\right| ; |\lambda| \to \infty, Re(\lambda) \geq 0\right\} < 1.$$

5/ le polynôme $|P_n(i\omega,\tau)|^2 - |P_{n-1}(i\omega,\tau)|^2$ doit posséder un nombre fini de racines réelles, et chaque racine $\omega(\tau)$ doit être continue et dérivable en $\tau$.

La condition 1/ est une condition nécessaire et suffisante pour la stabilité lorsque le retard est proche de zéro, et la condition 2/ assure que $\lambda = 0$ n'est pas valeur propre. Les conditions suivantes sont nécessaires pour qu'un changement de stabilité ait lieu. La condition 3/ assure que $P_n$ et $P_{n-1}$ n'ont pas de racine imaginaire pure commune. La condition 4/ est nécessaire pour assurer qu'aucune bifurcation ne peut venir de l'infini. La condition 5/ est nécessaire pour assurer l'existence d'un nombre fini de "fenêtres" dans lesquelles une bifurcation peut survenir, et pour pouvoir calculer la dérivée des valeurs propres imaginaires par rapport à $\tau$.

Dans le cas de l'équation (1.9), les conditions 1/ et 2/ sont équivalentes à

$$b(0) < d(0) \quad \text{et} \quad b(\tau) \neq d(\tau), \text{ pour tout } \tau \in [0,\overline{\tau}],$$

c'est-à-dire

$$b(\tau) < d(\tau), \text{ pour tout } \tau \in [0,\overline{\tau}].$$

Les conditions 3/, 4/ et 5/ sont trivialement vérifiées. Le théorème suivant illustre le résultat de stabilité obtenu pour l'équation (1.9).

**Théorème 1.2.2** ([**51**])**.** *Supposons $b(\tau) < d(\tau)$, pour tout $\tau \in [0,\overline{\tau}]$. Supposons de plus qu'il existe $\tau^* \in (0,\overline{\tau})$ tel que $d(\tau) < |b(\tau)|$ si et seulement si $\tau \in [0,\tau^*)$. Alors,*

*(i) si $Z_0$ (défini en (1.15)) n'a pas de racine sur l'intervalle $[0,\tau^*)$, l'équation (1.9) ne possède que des racines à parties réelles négatives pour $\tau \in [0,\overline{\tau})$.*

*(ii) si $Z_0$ possède au moins une racine $\tau_c \in (0,\tau^*)$, l'équation (1.9) ne possède que des racines à parties réelles négatives pour $\tau \in [0,\tau_c)$ et une paire de racines imaginaires pures conjuguées apparaît lorsque $\tau = \tau_c$.*

***Idée de la preuve.*** On vérifie tout d'abord que lorsque $\tau = 0$, le polynôme exponentiel donné par (1.9) possède une seule racine, $\lambda = P_1^{-1}(P_0(\lambda,0),0) = b(0) - d(0) < 0$. La stabilité ne peut alors être perdue, en augmentant $\tau$, que si des racines imaginaires pures apparaissent. Notons $\lambda = i\omega$, $\omega \in \mathbb{R}$, une racine imaginaire pure de (1.9). En séparant les parties réelles et imaginaires dans (1.9) on obtient :

$$d(\tau) - b(\tau)\cos(\omega\tau) = 0, \tag{1.11}$$

$$\omega + b(\tau)\sin(\omega\tau) = 0. \tag{1.12}$$

On constate que si $\omega$ est solution de (1.11)–(1.12) alors $-\omega$ l'est aussi, et que $\omega = 0$ n'est pas solution de (1.11)–(1.12). Une condition nécessaire et suffisante pour que (1.9) possède des racines imaginaires pures est donc

$$d(\tau) < |b(\tau)|.$$

Notons qu'en fonction du problème étudié, les propriétés de $d$ et $b$ peuvent être différentes. Supposons qu'il existe $\tau^* \in (0, \overline{\tau})$ tel que $d(\tau) < |b(\tau)|$ si et seulement si $\tau \in [0, \tau^*)$. En sommant les carrés des équations (1.11) et (1.12), on obtient alors

$$\omega = \omega(\tau) = \sqrt{b^2(\tau) - d^2(\tau)}. \tag{1.13}$$

En substituant cette expression dans (1.11)–(1.12), on obtient

$$\begin{aligned} \cos\left(\tau\sqrt{b^2(\tau) - d^2(\tau)}\right) &= \frac{d(\tau)}{b(\tau)}, \\ \sin\left(\tau\sqrt{b^2(\tau) - d^2(\tau)}\right) &= -\frac{\sqrt{b^2(\tau) - d^2(\tau)}}{b(\tau)}. \end{aligned} \tag{1.14}$$

On conclut que les valeurs de $\tau \in [0, \tau^*)$ satisfaisant (1.14) génèrent des racines imaginaires pures $\lambda = i\omega(\tau)$ de (1.9), où $\omega(\tau)$ est donné par (1.13).

Or, les solutions positives $\tau \in (0, \tau^*)$ de (1.14) sont des racines de

$$Z_k(\tau) = \tau - \tau_k(\tau), \qquad k \in \mathbb{N}^*, \tau \in [0, \tau^*), \tag{1.15}$$

où

$$\tau_k(\tau) = \frac{\arccos\left(\frac{d(\tau)}{b(\tau)}\right) + 2k\pi}{\sqrt{b^2(\tau) - d^2(\tau)}}, \qquad k \in \mathbb{N}^*, \tau \in [0, \tau^*).$$

Les racines de $Z_k$ sont difficiles à déterminer analytiquement. On peut toutefois établir les propriétés suivantes (voir [7]) :

**Lemme 1.2.3.** *Pour $k \in \mathbb{N}^*$,*

$$Z_k(0) < 0 \qquad \textit{et} \qquad \lim_{\tau \to \tau^*} Z_k(\tau) = -\infty.$$

*Ainsi, à condition qu'aucune racine de $Z_k$ ne soit un minimum local, le nombre de racines positives de $Z_k$, $k \in \mathbb{N}^*$ sur l'intervalle $[0, \tau^*)$ est pair. De plus, si $Z_k$ ne possède aucune racine dans l'intervalle $[0, \tau^*)$, alors les fonctions $Z_j$, avec $j > k$, n'en possèdent pas non plus.*

On peut alors conclure. □

Ce résultat permet de conclure à la stabilité asymptotique de l'équation linéaire (1.9)–(1.10). L'existence de racines $\tau_c$ des fonctions $Z_k$ correspond à l'existence de changements de stabilité. La méthode de résolution, adaptée des travaux de Beretta et Kuang [29], consiste à transformer la recherche de solutions $(\omega, \tau)$ d'un système trigonométrique

$$\begin{cases} \cos(\omega\tau) &= f(\omega, \tau), \\ \sin(\omega\tau) &= g(\omega, \tau), \end{cases}$$

où $\omega$ est la partie imaginaire de la valeur propre imaginaire pure associée à $\tau$ et $f$ et $g$ deux fonctions rationnelles, en la recherche de racines réelles $\tau_k^*$ de fonctions réelles sur un intervalle donné. L'utilisation de solveurs numériques est cependant nécessaire en général, les fonctions étant rarement explicites.

L'existence d'une bifurcation type Hopf dépend de la vérification d'une condition de transversalité, elle-même dépendant des propriétés des fonctions $d(\tau)$ et $b(\tau)$. Le résultat établi dans [51] montre qu'il existe une suite finie $\{\tau_k^*\}_k$, avec $\tau_k^* > 0$, telle qu'une bifurcation de Hopf survienne lorsque $\tau = \tau_1^*$ et que la stabilité locale de l'équation non-linéaire change (stable/instable/stable/etc.) chaque fois que le paramètre $\tau$ prend une valeur $\tau_k^*$.

Ce résultat a par la suite été étendu à une équation caractéristique de degré 2,

$$P_2(\lambda, \tau) + P_1(\lambda, \tau)e^{-\lambda\tau} = 0,$$

dans [56] et dans [52], et appliqué à un modèle de dynamique des cellules souches hématopoiétiques (voir Section 2.1) structuré en maturité [11]. J'ai publié en 2011 un article de revue [54] sur les résultats de stabilité linéaire concernant les équations à retard discret dont l'équation caractéristique s'écrit sous la forme d'un polynôme exponentiel de degré $n$, avec $n = 1$, 2 et 3 (cf. Section 5.2). L'augmentation du degré du polynôme exponentiel limite bien évidemment nos capacités à déterminer théoriquement des critères de stabilité. Tous ces résultats ne sont de plus valables que lorsqu'il y a un seul retard discret, or de nombreuses applications peuvent faire apparaître plusieurs retards, de natures diverses. Le cas de deux retards discrets montre des dynamiques et des difficultés analytiques très différentes [15].

Dans la suite, je présenterai des résultats concernant des équations avec retard distribué et retard dépendant de l'état.

### 1.2.2 Retard distribué

Je me suis intéressé à un autre type d'équations : les équations à retard continu, distribué selon un noyau de probabilité. Plus réalistes d'un point de vue biologique que les équations à retard discrets, car elles tiennent compte d'une variabilité dans l'expression du retard (on peut considérer qu'en général un retard discret représente un temps moyen), ces équations sont bien entendu un peu plus complexes et moins présentes dans la modélisation de phénomènes biologiques. Une équation linéaire à retard distribué s'écrit

$$\frac{d}{dt}x(t) = -dx(t) - b\int_0^{+\infty} x(t-a)d\eta(a), \tag{1.16}$$

où $\eta(a)$ est une fonction de distribution de probabilité, et dans le cas où $d\eta(a)/da = f(a)$, on obtient

$$\frac{d}{dt}x(t) = -dx(t) - b\int_{\text{supp }(f)} f(a)x(t-a)da = 0, \tag{1.17}$$

où

$$\text{supp }(f) := \{a \in [0, +\infty); f(a) \neq 0\}.$$

De façon plus générale, on peut considérer l'équation

$$\frac{d}{dt}x(t) = -dx(t) - b\int_0^{+\infty} F(a)x(t-a)da, \tag{1.18}$$

où $F$ est une fonction intégrable mais pas nécessairement une densité de probabilité. En effet, dans de nombreuses applications où le retard distribué apparaît suite à l'intégration d'un système structuré en âge (cf. 1.1), la fonction $F$ est le produit d'une densité de probabilité et d'un taux de survie, par exemple [13]

$$F(a) = e^{-\gamma a}f(a), \qquad \gamma \geq 0, \quad a \in \text{supp }(f).$$

Durant ma thèse, j'ai réalisé l'étude de la stabilité d'une équation à retard distribué décrivant la dynamique des cellules souches hématopoïétiques [13], dont l'équation linéarisée est donnée par (1.17). J'ai établi l'existence d'une bifurcation de Hopf déstabilisant l'unique état d'équilibre positif du système, sous certaines hypothèses sur la fonction $F(a)$.

Dans la section précédente, nous avons vu que déterminer l'existence d'une valeur propre imaginaire pure pour une équation linéaire à retard discret revenait à résoudre un système trigonométrique, pour lequel on pouvait utiliser la relation $\cos^2 + \sin^2 = 1$ (cf. la démonstration du Théorème 1.2.2). Dans le cas d'un retard distribué, cette propriété ne peut plus être utilisée que pour obtenir une condition nécessaire. En effet, l'équation caractéristique associée à (1.18) est

$$\lambda + d + b\int_0^{+\infty} F(a)e^{-\lambda a}da = 0. \tag{1.19}$$

Une racine imaginaire pure $\lambda = i\omega$ vérifie donc le système

$$d + b\int_0^{+\infty} F(a)\cos(\omega a)da = 0, \tag{1.20}$$

$$\omega + b\int_0^{+\infty} F(a)\sin(\omega a)da = 0, \tag{1.21}$$

et en sommant les carrés des deux équations on n'aboutit qu'à l'inégalité

$$\omega^2 + d^2 = b^2\left(\int_0^{\tau} F(a)\cos(\omega a)da\right)^2 + b^2\left(\int_0^{\tau} F(a)\sin(\omega a)da\right)^2 \leq b^2\left(\int_0^{\tau} F(a)da\right)^2,$$

qui ne permet pas d'identifier $\omega$.

De nombreux travaux se sont intéressés à l'analyse de la stabilité de l'équation (1.17). Chronologiquement, Boese [39] en 1989 a considéré le cas où $f(a)$ est la densité d'une loi Gamma,

$$f(a) = a^{n-1}\frac{e^{-a/\theta}}{\theta^n(n-1)!}, \quad \theta = \frac{\tau}{n},\ n \in \mathbb{N}^*.$$

Cette loi de probabilité a la propriété de réduire une équation à retard en un système d'équations différentielles sans retard, ainsi la stabilité de l'équation à retard est ramenée à l'étude de la stabilité d'un système d'équations ordinaires pour lesquelles des critères sont connus (le critère de Routh-Hurwitz, par exemple). Kuang [89], en 1994, a déterminé une condition pour la non-existence de valeurs propres imaginaires pures pour un système de deux équations à retard distribué. Il a obtenu des conditions suffisantes pour la stabilité asymptotique. Bernard et al [33] en 2001 ont déterminé des conditions suffisantes pour la stabilité de (1.17) lorsque la densité de probabilité est symétrique par rapport à sa moyenne. Ils ont alors émis la conjecture suivante :

> "the most destabilizing distribution of delays [with the same mean] is a single Dirac function."

Atay [26] a récemment apporté des arguments dans cette direction. Il a montré, en se plaçant, pour une équation linéaire, à proximité d'une bifurcation de Hopf, que si le retard avait un effet déstabilisant alors le retard discret était localement la distribution de retards la plus déstabilisante.

Huang and Vandewalle [82] et Tang [119] ont également contribué à l'analyse d'équations similaires à (1.17). Les premiers se sont intéressés à la stabilité numérique des équations à retard distribué, proposant une approche géométrique intéressante pour déterminer des conditions de stabilité, malheureusement limitée à la distribution qu'ils ont considérée. Tang a obtenu des conditions suffisantes pour la stabilité dans des cas très généraux, mais ses conditions se révèlent très techniques et difficilement utilisables en pratique. En 2008, Ozbay et al. [101] ont considéré une distribution exponentielle de retards, et ont obtenu des conditions nécessaires et suffisantes pour la stabilité en utilisant le *small gain theorem* et le critère de Nyquist. Berezansky et Braverman ont récemment obtenu des conditions suffisantes pour la stabilité d'équations à retard distribué non-autonomes [30].

Mentionnons enfin les travaux d'Anderson [17, 18], publiés en 1991 et 1992. Anderson a considéré les équations du *regulator model*, des équations à retard distribué consistant en un cas particulier de (1.16),

$$\frac{d}{dt}x(t) = -b\int_0^{+\infty} x(t-a)d\eta(a).$$

Anderson s'est concentré sur l'influence des propriétés de la distribution $\eta$ sur la stabilité de l'équation à retard distribué. Bien que ses résultats ne soient valables que pour une certaine classe de lois de probabilités, ils soulignent l'importance de la *forme* de la distribution (moyenne, variance, variance relative).

En 2010, j'ai publié un chapitre de livre [53] (cf. Section 5.3) traitant de la stabilité de l'équation à retard linéaire avec retard distribué (1.18), établissant la stabilité ou l'instabilité de l'équation en fonction des propriétés de la fonction $F(a)$. Il s'agit d'une généralisation du résultat de stabilité obtenu dans [13]. Ce résultat est présenté dans le théorème suivant. Notons

$$C(\omega) := \int_0^{+\infty} F(a)\cos(\omega a)da \quad \text{et} \quad S(\omega) := \int_0^{+\infty} F(a)\sin(\omega a)da.$$

**Théorème 1.2.4.** *Supposons que $F$ est une fonction décroissante vérifiant*

$$b\int_0^{+\infty} F(a)da > |d|. \tag{1.22}$$

*Alors il existe $b^* > 0$ vérifiant (1.22) tel que (1.18) est asymptotiquement stable pour tout $b$ tel que*

$$\frac{|d|}{\int_0^{+\infty} F(a)da} < b < b^*, \tag{1.23}$$

*et (1.18) devient instable lorsque $b \geq b^*$, une bifurcation de Hopf survenant pour $b = b^*$, à condition que*

$$\frac{\omega^* S'(\omega^*)}{C(\omega^*)S(\omega^*)} \neq \frac{d}{d\omega}\left(\frac{\omega}{C(\omega)}\right)\Big|_{\omega=\omega^*}, \tag{1.24}$$

*où $\pm i\omega^*$ sont des valeurs propres imaginaires pures de (1.18) lorsque $b = b^*$.*

***Idée de la preuve.*** L'élément clef de cette démonstration est de contrôler le signe de $S(\omega)$. La fonction $F$ étant décroissante, on montre que $S(\omega) > 0$ pour tout $\omega > 0$ (cf. [53], Lemme 3). On peut alors montrer l'existence de $(\omega^*, b^*)$, avec $\omega^* > 0$ et $b^*$ vérifiant (1.22), tels que $\pm i\omega^*$ soit une paire de valeurs propres imaginaires pures simples de l'équation (1.18) lorsque $b = b^*$. On en déduit que toutes les valeurs propres sont à parties réelles négatives lorsque $b < b^*$.

La condition (1.24) permit d'établir que

$$\Re\left(\frac{d\lambda}{db}(b^*)\right) > 0 \quad \text{ou} \quad \Re\left(\frac{d\lambda}{db}(b^*)\right) < 0.$$

En supposant, par contradiction, que

$$\Re\left(\frac{d\lambda}{db}(b^*)\right) < 0$$

pour $b < b^*$, $b$ proche de $b^*$, on montre qu'il existe une valeur propre $\lambda(b)$ de (1.18) à partie réelle positive et vérifiant $b < b^*$, ce qui est en contradiction avec le résultat précédent de stabilité de (1.18) pour $b < b^*$. Ainsi

$$\Re\left(\frac{d\lambda}{db}(b^*)\right) > 0,$$

et nous pouvons conclure à l'existence d'une bifurcation de Hopf lorsque $b = b^*$. □

La section suivante présente les résultats de stabilité obtenus pour une équation avec un retard dépendant de l'état.

### 1.2.3 Retard dépendant de l'état

Un autre type d'équation à retard auquel je me suis intéressé est l'équation à retard dépendant de l'état : l'évolution de la variable $x$ à l'instant $t$ dépend de la valeur de $x$ à l'instant $t - \tau(x(t))$, où le retard dépend également de la valeur de $x$. Une telle équation s'écrit sous la forme générale

$$\frac{d}{dt}x(t) = f(x(t), x(t - \tau(x(t)))), \quad t > 0.$$

Ces équations posent de nombreux problèmes théoriques. Sur quel intervalle définir la condition initiale par exemple ? Pour une équation à retard discret $\tau$, la condition initiale doit être définie sur un intervalle de longueur $\tau$, typiquement $[-\tau, 0]$. Pour une équation à retard dépendant de l'état, en $t = 0$ il est nécessaire d'accéder à la valeur $x(-\tau(x(0)))$. On pourrait donc considérer une condition initiale $\varphi$ définie sur l'intervalle $[-\tau(\varphi(0)), 0]$. Si la fonction $\tau$ est supposée croissante, alors en $t = \varepsilon > 0$ il faut accéder à la valeur $x(\varepsilon - \tau(x(\varepsilon)))$, et il se peut que $\varepsilon - \tau(x(\varepsilon)) < -\tau(x(0)) = -\tau(\varphi(0))$, c'est-à-dire

$$\frac{(\tau \circ x)(\varepsilon) - (\tau \circ x)(0)}{\varepsilon} > 1.$$

Ainsi, si la fonction $\tau \circ x$ est fortement croissante en $t = 0$, on peut faire face à un problème de définition de la condition initiale. On est rapidement amené à considérer des fonctions $\tau$ bornées, et des conditions initiales suffisamment régulières. Walther [122] a apporté un cadre théorique pour établir l'existence et l'unicité des solutions.

Les premiers travaux notables sur les équations à retard dépendant de l'état ont été réalisés dans les années 1960. Driver [64] a étudié l'existence, l'unicité et la dépendance aux conditions initiales des solutions, un travail complété par la suite par de nombreux auteurs qui se sont intéressés à l'existence de solutions périodiques pour ces équations : Aiello et al. [16], Arino et al. [24], Kazmerchuk et Wu [84], Kuang et Smith [90], Magal et Arino [95], Mallet-Paret et al. [98], Ouifki et Hbid [100], Rezounenko et Wu [107], Walther [121]. Pour certaines classes d'équations, les semi-groupes non-linéaires ont été

étudiés (Louihi et Hbid [92]). La linéarisation d'équations à retard dépendant de l'état a été étudiée par Cooke et Huang [50], Arino et Sanchez [25], Hartung [75], Hartung et Turi [77], Hartung et al. [76] et Walther [123]. Un théorème de bifurcation de Hopf a été obtenu par Eichmann [66]. Mentionnons également que des méthodes numériques pour ces équations ont été proposées par Hofer et al. [81], ainsi que par Shampine [114].

J'ai étudié un tel système décrivant la dynamique des cellules souches hématopoiétiques [10] (cf. Section 5.4). L'étude concerne l'existence et l'unicité des solutions, leur positivité, l'existence d'états d'équilibre et leur stabilité. En particulier, nous avons obtenu une condition suffisante pour la stabilité globale de l'état d'équilibre trivial (cf. Paragraphe 1.2.4), décrivant l'extinction de la population, l'existence d'une bifurcation transcritique, et une condition nécessaire et suffisante pour l'existence d'une bifurcation de Hopf locale de l'état d'équilibre positif. Ci-après, je présente brièvement le résultat de stabilité locale obtenu dans [10].

Nous avons considéré l'équation suivante

$$\frac{d}{dt}x(t) = -\left(\delta + \beta(x(t))\right)x(t) + 2e^{-\gamma\mu\tau(x(t))}\beta(x(t-\mu\tau(x(t))))x(t-\mu\tau(x(t))), \quad (1.25)$$

provenant de la description de la dynamique d'une population de cellules souches hématopoïétiques (cf. Section 2.1). Le paramètre $\mu$ est un paramètre de bifurcation, introduit afin de pouvoir réaliser l'étude de la stabilité locale [66], et $\tau$ est une fonction positive, croissante, bornée, et de classe $C^1$. Cette équation possède un unique état d'équilibre positif, noté $x^*(\mu)$, et vérifiant

$$\left(2e^{-\gamma\mu\tau(x^*(\mu))} - 1\right)\beta\left(x^*(\mu)\right) = \delta, \qquad \mu \in [0, \overline{\mu}),$$

à condition que

$$\beta(0) > \delta \qquad \text{et} \qquad 0 \leq \mu < \frac{1}{\tau(0)\gamma}\ln\left(\frac{2\beta(0)}{\delta + \beta(0)}\right) := \overline{\mu}. \quad (1.26)$$

L'équation caractéristique de (1.25) linéarisée autour de $x^*$ est donnée par

$$\begin{aligned}\lambda + \delta + \overline{\beta}(\mu) + \mu\tau'(x^*(\mu))\overline{\alpha}(\mu)e^{-\gamma\mu\tau(x^*(\mu))} \\ -2\overline{\beta}(\mu)e^{-\gamma\mu\tau(x^*(\mu))}e^{-\lambda\mu\tau(x^*(\mu))} = 0, \quad \lambda \in \mathbb{C},\end{aligned}$$

où

$$\overline{\alpha}\left(\mu\right) = 2\gamma\beta(x^*\left(\mu\right))x^*\left(\mu\right) \quad \text{et} \quad \overline{\beta}\left(\mu\right) = \beta(x^*\left(\mu\right)) + \beta'(x^*\left(\mu\right))x^*\left(\mu\right).$$

Cette équation est similaire à celle obtenue dans le cas d'un retard discret (cf. 1.2.1). Si $\tau$ est supposé constant, on retrouve l'équation (1.9).

On établit tout d'abord l'existence d'une bifurcation transcritique ([10], Theorème 6.1), assurant la stabilité de l'état d'équilibre lorsque $\mu = \overline{\mu}$.

**Théorème 1.2.5.** *Lorsque $\mu = \overline{\mu}$, l'état d'équilibre positif subit une bifurcation transcritique : pour $\mu < \overline{\mu}$, $\mu$ proche de $\overline{\mu}$, l'état d'équilibre positif est localement asymptotiquement stable tandis que l'état d'équilibre trivial $x = 0$ est instable, et pour $\mu > \overline{\mu}$ l'état d'équilibre trivial est le seul état d'équilibre et il est localement asymptotiquement stable.*

On montre ensuite trivialement la stabilité de $x^*$ lorsque $\mu = 0$ ([10], Lemme 6.2), sous la condition $\beta(0) > \delta$.

La recherche de valeurs propres imaginaires pures $\lambda = i\omega$, $\omega > 0$ consiste à résoudre le système

$$\left\{ \begin{array}{rcl} \omega & = & c(\mu)\sin(\omega\mu\tau\,(x^*(\mu))), \\ b(\mu) & = & -c(\mu)\cos(\omega\mu\tau\,(x^*(\mu))), \end{array} \right. \tag{1.27}$$

où, pour $\mu \in [0, \overline{\mu})$,

$$b(\mu) = \delta + \overline{\beta}(\mu) + \mu\tau'(x^*(\mu))\overline{\alpha}(\mu)e^{-\gamma\mu\tau(x^*(\mu))} \quad \text{et} \quad c(\mu) = -2\overline{\beta}(\mu)e^{-\gamma\mu\tau(x^*(\mu))}.$$

Une condition nécessaire pour obtenir des valeurs propres imaginaires pures est donc

$$\mid c(\mu) \mid > \mid b(\mu) \mid . \tag{1.28}$$

Une condition suffisante pour que (1.28) soit vérifiée est $b(\mu) < 0$, car par définition $b(\mu) + c(\mu) > 0$.

**Lemme 1.2.6** ([10], Lemme 6.3)**.** *Soit $\eta : [0, +\infty) \to (-\infty, 0]$ et $\sigma : [0, +\infty) \to [0, +\infty)$ définies, pour $y \geq 0$, par $\eta(y) = y\beta'(y)$ et $\sigma(y) = y\tau'(y)$. Supposons que*

*(H1) $\eta$ et $\sigma$ sont décroissantes sur $[0, \beta^{-1}(\delta)]$,*

*(H2) $\eta\left(\beta^{-1}(\delta)\right) < -2\delta$.*

*Alors il existe un unique $\mu^* \in (0, \overline{\mu})$ tel que $b(\mu) < 0$ soit vérifiée si et seulement si $\mu \in [0, \mu^*)$.*

Supposons à présent qu'il existe $\mu^* \in (0, \overline{\mu})$ tel que (1.28) soit vérifiée pour $\mu \in [0, \mu^*)$. on obtient alors, en utilisant (1.27),

$$\omega = \left(c^2(\mu) - b^2(\mu)\right)^{\frac{1}{2}},$$

et en revenant au système (1.27),

$$\left\{ \begin{array}{rcl} \cos\left(\mu\tau^*(\mu)\left(c^2(\mu) - b^2(\mu)\right)^{\frac{1}{2}}\right) & = & -\dfrac{b(\mu)}{c(\mu)}, \\ \sin\left(\mu\tau^*(\mu)\left(c^2(\mu) - b^2(\mu)\right)^{\frac{1}{2}}\right) & = & \dfrac{\left(c^2(\mu) - b^2(\mu)\right)^{\frac{1}{2}}}{c(\mu)}. \end{array} \right.$$

Similairement à ce que nous avons présenté dans le cas d'un retard discret, nous pouvons alors définir

$$Z_k(\mu) = \mu - \mu^k(\mu), \quad k \in \mathbb{N}_0, \mu \in [0, \mu^*), \tag{1.29}$$

où

$$\mu^k(\mu) := \frac{\arccos\left(-\frac{b(\mu)}{c(\mu)}\right) + 2k\pi}{\tau^*(\mu)\left(c^2(\mu) - b^2(\mu)\right)^{\frac{1}{2}}}, \qquad k \in \mathbb{N}_0, \mu \in [0, \mu^*).$$

L'existence de valeurs propres imaginaires pures devient équivalente à l'existence de racines réelles positives des fonctions $Z_k$ sur l'intervalle $[0, \mu^*)$. Nous pouvons alors conclure dans le théorème suivant.

**Théorème 1.2.7.** *Supposons que (1.26) est vérifiée, et que $\beta$ et $\tau$ sont des fonctions $C^2$. Si aucun $\mu \in [0, \overline{\mu})$ ne vérifie (1.28), alors l'état d'équilibre positif $x^*$ de (1.25) est localement asymptotiquement stable pour $\mu \in [0, \overline{\mu})$.*

*Supposons qu'il existe $\mu^* \in (0, \overline{\mu})$ tel que (1.28) soit vérifiée pour $\mu \in [0, \mu^*)$. Alors,*

*(i) Si $Z_0$, définie en (1.29), n'a aucune racine sur $[0, \mu^*)$, l'état d'équilibre positif $x^*$ de (1.25) est localement asymptotiquement stable pour $\mu \in [0, \mu^*)$ ;*

*(ii) Si $Z_0$ possède au moins une racine positive $\mu_c \in (0, \mu^*)$, $x^*$ est localement asymptotiquement stable pour $\mu \in [0, \mu_c)$, instable pour $\mu \geq \mu_c$, $\mu$ dans un voisinage de $\mu_c$, et une bifurcation de Hopf peut survenir pour $\mu = \mu_c$ .*

*Lorsque (ii) est vérifiée, plusieurs changements de stabilité peuvent être observés pour tout $\tau = \tau_c$ racine de $Z_k$.*

On peut noter que la stabilité asymptotique de l'état d'équilibre $x^*$ est obtenue en fonction des valeurs du paramètre $\mu$. N'importe quel autre paramètre aurait cependant pu être utilisé pour déterminer la stabilité, le paramètre $\mu$ a été choisi car il caractérise le retard.

Les retards dépendant de l'état apparaissent assez naturellement dans la modélisation de phénomènes biologiques : le retard décrit généralement une durée ou un phénomène temporel essentiel à la modélisation du processus biologique dans son ensemble (cycle cellulaire, externalisation d'une protéine, gestation d'une espèce animale, etc.) et la population considérée influence souvent cette durée ou ce processus. La complexité d'un modèle à retard dépendant de l'état et les difficultés mathématiques et numériques liées à sa résolution peuvent limiter l'utilisation de tels modèles. Les travaux réalisés ces dernières années [25, 75, 76, 77, 81, 84, 95, 100, 107, 114, 121, 123] ont cependant défini un cadre théorique assez complet pour l'étude des équations à retard dépendant de l'état, permettant de s'intéresser à des applications en biologie faisant intervenir de telles équations.

### 1.2.4 Stabilité asymptotique globale

J'ai discuté, dans les paragraphes précédents, les techniques mises en place pour déterminer la stabilité locale d'une équation à retard, par linéarisation et étude des valeurs propres. La plupart des résultats obtenus montrent qu'une modification du retard peut déstabiliser un état d'équilibre ou une équation stables autrement. Des résultats de stabilité indépendants du retard peuvent cependant parfois être obtenus.

Une question récurrente est celle de la stabilité asymptotique globale (GAS), c'est-à-dire de stabilité indépendamment des conditions initiales. J'ai obtenu plusieurs résultats de GAS, en utilisant des fonctions de Lyapunov. L'idée étant de diminuer l'énergie du système le long des solutions, la construction d'une telle fonction dépend du système étudié.

Considérons un modèle de dynamique de cellules souches hématopoïétiques "classique" [94], décrit par l'équation

$$\frac{d}{dt}x(t) = -\left(\delta + \beta(x(t))\right)x(t) + 2e^{-\gamma\tau}\beta(x(t-\tau))x(t-\tau), \tag{1.30}$$

où $x(t)$ est le nombre de cellules souches hématopoïétiques au temps $t$, $\delta > 0$ et $\gamma > 0$ des taux de mortalité, $\beta(x)$ un taux de transition entre phase de repos et phase de prolifération, $\tau$ la durée de la phase de prolifération, pouvant être constante (cf. 1.2.1), distribuée selon une loi de probabilité (cf. 1.2.2), ou dépendante de l'état (cf. 1.2.3). Cette équation possède, quelle que soit la nature du retard $\tau$, un état d'équilibre trivial $x = 0$. Un état d'équilibre positif peut exister, en fonction des valeurs de paramètres choisies : dans le cas de l'équation (1.30), un unique état d'équilibre positif existe si et seulement si

$$(2e^{-\gamma\tau} - 1)\beta(0) > \delta.$$

Dans le cas où cette condition n'est pas vérifiée, on peut généralement montrer la stabilité asymptotique globale de l'état d'équilibre trivial $x = 0$ en prouvant que la fonction

$$V(\varphi) = \int_0^{\varphi(0)} \beta(u)u\,du + e^{-\gamma\tau}\int_{-\tau}^{0} \left(\beta(\varphi(\theta))\varphi(\theta)\right)^2 d\theta,$$

définie pour $\varphi \in C^+$, l'ensemble des fonctions positives continues sur $[-\tau, 0]$, est une fonction de Lyapunov [73]. Cette méthode, ou une variante basée sur la même propriété, a été utilisée pour obtenir la stabilité asymptotique globale dans différents modèles [5, 7, 8, 10, 11, 51, 52]. Ces résultats sont disponibles dans les articles des Sections 5.1 et 5.4.

## 1.3 Conclusions et commentaires

J'ai abordé dans ce chapitre quelques questions liées à la stabilité des équations à retard, en me concentrant sur la stabilité asymptotique d'une équation linéaire en fonction de la nature du retard. J'ai volontairement laissé de côté certains aspects de l'étude de la stabilité, notamment le cas de plusieurs retards discrets, l'étude des bifurcations, l'existence de chaos et de solutions oscillantes stables.

De nombreuses applications proposent une description basée sur des modèles à plusieurs retards discrets. Le cas d'équations ou de systèmes d'équations à deux retards discrets a été assez largement étudié. J'ai moi-même étudié la stabilité du système

$$\left\{ \begin{array}{rcl} \dfrac{d}{dt}x(t) & = & -a(x(t),y(t))x(t) + f(\tau_1, x(t-\tau_1))x(t-\tau_1), \\ \dfrac{d}{dt}y(t) & = & -by(t) + g(y(t-\tau_2))x(t-\tau_2), \end{array} \right. \tag{1.31}$$

où $a$, $f$ et $g$ sont des fonctions positives et décroissantes en chaque variable, $b > 0$, et $\tau_1 \geq 0$ et $\tau_2 \geq 0$ sont deux retards [15].

Plusieurs méthodes ont été proposées pour analyser la stabilité d'un système à deux retards, basées soit sur une approche géométrique [74, 97], soit sur une approche analytique [68, 106, 109, 110]. Il est toutefois très difficile d'obtenir des conditions nécessaires et suffisantes pour la stabilité, et souvent seules des conditions suffisantes – et très limitées – sont obtenues. La représentation de la frontière entre les zones de stabilité et d'instabilité pour le système (1.31), en fonction des valeurs des retards, donne une assez bonne idée de la difficulté à déterminer exactement cette frontière (Figure 1.1).

L'étude des bifurcations dans le cas d'équations à retard est similaire à celle réalisée pour les équations différentielles ordinaires [72]. J'ai étudié en 2005 le cas d'une équation avec un retard distribué [9], et mis à part que le cadre théorique à mettre en place demande un peu plus de travail (il faut utiliser les bons espaces) il n'y a pas plus de difficulté dans ces études. L'existence de solutions oscillantes lorsqu'une équation est stable, ou l'apparition de chaos dans le cas d'une équation instable, sont déterminés au cas par cas. Dans les modèles à retard que j'ai étudiés, le chaos n'a jamais été ni attendu ni observé. De nombreuses fois en revanche des solutions oscillantes ont été observées numériquement alors même que le système était stable (il s'agit alors de solutions oscillantes amorties). Plusieurs auteurs se sont déjà intéressés à ces solutions, en particulier dans le cas de modèles dynamiques des cellules souches [31, 71, 112].

Concernant les méthodes et résultats présentés dans ce chapitre sur les équations à retard discret, on peut identifier deux éléments clefs. L'obtention de résultats de stabilité ou instabilité dépend de notre capacité à résoudre un système trigonométrique, et à déterminer les racines de polynômes de degrés potentiellement élevés (incluant la

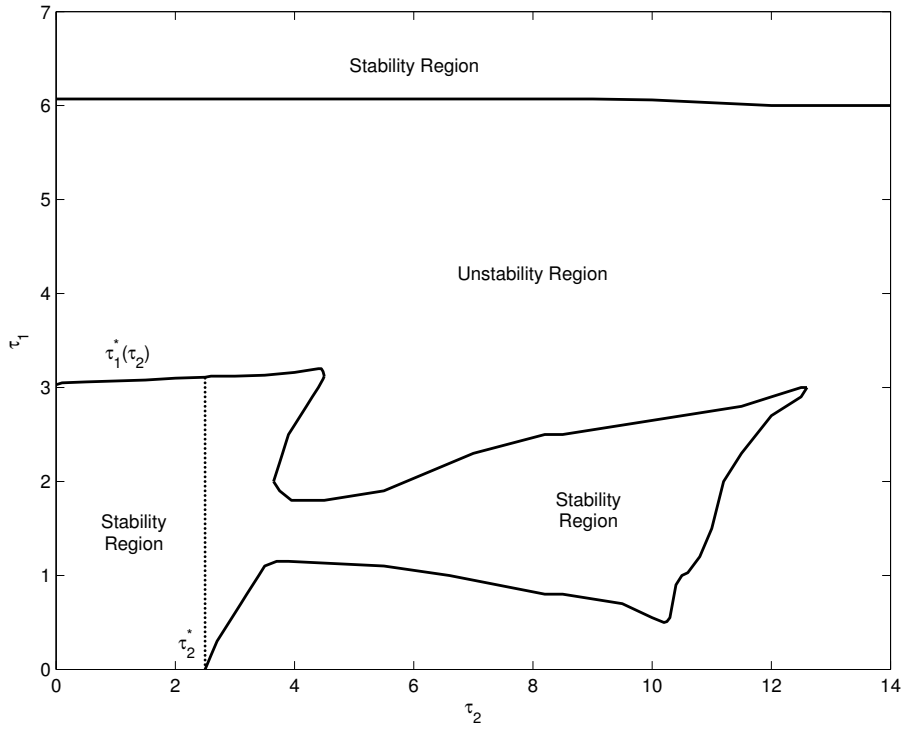


FIGURE 1.1 – **Diagramme de stabilité pour un système à deux retards.** La stabilité du système (1.31) est représentée dans le plan $(\tau_1, \tau_2)$. Les traits continus représentent les frontières entre les zones stables et instables. La zone de stabilité supérieure ($\tau_1 \geq 6.1$ jours) correspond à la stabilité de l'état d'équilibre trivial $(x, y) = (0, 0)$. Le trait pointillé délimite la zone de stabilité obtenue dans [15].

détermination de conditions nécessaires et suffisantes pour que ces polynômes possèdent des racines positives). Ce dernier élément est clairement limitant : il n'est pas raisonnable d'envisager déterminer explicitement, dans des systèmes de plus en plus complexes, des conditions nécessaires et suffisantes sur les paramètres des modèles pour obtenir des racines positives de polynômes de degrés élevés. L'intérêt se porte donc, motivé en partie par les applications, sur la détermination de conditions suffisantes pour la stabilité. En effet, même si pour les modèles de dynamique de cellules souches l'existence de solutions périodiques, associées à une instabilité, a été au coeur des recherches durant les 50 dernières années, de nombreuses applications s'intéressent uniquement à la stabilité des solutions. On peut ainsi envisager d'autres approches (géométriques par exemple, comme cela a déjà été réalisé [28, 97, 99]).

Ce raisonnement s'applique également aux équations à retard distribué. Pour ces équations, à part dans des cas particuliers, aucune condition nécessaire et suffisante n'a été déterminée pour la stabilité de l'équation. En revanche, l'existence de conditions

suffisantes, s'appuyant sur la forme du noyau de probabilité considéré, a été étudiée. De ce point de vue, la conjecture mentionnée par Anderson [18] puis Bernard et al. [33] (cf. Paragraphe 1.2.2) prend une grande importance : si la distribution de retards associée à la plus grande zone d'instabilité, pour un retard moyen donné, est la mesure de Dirac, ou en d'autre terme le retard discret, alors l'étude de l'équation à retard discret permet de déterminer des conditions optimales pour la stabilité de l'équation à retard distribué. Nous avons, Samuel Bernard et moi-même, déterminé récemment que cette conjecture est vraie, et ce résultat est actuellement soumis pour publication [35]. Il s'agit d'un résultat important, qui permet de revenir sur plusieurs applications et résultats déjà publiés en déterminant des conditions optimales pour la stabilité.

# Chapitre 2

# Applications en Dynamique de Populations Cellulaires

Ce chapitre sera consacré aux résultats obtenus dans l'étude de populations cellulaires proliférantes et de leurs rétro-contrôles. Je discuterai essentiellement des résultats liés à la modélisation de la dynamique des cellules souches hématopoïétiques et à la modélisation de l'érythropoïèse normale et de stress. Dans la dernière partie de ce chapitre, j'aborderai brièvement d'autres applications auxquelles je me suis intéressées : la modélisation de l'apparition d'une leucémie myéloïde aiguë [7, 58], et la modélisation de la réponse immunitaire [57, 120], en raison de leur pertinence tant par rapport aux outils et méthodes utilisées (équations à retard pour l'étude de la leucémie myéloïde aiguë) que pour l'attention que je leur porte actuellement (la réponse immunitaire).

La modélisation de la dynamique des cellules souches hématopoïétiques s'appuie principalement sur des systèmes d'équations à retard, déterministes. Les résultats obtenus à travers les différentes études que j'ai réalisées ne seront pas présentés en détails. Je me concentrerai sur un résultat caractéristique, obtenu d'après [51, 52], et mentionnerai brièvement d'autres résultats [6, 11].

La modélisation de l'érythropoïèse fait le lien entre mon activité ces dernières années, basée sur l'étude des équations à retards, et mon activité actuelle axée sur la modélisation multi-échelles. Je présenterai ces deux aspects à travers les résultats obtenus d'abord dans un travail collaboratif sur la modélisation de la réponse à une anémie sévère chez la souris [56], puis dans une série de publications sur la modélisation multi-échelles de l'érythropoïèse [55, 63, 69, 91].

## 2.1 Dynamiques de Cellules Souches Hématopoïétiques

Les cellules souches hématopoïétiques (CSH) sont des cellules majoritairement quiescentes (sans activité proliférative), une faible proportion étant activement proliférante et permettant à la fois le maintien d'un "stock" de CSH et la production de cellules engagées dans les différentes lignées sanguines. Le premier modèle mathématique de la dynamique des CSH est dû à Mackey [94], qui s'est inspiré d'un modèle de cycle cellulaire de Burns et Tannock [40].

Les modèles de dynamique des CSH ont été utilisés pour comprendre différentes maladies sanguines (dont les leucémies myéloïdes), en identifiant les causes potentielles de ces maladies. Il est en particulier intéressant de noter que plusieurs maladies sanguines font apparaître des oscillations temporelles d'un ou plusieurs types cellulaires touchés par la maladie : c'est le cas des leucémies myéloïdes chroniques, pour lesquelles des oscillations avec des périodes comprises entre 40 et 80 jours de tous les types cellulaires ont pu être observées [78].

Je me suis intéressé à différents modèles de dynamiques des CSH, inspirés par le modèle de Mackey [94]. J'ai en particulier considéré un modèle à retard discret, dans lequel la non-linéarité du modèle (le taux d'introduction en phase de prolifération) est supposée dépendre de toute la population de cellules souches, et non uniquement de la population de cellules au repos comme c'est habituellement supposé [94]. Les résultats obtenus à travers l'étude de ce modèle sont présentés dans les paragraphes suivants. J'ai également considéré le modèle de Mackey avec un retard distribué et un retard dépendant de l'état. Pour ces modèles, j'ai montré que les propriétés du modèle de Mackey étaient conservées, et en particulier qu'on pouvait observer des solutions périodiques pour certaines valeurs du retard (cf. Paragraphes 1.2.2 et 1.2.3). Les résultats de ces études sont similaires à ceux obtenus dans le cas discret, je ne les présenterai donc pas dans la suite.

A travers deux articles [51, 52] (cf. Section 5.1), je me suis intéressé à une variante du modèle de Mackey [94] avec un retard discret (Figure 2.1). Dans le modèle de Mackey, et les modèles qui se sont inspirés du modèle de Mackey, l'introduction des cellules souches au repos dans la phase de prolifération est supposée dépendante uniquement du nombre de cellules au repos. Rien dans la justification biologique de ce phénomène ne laisse penser que cette introduction (par exemple lorsque l'organisme a besoin de produire de nouvelles cellules) n'est pas sensible au nombre total de cellules souches. J'ai donc considéré ce cas, et essayé de comparer la dynamique du système à celle du modèle de Mackey.

En notant $N(t)$ la population de cellules souches au repos, et $S(t)$ le nombre total

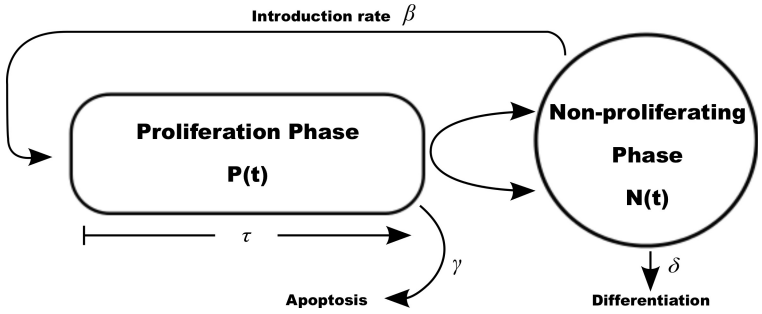


FIGURE 2.1 – **Modèle de cycle cellulaire avec phase de repos et phase de prolifération**, d'après Mackey [94]. La phase de prolifération est caractérisée par une durée de cycle $\tau$ et un taux d'apoptose $\gamma$. Chaque cellule proliférante atteignant la fin du cycle sans mourir se divise en deux cellules qui entrent en phase de repos. Les cellules au repos meurent ou se différencient avec un taux $\delta$ et sont ré-introduites en phase de prolifération avec un taux $\beta$, généralement non-linéaire [51, 52, 94].

de cellules souches (avec, bien entendu, $S(t) \geq N(t)$), le système que j'ai étudié est :

$$\frac{dN}{dt}(t) = -\delta N(t) - \beta(S(t))N(t) + 2e^{-\gamma\tau}\beta(S(t-\tau))N(t-\tau), \tag{2.1}$$

$$\frac{dS}{dt}(t) = -\gamma S(t) + (\gamma - \delta)N(t) + e^{-\gamma\tau}\beta(S(t-\tau))N(t-\tau), \tag{2.2}$$

où $\delta$ est le taux de mortalité des cellules au repos, $\gamma$ celui des cellules en prolifération, $\beta$ le taux d'introduction en phase de prolifération, et $\tau$ la durée moyenne d'un cycle cellulaire (Figure 2.1).

J'ai d'abord étudié ce modèle dans le cas où $\delta = \gamma$, c'est à dire le taux de mortalité est le même pour les cellules quiescentes et proliférantes [51], puis dans le cas général $\delta \neq \gamma$ [52]. L'étude de la stabilité asymptotique locale du système (2.1)–(2.2) est alors plus compliquée que celle du système de Mackey [94] équivalent, car il faut dans le second cas étudier les racines d'un polynôme exponentiel de degré 1, et de degré 2 dans le premier cas (cf Paragraphe 1.2.1).

L'étude complète de la stabilité locale, avec l'existence de changements de stabilité et d'une bifurcation de Hopf (de façon indentique aux résultats obtenus dans le Théorème 1.2.2, cf. Paragraphe 1.2.1), et globale *via* une fonction de Lyapunov (cf. Paragraphe 1.2.4), a permis de conclure que qualitativement ce modèle et celui de Mackey se comportaient de la même façon. On observe toutefois des différences quantitatives, dont on ne peut déterminer la pertinence par manque de données expérimentales validant les modèles.

Comme dans le modèle de Mackey, on retrouve un rôle prépondérant du taux d'apoptose $\gamma$ et de la durée de la phase de prolifération $\tau$ dans la stabilité du système. On

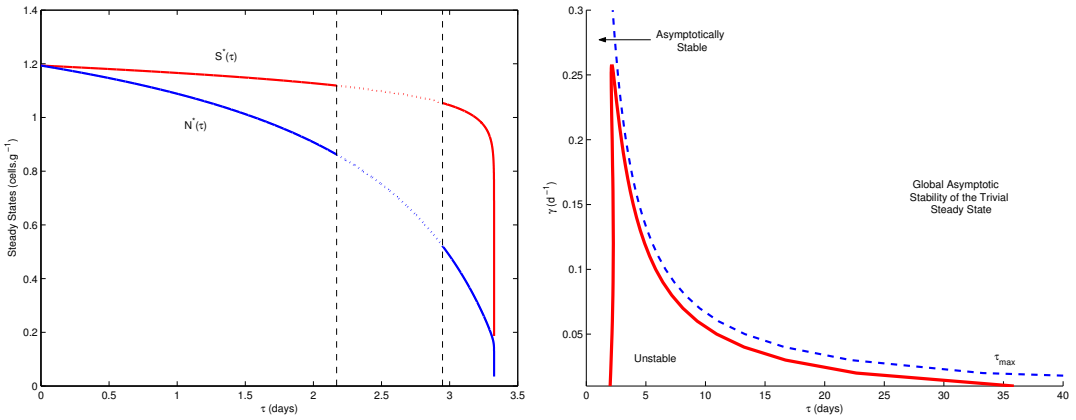


FIGURE 2.2 – **Changement de stabilité du système (2.1)–(2.2)**, d'après [52]. À gauche : États d'équilibre $N^*(\tau)$ et $S^*(\tau)$ du système (2.1)–(2.2), pour un taux d'apoptose $\gamma = 0.2\,\mathrm{j}^{-1}$. Les états d'équilibre sont instables lorsque $\tau \in (2.17; 2.95)$ jours, stables sinon. À droite : Valeurs critiques de $(\tau, \gamma)$ pour lesquelles un changement de stabilité survient. Pour chaque valeur de $\gamma$ dans l'intervalle $[0, 0.26]$ $\mathrm{j}^{-1}$ deux valeurs critiques de $\tau$ existent.

observe des changements de stabilité (Figure 2.2) associés à l'apparition de solutions oscillantes périodiques. Ces solutions ont auparavant été comparées à des oscillations observées dans certaines maladies hématologiques, dont la leucémie myéloïde chronique [13, 78, 104], et on retrouve bien avec le système (2.1)–(2.2) des solutions oscillantes de périodes similaires à celles observées dans les travaux précédemment cités.

Les modèles de dynamique cellulaire inspirés du modèle de Mackey [94] supposent, implicitement, que la dynamique des cellules souches explique à elle seule la dynamique observée dans les différentes lignées hématopoïétiques, et en particulier la dynamique des cellules différenciées (globules rouges, globules blancs, plaquettes). En effet, ni la différenciation des cellules souches (le paramètre $\delta$ peut être vu comme un taux de différenciation ou bien comme un taux de mort) ni la dynamique des différentes lignées n'est décrite. Plusieurs modèles ont ainsi ajouté la description de la dynamique des cellules différenciées : mentionnons les travaux de Bernard et al. [34] sur les globules blancs, Mahaffy et al. [96] sur les globules rouges, Santillan et al. [113] sur les plaquettes, ou encore les travaux plus récents de Colijn et Mackey [48, 47] qui ont décrit à la fois la dynamique des cellules souches hématopoïétiques et des trois lignées myéloïdes.

A travers deux manuscrits, publiés en 2009 et 2010, je me suis intéressé à l'influence d'une part de la prise en compte d'un contrôle explicite par des facteurs de croissance de la régulation de la dynamique des cellules souches [6], et d'autre part à

l'influence de la prise en compte de la différenciation dans la dynamique des cellules souches hématopoïétiques [11].

Dans le premier cas, il s'agissait de poursuivre un travail publié en 2007 [5], en comparant les actions d'un facteur de croissance contrôlant la prolifération des cellules souches, et un autre contrôlant leur apoptose [6]. Ces travaux ont permis de mieux comprendre les différents rôles possibles des facteurs de croissance dans la régulation de l'hématopoïèse, du point de vue de la modélisation. Ils ont également contribué au développement d'un modèle d'érythropoïèse [56] dont je discuterai plus loin (cf. Section 2.2).

Dans le deuxième travail mentionné ci-dessus, réalisé en collaboration avec Mostafa Adimy et Catherine Marquet [11], nous avons étudié un modèle décrivant la dynamique de deux populations cellulaires, une immature et une mature. La population de cellules immatures représente les cellules souches hématopoïétiques, qui peuvent proliférer ou bien demeurer au repos (comme dans le système (2.1)–(2.2)), la population de cellules matures décrit un stade plus avancé de la différenciation des cellules sanguines (progéniteurs/précurseurs). Cette dernière population contrôle la première, à travers son taux de différenciation, son taux d'introduction en cycle, ou sa mortalité. En notant $R(t)$ le nombre de cellules immatures au repos, et $M(t)$ le nombre de cellules matures, le système s'écrit

$$\begin{cases} \dfrac{dR}{dt}(t) = -\left[\delta + K_R + \beta(M(t))\right] R(t) + 2(1-K_P)e^{-\gamma\tau}\beta\left(M(t-\tau)\right) R(t-\tau), \\ \dfrac{dM}{dt}(t) = -\mu M(t) + K_R R(t) + 2K_P e^{-\gamma\tau}\beta\left(M(t-\tau)\right) R(t-\tau). \end{cases}$$

La population de cellules proliférantes n'est pas décrite ici, car l'équation qui régit sa dynamique est découplée du système (il s'agit d'une propriété du système de Mackey [94]) en raison du choix de la fonction $\beta$. Les paramètres $K_R$ et $K_P$ représentent les taux de différenciation, supposés constants, des cellules au repos et proliférantes respectivement. On observe que pour des taux de différenciation élevés le système n'oscille pas (Figure 2.3), et l'instabilité du compartiment de cellules souches peut se transmettre au compartiment de cellules différenciées uniquement pour de faibles taux de différenciation.

## 2.2 Modèles d'érythropoïèse

Le terme "érythropoïèse" désigne l'ensemble des phénomènes de différenciation, prolifération, maturation, et mort cellulaire permettant la production des globules rouges. Il s'agit d'un sous-processus de l'hématopoïèse. Les cellules souches hématopoïétiques produisent, par division et différenciation, des cellules engagées dans une voie de différenciation, la lignée érythrocytaire. Ces cellules, appelées progéniteurs érythrocytaires, ou

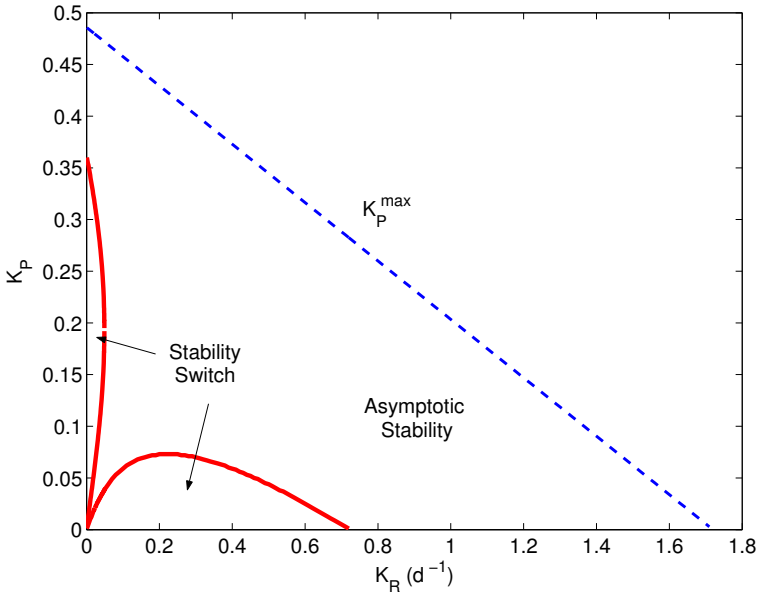


FIGURE 2.3 – **Stabilité dans le plan** $(K_R, K_P)$, d'après [11]. La ligne pointillée représente une valeur limite de $K_P$ au delà de laquelle l'état d'équilibre positif n'existe plus.

érythroïdes, sont peu matures et produiront, à leur tour et en quelques divisions, par différenciation et maturation des réticulocytes, puis des érythrocytes. Les réticulocytes sont des globules rouges immatures, les érythrocytes, une fois qu'ils ont quitté la moelle osseuse et ont rejoint le sang, deviennent des globules rouges fonctionnels (cf. Figure 2.5.A).

Depuis la fin des années 1980, et la découverte de Koury et Bondurant [87] concernant l'érythropoïétine (ou Epo) et sa fonction dans l'érythropoïèse, les mécanismes de régulation de l'érythropoïèse semblaient définitivement acquis : l'Epo, un facteur de croissance, est libéré par les reins lorsque le nombre de globules rouges dans le sang diminue, et inhibe l'apoptose des progéniteurs érythrocytaires en se fixant à leur surface (*via* le récepteur Epo) ; lorsque le nombre de globules rouges augmente, la production d'Epo cesse. On sait également, depuis bien plus longtemps, que l'hématopoïèse dans son ensemble fonctionne correctement car elle s'appuie sur une réserve de cellules souches qui ont la double capacité de se différencier (produire par division des cellules différentes, possédant un niveau de maturité plus élevé) et de s'auto-renouveler (produire par division une ou des cellules génétiquement identiques à la cellule mère). Depuis quelques années maintenant (fin des années 1990, début des années 2000), l'auto-renouvellement de progéniteurs érythrocytaires en situation de stress a été prouvé [27, 70]. Cette capacité des progéniteurs érythrocytaires à s'auto-renouveler éclaire sous un nouveau jour la

régulation de l'érythropoïèse.

Dans la Section suivante je présenterai les travaux de modélisation de l'érythropoïèse réalisés en collaboration avec des collègues de l'Institut Camille Jordan (S. Génieys, L. Pujo-Menjouet) et Olivier Gandrillon, biologiste au centre de Génétique et Physiologie Moléculaire et Cellulaire. Il s'agit d'une approche déterministe de la modélisation de l'érythropoïèse consistant à décrire des données expérimentales (anémie) en utilisant un modèle incluant l'auto-renouvellement des progéniteurs érythrocytaires.

La section 2.2.2 présentera d'autres approches basées sur des modèles stochastiques, hybrides discrets/continus, modélisant l'érythropoïèse de stress.

### 2.2.1 Modèles déterministes

J'ai proposé en 2008, en collaboration avec Laurent Pujo-Menjouet, Stéphane Génieys, Clément Molina et Olivier Gandrillon [56], un modèle d'érythropoïèse de stress chez la souris. Il s'agit d'un système d'équations structurées en âge (cf. 1.1) décrivant la dynamique de populations de progéniteurs érythrocytaires et d'érythrocytes circulant dans le sang (globules rouges). Je me suis intéressé à la régulation des populations cellulaires par des rétrocontrôles, essentiellement par l'Epo (inhibition de l'apoptose) et les glucocorticoïdes (GC) qui favorisent l'auto-renouvellement des progéniteurs [27, 70]. L'article dans lequel ce travail a été présenté est disponible au Chapitre 5.5.

Des souris ont été anémiées par injection de phenylhydrazine (cf. Figure 2.4), une substance détruisant la membrane des globules rouges, et la cinétique du retour à un hématocrite normal a été mesurée. Rappelons que l'hématocrite est le ratio entre le volume de globules rouges et le volume total de sang, ce dernier pouvant être approché par le volume des globules rouges et le volume du plasma (les plaquettes et les globules blancs sont négligeables dans la composition du sang). Les données expérimentales font apparaître, en réponse à l'anémie, une remontée très rapide du nombre de globules rouges suivie d'oscillations amorties autour d'une valeur d'équilibre (Figure 2.4).

L'objectif était de reproduire ces données expérimentales avec un modèle d'érythropoïèse, afin de déterminer si l'auto-renouvellement était utile pour expliquer les données ou s'il ne l'était pas. Pour cela, nous avons étudié les rôles respectifs de l'inhibition de l'apoptose des progéniteurs érythrocytaires en cas d'anémie, et la stimulation de leur auto-renouvellement. En notant $p(t,a)$ la densité de progéniteurs érythrocytaires au temps $t$, d'âge $a \in [0, \tau_p]$, $s(t,a)$ la densité de progéniteurs s'auto-renouvellant au temps $t$ et d'âge $a \in [0, \tau_c]$, et $e(t,a)$ la densité d'érythrocytes au temps $t$ et d'âge $a > 0$, le

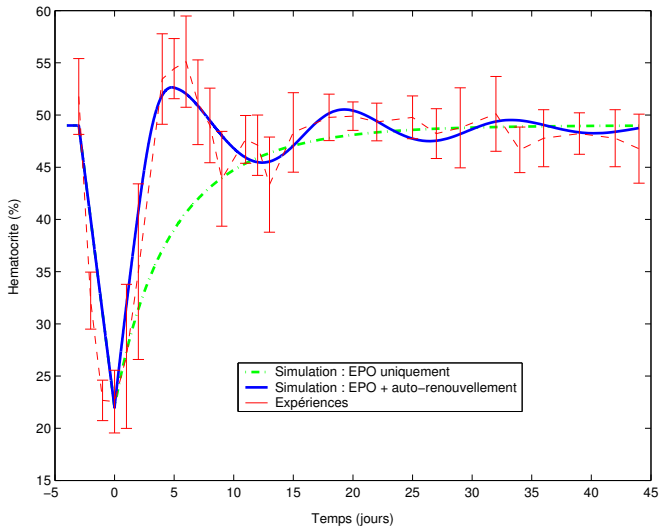


FIGURE 2.4 – **Résultats de simulations d'une anémie chez des souris**, d'après Crauste et al. [56]. Les données expérimentales sont représentées en rouge. Une anémie a été induite chez 9 souris, par injection de phenylhydrazine aux jours -3 et -2. Le retour à un hématocrite stable a été mesuré sur 44 jours. En vert le résultat obtenu en supposant que les progéniteurs érythrocytaires ne peuvent pas s'auto-renouveller. En bleu le résultat obtenu avec de l'auto-renouvellement.

système étudié est le suivant :

$$\begin{cases} \partial_t p(t,a) + \partial_a p(t,a) = -(\beta+\sigma)\, p(t,a), & p(t,0) = HSC + 2s(t,\tau_c), \\ \partial_t s(t,a) + \partial_a s(t,a) = -\beta s(t,a), & s(t,0) = \displaystyle\int_0^{\tau_p} \sigma p(t,a)da, \\ \partial_t e(t,a) + \partial_a (t,a) = -\gamma e(t,a), & e(t,0) = Ap(t,\tau_p), \end{cases} \tag{2.3}$$

où $\partial_y$ représente la dérivée partielle par rapport à la variable $y$, $HSC > 0$ est un flux supposé constant de cellules souches hématopoïétiques se différenciant en progéniteurs érythrocytaires, $A > 0$ est un facteur d'amplification, $\gamma > 0$ est le taux de mort des globules rouges dans le sang, et

$$\beta = \beta\left(\int_0^\infty e(t,a)da\right) \quad \text{et} \quad \sigma = \sigma\left(\int_0^\infty e(t,a)da\right).$$

La fonction $\beta$, taux d'apoptose des progéniteurs, est supposée croissante afin de décrire le contrôle négatif du nombre de globules rouges sur l'Epo (plus il y a de globules rouges, moins il y a d'Epo libéré par les reins) associé au contrôle négatif de l'Epo sur l'apoptose des progéniteurs (plus il y a d'Epo, moins il y a d'apoptose). La fonction $\sigma$, taux d'auto-renouvellement des progéniteurs, a un comportement opposé : elle est supposée décroissante pour décrire, implicitement, le contrôle négatif des globules rouges sur

les glucocorticoïdes, et le contrôle positif des glucocorticoïdes sur l'auto-renouvellement (plus il y a de glucocorticoïdes, plus les cellules s'auto-renouvellent).

Lorsqu'on suppose que les progéniteurs érythrocytaires ne peuvent pas s'auto-renouveller, le système (2.3) s'écrit

$$\begin{cases} \partial_t p(t,a) + \partial_a p(t,a) = \beta\left(\int_0^\infty e(t,a)da\right) p(t,a), & p(t,0) = HSC, \\ \partial_t e(t,a) + \partial_a (t,a) \ = -\gamma e(t,a), & e(t,0) = Ap(t,\tau_p). \end{cases} \tag{2.4}$$

On peut alors réduire ce système à un système de deux équations non-linéaires à retard (cf. 1.1), avec retard distribué,

$$\begin{cases} \dfrac{dP}{dt}(t) = -\beta(E(t))P(t) + HSC\left[1 - \exp\left(-\displaystyle\int_{t-\tau_p}^{t} \beta(E(s))ds\right)\right], \\ \dfrac{dE}{dt}(t) = -\gamma E(t) + A.HSC \exp\left(-\displaystyle\int_{t-\tau_p}^{t} \beta(E(s))ds\right), \end{cases} \tag{2.5}$$

où

$$P(t) := \int_0^{\tau_p} p(t,a)da, \qquad E(t) := \int_0^\infty e(t,a)da.$$

L'étude de la stabilité de ce système montre qu'il est stable lorsque le taux de mortalité $\gamma$ des globules rouges n'est pas trop grand, et qu'il peut devenir instable, à travers une bifurcation de Hopf. Bien que le système (2.5) puisse générer des oscillations amorties, ces dernières ne permettent toutefois pas de reproduire les données expérimentales (voir Figure 2.4). On observe un retour à l'équilibre de l'hématocrite monotone, capturant assez mal la cinétique autour des jours 3 à 8 post-anémie. Le modèle ne tenant pas compte de l'auto-renouvellement des progéniteurs n'est donc *a priori* pas capable de reproduire les données expérimentales.

Le système (2.3) peut également être réduit à un système de deux équations différentielles non-linéaires à retard (deux retards apparaissent naturellement dans la modélisation : la durée d'un cycle cellulaire $\tau_c$, et la longueur du compartiment des progéniteurs $\tau_p$) par intégration sur la variable d'âge, mais son étude n'est pas aisée.

Une étude numérique du modèle complet (2.3) a alors permis de conclure à l'importance de l'auto-renouvellement des progéniteurs dans la situation d'érythropoïèse de stress considérée, avec des résultats reproduisant très bien les données expérimentales (voir Figure 2.4). On observe en particulier que le retour à l'équilibre est bien capturé. Pour aboutir à ce résultat, il a toutefois fallu modifier la valeur du taux de mortalité $\gamma$ : en effet, la phenylhydrazine a pour conséquence de fragiliser les globules rouges non détruits lors de son injection, réduisant leur durée de vie.

Dans un travail récent, j'ai étudié plus en détail l'influence du protocole expérimental sur la sévérité de l'anémie et la capacité de l'organisme à récupérer rapidement. Le

protocole expérimental consiste en deux injections, à 24h d'intervalle, d'une même dose de phenylhydrazine. La première injection induit une anémie sévère, la seconde injection fait chuter l'hématocrite à des niveaux très faibles, induisant un stress important. Dans ce travail, en collaboration avec Oscar Angulo [19] et actuellement en cours de révision, il a tout d'abord fallu modéliser le protocole expérimental, qui était "caché" dans le modèle précédent : l'anémie était décrite comme condition initiale, et correspondait en fait à une perturbation de l'état d'équilibre du système. Pour cela, nous avons supposé que la phenylhydrazine n'affectait que la durée de vie des globules rouges, c'est-à-dire le paramètre $\gamma$, et ensuite que les globules rouges non détruits mais présents lors de l'injection étaient affectés par la phenylhydrazine, en conséquence leur taux de mortalité $\gamma$ était modifié.

Les premiers résultats obtenus mettent en évidence l'importance du protocole expérimental, qui est responsable de la sévérité de l'anémie et modifie la réponse de l'organisme en affectant durablement la durée de vie des globules rouges, mais également l'importance de l'auto-renouvellement (comme évoqué dans [56]) et de ne pas induire la différenciation de progéniteurs trop immatures.

L'étude théorique du système (2.3) est actuellement en cours. La difficulté réside dans la présence de non-linéarités et de deux retards distincts, qui rendent l'étude de l'existence d'états d'équilibre et de leur stabilité délicate. L'unicité d'un état d'équilibre n'est pas assurée sans des hypothèses assez fortes sur les taux d'auto-renouvellement et de différenciation (ce dernier n'est pas décrit dans (2.3), la différenciation est supposée survenir uniquement lorsque $a = \tau_p$). L'étude de la stabilité peut être appréhendée par des méthodes semblables à celles présentées au Chapitre 1, toutefois le système (2.3) est plus proche d'une équation à deux retards que d'une équation à retard distribué, et son étude est donc plus compliquée.

A partir de 2006, parallèlement au travail sus-cité, j'ai commencé à m'intéresser à la modélisation multi-échelles de l'érythropoïèse et sa régulation intra-cellulaire. L'idée initiale est de relier des observations à l'échelle d'une population de cellules à des événements moléculaires : il faut pour cela identifier les protéines contrôlant le choix entre auto-renouvellement, apoptose et différenciation, les facteurs de croissance responsables de l'activation de l'une ou l'autre protéine, et coupler les différentes échelles de régulation de l'érythropoïèse, de l'échelle moléculaire à l'échelle des populations de cellules, en tenant compte des différentes échelles de temps (l'activation d'une protéine est de l'ordre de quelques minutes, un cycle cellulaire de 24h, etc.). Le travail auquel j'ai participé, réalisé entre 2006 et 2013 sur ce sujet, est présenté dans la section suivante.

### 2.2.2 Modèles multi-échelles

Mon travail sur la modélisation multi-échelles de l'érythropoïèse a fait l'objet de plusieurs publications [63, 55, 69, 91] proposant deux approches différentes mais complémentaires.

Récemment, de nombreuses personnes se sont penchées sur l'intérêt d'une modélisation multi-échelles en biologie, et sur les méthodes et outils appropriés. Mentionnons les travaux de Byrne et Drasdo [41], Chauvière et al. [44], Billy et al. [38] Deisboeck et Stamatakos [62], Qu et al. [105], Bernard [32], ainsi que les nombreuses références qu'ils présentent. Il ressort de ces travaux que pour être "multi-échelles" un modèle doit à la fois imbriquer différentes échelles (temporelles et/ou spatiales, par exemple) mais également décrire des interactions entre les échelles. Je considèrerai cette définition d'un modèle multi-échelles dans la suite.

Plusieurs formalismes peuvent être utilisés pour modéliser un processus multi-échelles : modèles continus (équations différentielles, équations aux dérivées partielles), modèles discrets (à base d'agents), modèles hybrides discret/continu,... Le choix du formalisme utilisé dépend essentiellement des questions posées et des données biologiques venant soutenir le modèle. Concernant la modélisation de l'érythropoïèse, la question qui est posée est : peut-on déterminer les causes moléculaires responsables du comportement d'une population de cellules ? Les deux échelles spatiales à considérer sont donc l'échelle intra-cellulaire, à laquelle la régulation moléculaire a lieu, et l'échelle de la population de cellules, à laquelle a lieu l'observation. Entre les deux, il est nécessaire de décrire la "cellule" qui est l'élément faisant le lien entre les deux échelles. L'environnement extracellulaire doit généralement être décrit également (car certaines interactions passent par lui), et peut être considéré comme une troisième échelle. Les échelles temporelles vont de la minute (expression de protéines intra-cellulaires) à la journée (modification de la population de cellules).

Dans Demin et al. [63] et Crauste et al. [55], cf. Section 5.6, nous avons souhaité coupler une description de l'érythropoïèse à l'échelle d'une population de cellules (comme dans [56]) avec une description de la régulation intra-cellulaire, en utilisant des modèles continus. Pour cela, nous avons tout d'abord déterminé un réseau de protéines assurant le contrôle du choix entre auto-renouvellement, apoptose et différenciation dans un progéniteur érythrocytaire. Nous avons ensuite réduit ce réseau de régulation intracellulaire à sa plus simple expression : deux protéines. La première protéine, Erk, contrôle l'auto-renouvellement des progéniteurs ; la seconde, Fas, contrôle leur mort par apoptose et leur différenciation (cf. Figure 2.5.B). La dynamique de ce réseau est bi-stable : Erk stimule sa propre activation et inhibe la production de Fas, tandis que Fas inhibe

la production de Erk et favorise, indirectement, sa propre expression (en induisant la différenciation).

La seconde étape consiste à décrire le milieu extra-cellulaire, composé essentiellement de facteurs de croissance. Les facteurs de croissance, qui sont des facteurs externes à la cellule, peuvent activer ou inhiber une ou plusieurs voies de signalisation, et jouent ainsi un rôle essentiel dans le couplage des échelles intra-cellulaires et de populations de cellules. L'Epo, par exemple, peut inhiber la mort par apoptose (par une voie de signalisation indépendante de Erk et Fas) et favoriser la différenciation. Les glucocorticoïdes favorisent l'auto-renouvellement (cf. Figure 2.5.B).

Enfin, la dynamique de la population de progéniteurs est décrite à l'aide d'un modèle compartimental. Chaque compartiment représente un niveau de maturité/différenciation de ces cellules, correspondant à une capacité à s'auto-renouveler qui diminue avec la différenciation, jusqu'au dernier compartiment représentant les globules rouges (cellules matures, capables de transporter de l'oxygène). Ce modèle est représenté par la Figure 2.5.A. Les cellules exercent potentiellement un feedback (positif ou négatif) sur les réseaux de régulation intra-cellulaire. L'apoptose des progéniteurs dépend de la proximité des réticulocytes : ces derniers induisent, par contact avec un progéniteur, l'expression de la protéine Fas, *via* l'activation de son ligand, Fas-Ligand. Le schéma global du modèle multi-échelle est résumé dans la Figure 2.5.B.

Les différentes populations de cellules, notées $P_1$, $P_2$, etc., sont caractérisées par les niveaux moyens de Erk et Fas exprimés par les cellules appartenant à ce stade de différenciation. En fonction des niveaux d'expression des protéines Erk et Fas, notés $E_i$ et $F_i$ respectivement pour le compartiment $P_i$, les cellules d'une génération donnée auront une probabilité de s'auto-renouveler, de mourir par apoptose, et de se différencier. La probabilité de mourir sera également directement influencée par le niveau d'Epo à proximité de la cellule.

La dynamique des populations de progéniteurs érythrocytaires et des cellules matures a été décrite par un système d'équations différentielles ordinaires. Il en va de même pour les facteurs de croissance. En notant $HSC$ le flux constant de cellules souches hématopoïétiques se différenciant en progéniteurs érythrocytaires, les équations que nous

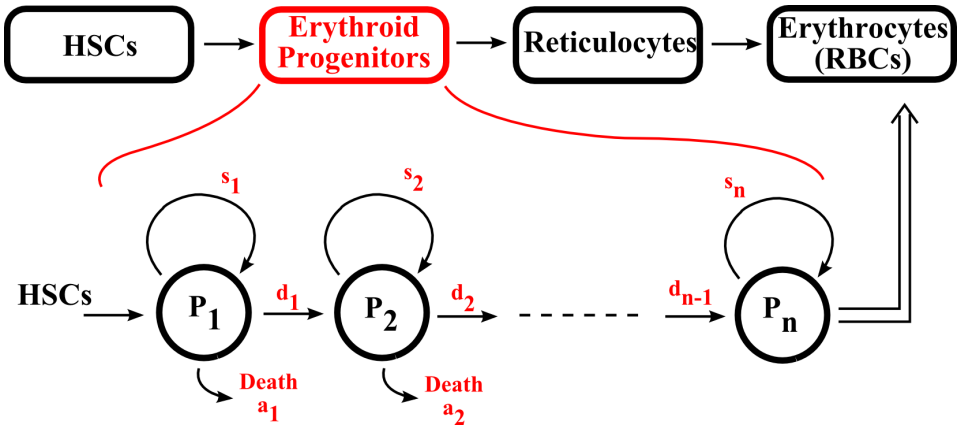


A.

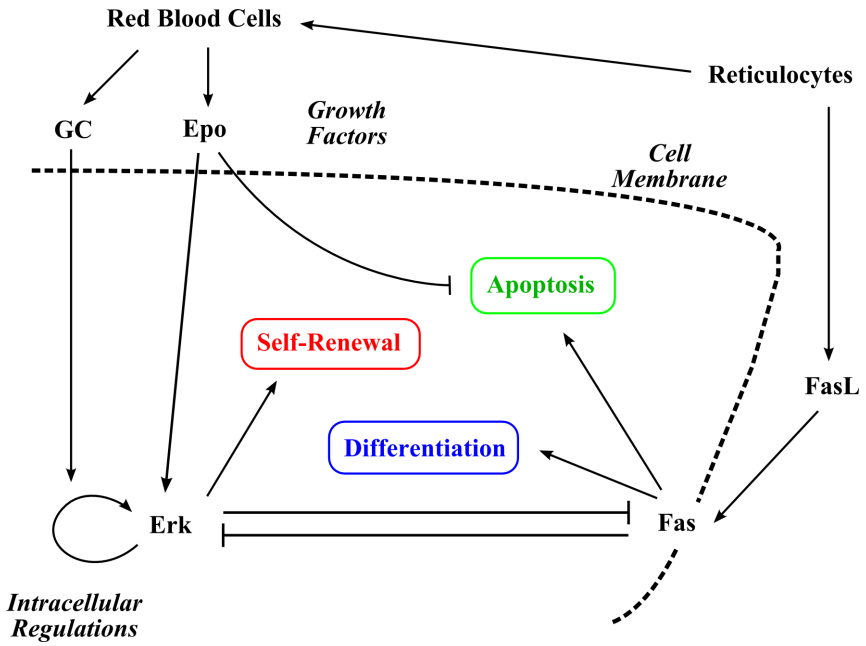


B.

FIGURE 2.5 – **Modélisation multi-échelle de l'érythropoïèse**, d'après Demin et al. [63]. A : modèle compartimental de différenciation cellulaire. B : modèle multi-échelle, incluant la description de la régulation intra-cellulaire (basée sur les protéines Erk et Fas), de la dynamique cellulaire (red blood cells et réticulocytes), du milieu extra-cellulaire (Epo et GC), et du destin cellulaire (différenciation en bleu, auto-renouvellement en rouge et apoptose en vert).

avons proposées sont les suivantes.

$$\begin{cases} \dfrac{dP_1}{dt} &= HSC + s_1P_1 - d_1P_1 - a_1P_1, \\ \dfrac{dP_i}{dt} &= 2d_{i-1}P_{i-1} + s_iP_i - d_iP_i - a_iP_i, \quad i = 2, \dots, n, \\ \dfrac{dM}{dt} &= d_nP_n - \delta M, \\ \dfrac{dEpo}{dt} &= f_{Epo}(M) - k_{Epo}Epo, \\ \dfrac{dGC}{dt} &= f_{GC}(M) - k_{GC}GC. \end{cases}$$

La compétition entre les deux protéines intra-cellulaires est décrite par un système bistable :

$$\begin{cases} \dfrac{dE_i}{dt} &= (\alpha(Epo, GC) + \beta E_i^k)(E_0 - E) - aE_i - bE_iF_i, \\ \dfrac{dF_i}{dt} &= \gamma(P_n)(F_0 - F_i) - cE_iF_i - dF_i. \end{cases} \tag{2.6}$$

Le couplage entre les deux échelles physiques est réalisé à travers les taux d'auto-renouvellement ($s_i$), d'apoptose ($a_i$) et de différenciation ($d_i$), de la façon suivante : on considère une fonction $a$ définissant le taux d'apoptose, et une probabilité $p_s$ d'auto-renouvellement en l'absence d'apoptose. Alors

$$s = (1 - a)p_s, \qquad s + d + a = 1,$$

et

$$s_i := s(E_i, F_i), \quad d_i := d(E_i, F_i), \quad a_i := a(E_i, F_i)f(Epo).$$

Le dernier terme tient compte d'une inhibition de l'apoptose par l'Epo indépendante du réseau de régulation intra-cellulaire basé sur Erk et Fas.

L'étude théorique de ce modèle a consisté à déterminer le nombre d'états d'équilibre et leur stabilité. Le travail principal a consisté à écrire le modèle, qui est entièrement nouveau, fruit d'une collaboration entre mathématiciens et biologistes. Numériquement, le modèle a permis de déterminer les rôles respectifs des rétro-contrôles indépendants des protéines intra-cellulaire Erk et Fas et ceux complètement dépendants [55, 63] : nous avons montré que l'inhibition de l'apoptose par l'Epo est le principal facteur permettant une production rapide et intense de globules rouges dans les premières heures suivant une anémie, alors que la régulation intra-cellulaire basée sur Erk et Fas s'inscrit sur une plus longue période (plusieurs jours) pour réguler l'érythropoïèse, même une fois l'action de l'Epo sur l'apoptose inexistante.

Une hypothèse importante et limitante, dans ce modèle, concerne toutefois la modélisation de l'échelle cellulaire. La "cellule" n'est pas modélisée en tant que telle, mais à travers la modélisation des échelles intra-cellulaire et de la population de cellules

émerge une définition de la "cellule". Or, l'utilisation de compartiments décrivant des niveaux de différenciation implique la définition d'une "cellule moyenne", représentant toutes les cellules d'un compartiment en terme de niveaux d'expression des protéines intra-cellulaires. Le nombre de compartiments étant fixe, le modèle dans son ensemble introduit une hétérogénéité à l'échelle cellulaire plus importante que dans le modèle présenté au Paragraphe 2.2.1 mais cependant limitée. Pour essayer de corriger cet effet, nous avons ensuite proposé un nouveau modèle d'érythropoïèse.

Ce travail a été poursuivi par la modélisation multi-échelles de l'érythropoïèse à partir de modèles hybrides discret/continu. Dans ces modèles, les réseaux moléculaires intra-cellulaires sont toujours décrits par des modèles continus, les cellules en revanche sont des objets discrets disposés sur une grille, ou pas (modèles *off-lattice*). Il s'agit d'une approche computationelle associée à une approche mathématique. Elle permet une description de l'espace physique extra-cellulaire (le domaine de calcul) et une prise en compte d'événements stochastiques (les déplacements des cellules, la division physique d'une cellule, etc.). Elle est également plus couteuse, computationnellement, qu'une approche continu/continu, comme mentionnée ci-dessus.

Le modèle hybride d'érythropoïèse et les résultats que nous avons obtenus ont été présentés à travers trois publications (Kurbatova et al [91], Bessonov et al [36], et Fisher et al [69]). Je présenterai ici le modèle et les résultats obtenus dans [69], cf. Section 5.7.

La dynamique moléculaire est décrite par le système d'équations différentielles ordinaires bistable (2.6). Chaque cellule est en revanche "unique" dans ce modèle, dans le sens où on ne considère pas des niveaux de Erk et Fas correspondant à un stade de différenciation donné. Chaque cellule possède le même réseau de régulation intracellulaire, qui évolue en fonction des règles internes au réseau (modèle bi-stable, à base d'équations ordinaires) mais aussi en fonction de l'environnement de la cellule (niveau de facteurs de croissance, contact avec une ou plusieurs autres cellules).

La diffusion des facteurs de croissance dans le domaine de calcul est réalisée par des équations de réaction-diffusion. En pratique, les facteurs de croissance comme l'Epo diffusent assez rapidement dans la moelle osseuse, et lorsqu'on considère un domaine de petite taille on peut, sans perte de généralité, supposer un coefficient de diffusion infini. Chaque cellule détecte le niveau de facteurs de croissance dans son voisinage.

Les cellules sont des objets circulaires (en 2D), évoluant *off-lattice*, avec une partie incompressible correspondant au noyau de la cellule et un cytoplasme déformable [36], cf. Figure 2.6. Les cellules se déplacent dans l'environnement, et interagissent en suivant des lois classiques de la physique. En particulier, la division d'une cellule en deux cellules filles induit une modification de la pression locale, et un déplacement des cellules. La

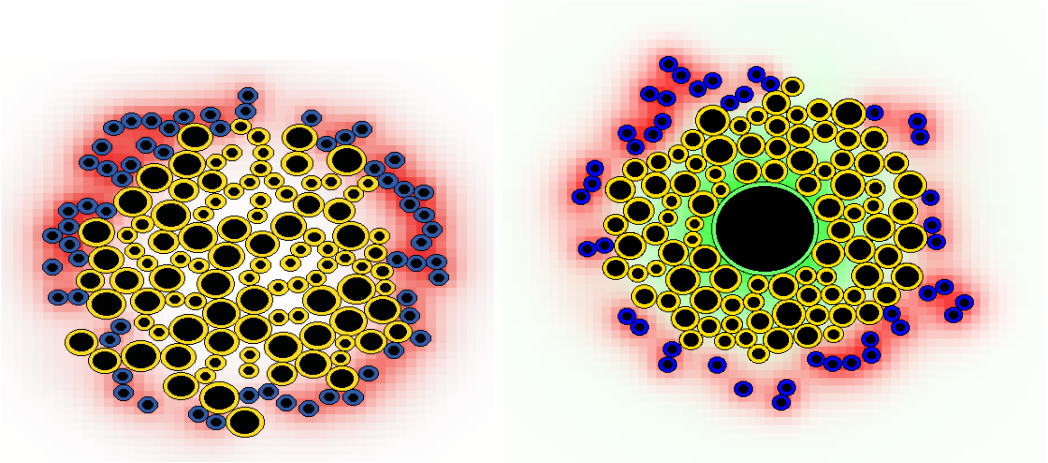

FIGURE 2.6 – **Modèle hybride de l'érythropoïèse**, d'après Fisher et al. [69]. A droite, un îlot érythroblastique "typique", constitué d'un macrophage central, sécrétant des facteurs de survie (en vert), entouré de progéniteurs (jaunes), et de cellules différenciées à sa périphérie (réticulocytes et érythrocytes, bleus). A gauche, un îlot érythroblastique sans macrophage. La concentration en Fas-Ligand est exprimée par le niveau de rouge.

survie d'une cellule, sa différenciation, sa division, et sa mort, dépendent de l'état de son réseau de régulation intra-cellulaire.

Nous nous sommes intéressés à une structure typique de la moelle osseuse : l'îlot érythroblastique. Il s'agit d'un amas de cellules, comprenant en son centre un macrophage entouré de progéniteurs érythrocytaires. Cette structure est à la base de la production des globules rouges. Les cellules les plus immatures sont situées à proximité du macrophage, et plus les cellules se différencient plus elles perdent en adhésion et s'éloignent du macrophage. Les érythrocytes sont donc situés à la périphérie de l'îlot. La Figure 2.6 présente cette structure simulée.

Nous avons mis en évidence deux rôles essentiels du macrophage au sein de l'îlot érythroblastique [69]. Tout d'abord, il assure la stabilisation de l'îlot. En l'absence de macrophage, soit la durée de vie de l'îlot est très courte, et il disparaît, soit il croît de façon non-contrôlée. Dans les deux cas, la structure est incapable de trouver un équilibre entre la prolifération (*via* l'auto-renouvellement) et la mort des progéniteurs érythrocytaires (Figure 2.7). Les rétro-contrôles *via* l'inhibition de l'apoptose et la stimulation de l'auto-renouvellement s'avèrent incapables de maintenir un îlot stable suffisamment longtemps. La régulation spatiale influence plus rapidement la structure de l'îlot que la régulation par les rétro-contrôles.

Ensuite, le macrophage permet à l'îlot de réguler de façon stricte ses capacités auto-

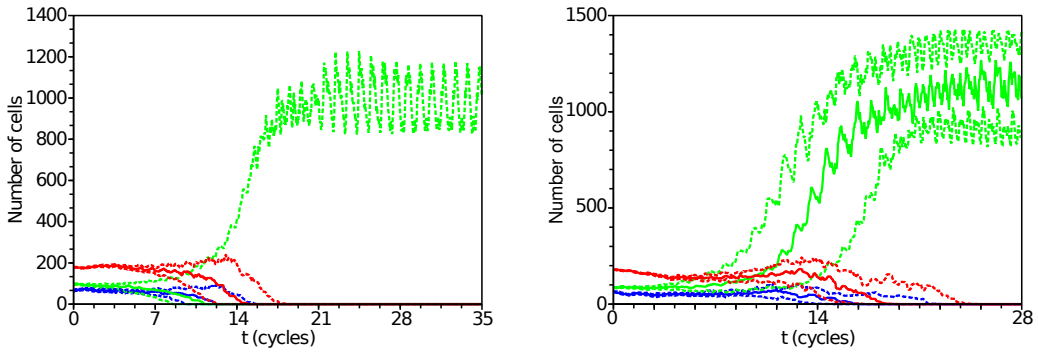


FIGURE 2.7 – **Destin d'un îlot érythroblastique en l'absence de macrophage.** Deux hypothèses concernant la division cellulaire sont considérées (scénario "out of equilibrium", à gauche, et "hysteresis cycle", à droite, cf. [69]). Le nombre de progéniteurs est représenté en vert, de réticulocytes en bleu, et de globules rouges circulant en rouges. Les médianes sont représentées par un trait plein, les quartiles par un trait pointillé. La saturation observée n'est due qu'à la limitation spatiale liée à la taille du domaine computationnel.

renouvelantes et de prolifération, lors d'une érythropoïèse normale. Bien que le rôle du macrophage ait été identifié lors d'une érythropoïèse de stress [111], il n'a pas encore été identifié pour une érythropoïèse normale. Or, durant la réponse à un stress, l'érythropoïèse est un processus intense durant lequel de très grandes quantités de cellules sont produites en un temps court. Le système doit donc pouvoir modifier fortement son fonctionnement habituel, en particulier le ratio entre le nombre de réticulocytes et le nombre de progéniteurs ne devrait pas être constant. Notre hypothèse est que le macrophage contrôle, à l'intérieur de l'îlot, l'explosivité de l'érythropoïèse, qui est nécessaire à la production de grandes quantités de cellules en peu de temps, et assure également sa stabilité. Notons que la stabilité ne s'obtient pas au détriment de la réactivité du système [67].

## 2.3 Autres applications

Pour conclure ce chapitre, je mentionnerai deux applications auxquelles j'ai consacré une partie de mon activité ces dernières années : la modélisation de l'apparition d'une leucémie myéloïde aiguë (Paragraphe 2.3.1) et la modélisation de la réponse immunitaire T CD8 (Paragraphe 2.3.2).

### 2.3.1 Leucémie myéloïde aiguë (LMA)

A travers deux articles en collaboration avec Mostafa Adimy et Abderrahim El Abddlaoui [7, 58], je me suis intéressé à un système d'équations différentielles non-linéaires à retard (issues d'équations aux dérivées partielles structurées en âge) décrivant la dynamique des cellules souches hématopoïétiques (cf 2.1) et l'apparition d'une leucémie myéloïde aiguë à travers le blocage de la différenciation cellulaire. Un troisième article [8] a été consacré aux propriétés mathématiques du système étudié, je n'en parlerai pas ici.

La leucémie myéloïde aiguë, ou LMA, est une forme de leucémie de la branche myéloïde très répandue (la fréquence augmente avec l'âge, environ 4 cas pour 100 000 personnes de plus de 60 ans annuellement, soit 1% des cancers en France [79]), caractérisée par un dysfonctionnement de la moelle osseuse : la différenciation des cellules hématopoïétiques est bloquée à un stade immature (progéniteur), les cellules ne meurent plus et prolifèrent fortement. Contrairement aux leucémies myéloïdes chroniques, les LMA sont rapidement mortelles sans traitement.

Le modèle que nous avons proposé est composé de $n$ équations non-linaires à retard, correspondant chacune à un niveau de maturité de plus en plus élevé des cellules hématopoïétiques. Les cellules les moins matures sont des cellules souches hématopoïétiques, les cellules les plus matures des cellules différenciées (globules blancs). Durant les premiers stades de différenciation les cellules conservent une capacité à s'auto-renouveler. Une représentation schématique du modèle est donnée par la Figure 2.8.

Chaque équation est du type

$$\begin{aligned}\frac{dx_i}{dt}(t) = &-(\delta_i + \beta_i(x_i(t))\, x_i(t) + 2(1-K_i)\int_0^{\tau_i} e^{-\gamma_i a} f_i(a)\beta_i(x_i(t-a))x_i(t-a)da \\ &+2K_{i-1}\int_0^{\tau_{i-1}} e^{-\gamma_{i-1}a} f_{i-1}(a)\beta_{i-1}(x_{i-1}(t-a))x_{i-1}(t-a)da,\end{aligned}$$

où $x_i(t)$ représente le nombre ou la densité de cellules au stade $i$ de différenciation, au temps $t$. Les caractéristiques de chaque stade de différenciation (durée de cycle $\tau_i$, probabilité de s'auto-renouveler $K_i$, taux de mort $\delta_i$ et $\gamma_i$, temps moyen de séjour dans la phase de repos $1/\beta_i$) dépendent du stade de différenciation.

Ce modèle a mis en évidence l'importance de la régulation des taux de différenciation à chaque niveau de maturité, et des durées de cycles cellulaires, de légères variations pouvant déstabiliser (ou au contraire stabiliser) la population totale, ou la population de cellules matures (qui est, d'un certain point de vue, la plus importante, puisque celle sur laquelle portent généralement les mesures cliniques).

Nous avons en particulier utilisé ce modèle pour illustrer l'effet d'un blocage de la différenciation : à un certain moment, dans le processus de maturation, les cellules

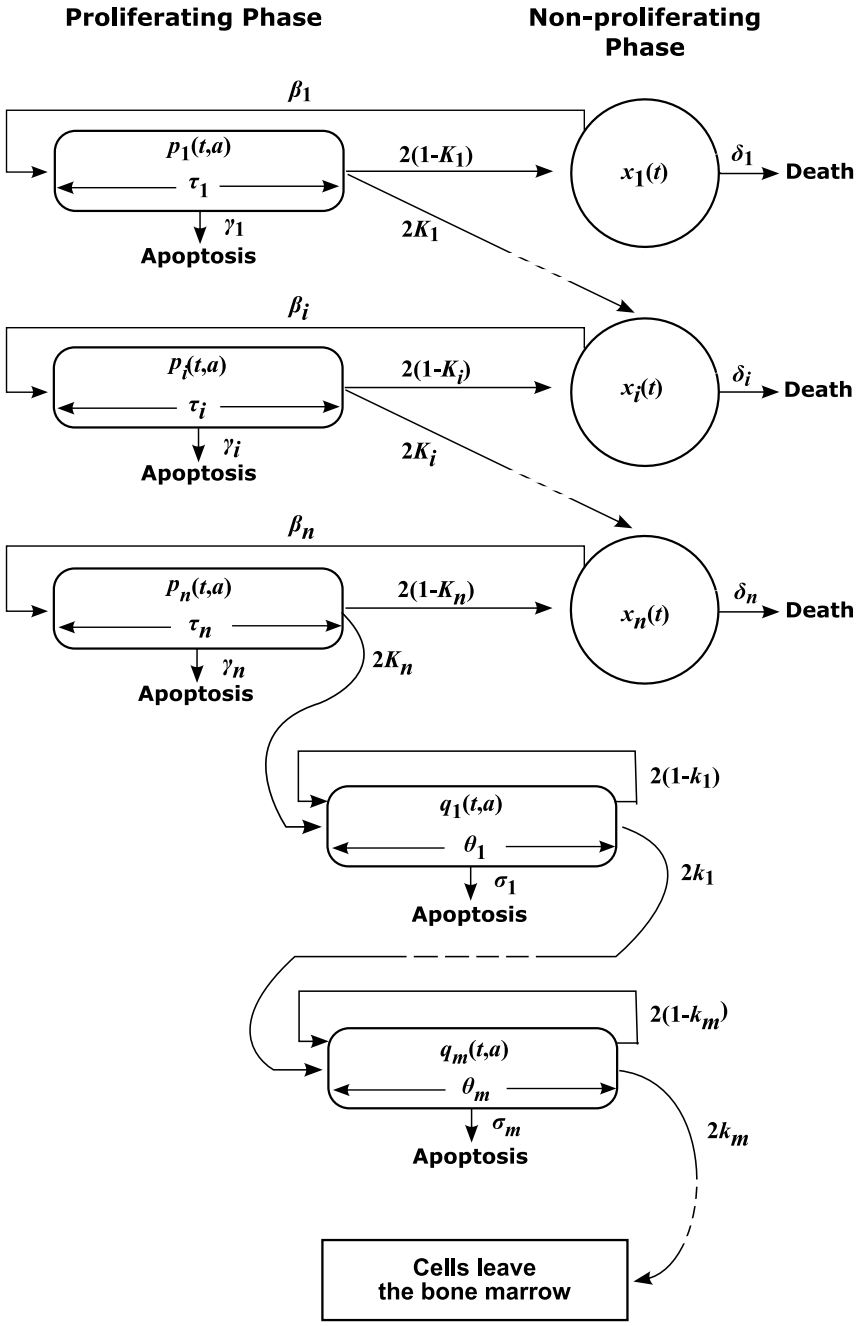


FIGURE 2.8 – **Modèle de différenciation cellulaire**, d'après [58]. Les cellules immatures prolifèrent en passant par une phase de repos (densités notées $x_i$) entre deux phases de prolifération (densités notées $p_i$) et possèdent une capacité d'auto-renouvellement, $1 - K_i$ dénotant la probabilité de s'auto-renouveler lors d'une division, $K_i$ la probabilité de se différencier. A partir d'un certain nombre de divisions (ici $n$) les cellules prolifèrent sans phase de repos (densités notées $q_i$) et chaque division correspond à de la différenciation.

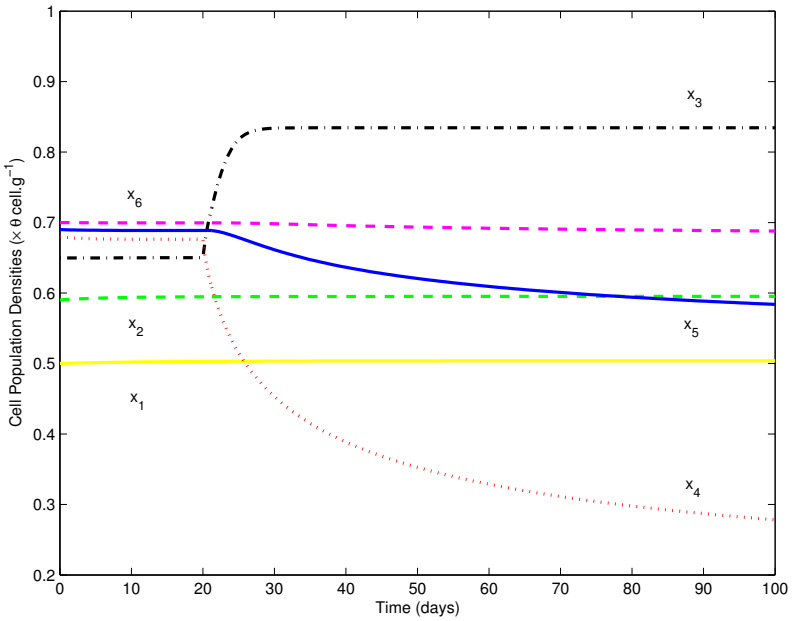


FIGURE 2.9 – **Blocage de la différenciation**, d'après [58]. A partir du vingtième jour, les cellules du stade 3 ($x_3(t)$) ne se différencient plus. Le nombre de cellules au stade 3 augmente, et dans le même temps le nombre de cellules dans les générations 4, 5, et 6 diminue, aboutissant à une population essentiellement composée de cellules immatures.

cessent de se différencier, il y a alors accumulation de cellules immatures. Il s'agit d'une des causes probables de l'apparition d'une LMA. Ce n'est cependant pas la seule cause : les cellules immatures ne meurent quasiment plus et s'auto-renouvellent énormément.

Notre étude a tout d'abord mis en évidence le fait qu'une perturbation des taux de différenciation usuels des différentes populations cellulaires (correspondant aux différents niveaux de maturité des cellules hématopoïétiques) modifie le nombre de cellules dans les générations proches mais ce phénomène est atténué dans la suite de la différenciation (on observe en fait des oscillations amorties du nombre de cellules dans chaque compartiment). Cependant, certaines perturbations peuvent conduire à un comportement oscillant du nombre de cellules dans chaque compartiment. Ces perturbations peuvent globalement être soutenues et aboutir à une situation où le nombre de cellules immatures devient plus important que le nombre de cellules matures lorsque la différenciation est définitivement bloquée pour une génération (taux de différenciation $K_i$ nul, cf. Figure 2.9). On obtient alors une situation correspondant à une LMA. L'hypothèse du blocage de la différenciation pour expliquer une LMA est ainsi soutenue par un modèle.

Notons toutefois que le nombre de cellules immatures est difficilement "très grand" si on n'empêche pas dans le même temps les cellules de mourir et si on ne leur permet

pas de proliférer anormalement. Ces travaux ont été utilisés par Clairambault [45, 46] et Özbay et al. [125] pour l'étude de la LMA, ainsi que par Precup et al. [103], Billy et Clairambault [37], Dupuy [65].

### 2.3.2 Réponse immunitaire

D'octobre 2009 à novembre 2012, j'ai co-encadré la thèse d'Emmanuelle Terry sur la modélisation de la réponse immunitaire T CD8. Cette thèse a permis de concrétiser des discussions débutées avec des collègues immunologistes lyonnais (l'équipe de Jacqueline Marvel) plus d'un an auparavant.

La réponse immunitaire consiste en un ensemble de processus mis en oeuvre par l'organisme pour lutter contre une infection, c'est-à-dire détecter, attaquer, et éliminer un pathogène. La réponse immunitaire acquise permet une réponse spécifique contre un pathogène donné. Nous nous sommes intéressés à la réponse immunitaire acquise cellulaire (et non humorale), c'est-à-dire consistant à déployer une réponse basée sur l'interaction entre cellules (une cellule en détruisant une autre), et en particulier la réponse impliquant les cellules T CD8. Il s'agit, par exemple, de la réponse mise en jeu contre le virus de la grippe.

L'organisme possède une réserve de cellules T-CD8, dites naïves, capables d'entrer en prolifération suite à la présentation d'un antigène (un marqueur du pathogène). Le nombre de cellules T CD8, suite à la présentation de l'antigène, augmente rapidement en raison d'une forte prolifération cellulaire. Lors de cette phase, dite d'expansion cellulaire, des cellules effectrices sont produites : ce sont des cellules cytotoxiques, capables d'aller détruire les cellules reconnues comme infectées. Les cellules effectrices sont ensuite presque toutes éliminées lors d'une phase dite de contraction cellulaire, durant laquelle elles meurent par apoptose. Des cellules mémoires sont produites au cours de cette réponse. Elles seront capables, lorsqu'on leur présentera de nouveau l'antigène du pathogène de répondre rapidement et efficacement.

Nous avons proposé un modèle de la cinétique des cellules T CD8 en réponse à un pathogène, décrivant l'activation des cellules naives, l'expansion cellulaire, la contraction, et la génération des cellules mémoires. Il s'agit d'un modèle composé de 3 équations différentielles ordinaires non-linéaires et d'une équation de transport non-linéaire structurée en âge, inspiré des travaux d'Antia et al. [21, 22]. Plusieurs modèles avaient auparavant été proposés pour décrire la cinétique d'une réponse T CD8, basés sur des équations différentielles ordinaires [60, 86, 108]. Ces modèles supposaient que la réponse était liée à la présence de pathogène (la réponse débute quand le pathogène est détecté, et s'arrête une fois que la charge virale est redevenue faible), alors que plusieurs travaux montrent que même une présentation brève de l'antigène induit une réponse complète [83, 116].

Le modèle d'Antia et al. [21, 22] considère une structuration en âge de la population de cellules effectrices : un âge limite correspond à la différenciation des cellules effectrices en cellules mémoires. Malgré la prise en compte de taux de prolifération et mort linéaires (en particulier, les cellules T ne sont pas supposées éliminer le pathogène), le schéma de différenciation utilisé dans ce modèle et la structuration en âge de la dynamique des cellules effectrices et mémoires nous ont paru pertinents, et nous avons construit notre modèle à partir de celui-ci, en incluant des processus non-linéaires [23, 85].

En notant $N(t)$ le nombre de cellules naïves au temps $t$, $M(t)$ le nombre de cellules mémoires, $e(t,\tau)$ le nombre de cellules effectrices d'âge $\tau$, et $P(t)$ la quantité de pathogène, le système s'écrit [120] :

$$\left\{\begin{array}{rcl} \dfrac{dN}{dt}(t) & = & H - \mu_N N(t) - \delta_{NE}(P(t))N(t), \\ \partial_t e(t,\tau) + \partial_\tau e(t,\tau) & = & [\rho_E(P(t)) - \mu_E(E(t)) - k(\tau)]e(t,\tau), \\ \dfrac{dP}{dt}(t) & = & I(t) - \mu_P(E(t))P(t), \\ \dfrac{dM}{dt}(t) & = & \displaystyle\int_0^{\bar\tau} k(\tau)e(t,\tau)\,d\tau - \mu_M M(t), \end{array}\right. \tag{2.7}$$

avec

$$e(t,0) = \delta_{NE}(P(t))N(t), \quad \text{et} \quad e(0,\tau) = e_0(\tau), \quad E(t) := \int_0^{+\infty} e(t,\tau)d\tau,$$

et

$$N(0) = N_0, \quad M(0) = M_0, \quad P(0) = P_0.$$

La quantité $E(t)$ représente le nombre total de cellules effectrices au temps $t$.

Les cellules naïves et mémoires sont supposées mourir avec des taux constants $\mu_N$ et $\mu_M$. Les cellules naïves se différencient en cellules effectrices en interagissant avec le pathogène (*via* les cellules présentatrices d'antigène) [23] et on note $\delta_{NE}$ ce taux d'interaction. Les cellules effectrices prolifèrent avec un taux $\rho_E$ dépendant de la quantité de pathogène [23, 85, 86], meurent par apoptose avec un taux $\mu_E$ dépendant du nombre de cellules effectrices (en particulier, cette dépendance décrit la compétition pour des ressources limitées et la mort fratricide [85, 117]), et se différencient en cellules mémoires avec un taux $k(\tau)$ dépendant de l'âge des cellules. L'élimination du pathogène est supposée dépendante du nombre de cellules effectrices [21], et on note $\mu_P$ le taux d'élimination du pathogène.

Ce système peut être étudié directement, ou bien réduit par intégration à un système à retard (cf. 1.1). Nous avons initialement établi l'existence et l'unicité des solutions, ainsi que leur caractère borné. Ensuite, nous avons montré que le système possédait un et un seul état d'équilibre, et nous avons établi sa stabilité locale. Nous nous sommes

ensuite intéressés à la stabilité globale du système, et nous avons montré que l'unique état d'équilibre, correspondant à l'élimination des différentes populations excepté la population de cellules naives (en raison du terme de production $H$), était globalement asymptotiquement stable. Ce résultat a été obtenu en déterminant une fonction qui n'est pas une fonction de Lyapunov, mais en est proche, et permet de conclure à la convergence de la solution de l'équation aux dérivées partielles vers zéro [120].

En collaboration avec l'équipe Inserm U851, dirigée par Jacqueline Marvel, nous avons ensuite réalisé une estimation des paramètres du modèle, en nous appuyant sur des données expérimentales décrivant des réponses au virus de la grippe, de la vaccine, et à la bactérie *Listeria monocytogenes*, chez des souris. Ce travail, basé sur une exploration systématique d'un espace de paramètres de grande dimension (9 paramètres), est actuellement soumis pour publication [57].

Le système (2.7) a été tout d'abord simplifié, en considérant uniquement la dynamique des populations totales (pas de structuration en âge), en négligeant la production de cellules naïves (pour être en accord avec le protocole expérimental), en précisant la dynamique du pathogène (dont la prolifération est supposée dépendante de la quantité de pathogène), et en régissant les interactions entre cellules par des lois d'action de masse. Le système étudié est donc

$$\left\{\begin{array}{rcll} \dfrac{d}{dt}N &=& -\mu_N N - \delta_{NE} PN, & N(0) = N_0, \\ \dfrac{d}{dt}E &=& \delta_{NE} PN + \rho_E PE - \mu_E E^2 - \delta_{EM} E, & E(0) = E_0, \\ \dfrac{d}{dt}M &=& -\mu_M M + \delta_{EM} E, & M(0) = M_0, \\ \dfrac{d}{dt}P &=& \rho_P P^2 - \mu_P EP - \mu_P^0 P, & P(0) = P_0. \end{array}\right.$$

Ce modèle possède 9 paramètres constants ($\mu_N$, $\delta_{NE}$, $\rho_E$, $\mu_E$, $\delta_{EM}$, $\mu_M$, $\rho_P$, $\mu_P$, $\mu_P^0$) et 4 conditions initiales, dont une (celle du pathogène) qui n'est pas fournie expérimentalement. En rescalant le système, on peut toutefois contourner cette difficulté et éviter d'avoir à estimer la valeur d'un dixième paramètre.

Le recherche de valeurs de paramètres réalisée a permis d'établir d'un côté que nos résultats étaient conformes à ceux établis dans des travaux précédents, et d'un autre côté que certains paramètres étaient caractéristiques de la réponse T CD8 alors que d'autres semblaient spécifiques du pathogène induisant la réponse. Ces résultats doivent toutefois être confrontés à de nouvelles données expérimentales permettant de discriminer les différents phénotypes (naïf, effecteur, mémoire), comme mentionné ci-dessous. Un résultat de cette optimisation paramétrique est présenté en Figure 2.10.

Ce travail de modélisation de la réponse immunitaire est actuellement poursuivi dans deux directions complémentaires. Tout d'abord, nous tentons d'estimer certains

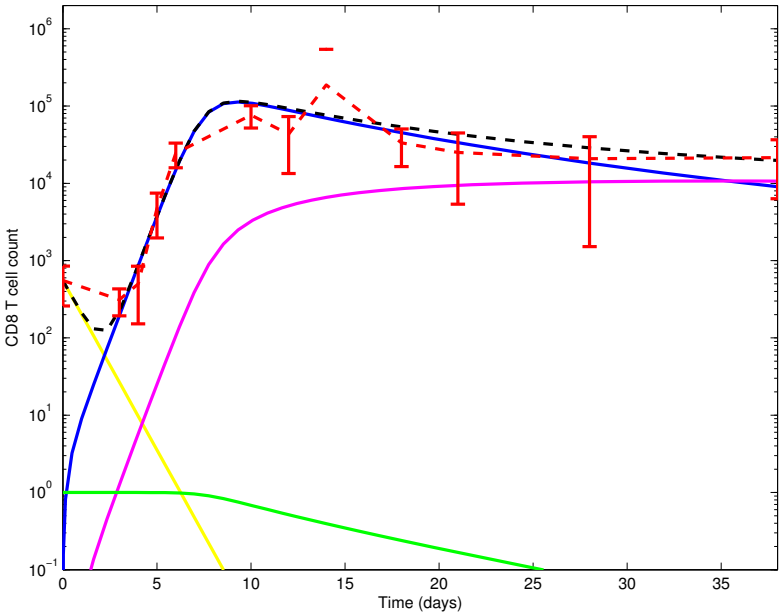


FIGURE 2.10 – **Cinétique des sous-populations de cellules T CD8 en réponse à une infection par le virus de la grippe.** Les données expérimentales sont représentées en rouge et pointillés, et le nombre total de cellules T CD8 en noir et pointillés. La population de cellules naïves est représentée en jaune, de cellules effectrices en bleu, de cellules mémoires en rose, et la quantité de pathogène en vert.

paramètres caractérisant les cellules T CD8 (durées des cycles cellulaires, taux de prolifération, taux de mort) à partir de données de fluorescence (type CFSE [93]) et en utilisant des modèles type Smith-Martin [61]. Les données expérimentales utilisées ont été générées *in vivo* et tous les modèles adaptés à de telles données ont été calibrés sur des données obtenues *in vitro*. Dans ce contexte, il est difficile d'obtenir des résultats pertinents sans modifier les modèles : l'évolution *in vivo* nécessite la description de phénomènes ou processus négligeables dans l'*in vitro*, comme par exemple la re-circulation des cellules dans l'organisme. Ensuite, des cinétiques correspondant aux différents phénotypes précédemment définis (naïves, effectrices, mémoires) ont pu être récemment mesurées. Il est donc pertinent de revenir sur notre estimation de valeurs de paramètres, afin d'essayer de caractériser les différents phénotypes. Ces travaux sont en cours.

Récemment, je me suis intéressé à la modélisation multi-échelle de la réponse immunitaire T CD8. De façon similaire à ce que j'ai réalisé pour l'érythropoïèse (cf. 2.2), je me suis intéressé, en collaboration avec Olivier Gandrillon et l'équipe de Jacqueline Marvel, à l'influence d'événements moléculaires sur le comportement d'une population de cellules. La réponse immunitaire étant un processus par nature multi-compartiment

(site d'infection, ganglions, rate, sang), nous avons décidé de nous concentrer sur l'activation des T CD8 naïves par les cellules présentatrices d'antigène dans un ganglion. Cet événement survient environ 72 heures post-infection et dure approximativement 60 heures. Il consiste en l'activation des cellules naïves, leur différenciation en cellules effectrices et la prolifération de ces dernières.

La première étape a consisté à déterminer les éléments clefs d'un réseau de régulation intra-cellulaire correspondant à une cellule T CD8. Une fois obtenu un réseau assez grand, nous avons réduit ce réseau à quelques éléments, en raisons de leur centralité dans le réseau mais également de la disponibilité des mesures expérimentales de leurs niveaux d'expressions. Ce réseau a ensuite été implémenté dans un modèle computationnel à base d'agents, pour former un modèle hybride discret/continu. Afin de décrire les premières heures de l'activation des cellules T CD8 dans un ganglion, nous avons choisi un modèle de Potts cellulaire, implémenté dans le logiciel CompuCell 3D [118]. Le modèle obtenu permet, après avoir réalisé une optimisation paramétrique, de reproduire qualitativement la dynamique observée chez une souris (cf. Figure 2.11).

L'objectif suivant est de coupler le modèle de régulation intra-cellulaire au modèle complet de réponse immunitaire T CD8 proposé dans Terry et al. [120], pour obtenir un modèle multi-échelles "complet" de la réponse immunitaire T CD8 chez la souris.

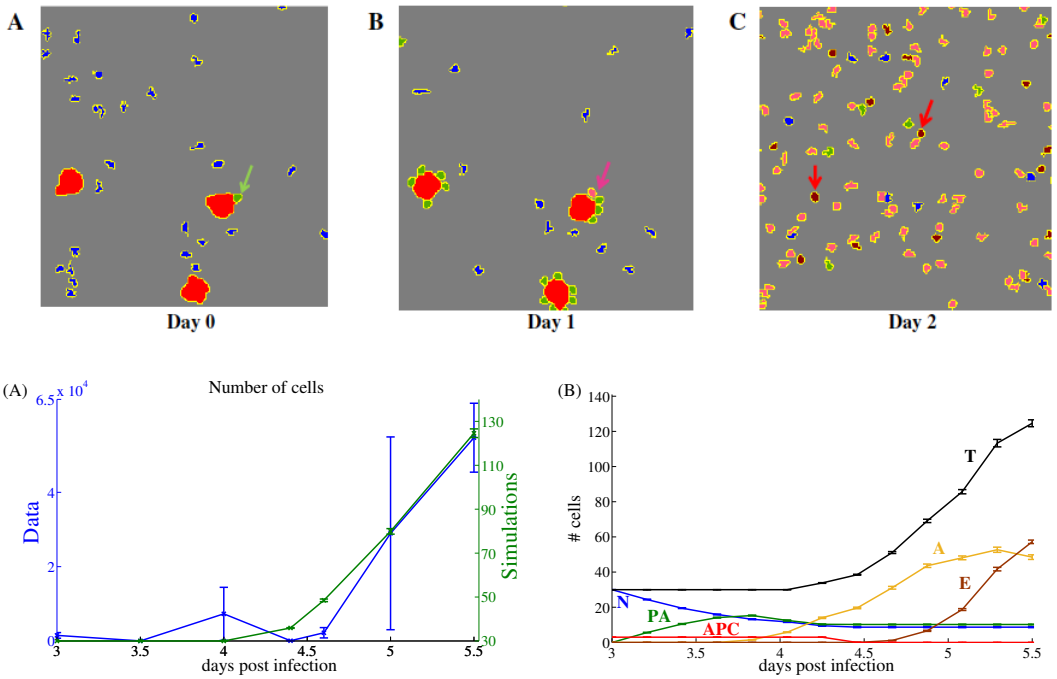


FIGURE 2.11 – **Modélisation multi-échelle de l'activation des cellules T CD8 dans un ganglion.** Haut : Captures d'écrans du logiciel CompuCell 3D. Les cellules rouges sont des cellules présentatrices d'antigènes, les cellules bleues des T CD8 naïves, les cellules vertes des T CD8 pré-activées, les cellules oranges des cellules activées, les cellules violettes des cellules effectrices. Bas : Résultats des simulations (en vert, (A)) et comparaison avec les données expérimentales (en bleu, (A)), et dynamique des différents phénotypes cellulaires (B).

# Chapitre 3

# Fin. . . et Suite

J'ai présenté, à travers les Chapitres 1 et 2, un aperçu partiel de mon activité de recherche lors des huit dernières années. J'ai choisi de présenter séparément les méthodes mathématiques et les applications en biologie, bien qu'en pratique cette séparation n'existe pas la plupart du temps. Il s'agit d'un choix délibéré, visant à présenter de façon claire les deux aspects, l'analyse mathématique d'un côté, la modélisation et l'interprétation des résultats en rapport avec la question biologique de l'autre. En pratique, ces deux aspects sont mêlés, et se complètent au fur et à mesure de l'avancée du travail de recherche.

Il s'agit d'un aspect essentiel des travaux que j'ai menés ces dernières années et que je poursuis actuellement. Il y a généralement, au départ, une question biologique qui motive le choix d'un formalisme mathématique, menant à une étude mathématique en parallèle d'une étude computationnelle (à base de simulations). Les résultats obtenus (ou non-obtenus) permettent un retour à la question initiale, et participent à la résolution de cycles menant *in fine* à proposer une ou plusieurs réponses à la question initiale. Cet aspect du travail que je réalise apparaît en filigrane dans les chapitres 1 et 2 : l'étude de la dynamique des cellules souches hématopoïétiques et de la leucémie myéloïde aiguë (Sections 2.1 et 2.3.1) a posé la question du choix des modèles (équations à retard discret, distribué, ou dépendant de l'état ?) et mené à l'étude de la stabilité d'équations à retard (Section 1.2), aboutissant à l'obtention de résultats mathématiques nouveaux tout en répondant à des questions biologiques (apparition d'oscillations) ; plus récemment, l'étude de l'érythropoïèse de stress (Section 2.2) a permis de proposer différents modèles, déterministe structuré en âge ou stochastiques continu ou hybride, pour répondre à la même question mais avec des points de vue différents (échelle de la population de cellules *vs* échelle intra-cellulaire).

Récemment, je me suis concentré sur la modélisation multi-échelles de processus biologiques, l'érythropoïèse (Section 2.2.2) et la réponse immunitaire T CD8 (Section

2.3.2). Ce type de modélisation pose beaucoup de questions : qu'est-ce-qu'un modèle multi-échelles tout d'abord ? Quel formalisme utiliser, et quels outils mathématiques possède-t-on pour étudier ces modèles ? Comment valider les modèles proposés ? Ce dernier aspect n'a pas été abordé dans ce manuscrit, il représente pourtant un des axes principaux de mes recherches actuelles : l'optimisation paramétrique est essentielle pour faire le lien entre un modèle et la question biologique à son origine. A chaque stade de l'étude, de nombreuses compétences sont nécessaires : en biologie, mais également en analyse non-linéaire, en probabilités, en calcul scientifique, en théorie du contrôle, en problèmes inverses, etc.

Les biomathématiques – ou *la* biomathématique ( ?), ou encore les maths-bio, ou la biologie mathématique, autant de noms que de langues et de communautés – sont synonymes d'interdisciplinarité. À partir du moment où l'on souhaite appliquer les mathématiques, il est nécessaire de se rapprocher de la source des questions, au moins pendant un certain temps, un temps de maturation, avant de poursuivre la quête de résultats théoriques indépendamment des applications. Dans son ouvrage de vulgarisation, *Les mathématiques du vivant* [115], Ian Stewart annonce une nouvelle révolution en biologie, la sixième après l'invention du microscope, de la classification de Linné, après la théorie de l'évolution, après la génétique et la découverte de la structure de l'ADN :

> "l'étude des processus biologiques à la lumière des mathématiques"

En d'autres termes, la biologie mathématique (Ian Stewart est mathématicien, il adopte pour le coup la position d'un biologiste). A quoi tient finalement cette sixième révolution de la biologie ? A la diversité des méthodes mathématiques utilisées et à l'importance croissante quelles prennent dans de nombreux domaines de la biologie actuelle. "Les frontières traditionnelles entre les disciplines explosent" énonce Ian Stewart en conclusion, et permettent d'obtenir des "résultats impossibles à atteindre" sans que des communautés spécialisées, autrefois étrangères l'une à l'autre, ne prennent conscience de leur complémentarité.

Cette révolution annoncée en biologie pourrait également être, pour les mathématiques, à défaut d'un changement, une nouvelle orientation. De nombreux problèmes biologiques ne trouvent actuellement pas de réponse dans l'accumulation de données et leur traitement statistique. Les mathématiques, déterministes ou probabilistes, permettent d'appréhender ces problèmes sous un angle différent, et les aller-retour entre biologie et mathématiques nourrissent à la fois la première et les secondes, en apportant des éclairages nouveaux et en impliquant le développement de nouveaux outils, de nouvelles méthodes, voire de nouvelles pensées.

# Chapitre 4

# Curriculum Vitæ

## 4.1 Informations générales

**Fabien Crauste**

Docteur en Mathématiques Appliquées
Chargé de Recherches Première Classe au CNRS (depuis le 1er octobre 2010)
34 ans, né le 17 janvier 1980 à St-Gaudens (31)
Nationalité : Français

### 4.1.1 Affiliation et coordonnées

1/ **CNRS UMR5208 Institut Camille Jordan**
Université Claude Bernard Lyon 1, Villeurbanne (http ://math.univ-lyon1.fr/)

2/ **Équipe-Projet Inria Dracula**
Centre Inria Grenoble Rhône Alpes
Antenne Lyon la Doua, Villeurbanne (http ://dracula.univ-lyon1.fr/)

**Numéro de téléphone :** +33 (0) 4 72 44 85 16 [UCBL] / +33 (0) 4 72 43 74 89 [Inria]
**Numéro de télécopie :** +33 (0) 4 72 43 16 87
**Adresses électroniques :** crauste@math.univ-lyon1.fr, fabien.crauste@inria.fr
**Page web :** http ://math.univ-lyon1.fr/∼crauste/

### 4.1.2 Activités professionnelles

| | |
|---|---|
| 1/10/2006 | **Chargé de Recherches Deuxième Classe au CNRS** |
| au 1/10/2010 | CNRS UMR5208 Institut Camille Jordan, UCBL, Villeurbanne |
| 09/2005 - 09/2006 | **ATER**, à l'université de Pau et des Pays de l'Adour (UPPA) |

### 4.1.3 Formation

2005 **Doctorat en Mathématiques Appliquées.**

Thése de doctorat de l'UPPA, soutenue le 21 juin 2005, mention : Trés Honorable.
Directeur de thèse : Mostafa Adimy (Maître de Conférences HDR).
Titre de la thèse : **Etude mathématique d'équations aux dérivées partielles hyperboliques modélisant les processus de régulation des cellules sanguines - Applications aux maladies hématologiques cycliques**.

Rapporteurs de la thèse :

M. B. Perthame – Prof. à l'École Normale Supérieure de Paris
M. V. Volpert – DR CNRS à l'Université Lyon 1
M. G. F. Webb – Prof. à l'Université Vanderbilt (Nashville, USA)

Allocataire du Ministère de la Recherche et des Nouvelles Technologies et moniteur de l'enseignement supérieur, attaché au CIES d'Aquitaine et d'Outre-Mer.

2002 **Diplôme d'Études Approfondies** de Mathématiques Appliquées à la Résolution de Problèmes de la Physique et de la Mécanique à l'UPPA.
Mention : Très Bien, avec les félicitations du jury.

### 4.1.4 Principaux thèmes de recherche

- Modélisation mathématique du vivant / Biomathématiques
- Modélisation multi-échelles
- Dynamique des populations
- Modèles structurés en âge et/ou maturité
- Équations aux dérivées partielles de transport
- Équations différentielles à retard
- Modéles à base d'agents
- Stabilité asymptotique et bifurcation de Hopf
- Modèles de production du sang (hématopoïèse, érythropoïèse, leucopoïèse)
- Modèles de réponse immunitaire (infection grippale, vaccination)

### 4.1.5 Responsabilités administratives et collectives

**En cours**

- Membre élu du **conseil de laboratoire** de l'Institut Camille Jordan UMR 5208 (depuis 2010)
- Membre élu du **comité de pilotage de l'Institut des Systèmes Complexes (IXXI)** en Rhône Alpes (http ://www.ixxi.fr) (depuis 2010)

**Précédemment**

- Organisateur du **séminaire de biomathématiques** de l'Institut Camille Jordan UMR 5208 (2009 - 2012)
- Co-organisateur du **séminaire INRIabcd**, séminaire commun aux équipes Inria "Dracula" et "Beagle" de l'Antenne de la Doua du Centre Inria Grenoble Rhône Alpes (2011 - 2012).
- Membre nommé du **conseil de laboratoire** de l'Institut Camille Jordan UMR 5208 (2007 - 2010)
- Membre élu du **comité consultatif 25/26** de l'UCB Lyon 1 (2007 - 2011)
- Responsable du **Groupe de Travail Biomathématiques** du Laboratoire de Mathématiques Appliquées de Pau UMR 5142 (2005 - 2006)
- Membre du **Conseil de Laboratoire** de l'unité CNRS UMR 5142, Laboratoire de Mathématiques Appliquées de Pau (2005 - 2006)
- Membre du **Conseil Scientifique** de l'Université de Pau et des Pays de l'Adour (2005 - 2006)

## 4.2 Implication dans des contrats de recherche

**ANR RPIB "PrediVac"** (jan 2013 - dec 2015). Budget : 990 540 €

- ▷ Titre : *Outils de modélisation innovants pour la prédiction de l'efficacité de vaccins basés sur les lymphocytes T CD8.*
- ▷ Responsable du projet : Jacqueline Marvel (U1111 Inserm).
- ▷ Responsable du partenaire Inria : Fabien Crauste.

**ANR JCJC "ProCell"** (sep 2009 - fev 2014). Budget : 90 000 €

- ▷ Titre : *Mathematical Methods for Erythropoiesis Modelling : from Proteins to Cell Populations.*
- ▷ Responsable du projet : Fabien Crauste.

**ANR JCJC "Madcow"** (2008 - 2013).

- ▷ Titre : *Modelling amyloid dynamics and computation output work : applications to prion and Alzheimer's disease.*
- ▷ Responsable du projet : Laurent Pujo-Menjouet (ICJ UMR 5208, Lyon).

**ANR Blanc "Anatools"** (2007 - 2010).

- ▷ Titre : *Analytical Tools for Cancer Chemotherapy Improvement.*
- ▷ Responsable du projet : Ch. Perigaud (LCOBS, Montpellier).
- ▷ Responsable du partenaire math : V. Volpert (ICJ UMR 5208, Lyon).

**Projet ANUBIS, INRIA Futurs** (de 2004 à 2006).

- ▷ Titre : *Outils de l'automatique pour le Calcul Scientifique, Modèles et Méthodes en Bio-Mathématique.*
- ▷ Responsable du projet : Jacques Henry (Directeur de Recherche, INRIA).

**Action Intégrée Brâncusi** n° 08810RJ (2005 et 2006).
Partenaires : LMA de l'université de Pau / Département de Mathématiques, université Polytechnique de Bucarest (Roumanie)

- ▷ Titre : *Stabilité, bifurcation et contrôle pour des équations différentielles à retard issues de modèles biologiques.*
- ▷ Responsable du projet : Mostafa Adimy (Maître de Conférences HDR, Pau).

## 4.3 Encadrements de post-Docs, thèses et stages

### 4.3.1 Encadrements de post-docs

**Xuefeng Gao**

PhD de University College Cork (supervisors : Sabin Tabirca and Mark Tangney)
Post-Doc sur contrat ANR PrediVac, d'avril 2014 à mars 2015.

**Sotiris Prokopiou**

PhD de Nottingham University (supervisors : Helen Byrne and Markus Owen)
Post-Doc sur contrat ANR PrediVac, d'avril 2013 à février 2014.

**Floriane Lignet**

PhD de l'ENS de Lyon (supervisors : Emmanuel Grenier et Benjamin Ribba)
Post-Doc sur contrat ANR PrediVac, de février 2013 à janvier 2014.

### 4.3.2 Encadrements de thèses

**Marine Jacquier**

Thése débutée en octobre 2012, sur le théme : *"Contribution à l'étude de modéles à retards modélisant l'impact physiologique du comportement de prise alimentaire"*
Direction : Mostafa Adimy (DR Inria) et Fabien Crauste.

**Emmanuelle Terry**

Thése soutenue le 12 novembre 2012, sur le théme *"Modélisation mathématique des dynamiques de la réponse immunitaire T CD8, aux échelles moléculaire et cellulaire"*
Direction : Olivier Gandrillon (DR CNRS) et Fabien Crauste.

### 4.3.3 Encadrements de stages

**Antoine Burg**

Éléve à l'École Centrale de Lyon
Stage de recherche (année de césure) en 2014
Sujet : "Contribution à l'étude d'un modèle de la réponse immunitaire T CD8"

**Merlin Legrain**

Éléve à l'INSA de Lyon
Stage de recherche M2 au printemps 2014
Sujet : "Modélisation multi-échelle et multi-agents de l'érythropoïèse"

**Cigdem Ak**

Éléve à l'École Normale Supérieure de Lyon

Stage de recherche M2 au printemps 2013

Sujet : "Stabilité d'un Systéme Linéaire Structuré en Age Décrivant la Production des Globules Rouges"

**Camille Pommier**

Élève en dernière année à l'Ecole Centrale de Lyon

Stage de recherche au printemps 2012

Sujet : "Modélisation du processus de production des globules rouges : analyse et simulation d'un modèle multi-échelles"

**Loic Barbarroux**

Élève en dernière année à l'Ecole Centrale de Lyon

Stage de recherche au printemps 2012

Sujet : "Modélisation multi-échelle de la réponse immunitaire T-CD8"

**Adour Mikirditsian**

Étudiant à l'Université Paris 6

Stage de recherche M2 au printemps 2011

Sujet "Modélisation mathématique de la réponse immunitaire CD4"

**Rana Abu Eisheh**

Étudiante en master 2 à l'Université de Hebron, en Palestine

Stage de recherche M2 au printemps 2010

Sujet : "Contribution to the study of a model of erythropoiesis".

**Emmanuelle Terry**

Étudiante en master systèmes complexes à l'École Normale Supérieure de Lyon

Stage de recherche M2 au printemps 2009

Sujet : "Etude mathématique d'équations différentielles ordinaires et d'équations aux dérivées partielles à retard modélisant la réponse immunitaire des lymphocytes T CD8".

**Xavier Pellegrin**

Éléve à l'École Normale Supérieure de Lyon

Stage de recherche M2 au printemps 2007

Sujet : "Une équation intégro-différentielle en dynamique des populations"

## 4.4 Publications

### 4.4.1 Publications dans des revues avec comités de lectures (au 1 juillet 2014)

Les publications marquées par une astérisque * sont celles sur lesquelles s'appuie la discussion des premiers chapitres (cf. Chapitre 5).


38. S. Bernard, F. Crauste. *Optimal linear stability condition for scalar differential equations with distributed delay.* Discrete and Continuous Dynamical Systems Series B (submitted).
37. F. Crauste, E. Terry, I. Le Mercier, J. Mafille, S. Djebali, T. Andrieu, B. Mercier, G. Kaneko, C. Arpin, J. Marvel, O. Gandrillon, *Predicting Pathogen-Specific CD8 T Cell Immune Response from a Modelin Approach*, Journal of Theoretical Biology (submitted).
36. S.A. Prokopiou, L. Barbarroux, S. Bernard, J. Mafille, Y. Leverrier, C. Arpin, J. Marvel, O. Gandrillon, F. Crauste, *Multiscale Modeling of the Early CD8 T Cell Immune Response in Lymph Nodes : An Integrative Study*, Computation (in revision).
35. O. Angulo, F. Crauste, JC Lopez-Marcos, *A Model of Phenylhydrazine-Induced Anemia in Mice : Investigating the Roles of the Experimental Protocol and of Age-Dependent Feedback Controls*, Journal of Theoretical Biology (in revision).
34. M. Jacquier, F. Crauste, Ch. Soulage, H. Soula, *A predictive model of the dynamics of body weight and food intake in rats submitted to caloric restrictions.* PLoS ONE, 9(6) : e100073.
33. M. Adimy, F. Crauste, *Delay Differential Equations and Autonomous Oscillations in Hematopoietic Stem Cell Dynamics Modeling*, Math. Model. Nat. Phenom., 7 (6), 1–22 (2012)
32. E. Terry, J. Marvel, C. Arpin, O. Gandrillon, F. Crauste, *Mathematical Model of the primary CD8 T Cell Immune Response : Stability Analysis of a Nonlinear Age-Structured System*, J. Math. Biol., 65, 263–291 (2012)
31. * S. Fischer, P. Kurbatova, N. Bessonov, O. Gandrillon, V. Volpert, F. Crauste, *Modelling erythroblastic islands : using a hybrid model to assess the function of central macrophage*, Journal of Theoretical Biology, 298, 92–106 (2012).
30. N. Bessonov, F. Crauste, S. Fischer, P. Kurbatova, V. Volpert, *Application of Hybrid Models to Blood Cell Production in the Bone Marrow*, Math. Model. Nat. Phenom., 6 (7), 2–12 (2011).

29. N. Bessonov, F. Crauste, V. Volpert, *Modelling of Plant Growth with Apical or Basal Meristem*, Math. Model. Nat. Phenom., 6 (2), 107–132 (2011).

28. P. Kurbatova, S. Bernard, N. Bessonov, F. Crauste, I. Demin, C. Dumontet, S. Fischer, V. Volpert, *Hybrid model of erythropoiesis and leukemia treatment with cytosine arabinoside*, SIAM J. App. Math., 71 (6), 2246–2268 (2011).

27. * F. Crauste, *A review on local asymptotic stability analysis for mathematical models of hematopoiesis with delay and delay-dependent coefficients*, Annals of the Tiberiu Popoviciu Seminar of functionnal equations, approximation and convexity, vol 9, 121–143 (2011).

26. M. Adimy, F. Crauste, A. El Abdllaoui, *Boundedness and Lyapunov Function for a Nonlinear System of Hematopoietic Stem Cell Dynamics*, Comptes Rendus Mathematique, 348 (7-8), 373–377 (2010).

25. M. Adimy, F. Crauste, C. Marquet, *Asymptotic behavior and stability switch for a mature-immature model of cell differentiation*, Nonlinear Analysis : Real World Applications, 11 (4), 2913–2929 (2010).

24. * F. Crauste, *Stability and Hopf bifurcation for a first-order linear delay differential equation with distributed delay*, in Complex Time Delay Systems (Ed. F. Atay), Springer, 1st edition, 320 p., ISBN : 978-3-642-02328-6 (2010).

23. * F. Crauste, I. Demin, O. Gandrillon, V. Volpert, *Mathematical study of feedback control roles and relevance in stress erythropoiesis*, Journal of Theoretical Biology, 263 (3), 303–316 (2010).

22. * M. Adimy, F. Crauste, My L. Hbid, R. Qesmi, *Stability and Hopf bifurcation for a cell population model with state-dependent delay*, SIAM J. Appl. Math, 70 (5), 1611–1633 (2010).

21. I. Demin, F. Crauste, O. Gandrillon, V. Volpert, *A multi-scale model of erythropoiesis*, Journal of Biological Dynamics, 4 (1), 59–70 (2010).

20. N. Bessonov, F. Crauste, I. Demin, V. Volpert, *Dynamics of erythroid progenitors and erythroleukemia*, Mathematical Modeling of Natural Phenomena, 4 (3), 210–232 (2009).

19. F. Crauste, *Delay Model of Hematopoietic Stem Cell Dynamics : Asymptotic Stability and Stability Switch*, Mathematical Modeling of Natural Phenomena, 4 (2), 28–47 (2009).

18. M. Adimy, F. Crauste, *Mathematical Model of Hematopoiesis Dynamics with Growth Factor-Dependent Apoptosis and Proliferation Regulations*, Mathematical and Computer Modelling, 49, 2128–2137 (2009).

17. M. Adimy, S. Bernard, J. Clairambault, F. Crauste, S. Génieys, L. Pujo-Menjouet, *Modélisation de la dynamique de l'hématopoïèse normale et pathologique*, Hématologie, 14(5), 339–350 (2008).

16. M. Adimy, F. Crauste, A. El Abddlaoui, *Discrete Maturity-Structured Model of Cell Differentiation with Applications to Acute Myelogenous Leukemia*, Journal of Biological Systems, 16 (3), 395–424 (2008).

15. F. Crauste, M.L. Hbid, A. Kacha, *A Delay Reaction-Diffusion Model of the Dynamics of Botulinum in Fish*, Mathematical Biosciences, 216, 17–29 (2008).

14. M. Adimy, O. Angulo, F. Crauste, J.C. Lopez-Marcos, *Numerical integration of a mathematical model of hematopoietic stem cell dynamics*, Computer and Mathematics with Applications, 56, 594–606 (2008).

13. * F. Crauste, L. Pujo-Menjouet, S. Génieys, C. Molina, O. Gandrillon, *Adding Self-Renewal in Committed Erythroid Progenitors Improves the Biological Importance of a Mathematical Model of Erythropoiesis*, Journal of Theoretical Biology, 250, 322–338 (2008).

12. M. Adimy, F. Crauste, *Modelling and asymptotic stability of a growth factor-dependent stem cells dynamics model with distributed delay*, Discrete and Continuous Dynamical Systems Series B, 8 (1), 19–38 (2007).

11. M. Adimy, F. Crauste, A. El Abddlaoui, *Asymptotic Behavior of a Discrete Maturity Structured System of Hematopoietic Stem Cells Dynamics with Several Delays*, Mathematical Modelling of Natural Phenomena, 1 (2), 1–22 (2006).

10. M. Adimy, F. Crauste, S. Ruan, *Modelling hematopoiesis mediated by growth factors with applications to periodic hematological diseases*, Bulletin of Mathematical Biology, 68 (8), 2321–2351 (2006).

9. M. Adimy, F. Crauste, S. Ruan, *Periodic Oscillations in Leukopoiesis Models with Two Delays*, Journal of Theoretical Biology, 242, 288–299 (2006).

8. * F. Crauste, *Global Asymptotic Stability and Hopf Bifurcation for a Blood Cell Production Model*, Mathematical Biosciences and Engineering, 3 (2), 325–346 (2006).

7. M. Adimy, F. Crauste, A. Halanay, M. Neamţu, D. Opriş, *Stability of Limit Cycles in a Pluripotent Stem Cell Dynamics Model*, Chaos, Solitons and Fractals, 27 (4), 1091–1107 (2006).

6. M. Adimy, F. Crauste, S. Ruan, *A mathematical study of the hematopoiesis process with applications to chronic myelogenous leukemia*, SIAM Journal of Applied Mathematics, 65 (4), 1328–1352 (2005).

5. M. Adimy, F. Crauste, S. Ruan, *Stability and Hopf bifurcation in a mathematical model of pluripotent stem cell dynamics*, Nonlinear Analysis : Real World Applications, 6 (4), 651–670 (2005).
4. M. Adimy, F. Crauste, L. Pujo-Menjouet, *On the stability of a nonlinear maturity structured model of cellular proliferation*, Discrete and Continuous Dynamical Systems Series A, 12 (3), 501–522 (2005).
3. M. Adimy, F. Crauste, *Existence, positivity and stability for a nonlinear model of cellular proliferation*, Nonlinear Analysis : Real World Applications, 6 (2), 337–366 (2005).
2. M. Adimy, F. Crauste, *Global stability of a partial differential equation with distributed delay due to cellular replication*, Nonlinear Analysis, 54, 1469–1491 (2003).
1. M. Adimy, F. Crauste, *Un modèle non-linéaire de prolifération cellulaire : extinction des cellules et invariance*, Comptes Rendus Mathématiques, 336, 559–564 (2003).

### 4.4.2 Publications dans des actes de colloques

▷ M. Adimy et F. Crauste, *Stability and instability induced by time delay in an erythropoiesis model*, Monografias del Seminario Matematico Garcia de Galdeano, 31, 3–12 (2004).

### 4.4.3 Autres publications

▷ F. Crauste, *Equations aux dérivées partielles structurées en âge et équations à retard : Deux exemples d'applications en biologie*, MATAPLI, volume 97 (2012).

▷ F. Crauste et M. Adimy, *Bifurcation dans un modèle non-linéaire de production du sang*, Comptes-rendus de la 7ième Rencontre du Non-Linéaire, Non-Linéaire Publications, Paris, 73–78 (2004).

## 4.5 Conférences, workshops, écoles d'été, et séminaires

Les ** indiquent des participations sans présentation (ni orale, ni poster).

| | |
|---|---|
| 19-21/11/2014 | Conference "LyonSysBio" (Lyon Systems Biology), à Lyon (France)<br>Organisateur. |
| 25-30/08/2014 | 12e Colloque Franco-Roumain de Mathématiques Appliquées, à Lyon (France)<br>Organisateur. |
| 7-11/07/2014 | 10th AIMS Conference on Dynamical Systems, Differential Equations and Applications, à Madrid (Espagne)<br>Invité et Organisateur d'une session. |
| 27-28/01/2014 | Workshop et réunion du consortium 3+3 EuroMed (Inria), à Marrakech (Maroc) |
| 10/01/2014 | Journée sur la Biologie intégrative de l'UMR Pegase, à l'INRA de Rennes (France)<br>Invité. |
| 11-13/12/2013 | Conférence Mathematical Modeling of Complex Systems, à l'Ecole Centrale de Paris (France)** |
| 25-29/11/2013 | French Mexican Meeting on Industrial and Applied Mathematics, à Villahermosa (Mexique)<br>Invité. |
| 11-12/06/2013 | Colloque MB2 : journées de Modélisation BioMathémathique de Besançon, à Besançon (France)<br>Invité. |
| 3-6/06/2013 | Conference "In honour of Michael Mackey's 70th birthday", à Lyon (France)<br>Organisateur. |
| 13-15/05/2013 | SBIP'13 "Systems Biology Approach to Infectious Processes", à Lyon (France)<br>Organisateur. |
| 8-9/04/2013 | ImmunocomplexiT, à Paris (France)<br>Invité. |

| | |
|---|---|
| 02-06/2013 | Trimestre thématique biomathématiques "Mathematical Biology", incluant<br>▶ Invitations de chercheurs (étrangers et nationaux)<br>▶ Organisation de 4 conférences et 1 école d'été :<br>- Biological invasions and evolutionary biology, stochastic and deterministic models, 11-15 Mars<br>- Mathematical Modeling in Cell Biology, 25-29 Mars<br>- Systems Biology Approach to Infectious Processes, 13-15 Mai<br>- Ecole d'été "Multiscale modeling in the life sciences", 27-31 Mai<br>- Conference in honour of Michael Mackey's 70th birthday<br>Co-organisateur. |
| 7/01/2013 | Séminaire de l'équipe COMMANDS à L'École Polytechnique, Palaiseau (France)<br>Invité. |
| 2-7/07/2012 | European Congress of Mathematics, à Cracovie (Pologne).<br>Invité. |
| 26/06/2012 | Journée Scientifique de la Faculté des Sciences et Techniques de l'UCB Lyon 1, à Lyon (France). |
| 10-13/06/2012 | Conférence de la Société Francophone de Biologie Théorique, à St Flour (France). |
| 19-23/03/2012 | Workshop "present challenges of mathematics in oncology and biology of cancer : modelling and mathematical analysis", au CIRM à Luminy (France).** |
| 4-9/07/2011 | ICNODEA 11, International conference on nonlinear operators and differential equations and applications, à Cluj (Roumanie).<br>Invité. |
| 28/06/2011 au 2/07/2011 | ECMTB 2011, 8th European Conference on Mathematical and Theoretical Biology and Annual Meeting of The Society for Mathematical Biology, à Cracovie (Pologne). |
| 25-26/11/2010 | Integrative Post Genomics IPG'10, à Lyon (France).<br>Organisateur. |
| 26-31/08/2010 | 10ème Colloque Franco-Roumain de Mathématiques Appliquées, à Poitiers (France).<br>Organisateur d'une session. |

| | |
|---|---|
| 28-30/06/2010 | Second Congrès de la Société Marocaine de Mathématiques Appliquées ($SM^2A$), à Rabat (Maroc).<br>Organisateur d'une session. |
| 10-11/06/2010 | RIMM-2010, Premier Atelier International sur Le Rôle et l'Impact des Mathématiques en Médecine, à Paris (France).** |
| 31/05/2010 au 4/06/2010 | Computational and Mathematical Population Dynamics CMPD 3, à Bordeaux (France).<br>Invité. |
| 30/11/2009 et 1/12/2009 | "Vingt-Deuxièmes Entretiens" du Centre Jacques Cartier Rhône-Alpes, à Lyon (France).<br>Invité. |
| 18-20/11/2009 | Integrative Post Genomics IPG'09, à Lyon (France).<br>Organisateur. |
| 17/06/2009 | Semovi – Séminaire de Modélisation du Vivant de la région Rhône-Alpes, à Lyon (France).<br>Invité. |
| 15-17/06/2009 | Conférence de la Société Francophone de Biologie Théorique, à St Flour (France).** |
| 27/04/2009 au 2/05/2009 | Workshop Mathematical Modelling in Biology and Medicine, à Dubrovnik (Croatie).<br>Organisateur. |
| 19-21/11/2008 | Integrative Post Genomics IPG'08, à Lyon (France).** |
| 16-20/06/2008 | Workshop on Population Dynamics and Mathematical Biology, au CIRM, à Luminy (France).<br>Invité. |
| 10/04/2008 | Journées "Modélisation de la Croissance des Plantes", à Lyon (France).<br>Organisateur. |
| 20-21/03/2008 | Workshop "Haematopoiesis ant Its Disorders. Modelling, Experimental and Clinical Approaches", à Paris (France).<br>Organisateur. |
| 6-8/02/2008 | Premier Congrès de la Société Marocaine de Mathématiques Appliquées ($SM^2A$), à Rabat (Maroc).<br>Invité. |

| | |
|---|---|
| 3-8/01/2008 | Marrakesh International Conference and Workshop on Mathematical Biology, à Marrakesh (Maroc). |
| 28-30/11/2007 | Integrative Post Genomics IPG'07, à Lyon (France).** |
| 5-8/11/2007 | Workshop "Modelling Blood Diseases", à Lyon (France).<br>Organisateur. |
| 18-22/06/2007 | "Mathematical Models in Medicine and Biology", Premier colloque IXXI, à Lyon (France). |
| 11-12/12/2006 | Journées de Gerland "Systèmes complexes et biologie", à Lyon (France).** |
| 29/11/2006 au 1/12/2006 | Integrative Post Genomics IPG'06, à Lyon (France).** |
| 12-14/07/2006 | Conférence Francophone sur la Modélisation Mathématique en Biologie et en Médecine, à Craiova (Roumanie).<br>Organisateur. |
| 25-28/06/2006 | AIMS' 6th International Conference on Dynamical Systems, Differential Equations and Applications, à Poitiers (France). |
| 15-20/06/2006 | Marrakesh World Conference on Differential Equations and Applications, à Marrakesh (Maroc).<br>Invité. |
| 1-2/12/2005 | Integrative Post-Genomics IPG'05, à Lyon (France). |
| 14-18/11/2005 | European Conference on Complex Systems, à Paris (France). |
| 19-21/09/2005 | IXèmes Journées de Mathématiques Appliquées Pau-Saragosse, à Jaca (Espagne). |
| 11-13/07/2005 | International Workshop on Differential Equations in Mathematical Biology, au Havre (France).<br>Invité. |
| 13/04/2005 | Demi-journée scientifique ISPED/MAB/ANUBIS (Groupe de Travail du projet INRIA ANUBIS), à Bordeaux. |
| 1-2/10/2004 | Journées Bordeaux-Pau-Toulouse, à Anglet (France).** |
| 14-20/09/2004 | XXXIIIième Conférence Nationale de Pologne sur les Applications des Mathématiques (Ogòlnoposka Konferencja Zastosowan Matematyki), à Zakopane (Pologne).<br>Invité. |

| | |
|---|---|
| 26/07/2004 au 3/09/2004 | CEMRACS 2004 "Mathematics and Applications in Biology and Medicine", au CIRM, à Luminy (France).<br>Participation au projet ONCO (coordinateurs : B. Perthame et F. Filbet). |
| 12-15/07/2004 | Premier congrès Canada-France des sciences mathématiques, à Toulouse (France). |
| 2/07/2004 | Journée Bio-Mathématiques à la mémoire du Professeur Ovide Arino, à Pau (France).<br>Organisateur. |
| 21-25/06/2004 | Computational and Mathematical Population Dynamics (CMPD), à Trento (Italie). |
| 7-18/06/2004 | ESMTB Summer school Cell Biology and Mathematical Modelling, à Hvar (Croatie). |
| 10/03/2004 | Colloque "Le non linéaire en médecine et en biologie", lors de la 7ième Rencontre du Non Linéaire, à l'Institut Henri Poincaré, à Paris (France). |
| 14-16/09/2003 | VIIIièmes Journées de Mathématiques Appliquées Pau-Saragosse, à Jaca (Espagne). |
| 5-9/09/2003 | Second International Conference on Mathematical Ecology (AICME), à Alcala de Henares (Espagne). |
| 16-21/06/2003 | Workshop Internet Seminar, à Blaubeuren (Allemagne). |
| 14-16/05/2003 | Conférence de Prospective sur la Modélisation Mathématique en Biologie et en Médecine, à Paris (France).<br>Conférence organisée par la SMAI, la SMF et l'Institut Fédératif du Chevaleret à l'occasion du vingtième anniversaire de la SMAI. |
| 10-13/02/2003 | Applied Mathematics and Applications of Mathematics (AMAM), à Nice (France). |
| 27-28/09/2002 | Journées Bordeaux-Pau-Toulouse, à Anglet (France).** |
| 9-21/09/2002 | School on Delay Differential Equations and Applications, à Marrakech (Maroc). |
| 8-19/07/2002 | Biomathematics Euro Summer School - Dynamical Systems in Physiology and Medicine, à Urbino (Italie).** |

## 4.6 Organisation de conférences

2014

*Conference "LyonSysBio" (Lyon Systems Biology)*, à Lyon (France), du 19 au 21 novembre.

*12e Colloque Franco-Roumain de Mathématiques Appliquées*, à Lyon (France), du 25 au 30 août.

*10th AIMS Conference on Dynamical Systems, Differential Equations and Applications*, à Madrid (Espagne), organisateur d'une session "Deterministic and stochastic models in biology and medicine", du 7 au11 juillet.

2013

*Conference "In honour of Michael Mackey's 70th birthday"*, à Lyon (France), du 3 au 6 juin.

*SBIP'13 "Systems Biology Approach to Infectious Processes"*, à Lyon (France), du 13 au 15 mai.

*Trimestre thématique biomathématiques "Mathematical Biology"*, incluant des invitations de chercheurs et l'organisation de 4 conférences et une école d'été, à Lyon (France), de février à juin.

2010

*Integrative Post Genomics IPG'10*, à Lyon (France), les 25-26 novembre.

*10ème Colloque Franco-Roumain de Mathématiques Appliquées*, à Poitiers (France), organisateur d'une session "Biomathématiques", du 26 au 31 août.

*Second Congrès de la Société Marocaine de Mathématiques Appliquées ($SM^2A$)*, à Rabat (Maroc), organisateur d'une session "Biomathématiques", du 28 au 30 juin.

2009

*Integrative Post Genomics IPG'09*, à Lyon (France), du 18 au 20 novembre.

*Workshop Mathematical Modelling in Biology and Medicine*, à Dubrovnik (Croatie), du 27 avril au 2 mai.

2008

*Journée thématique "Modélisation de la Croissance des Plantes"*, à Lyon (France), le 10 avril.

*Workshop "Haematopoiesis and its Disorders. Modelling, Experimental and Clinical Approaches"*, à Paris (France), les 20 et 21 mars.

2007

*Workshop "Modelling Blood Diseases"*, à Lyon (France), du 5 au 8 novembre.

2006

*Conférence Francophone sur la Modélisation Mathématique en Biologie et en Médecine*, à Craiova (Roumanie), du 12 au 14 juillet. (Année de la francophonie en Roumanie)

2004

*Journée Bio-Mathématiques à la mémoire du Professeur Ovide Arino*, à Pau, le 2 juillet.

## 4.7 Séjours scientifiques

22/11 au 2/12/2011

Séjour au **Département de Mathématiques de l'Université de Valladolid**, à Valladolid (Espagne), dans le cadre d'une collaboration avec Oscar Angulo.

25-29/10/2010

Séjour au **Département de Mathématiques de l'Université de Valladolid**, à Valladolid (Espagne), dans le cadre d'une collaboration avec Oscar Angulo.

18-30/10/2008

Séjour au **Laboratoire de Mathématiques et Dynamique des Populations du Département de Mathématiques de l'Université Caddy Ayyad**, à Marrakech (Maroc), dans le cadre d'une collaboration avec Hassan Hbid.

22-29/05/2005

Séjour au **Département de Mathématiques de l'Université Polytechnique de Bucarest**, à Bucarest (Roumanie), dans le cadre de l'action intégrée Brâncusi n° 08810RJ.

22-29/05/2005

Séjour au **Département de Mathématiques de l'Université Polytechnique de Bucarest**, à Bucarest (Roumanie), dans le cadre de l'action intégrée Brâncusi n° 08810RJ.

6-20/09/2004

Séjour à **l'Institut de Mathématiques de l'Université de Silésie**, à Katowice (Pologne), avec une bourse du Centre of Excellence Program.
Invité du Prof.r Ryszard Rudnicki, chercheur à l'Académie des Sciences de Pologne.

## 4.8 Jury de thèses

10 Octobre 2013 - Soutenance de M. Qasim ALI, à l'Ecole des Mines de St Etienne
Sujet : "Contribution to the mathematical modeling of immune response"
Rôle : examinateur

13 Novembre 2013 - Soutenance de M. Xavier DUPUIS, à l'Ecole Polytechnique
Sujet : "Contrôle optimal d'équations différentielles avec – ou sans – mémoire"
Rôle : examinateur

## 4.9 Diffusion scientifique pour non-spécialistes

Depuis 2009, je participe au cycle "Mathématiques et médecine" de l'**Université Ouverte** : il s'agit de conférences à destination d'un public non-spécialiste, sur l'application des mathématiques à des problèmes de médecine. J'ai donné les conférences :

— "Quand les cellules tueuses se réveillent...", traitant de la modélisation de la réponse immunitaire et du développement des vaccins, le 7 mai 2009, le 4 mars 2010, le 19 avril 2011, et le 27 mars 2012,

— "Grippe saisonnière, épidémie, pandémie : quel apport des mathématiques ?", le 21 février 2013 et le 25 mars 2014.

Entre le mois de décembre 2008 et le mois de juillet 2011, j'ai collaboré au site **Images des Mathématiques** (http ://images.math.cnrs.fr/), en tant que membre de l'équipe Liens-Actualités, alors coordonnée par Vincent Borelli (reprise depuis par Sylvie Benzoni), chargée de la rédaction de la revue de presse mensuelle et des "actualités brèves".

# Chapitre 5

# Publications Sélectionnées

Le lecteur trouvera dans ce chapitre les manuscrits de quelques publications ayant été utilisées dans les chapitres précédents. Ces articles ont été choisis soit parce qu'ils présentaient un résultat ou une approche notables (Sections 5.3, 5.4, 5.5, 5.7), soit parce qu'ils permettaient de présenter un ensemble de résultats dans un seul manuscrit (Sections 5.1, 5.2, 5.6).

## 5.1 Crauste (2006)

Manuscrit de l'article : [51] F. Crauste, *Global Asymptotic Stability and Hopf Bifurcation for a Blood Cell Production Model*, Mathematical Biosciences and Engineering, 3 (2), 325–346 (2006).

MATHEMATICAL BIOSCIENCES AND ENGINEERING
Volume **3**, Number **2**, April **2006**
http://www.mbejournal.org/
pp. **325–346**

# GLOBAL ASYMPTOTIC STABILITY AND HOPF BIFURCATION FOR A BLOOD CELL PRODUCTION MODEL

Fabien Crauste

Laboratoire de Mathématiques Appliquées UMR 5142,
Université de Pau et des Pays de l'Adour,
Avenue de l'université, 64000 Pau, France,
ANUBIS project, INRIA Futurs

(Communicated by Yasuhiro Takeuchi)

Abstract. We analyze the asymptotic stability of a nonlinear system of two differential equations with delay, describing the dynamics of blood cell production. This process takes place in the bone marrow, where stem cells differentiate throughout division in blood cells. Taking into account an explicit role of the total population of hematopoietic stem cells in the introduction of cells in cycle, we are led to study a characteristic equation with delay-dependent coefficients. We determine a necessary and sufficient condition for the global stability of the first steady state of our model, which describes the population's dying out, and we obtain the existence of a Hopf bifurcation for the only nontrivial positive steady state, leading to the existence of periodic solutions. These latter are related to dynamical diseases affecting blood cells known for their cyclic nature.

1. **Introduction.** The blood cell production process is based on the differentiation of so-called hematopoietic stem cells, located in the bone marrow. These undifferentiated and unobservable cells have unique capacities of differentiation (the ability to produce cells committed to one of the three blood cell types: red blood cells, white cells or platelets) and self-renewal (the ability to produce cells with the same properties).

Mathematical modelling of hematopoietic stem cell dynamics was introduced at the end of the seventies by Mackey [20]. He proposed a system of two differential equations with delay where the time delay describes the cell cycle duration. In this model, hematopoietic stem cells are separated in proliferating and nonproliferating cells, these latter being introduced in the proliferating phase with a nonlinear rate depending only upon the nonproliferating cell population. The resulting system of delay differential equations is then uncoupled, with the nonproliferating cells equation containing the whole information about the dynamics of the hematopoietic stem cell population. The stability analysis of the model in [20] highlighted the existence of periodic solutions, through a Hopf bifurcation, describing in some cases diseases affecting blood cells, characterized by periodic oscillations [18].

2000 *Mathematics Subject Classification.* 34K20, 92C37, 34D05, 34C23, 34K99.
*Key words and phrases.* asymptotic stability, delay differential equations, characteristic equation, delay-dependent coefficients, Hopf bifurcation, blood cell model, stem cells.

Mackey's model [20] has been studied by many authors, mainly since the beginning of the nineties. Mackey and Rey [22, 23, 24] numerically studied the behavior of a structured model based on the model in [20], stressing the existence of strange behaviors of the cell populations (such as oscillations or chaos). Mackey and Rudnicky [25, 26] developed the description of blood cell dynamics through an age-maturity structured model, stressing the influence of hematopoietic stem cells on blood production. Their model has been further developed by Dyson et al. [12, 13, 14], Adimy and Pujo-Menjouet [6], Adimy and Crauste [1, 2] and Adimy et al. [3]. Recently, Adimy et al. [4, 5] studied the model proposed in [20], taking into account that cells in cycle divide according to a density function (usually gamma distributions play an important role in cell cycle durations), contrary to what has been assumed in the works cited above, where the division has always been assumed to occur at the same time.

More recently, Pujo-Menjouet and Mackey [29] and Pujo-Menjouet et al. [28] gave a better insight into the Mackey's model [20], highlighting the role of each parameter of the model on the appearance of oscillations and, more particularly, of periodic solutions, when the model is applied to the study of chronic myelogenous leukemia [15].

Contrary to the assumption used in all of the works cited above, we study, in this paper, the model introduced by Mackey [20], considering that the rate of introduction in the proliferating phase, which contains the nonlinearity of this model, depends upon the total population of hematopoietic stem cells and not only upon the nonproliferating cell population. The introduction in cell cycle is partly known to be a consequence of activation of hematopoietic stem cells due to molecules fixing on them. Hence, the entire population is in contact with these molecules, and it is reasonable to think that the total number of hematopoietic stem cells plays a role in the introduction of nonproliferating cells in the proliferating phase.

The first consequence is that the model is not uncoupled, and the nonproliferating cell population equation does not contain all the information about the dynamics of blood cell production, contrary to the model in [20, 28, 29]. Therefore, we are led to the study of a modified system of delay differential equations (system (3)–(4)), where the delay describes the cell cycle duration, with a nonlinear part depending on one of the two populations.

Second, while studying the local asymptotic stability of the steady states of our model, we have to determine roots of a characteristic equation taking the form of a first-degree exponential polynomial with delay-dependent coefficients. For such equations, Beretta and Kuang [8] developed a very useful and powerful technique, which we will apply to our model.

Our aim is to show, through the study of the steady states' stability, that our model, described in (3)–(4), exhibits properties similar to those in [20] and that it can be used to model blood cell production dynamics with good results, particularly when one is interested in the appearance of periodic solutions in blood cell dynamics models. We want to point out that the usually accepted assumption about the introduction rate may be limitative and that our model can display interesting dynamics, such as stability switches, that have never been noted before.

The present work is organized as follows. In the next section we present our model, stated in equations (3) and (4). We then determine the steady states of this model. In section 3, we linearize the system (3)–(4) about a steady state, and we

deduce the associated characteristic equation. In section 4, we establish necessary and sufficient conditions for the global asymptotic stability of the trivial steady state (which describes the extinction of the hematopoietic stem cell population). In section 5, we focus on the asymptotic stability of the unique nontrivial steady state. By studying the existence of pure imaginary roots of a first degree exponential polynomial with delay-dependent coefficients, we obtain the existence of a critical value of the time delay for which a Hopf bifurcation occurs at the positive steady state, leading to the appearance of periodic solutions. Using numerical illustrations, we show how these solutions can be related to periodic hematological diseases in section 6, and we note the existence of a stability switch. We conclude with a discussion.

2. **A Nonlinear Model of Blood Cell Production.** Let us consider a population of hematopoietic stem cells located in the bone marrow. These cells actually perform a succession of cell cycles, to differentiate into blood cells (white cells, red blood cells and platelets). According to early works, Burns and Tannock [10] for example, we assume that cells in cycle are divided in two groups: proliferating and nonproliferating cells. The respective proliferating and nonproliferating cell populations are denoted by $P$ and $N$.

All hematopoietic stem cells die with constant rates, namely $\gamma > 0$ for proliferating cells and $\delta > 0$ for nonproliferating cells. The latter are introduced in the proliferating phase, in order to mature and divide, with a rate $\beta$. At the end of the proliferating phase, cells divide into two daughter cells, which immediately enter the nonproliferating phase.

Then the populations $P$ and $N$ satisfy the following evolution equations (see Mackey [20] or Pujo-Menjouet and Mackey [29]):

$$\frac{dP}{dt}(t) = -\gamma P(t) + \beta N(t) - e^{-\gamma\tau}\beta N(t-\tau), \tag{1}$$

$$\frac{dN}{dt}(t) = -\delta N(t) - \beta N(t) + 2e^{-\gamma\tau}\beta N(t-\tau). \tag{2}$$

In each of the above equations, $\tau$ denotes the average duration of the proliferating phase. The term $e^{-\gamma\tau}$ then describes the survival rate of proliferating cells. The last terms in the right-hand side of equations (1) and (2) account for cells that have performed a whole cell cycle and leave the proliferating phase (in (1)) or enter the nonproliferating phase (in (2)). These cells are in fact nonproliferating cells introduced in the proliferating phase a time $\tau$ earlier. The factor 2 in equation (2) represents the division of each proliferating hematopoietic stem cell in two daughter cells.

We assume that the rate of introduction $\beta$ depends on the total population of hematopoietic stem cells, which we denote by $S$. With our notations, $S = P + N$. This assumption stresses the fact that the nature of the trigger signal for introduction in the proliferating phase is the result of an action on the entire cell population. For example, it can be caused by molecules entering the bone marrow and fixing on hematopoietic stem cells, activating or inhibiting their proliferating capacity. This occurs in particular for the production of red blood cells. Their regulation is mainly mediated by a hormone (a growth factor, in fact) called erythropoietin, produced by the kidneys under a stimulation by circulating blood cells (see Bélair et al. [7], Mahaffy et al. [27]).

Hence we assume that

$$\beta = \beta(S(t)).$$

The function $\beta$ is supposed to be continuous and positive on $[0, +\infty)$, and strictly decreasing. This latter assumption describes the fact that the fewer hematopoietic stem cells in the bone marrow, the more cells introduced in the proliferative compartment [20, 29]. Furthermore, we assume that

$$\lim_{S\to\infty} \beta(S) = 0.$$

Adding equations (1) and (2), we can then deduce an equation satisfied by the total population of hematopoietic stem cells $S(t)$. We assume, for the sake of simplicity, that proliferating and nonproliferating cells die with the same rate, that is $\delta = \gamma$. Then the populations $N$ and $S$ satisfy the following nonlinear system with time delay $\tau$, corresponding to the cell cycle duration,

$$\frac{dS}{dt}(t) = -\delta S(t) + e^{-\delta\tau}\beta(S(t-\tau))N(t-\tau), \tag{3}$$

$$\frac{dN}{dt}(t) = -\delta N(t) - \beta(S(t))N(t) + 2e^{-\delta\tau}\beta(S(t-\tau))N(t-\tau). \tag{4}$$

From Hale and Verduyn Lunel [17], for each continuous initial condition, system (3)–(4) has a unique continuous solution $(S(t), N(t))$, well-defined for $t \geq 0$.

LEMMA 2.1. *For all nonnegative initial condition, the unique solution $(S(t), N(t))$ of (3)–(4) is nonnegative.*

*Proof.* First assume that there exists $\xi > 0$ such that $N(\xi) = 0$ and $N(t) > 0$ for $t < \xi$. Then, from (4) and since $\beta$ is a positive function,

$$\frac{dN}{dt}(\xi) = 2e^{-\delta\tau}\beta(S(\xi-\tau))N(\xi-\tau) > 0.$$

Consequently, $N(t) \geq 0$ for $t > 0$.

If there exists $\zeta > 0$ such that $S(\zeta) = 0$ and $S(t) > 0$ for $t < \zeta$, then the same reasoning, using (3), leads to

$$\frac{dS}{dt}(\zeta) = e^{-\delta\tau}\beta(S(\zeta-\tau))N(\zeta-\tau) > 0,$$

and we deduce that $S(t) \geq 0$ for $t > 0$. □

REMARK 1. *The positivity of $S$ and $N$, solutions of system (3)–(4), does not a priori imply that $P = S - N$ is nonnegative.*

*Using a classical variation of constant formula, the solutions $P(t)$ of (1) are given, for $t \geq 0$, by*

$$P(t) = e^{-\delta t}P(0) + e^{-\delta t}\int_0^t e^{\delta\theta}\beta(S(\theta))N(\theta) - e^{\delta(\theta-\tau)}\beta(S(\theta-\tau))N(\theta-\tau)d\theta.$$

*Setting the change of variable $\sigma = \theta - \tau$, we obtain*

$$P(t) = e^{-\delta t}\left[P(0) - \int_{-\tau}^0 e^{\delta\theta}\beta(S(\theta))N(\theta)d\theta\right] + e^{-\delta t}\int_{t-\tau}^t e^{\delta\theta}\beta(S(\theta))N(\theta)d\theta.$$

*Consequently, $P(t) \geq 0$ for $t \geq 0$ if*

$$P(0) \geq \int_{-\tau}^0 e^{\delta\theta}\beta(S(\theta))N(\theta)d\theta;$$

*that is, if*

$$S(0) \geq N(0) + \int_{-\tau}^{0} e^{\delta\theta}\beta(S(\theta))N(\theta)d\theta.$$

*This condition is biologically relevant, since* $\int_{-\tau}^{0} e^{\delta\theta}\beta(S(\theta))N(\theta)d\theta$ *represents the population of cells that have been introduced in the proliferating phase at time* $\theta \in [-\tau, 0]$ *and that have survived at time* $t = 0$*. Hence, from a biological point of view, the population in the proliferating phase at time* $t = 0$ *should be larger than this quantity.*

In the stability analysis of system (3)–(4), the existence of stationary solutions, called steady states, is relevant since these particular solutions are potential limits of system (3)–(4).

A steady state of system (3)–(4) is a solution $(\overline{S}, \overline{N})$ satisfying

$$\frac{d\overline{S}}{dt} = \frac{d\overline{N}}{dt} = 0.$$

Let $(\overline{S}, \overline{N})$ be a steady state of (3)–(4). Then

$$\delta\overline{S} = e^{-\delta\tau}\beta(\overline{S})\overline{N}, \tag{5}$$

$$(\delta + \beta(\overline{S}))\overline{N} = 2e^{-\delta\tau}\beta(\overline{S})\overline{N}. \tag{6}$$

We immediately notice that $(0, 0)$ is a steady state of system (3)–(4), which we will denote, in the following, by $E^0$. This steady state always exists. It describes the extinction of the hematopoietic stem cell population.

Assume that $(\overline{S}, \overline{N})$ is a steady state of (3)–(4) with $\overline{S}, \overline{N} \neq 0$. Then, from (5) and (6),

$$(2e^{-\delta\tau} - 1)\beta(\overline{S}) = \delta \qquad \text{and} \qquad \overline{N} = \frac{\delta\overline{S}}{e^{-\delta\tau}\beta(\overline{S})}.$$

A necessary condition to obtain a nontrivial steady state is then $2e^{-\delta\tau} - 1 > 0$, that is

$$\tau < \frac{\ln(2)}{\delta}.$$

Under this condition, since the function $\beta$ is decreasing, positive, and tends to zero at infinity, there exists $\overline{S} > 0$ satisfying

$$(2e^{-\delta\tau} - 1)\beta(\overline{S}) = \delta, \tag{7}$$

if and only if

$$(2e^{-\delta\tau} - 1)\beta(0) > \delta. \tag{8}$$

One can easily check that condition (8) is equivalent to

$$\delta < \beta(0) \qquad \text{and} \qquad 0 \leq \tau < \overline{\tau} := \frac{1}{\delta}\ln\left(\frac{2\beta(0)}{\delta + \beta(0)}\right). \tag{9}$$

In this case, $\overline{S} > 0$ solution of (7) is unique, and

$$\overline{N} = \frac{2e^{-\delta\tau} - 1}{e^{-\delta\tau}}\overline{S}.$$

One can check that $\overline{N} \leq \overline{S}$. These results are summed up in the next proposition.

PROPOSITION 2.1. *If inequality (8) holds true, the system (3)–(4) has exactly two steady states:* $E^0 = (0,0)$ *and* $E^* = (S^*, N^*)$*, where* $S^* > 0$ *is the unique solution of equation (7) and* $N^* = (2e^{-\delta\tau} - 1)e^{\delta\tau}S^*$.

*If*

$$(2e^{-\delta\tau} - 1)\beta(0) \leq \delta,$$

*then system (3)–(4) has only one steady state, namely* $E^0 = (0,0)$.

In the next section, we linearize the system (3)–(4) about one of its steady states to analyze its local asymptotic stability.

3. **Linearization and Characteristic Equation.** We are interested in the asymptotic stability of the steady states of system (3)–(4). To that aim, we linearize system (3)–(4) about one of its steady state and we determine the associated characteristic equation. We assume that $\beta$ is continuously differentiable on $[0, +\infty)$.

Let $(\overline{S}, \overline{N})$ be a steady state of system (3)–(4). From Proposition 2.1, $(\overline{S}, \overline{N})$ is either $E^0$ or $E^*$.

The linearization of system (3)–(4) about $(\overline{S}, \overline{N})$ leads to the following system,

$$\begin{aligned} \frac{dS}{dt}(t) &= -\delta S(t) + e^{-\delta\tau}\beta(\overline{S})N(t-\tau) + e^{-\delta\tau}\overline{N}\beta'(\overline{S})S(t-\tau), \qquad (10) \\ \frac{dN}{dt}(t) &= -(\delta + \beta(\overline{S}))N(t) - \overline{N}\beta'(\overline{S})S(t) \\ &\quad +2e^{-\delta\tau}\left[\beta(\overline{S})N(t-\tau) + \overline{N}\beta'(\overline{S})S(t-\tau)\right], \qquad (11) \end{aligned}$$

where we have used the notations $S(t)$ and $N(t)$ instead of $S(t) - \overline{S}$ and $N(t) - \overline{N}$ for the sake of simplicity.

The system (10)–(11) can be written

$$\begin{pmatrix} \frac{dS}{dt}(t) \\ \frac{dN}{dt}(t) \end{pmatrix} = \mathcal{A}_1 \begin{pmatrix} S(t) \\ N(t) \end{pmatrix} + \mathcal{A}_2 \begin{pmatrix} S(t-\tau) \\ N(t-\tau) \end{pmatrix},$$

where

$$\mathcal{A}_1 := \begin{pmatrix} -\delta & 0 \\ -\alpha & -(\delta + \beta(\overline{S})) \end{pmatrix}, \qquad \mathcal{A}_2 := e^{-\delta\tau}\begin{pmatrix} \alpha & \beta(\overline{S}) \\ 2\alpha & 2\beta(\overline{S}) \end{pmatrix},$$

and

$$\alpha = \alpha(\overline{N}, \overline{S}) := \overline{N}\beta'(\overline{S}). \qquad (12)$$

The characteristic equation of system (10)–(11) associated with the steady state $(\overline{S}, \overline{N})$ is defined by

$$\det(\lambda - \mathcal{A}_1 - e^{-\lambda\tau}\mathcal{A}_2) = 0.$$

After calculations, this equation reduces to

$$(\lambda + \delta)\left[\lambda + \delta + \beta(\overline{S}) - (2\beta(\overline{S}) + \alpha(\overline{N}, \overline{S}))e^{-\delta\tau}e^{-\lambda\tau}\right] = 0. \qquad (13)$$

We recall that the steady state $(\overline{S}, \overline{N})$ is locally asymptotically stable when all roots of (13) have negative real parts, and the stability can only be lost if eigenvalues cross the imaginary axis; that is, if pure imaginary roots appear.

One can notice that $\lambda = -\delta < 0$ is always an eigenvalue of (13). Therefore, we focus only on the equation

$$\lambda + \delta + \beta(\overline{S}) - (2\beta(\overline{S}) + \alpha(\overline{N}, \overline{S}))e^{-\delta\tau}e^{-\lambda\tau} = 0. \qquad (14)$$

We first analyze, in the next section, the stability of the trivial steady state $E^0$. We establish necessary and sufficient conditions for the population's dying out. Then, in section 5, we concentrate on the behavior of the positive steady state $E^*$.

4. **Global Asymptotic Stability of the Trivial Steady State: Cells' Dying Out.** We concentrate, in this section, on the stability of the steady state $E^0 = (0,0)$. From (12), $\alpha(0,0) = 0$, so, for $\overline{S} = \overline{N} = 0$, the characteristic equation (14) becomes

$$\lambda + \delta + \beta(0) - 2\beta(0)e^{-\delta\tau}e^{-\lambda\tau} = 0. \tag{15}$$

It is straightforward to see that equation (15) has a unique real eigenvalue, say $\lambda_0$, and all other eigenvalues $\lambda \neq \lambda_0$ of (15) satisfy $\mathrm{Re}(\lambda) < \lambda_0$.

Let us consider the mapping $\lambda \mapsto \lambda + \delta + \beta(0) - 2\beta(0)e^{-\delta\tau}e^{-\lambda\tau}$ as a function of real $\lambda$. Then it is an increasing function from $-\infty$ to $+\infty$, yielding the existence and uniqueness of $\lambda_0$.

Assume that $\lambda = \mu + i\omega \neq \lambda_0$ satisfies (15). Then, considering the real part of (15), we get

$$\mu - \lambda_0 = 2\beta(0)e^{-\delta\tau}\left[e^{-\mu\tau}\cos(\omega\tau) - e^{-\lambda_0\tau}\right].$$

By contradiction, we assume that $\mu > \lambda_0$. Then $e^{-\mu\tau}\cos(\omega\tau) - e^{-\lambda_0\tau} < 0$ and we obtain a contradiction. So $\mu \leq \lambda_0$. Now if $\mu = \lambda_0$, then the previous equality implies that

$$\cos(\omega\tau) = 1, \qquad \text{for } \tau \geq 0.$$

It follows that $\sin(\omega\tau) = 0$ and, considering the imaginary part of (15) with $\lambda = \mu + i\omega$, given by

$$\omega + 2\beta(0)e^{-\delta\tau}e^{-\mu\tau}\sin(\omega\tau) = 0,$$

we obtain $\omega = 0$ and $\lambda = \lambda_0$, which gives a contradiction. Therefore, $\mu < \lambda_0$.

The real root $\lambda_0$ is negative if

$$(2e^{-\delta\tau} - 1)\beta(0) < \delta,$$

and all eigenvalues of (15) have negative real parts in this case. When condition (8) holds, $\lambda_0$ is positive. We can then conclude in the next proposition to the stability of $E^0$.

PROPOSITION 4.1. *The trivial steady state $E^0 = (0,0)$ of system (3)–(4) is locally asymptotically stable when*

$$(2e^{-\delta\tau} - 1)\beta(0) < \delta, \tag{16}$$

*and unstable when*

$$(2e^{-\delta\tau} - 1)\beta(0) > \delta.$$

REMARK 2. *When*

$$(2e^{-\delta\tau} - 1)\beta(0) = \delta,$$

*then the unique real root of (15) is $\lambda_0 = 0$, and all other eigenvalues have negative real parts. One can easily check that $\lambda_0 = 0$ is a simple root of (15), since the first derivative of the mapping $\lambda \mapsto \lambda + \delta + \beta(0) - 2\beta(0)e^{-\delta\tau}e^{-\lambda\tau}$ at $\lambda_0 = 0$ is*

$$1 + 2\beta(0)\tau e^{-\delta\tau} > 0.$$

*Then the linear system is stable, but we cannot conclude to the asymptotic stability of the trivial steady state $E^0 = (0,0)$ of system (3)–(4) without further analysis. This is done in Proposition 4.2.*

When condition (16) holds true, $E^0$ is in fact the only steady state of system (3)–(4) (see Proposition 2.1). In this case, we can show that $E^0$ is globally asymptotically stable.

We first show the following result.

LEMMA 4.1. *Let $(S(t), N(t))$ be a solution of (3)–(4). If $\lim_{t\to+\infty} N(t) = 0$, then $\lim_{t\to+\infty} S(t) = 0$.*

*Proof.* Using (3), a classical variation of constant formula gives us, for $t \geq 0$,

$$S(t) = e^{-\delta t}S(0) + e^{-\delta t}\int_0^t e^{\delta(\theta-\tau)}\beta(S(\theta-\tau))N(\theta-\tau)d\theta.$$

Setting $\sigma = \theta - \tau$, this expression becomes

$$S(t) = e^{-\delta t}S(0) + e^{-\delta t}\int_{-\tau}^{t-\tau} e^{\delta\sigma}\beta(S(\sigma))N(\sigma)d\sigma.$$

Let $\varepsilon > 0$ be fixed. Since $N$ is assumed to tend to zero when $t$ tends to $\infty$, there exists $T > 0$ such that

$$N(t) < \varepsilon\frac{\delta e^{\delta\tau}}{2\beta(0)}, \qquad \text{for } t \geq T. \tag{17}$$

Then, for $t \geq T + \tau$,

$$S(t) = e^{-\delta t}\left[S(0) + \int_{-\tau}^{T} e^{\delta\sigma}\beta(S(\sigma))N(\sigma)d\sigma\right] + e^{-\delta t}\int_{T}^{t-\tau} e^{\delta\sigma}\beta(S(\sigma))N(\sigma)d\sigma.$$

Using (17) and the fact that $\beta(0)$ is a bound of $\beta$, we obtain, for $t \geq T + \tau$,

$$\begin{aligned} S(t) &\leq e^{-\delta t}\left[S(0) + \int_{-\tau}^{T} e^{\delta\sigma}\beta(S(\sigma))N(\sigma)d\sigma\right] + \varepsilon\frac{\delta e^{\delta\tau}}{2}e^{-\delta t}\int_{T}^{t-\tau} e^{\delta\sigma}d\sigma, \\ &\leq e^{-\delta t}\left[S(0) + \int_{-\tau}^{T} e^{\delta\sigma}\beta(S(\sigma))N(\sigma)d\sigma\right] + \varepsilon\frac{e^{\delta\tau}}{2}\left(e^{-\delta\tau} - e^{-\delta(t-T)}\right), \\ &\leq e^{-\delta t}\left[S(0) + \int_{-\tau}^{T} e^{\delta\sigma}\beta(S(\sigma))N(\sigma)d\sigma\right] + \frac{\varepsilon}{2}. \end{aligned}$$

Let $\bar{t} > 0$ be such that

$$e^{-\delta t}\left[S(0) + \int_{-\tau}^{T} e^{\delta\sigma}\beta(S(\sigma))N(\sigma)d\sigma\right] < \frac{\varepsilon}{2}, \qquad \text{for } t \geq \bar{t}.$$

Then, for $t \geq \max\{\bar{t}, T + \tau\}$, we obtain

$$S(t) < \varepsilon.$$

Thus, $S(t)$ tends to zero as $t$ tends to $+\infty$, and the proof is complete. □

We recall a very useful lemma, proved by Barbălat (see Gopalsamy [16]).

LEMMA 4.2. *Let $f : [a, +\infty) \to \mathbb{R}$, $a \in \mathbb{R}$, be a differentiable function. If $\lim_{t\to+\infty} f(t)$ exists and $f'(t)$ is uniformly continuous on $(a, +\infty)$, then*

$$\lim_{t\to+\infty} f'(t) = 0.$$

We then prove the following result, dealing with the global asymptotic stability of $E^0$.

PROPOSITION 4.2. *Assume that*

$$(2e^{-\delta\tau} - 1)\beta(0) \leq \delta. \tag{18}$$

*Then all solutions* $(S(t), N(t))$ *of system (3)–(4) converge to the trivial solution* $(0, 0)$. *Hence* $E^0$ *is globally asymptotically stable and the cell populations die out.*

*Proof.* Let $(S(t), N(t))$ be a solution of (3)–(4). We define, for $t \geq 0$,

$$Y(t) = N(t) + 2e^{-\delta\tau} \int_{t-\tau}^{t} \beta(S(\theta))N(\theta)d\theta.$$

Using (4), we can check that

$$Y'(t) = N(t) \left[(2e^{-\delta\tau} - 1)\beta(S(t)) - \delta\right]. \tag{19}$$

From condition (18) and the fact that $\beta$ is decreasing, it follows that

$$Y'(t) \leq 0 \qquad \text{for } t > 0.$$

Thus, $Y$ is decreasing. Since $Y$ is a nonnegative function, we deduce that there exists $y \geq 0$ such that

$$\lim_{t\to+\infty} Y(t) = y.$$

In particular, $Y$ is bounded, and consequently $N$ is also bounded.

We then deduce, with (4), that $N'$ is bounded and, using a similar technique as the one used in the proof of Lemma 4.1, that $S$ is bounded. Consequently, with (3), we obtain that $S'$ is bounded.

From (19), since $N$, $S$, $N'$ and $S'$ are bounded, $Y'$ is uniformly continuous.

Since $\lim_{t\to+\infty} Y(t)$ exists and $Y'$ is uniformly continuous on $(0, +\infty)$, Lemma 4.2 implies that

$$\lim_{t\to+\infty} Y'(t) = 0.$$

Consequently, from (19), we obtain either

$$\lim_{t\to+\infty} N(t) = 0 \qquad \text{or} \qquad \lim_{t\to+\infty} (2e^{-\delta\tau} - 1)\beta(S(t)) = \delta.$$

First, assume that (16) holds true, that is,

$$(2e^{-\delta\tau} - 1)\beta(0) < \delta.$$

If $2e^{-\delta\tau}-1 > 0$, then, since $\beta$ is a decreasing function satisfying (16), we deduce that $(2e^{-\delta\tau}-1)\beta(S(t)) \leq (2e^{-\delta\tau}-1)\beta(0) < \delta$. If $2e^{-\delta\tau}-1 \leq 0$, then $(2e^{-\delta\tau}-1)\beta(S(t)) \leq 0 < \delta$. Consequently, if it exists, $\lim_{t\to+\infty}(2e^{-\delta\tau} - 1)\beta(S(t))$ cannot be equal to $\delta$ and it follows that

$$\lim_{t\to+\infty} N(t) = 0.$$

From Lemma 4.1, we deduce that $\lim_{t\to+\infty} S(t) = 0$, and the conclusion follows.

Second, assume that

$$(2e^{-\delta\tau} - 1)\beta(0) = \delta.$$

Then, $\lim_{t\to+\infty}(2e^{-\delta\tau} - 1)\beta(S(t)) = \delta$ is equivalent to $\lim_{t\to+\infty} \beta(S(t)) = \beta(0)$. Since $\beta$ is positive and decreasing, this is equivalent to $\lim_{t\to+\infty} S(t) = 0$. It follows that either

$$\lim_{t\to+\infty} N(t) = 0 \qquad \text{or} \qquad \lim_{t\to+\infty} S(t) = 0.$$

If $\lim_{t\to+\infty} N(t) = 0$, we conclude similarly to the previous case with Lemma 4.1. So we assume that $\lim_{t\to+\infty} S(t) = 0$.

From (3), we deduce that

$$\lim_{t\to+\infty} \beta(S(t-\tau))N(t-\tau) = 0.$$

Consequently, either

$$\lim_{t\to+\infty} \beta(S(t-\tau)) = 0 \qquad \text{or} \qquad \lim_{t\to+\infty} N(t-\tau) = 0.$$

Since $\lim_{t\to+\infty} S(t) = 0$, then $\lim_{t\to+\infty} \beta(S(t-\tau)) = \beta(0) > 0$. Hence, $\lim_{t\to+\infty} N(t-\tau) = 0$, and it follows that $\lim_{t\to+\infty} N(t) = 0$.

This concludes the proof. □

REMARK 3. *Let $C$ denote the set of continuous functions mapping $[-\tau, 0]$ into $\mathbb{R}^+$. One can check that the function $V$, defined for $(\varphi, \psi) \in C^2$ by*

$$V(\varphi, \psi) = \psi(0) + 2e^{-\delta\tau} \int_{-\tau}^{0} \beta(\varphi(\theta))\psi(\theta)d\theta,$$

*satisfies*

$$\dot{V}(\varphi, \psi) = \psi(0)\left[(2e^{-\delta\tau} - 1)\beta(\varphi(0)) - \delta\right].$$

*Hence, $V$ is a Lyapunov functional (see Hale and Verduyn Lunel [17]) on the set*

$$G = \left\{(\varphi, \psi) \in C^2;\ \psi(0)\left[(2e^{-\delta\tau} - 1)\beta(\varphi(0)) - \delta\right] \le 0\right\}.$$

*With assumption (18), $G = C^2$. In the proof of Proposition 4.2, we did not directly use the properties of Lyapunov functionals, but the function $Y$ is defined by*

$$Y(t) = V(S_t, N_t), \qquad \text{for } t \ge 0,$$

*where $S_t$ (respectively, $N_t$) is defined by $S_t(\theta) = S(t+\theta)$ (respectively, $N_t(\theta) = N(t+\theta)$), $\theta \in [-\tau, 0]$.*

Through Propositions 4.1 and 4.2, we obtained necessary and sufficient conditions for the global asymptotic stability of $E^0$. Therefore, in the next section, we concentrate on the behavior of $E^*$, the unique positive steady state of (3)–(4).

5. **Local Asymptotic Stability of the Positive Steady State.** We now turn our considerations on the stability of the unique nontrivial steady state of system (3)–(4), namely $E^* = (S^*, N^*)$, where, from Proposition 2.1, $S^*$ is the unique solution of (7), and $N^* = (2e^{-\delta\tau} - 1)e^{\delta\tau}S^*$.

To ensure the existence of this steady state, we assume that condition (8), or equivalently condition (9), holds true. That is,

$$\delta < \beta(0) \qquad \text{and} \qquad 0 \le \tau < \overline{\tau} := \frac{1}{\delta}\ln\left(\frac{2\beta(0)}{\delta + \beta(0)}\right).$$

In particular, $2e^{-\delta\tau} - 1 > 0$.

In this case, Proposition 4.1 indicates that the unique other steady state $E^0$ is unstable.

From their definitions in Proposition 2.1, the steady states $S^*$ and $N^*$ depend on the time delay $\tau$. In fact,

$$S^* = S^*(\tau) = \beta^{-1}\left(\frac{\delta}{2e^{-\delta\tau} - 1}\right) \quad \text{and} \quad N^* = N^*(\tau) = \frac{2e^{-\delta\tau} - 1}{e^{-\delta\tau}}S^*(\tau),$$

where $\beta^{-1} : (0, \beta(0)] \to [0, +\infty)$ is a decreasing function.

Using these expressions, we can stress that $S^*$ and $N^*$ are positive decreasing continuous functions of $\tau \in [0, \overline{\tau})$, continuously differentiable, such that $S^*(0) = N^*(0) = \beta^{-1}(\delta)$, and $\lim_{\tau \to \overline{\tau}}(S^*(\tau), N^*(\tau)) = (0, 0) = E^0$.

The characteristic equation (14), with $\overline{S} = S^*$ and $\overline{N} = N^*$, is then given by

$$\lambda + A(\tau) - B(\tau)e^{-\lambda\tau} = 0, \tag{20}$$

with

$$A(\tau) := \delta + \beta(S^*(\tau)) \qquad \text{and} \qquad B(\tau) := [2\beta(S^*(\tau)) + N^*(\tau)\beta'(S^*(\tau))]e^{-\delta\tau}.$$

Notice that $A(\tau) > 0$ for all $\tau \in [0, \overline{\tau})$. Moreover, from (7), we obtain

$$B(\tau) = A(\tau) + (2e^{-\delta\tau} - 1)S^*(\tau)\beta'(S^*(\tau)), \quad \text{for } \tau \in [0, \overline{\tau}). \tag{21}$$

In particular, $B(\tau) < A(\tau)$ for $\tau \in [0, \overline{\tau})$.

Taking $\tau = 0$ in (20), we obtain

$$\lambda + A(0) - B(0) = 0,$$

that is

$$\lambda = \beta^{-1}(\delta)\beta'(\beta^{-1}(\delta)).$$

Since $\beta$ is decreasing, we deduce that the only eigenvalue of (20) is then negative. The ensuing lemma follows.

LEMMA 5.1. *When $\delta < \beta(0)$ and $\tau = 0$, the nontrivial steady-state $E^*$ of system (3)–(4) is locally asymptotically stable, and the system (3)–(4) undergoes a transcritical bifurcation.*

When $\tau$ increases and remains in the interval $[0, \overline{\tau})$, the stability of the steady state can only be lost if purely imaginary roots appear. Therefore, we investigate the existence of purely imaginary roots of (20).

Let $\lambda = i\omega$, $\omega \in \mathbb{R}$, be a pure imaginary eigenvalue of (20). Separating real and imaginary parts, we obtain

$$A(\tau) - B(\tau)\cos(\omega\tau) = 0, \tag{22}$$

$$\omega + B(\tau)\sin(\omega\tau) = 0. \tag{23}$$

One can notice, first, that if $\omega$ is a solution of (22)–(23) then $-\omega$ also satisfies this system. Second, $\omega = 0$ is not a solution of (22)–(23). Otherwise, we would obtain $A(\tau) = B(\tau)$ for some $\tau \in [0, \overline{\tau})$, which contradicts $B(\tau) < A(\tau)$ for $\tau \in [0, \overline{\tau})$. Therefore $\omega = 0$ cannot be a solution of (22)–(23). Thus, in the following, we will look only for positive solutions $\omega$ of (22)–(23).

From (22), a necessary condition for equation (20) to have purely imaginary roots is that

$$A(\tau) < |B(\tau)|.$$

Since $B(\tau) < A(\tau)$, this implies in particularly that $B(\tau)$ must be negative. Moreover, from (21), the above condition is equivalent to

$$2A(\tau) + (2e^{-\delta\tau} - 1)S^*(\tau)\beta'(S^*(\tau)) < 0.$$

Using the definitions of $A(\tau)$, $N^*(\tau)$, $S^*(\tau)$ and equality (5), this inequality becomes the following condition on $\tau$,

$$\frac{4\delta e^{-\delta\tau}}{2e^{-\delta\tau} - 1} + (2e^{-\delta\tau} - 1)\beta^{-1}\left(\frac{\delta}{2e^{-\delta\tau} - 1}\right)\beta'\left(\beta^{-1}\left(\frac{\delta}{2e^{-\delta\tau} - 1}\right)\right) < 0. \tag{24}$$

LEMMA 5.2. *Let $\chi : [0, +\infty) \to (-\infty, 0]$ be defined, for $y \geq 0$, by*

$$\chi(y) = y\beta'(y).$$

*Assume that*

*(H$_1$)* $\chi$ *is decreasing on the interval* $\left[0, \beta^{-1}(\delta)\right]$.

*(H$_2$)* $\chi\left(\beta^{-1}(\delta)\right) < -4\delta$.

*Then there exists a unique $\tau^* \in (0, \overline{\tau})$ such that condition (24) is satisfied if and only if $\tau \in [0, \tau^*)$.*

*Proof.* Consider the negative functions $f_1(\tau)$ and $f_2(\tau)$, defined for $\tau \in [0, \overline{\tau}]$ by

$$f_1(\tau) = \chi\left(\beta^{-1}\left(\frac{\delta}{2e^{-\delta\tau} - 1}\right)\right) \qquad \text{and} \qquad f_2(\tau) = -\frac{4\delta e^{-\delta\tau}}{(2e^{-\delta\tau} - 1)^2}.$$

Then

$$\{\tau \in [0, \overline{\tau}) \,; \text{condition (24) is satisfied}\} = \{\tau \in [0, \overline{\tau}) \,; f_1(\tau) < f_2(\tau)\}.$$

The function $f_2$ satisfies

$$f_2(0) = -4\delta \qquad \text{and} \qquad f_2(\overline{\tau}) = -2\frac{\delta + \beta(0)}{\delta}\beta(0),$$

and, for $\tau \in [0, \overline{\tau}]$,

$$f_2'(\tau) = -\frac{4\delta^2 e^{-\delta\tau}(2e^{-\delta\tau} + 1)}{(2e^{-\delta\tau} - 1)^3} < 0.$$

Hence $f_2$ is decreasing from $-4\delta$ to $-2(\delta + \beta(0))\beta(0)/\delta$.

For $\tau \in [0, \overline{\tau})$,

$$\delta \leq \frac{\delta}{2e^{-\delta\tau} - 1} < \beta(0).$$

Since $\beta^{-1}$ is decreasing on $(0, \beta(0)]$ and, from (H$_1$), $\chi$ is decreasing on $[0, \beta^{-1}(\delta)]$, we deduce that $f_1$ is increasing. Moreover,

$$f_1(0) = \chi\left(\beta^{-1}(\delta)\right) \qquad \text{and} \qquad f_1(\overline{\tau}) = 0.$$

From (H$_2$),

$$f_1(0) < f_2(0).$$

Since $f_1(\overline{\tau}) > f_2(\overline{\tau})$, there exists $\tau^* \in (0, \overline{\tau})$, which is unique since $f_1$ is increasing and $f_2$ decreasing, such that

$$\{\tau \in [0, \overline{\tau}) \,; f_1(\tau) < f_2(\tau)\} = [0, \tau^*).$$

This concludes the proof. □

REMARK 4. *Assumption (H$_1$) is not necessary for the existence of $\tau^*$; it just implies the uniqueness. This latter can be achieved with weaker conditions, as we will check in an example in section 6.*

We assume, in the following, that (H$_1$) and (H$_2$) are fulfilled and $\tau \in [0, \tau^*)$.

System (22)–(23) is equivalent to

$$\cos(\omega\tau) = \frac{A(\tau)}{B(\tau)}, \qquad \sin(\omega\tau) = -\frac{\omega}{B(\tau)}. \tag{25}$$

Note that for $\tau \in [0, \tau^*)$, $B(\tau) < 0$.

Therefore, adding the squares of both sides of (25), purely imaginary eigenvalues $i\omega$ of (20), with $\omega > 0$, must satisfy

$$\omega = \sqrt{B^2(\tau) - A^2(\tau)}. \tag{26}$$

So, in the following, we will think of $\omega$ as $\omega(\tau)$.

Substituting this expression for $\omega$ in (25), we obtain

$$\begin{aligned} \cos\left(\tau\sqrt{B^2(\tau) - A^2(\tau)}\right) &= \frac{A(\tau)}{B(\tau)}, \\ \sin\left(\tau\sqrt{B^2(\tau) - A^2(\tau)}\right) &= -\frac{\sqrt{B^2(\tau) - A^2(\tau)}}{B(\tau)}. \end{aligned} \tag{27}$$

From the above reasoning, values of $\tau \in [0, \tau^*)$ solutions of system (27) generate positive $\omega(\tau)$, given by (26), and hence yield imaginary eigenvalues of (20). Consequently, we look for positive solutions $\tau$ of (27) in the interval $(0, \tau^*)$.

Positive solutions $\tau \in (0, \tau^*)$ of (27) satisfy

$$\tau\sqrt{B^2(\tau) - A^2(\tau)} = \arccos\left(\frac{A(\tau)}{B(\tau)}\right) + 2k\pi, \qquad k \in \mathbb{N}_0,$$

where $\mathbb{N}_0$ denotes the set of all nonnegative integers. We set

$$\tau_k(\tau) = \frac{\arccos\left(\frac{A(\tau)}{B(\tau)}\right) + 2k\pi}{\sqrt{B^2(\tau) - A^2(\tau)}}, \qquad k \in \mathbb{N}_0, \tau \in [0, \tau^*).$$

Values of $\tau$ for which $\omega(\tau) = \sqrt{B^2(\tau) - A^2(\tau)}$ is a solution of (25) are roots of the functions

$$Z_k(\tau) = \tau - \tau_k(\tau), \qquad k \in \mathbb{N}_0, \tau \in [0, \tau^*). \tag{28}$$

The roots of $Z_k$ can be found using popular software like Maple, but are hard to determine with analytical tools [8]. The following lemma states some properties of the $Z_k$ functions.

LEMMA 5.3. *For $k \in \mathbb{N}_0$,*

$$Z_k(0) < 0 \qquad \textit{and} \qquad \lim_{\tau \to \tau^*} Z_k(\tau) = -\infty.$$

*Therefore, provided that no root of $Z_k$ is a local extremum, the number of positive roots of $Z_k$, $k \in \mathbb{N}_0$, on the interval $[0, \tau^*)$ is even.*

*Moreover, if $Z_k$ has no root on the interval $[0, \tau^*)$, then $Z_j$, with $j > k$, does not have positive roots.*

*Proof.* Notice first that $\tau_k(0) > 0$ and, second, that

$$\lim_{\tau \to \tau^*} \arccos\left(\frac{A(\tau)}{B(\tau)}\right) = \pi \qquad \text{and} \qquad \lim_{\tau \to \tau^*} \sqrt{B^2(\tau) - A^2(\tau)} = 0,$$

so $\lim_{\tau \to \tau^*} \tau_k(\tau) = +\infty$. Then the first statement holds.

To prove the second statement, one can notice that $\tau_{k+1}(\tau) > \tau_k(\tau)$, for $\tau \in [0, \tau^*)$ and $k \in \mathbb{N}_0$, so

$$Z_{k+1}(\tau) < Z_k(\tau), \qquad \tau \in [0, \tau^*), k \in \mathbb{N}_0.$$

Using the fact that $Z_k(0) < 0$, we conclude. This ends the proof. □

REMARK 5. *The second statement in Lemma 5.3 implies, in particular, that, if $Z_0$ has no positive root, then (25) has no positive solution, and equation (20) does not have pure imaginary roots.*

In the following proposition, we establish some properties of pure imaginary roots of equation (20) using a method described in [19].

PROPOSITION 5.1. *Let $\pm i\omega(\tau_c)$, with $\omega(\tau_c) > 0$, be a pair of pure imaginary roots of equation (20) when $\tau = \tau_c$. Then $\pm i\omega(\tau_c)$ are simple roots of (20) such that*

$$sign\left\{\frac{dRe(\lambda)}{d\tau}\bigg|_{\tau=\tau_c}\right\} = sign\Big\{-B^3 - B^2B'\tau_c + B(A^2 + A' + AA'\tau_c) - B'A\Big\}, \quad (29)$$

*where $A = A(\tau_c)$, $B = B(\tau_c)$, $A' = A'(\tau_c)$ and $B' = B'(\tau_c)$.*

*Proof.* We set

$$\Delta(\lambda, \tau) = \lambda + A(\tau) - B(\tau)e^{-\lambda\tau}.$$

Let $\lambda(\tau)$ be a family of roots of (20), so $\Delta(\lambda(\tau), \tau) = 0$, such that $\lambda(\tau_c)$ is a pure imaginary root of (20), given by $\lambda(\tau_c) = i\omega(\tau_c)$. Then,

$$\frac{d\lambda}{d\tau}(\tau)\Delta_\lambda(\lambda, \tau) + \Delta_\tau(\lambda, \tau) = 0, \quad (30)$$

where

$$\Delta_\lambda(\lambda, \tau) := \frac{d\Delta}{d\lambda}(\lambda, \tau) = 1 + B(\tau)\tau e^{-\lambda\tau},$$

and

$$\Delta_\tau(\lambda, \tau) := \frac{d\Delta}{d\tau}(\lambda, \tau) = A'(\tau) + [B(\tau)\lambda - B'(\tau)]e^{-\lambda\tau}.$$

Assume, by contradiction, that $\lambda(\tau_c) = i\omega(\tau_c)$ is not a simple root of (20). Then, from (30), $\Delta_\tau(i\omega(\tau_c), \tau_c) = A'(\tau_c) + [iB(\tau_c)\omega(\tau_c) - B'(\tau_c)]e^{-i\omega(\tau_c)\tau_c} = 0$. Separating real and imaginary parts in this equality, we deduce

$$\begin{aligned} B'(\tau_c)\cos(\omega(\tau_c)\tau_c) - B(\tau_c)\omega(\tau_c)\sin(\omega(\tau_c)\tau_c) &= A'(\tau_c), \\ B(\tau_c)\omega(\tau_c)\cos(\omega(\tau_c)\tau_c) + B'(\tau_c)\sin(\omega(\tau_c)\tau_c) &= 0. \end{aligned}$$

We recall that $B(\tau_c)$ is necessarily strictly negative. Using (25), the above system is equivalent to

$$\begin{aligned} \omega(\tau_c)^2 &= \frac{A(\tau_c)B'(\tau_c) - B(\tau_c)A'(\tau_c)}{B(\tau_c)}, \\ \omega(\tau_c)\left[A(\tau_c) + \frac{B'(\tau_c)}{B(\tau_c)}\right] &= 0. \end{aligned}$$

Since $\omega(\tau_c) > 0$ and satisfies, from (26), $\omega(\tau_c)^2 = B(\tau_c)^2 - A(\tau_c)^2$, we obtain

$$\begin{aligned} B(\tau_c)^2 - A(\tau_c)^2 &= \frac{A(\tau_c)B'(\tau_c) - B(\tau_c)A'(\tau_c)}{B(\tau_c)}, \\ A(\tau_c)B(\tau_c) &= -B'(\tau_c). \end{aligned}$$

Substituting the second equation in the first one, this yields $B(\tau_c)^2 - A(\tau_c)^2 = -A'(\tau_c) - A(\tau_c)^2$, so

$$B(\tau_c)^2 = -A'(\tau_c).$$

Since $B(\tau_c)^2 > 0$ and $A'(\tau_c) > 0$, we obtain a contradiction. Hence $\lambda(\tau_c) = i\omega(\tau_c)$ is a simple root of (20).

In the following, we do not mention the dependence of the coefficients $A$ and $B$ (and their derivatives) with respect to $\tau$.

Now, from (30), we obtain

$$\left(\frac{d\lambda}{d\tau}\right)^{-1} = \frac{e^{\lambda\tau} + B\tau}{B' - B\lambda - A'e^{\lambda\tau}}.$$

Since $\Delta(\lambda, \tau) = 0$, we deduce

$$e^{\lambda\tau} = \frac{B}{\lambda + A}.$$

Therefore,

$$\left(\frac{d\lambda}{d\tau}\right)^{-1} = \frac{B + B\tau(\lambda + A)}{(B' - B\lambda)(\lambda + A) - A'B}.$$

For $\tau = \tau_c$, we obtain

$$\begin{aligned}\left(\frac{d\lambda}{d\tau}\right)^{-1}\Big|_{\tau=\tau_c} &= \frac{B + B\tau_c(i\omega(\tau_c) + A)}{(B' - iB\omega(\tau_c))(i\omega(\tau_c) + A) - A'B},\\ &= \frac{B(1 + A\tau_c) + iB\omega(\tau_c)\tau_c}{B'A - AB' + B\omega^2(\tau_c) + i(B' - AB)\omega(\tau_c)}.\end{aligned}$$

Then,

$$\mathrm{Re}\left(\frac{d\lambda}{d\tau}\right)^{-1}\Big|_{\tau=\tau_c} = \frac{[B^2(1 + A\tau_c) + B\tau_c(B' - AB)]\omega(\tau_c)^2 + B(1 + A\tau_c)(B'A - A'B)}{[B'A - A'B + B\omega(\tau_c)^2] + [B' - AB]^2\omega(\tau_c)^2}.$$

Noticing that

$$\mathrm{sign}\left\{\frac{d\mathrm{Re}(\lambda)}{d\tau}\right\} = \mathrm{sign}\left\{\mathrm{Re}\left(\frac{d\lambda}{d\tau}\right)^{-1}\right\},$$

we get

$$\begin{aligned}\mathrm{sign}\left\{\frac{d\mathrm{Re}(\lambda)}{d\tau}\Big|_{\tau=\tau_c}\right\} = \mathrm{sign}\Big\{&[B^2(1 + A\tau_c) + B\tau_c(B' - AB)]\omega(\tau_c)^2\\ &+B(1 + A\tau_c)(B'A - A'B)\Big\}.\end{aligned} \tag{31}$$

Since $i\omega(\tau_c)$ is a purely imaginary root of (20), then, from (26),

$$\omega(\tau_c)^2 = B^2 - A^2.$$

Substituting this expression in (31), we obtain, after simplifications

$$\mathrm{sign}\left\{\frac{d\mathrm{Re}(\lambda)}{d\tau}\Big|_{\tau=\tau_c}\right\} = \mathrm{sign}\Big\{B\left[B^3 + B^2B'\tau_c - B(A^2 + A' + AA'\tau_c) + B'A\right]\Big\}.$$

As we already noticed, if equation (20) has pure imaginary roots then necessarily $B < 0$. We then deduce (29) and the proof is complete. □

Using this last proposition and the previous results about the existence of purely imaginary roots of (13), we can state and prove the following theorem, dealing with the asymptotic stability of $E^*$.

THEOREM 5.1. *Assume that (9) holds true and ($H_1$) and ($H_2$) are fulfilled.*

(i) *If $Z_0$ (defined in (28)) has no root on the interval $[0, \tau^*)$, $\tau^*$ defined in Lemma 5.2, then the positive steady state $E^* = (S^*, N^*)$ of (3)–(4) is locally asymptotically stable for $\tau \in [0, \overline{\tau})$.*

(ii) *If $Z_0$ has at least one positive root $\tau_c \in (0, \tau^*)$, then $E^*$ is locally asymptotically stable for $\tau \in [0, \tau_c)$ and a Hopf bifurcation occurs at $E^*$ for $\tau = \tau_c$ if*

$$B(A^2 + A' + AA'\tau_c) - B^3 - B^2B'\tau_c - B'A \neq 0, \tag{32}$$

*where $A = A(\tau_c)$, $B = B(\tau_c)$, $A' = A'(\tau_c)$ and $B' = B'(\tau_c)$.*

*Proof.* First, from Lemma 5.1, we know that $E^*$ is locally asymptotically stable when $\tau = 0$.

If $Z_0$ has no positive root on the interval $(0, \tau^*)$, then the characteristic equation (13) has no pure imaginary root (see Remark 5 and Lemma 5.3). Consequently, the stability of $E^*$ cannot be lost when $\tau$ increases. We obtain the statement in (i).

Now, if $Z_0$ has at least one positive root, say $\tau_c \in (0, \tau^*)$, then equation (13) has a pair of simple conjugate pure imaginary roots $\pm i\omega(\tau_c)$ for $\tau = \tau_c$. From (32) together with Proposition 5.1, we have either

$$\left.\frac{d\mathrm{Re}(\lambda)}{d\tau}\right|_{\tau=\tau_c} > 0 \qquad \text{or} \qquad \left.\frac{d\mathrm{Re}(\lambda)}{d\tau}\right|_{\tau=\tau_c} < 0.$$

By contradiction, we assume that there exists a branch of characteristic roots $\lambda(\tau)$ such that $\lambda(\tau_c) = i\omega_c$ and

$$\frac{d\mathrm{Re}(\lambda(\tau))}{d\tau} < 0$$

for $\tau < \tau_c$, $\tau$ close to $\tau_c$. Then there exists a characteristic root $\lambda(\tau)$ such that $\mathrm{Re}(\lambda(\tau)) > 0$ and $\tau < \tau_c$. Since $E^*$ is locally asymptotically stable when $\tau = 0$, applying Rouché's Theorem [11], we obtain that all characteristic roots of (13) have negative real parts when $\tau \in [0, \tau_c)$, and we obtain a contradiction. Thus,

$$\left.\frac{d\mathrm{Re}(\lambda)}{d\tau}\right|_{\tau=\tau_c} > 0.$$

In this case, a Hopf bifurcation occurs at $E^*$ when $\tau = \tau_c$. □

The result stated in (ii) leads, through the Hopf bifurcation, to the existence of periodic solutions for system (3)–(4).

In the next section, we apply the above-mentioned results of stability to a particular introduction rate $\beta$ and we present some numerical illustrations.

6. **Example and Numerical Simulations.** We develop, in this section, numerical illustrations of the above mentioned results (mainly the ones stated in Theorem 5.1).

Let us define (see [20, 21, 28, 29]) the introduction rate $\beta$ by

$$\beta(S) = \beta_0 \frac{\theta^n}{\theta^n + S^n}, \qquad \beta_0, \theta \geq 0,\ n > 1.$$

The parameter $\beta_0$ represents the maximal rate of introduction in the proliferating phase, $\theta$ is the value for which $\beta$ attains half of its maximum value, and $n$ is the sensitivity of the rate of reintroduction. The coefficient $n$ describes the reaction of $\beta$ due to external stimuli, the action of a growth factor for example (some growth factors are known to trigger the introduction of nonproliferating cells in the proliferating phase [7, 27]).

Then, from (9), the unique positive steady state of (3)–(4) exists if and only if

$$\delta < \beta_0 \qquad \text{and} \qquad 0 \leq \tau < \overline{\tau} = \frac{1}{\delta} \ln\left(\frac{2\beta_0}{\delta + \beta_0}\right).$$

From (5)–(6), it is defined by

$$S^* = \theta\left(\frac{(2e^{-\delta\tau}-1)\beta_0}{\delta}-1\right)^{1/n} \quad \text{and} \quad N^* = \theta\frac{2e^{-\delta\tau}-1}{e^{-\delta\tau}}\left(\frac{(2e^{-\delta\tau}-1)\beta_0}{\delta}-1\right)^{1/n}$$

Note that the function $\beta^{-1}$ is defined by $\beta^{-1}(x) = \theta(\beta_0/x-1)^{1/n}$ for $x \in (0,\beta_0]$.

After computations, we can state that condition (24) is equivalent to

$$\tau < \tau^* := \frac{1}{\delta}\ln\left(\frac{2\beta_0(n-2)}{n(\beta_0+\delta)}\right),$$

provided that

$$n > \frac{4\beta_0}{\beta_0-\delta}. \tag{33}$$

Noticing that the function $\chi$, defined in Lemma 5.2, is given by

$$\chi(y) = -n\beta_0\frac{\theta^n y^n}{(\theta^n+y^n)^2},$$

one can check that (33) is equivalent to $(H_2)$.

However, the function $\chi$ does not necessarily satisfy $(H_1)$, which is too strong (as mentioned in Remark 4). For $y \geq 0$,

$$\chi'(y) = \frac{\beta_0 n^2\theta^n y^{n-1}}{(\theta^n+y^n)^3}(y^n-\theta^n).$$

Consequently, $\chi$ is decreasing for $y \leq \theta$ and increasing for $y > \theta$. Taking $y = \beta^{-1}(\delta)$, we find that $\chi$ is decreasing on $[0,\beta^{-1}(\delta)]$ if and only if $\beta_0 < 2\delta$. In this case, $(H_1)$ is fulfilled. If $\beta_0 > 2\delta$, then $\chi$ is decreasing on the interval $[0,\theta]$ and increasing on $[\theta,\beta^{-1}(\delta)]$, yet $\tau^*$ is uniquely defined.

Note that

$$A(\tau) = \frac{2\delta e^{-\delta\tau}}{2e^{-\delta\tau}-1} \quad \text{and} \quad B(\tau) = \frac{2\delta\beta_0 e^{-\delta\tau} - n\delta[(2e^{-\delta\tau}-1)\beta_0-\delta]}{(2e^{-\delta\tau}-1)\beta_0},$$

with

$$A'(\tau) = \frac{2\delta^2 e^{-\delta\tau}}{(2e^{-\delta\tau}-1)^2} \qquad \text{and} \qquad B'(\tau) = \frac{2\delta^2 e^{-\delta\tau}(\beta_0+n\delta)}{(2e^{-\delta\tau}-1)^2\beta_0}.$$

Then, assuming that (33) holds true, we define the $Z_k$ functions, as in (28), for $\tau \in [0,\tau^*)$ by

$$Z_k(\tau) = \tau - \frac{\arccos\left(\frac{A(\tau)}{B(\tau)}\right)+2k\pi}{\sqrt{B^2(\tau)-A^2(\tau)}}, \quad k \in \mathbb{N}_0, \tau \in [0,\tau^*).$$

We choose the parameters according to [20, 28, 29]:

$$\delta = 0.05 \text{ days}^{-1}, \quad \beta_0 = 1.77 \text{ days}^{-1}, \quad \theta = 1. \tag{34}$$

Notice that the value of $\theta$ is in fact normalized and does not influence the stability of system (3)–(4) since all coefficients actually do not depend on $\theta$. The value of $\theta$ only influences the shape of the oscillations and the values of the steady states.

Using Maple to determine the roots of $Z_n$, we first check that $Z_0$ (and consequently all $Z_k$ functions) is strictly negative on $[0,\tau^*)$ for $n \leq 10$. Hence, from Theorem 5.1, the positive steady state $E^* = (S^*, N^*)$ of (3)–(4) is locally asymptotically stable for $\tau \in [0,\overline{\tau})$.

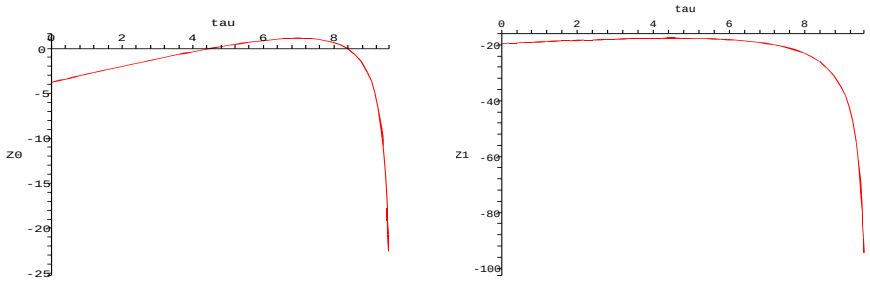


FIGURE 1. The functions $Z_0$ (left) and $Z_1$ (right) are drawn on the interval $[0, \tau^*)$ for parameters given by (34) and $n = 12$. One can see that $Z_0$ has exactly two roots, $\tau_1 \simeq 4.52$ and $\tau_2 \simeq 8.36$, and $Z_1$ has no root.

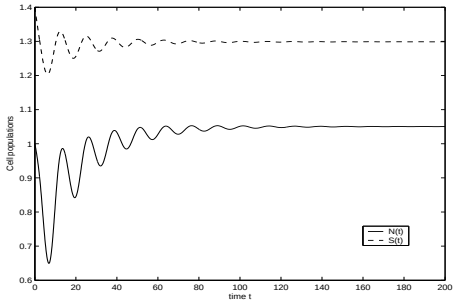


FIGURE 2. For $\tau = 3.5$ days and the other parameters given by (34) with $n = 12$, the solutions $S(t)$ (dashed line) and $N(t)$ (solid line) oscillate transiently to the steady state, which is asymptotically stable. Damped oscillations are observed.

For $n \geq 10$, Pujo-Menjouet et al. [28, 29] noticed, for the model (1)–(2) with the introduction rate $\beta$ depending only upon the nonproliferating phase population $N(t)$, that oscillations may be observed.

We choose $n = 12$, in keeping with values in [28, 29]. Then, we find that

$$\overline{\tau} \simeq 13.3 \text{ days} \qquad \text{and} \qquad \tau^* \simeq 9.66 \text{ days}.$$

One can see in Figure 1 that $Z_0$ has two positive roots in this case, $\tau_1 \simeq 4.52$ days and $\tau_2 \simeq 8.36$ days, and that $Z_1$ is strictly negative, so all $Z_k$ functions with $k \geq 1$ have no roots. Consequently, there exist two critical values, $\tau_1$ and $\tau_2$, for which a stability switch can occur at $E^*$.

For $\tau < \tau_1$, one can check that the populations are asymptotically stable on Figure 2. In this case $\tau = 3.5$ days and the solutions of (3)–(4) oscillate transiently to the steady state. Numerical simulations of the solutions of (3)–(4) are carried out with dde23 [30], a MATLAB solver for delay differential equations.

When $\tau = \tau_1$, one can check that

$$B(A^2 + A' + AA'\tau_c) - B^3 - B^2B'\tau_c - B'A \simeq 0.053,$$

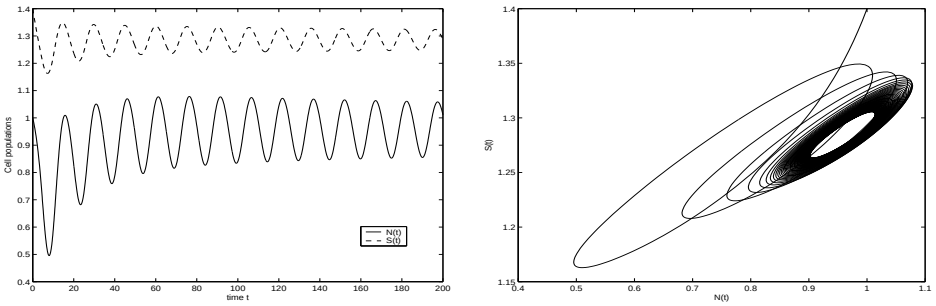


(a) (b)

FIGURE 3. For $\tau = 4.52$ days and the other parameters given by (34) with $n = 12$, a Hopf bifurcation occurs and the steady state $(S^*, N^*)$ of (3)–(4) is unstable. The periodic solutions $S(t)$ (dashed line) and $N(t)$ (solid line) are represented in (a), and we can observe the solutions in the $(S, N)$-plane in (b). Periods of the oscillations are about 15 days.

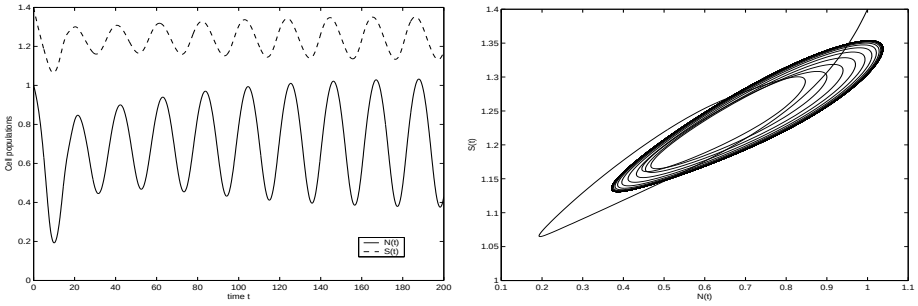


FIGURE 4. For $\tau = 7$ days and the other parameters given by (34) with $n = 12$, long periods oscillations are observed, with periods about 20-25 days. The steady state $E^*$ is unstable.

so condition (32) holds, and a Hopf bifurcation occurs at $(S^*, N^*)$, from Theorem 5.1. This is illustrated on Figure 3. Periodic solutions with periods about 15 days are observed at the bifurcation, and the steady state $E^*$ becomes unstable.

When $\tau$ increases after the bifurcation, one can observe oscillating solutions with longer periods (in the order of 20 to 30 days), as it can be seen in Figure 4.

This phenomenon has already been observed by Pujo-Menjouet et al. [28, 29]. It can be related to diseases affecting blood cells, the so-called periodic hematological diseases [18], which are characterized by oscillations of circulating blood cell counts with long periods compared to the cell cycle duration. Among the wide variety of periodic hematological diseases, we can cite chronic myelogenous leukemia [5, 15, 28], a cancer of white blood cells with periods usually falling in the range of 70 to 80 days, and cyclical neutropenia [9, 18], which is known to exhibit oscillations around 3 weeks of circulating neutrophils (white cells), as observed in Figure 4.

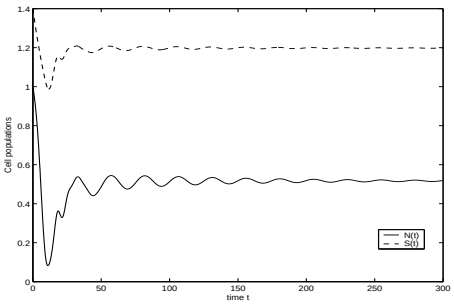


FIGURE 5. For $\tau = 9$ days and the other parameters given by (34) with $n = 12$, damped oscillations are observed and the steady state is stable.

Eventually, one can note that when $\tau$ passes through the second critical value $\tau_2$, stability switches, and then the steady state $(S^*, N^*)$ becomes stable again (see Figure 5).

7. **Discussion.** We considered a nonlinear model of blood cell dynamics in which the nonlinearity depends upon the entire hematopoietic stem cell population, contrary to the common assumption used in previous works [4, 5, 9, 20, 21, 28, 29] dealing with blood cell production models. Then we were led to the study of a new nonlinear system of two differential equations with delay (describing the cell cycle duration) modelling the hematopoietic stem cells dynamics.

We obtained the existence of two steady states for this model: a trivial one and a positive delay-dependent steady state. Through sections 4 and 5, we performed the stability analysis of our model. We determined necessary and sufficient conditions for the global asymptotic stability of the trivial steady state of system (3)–(4), which describes the population's dying out. Using an approach proposed by Beretta and Kuang [8], we analyzed a first-degree exponential polynomial characteristic equation with delay-dependent coefficients to obtain the existence of a Hopf bifurcation for the positive steady state (see Theorem 5.1) leading to the existence of periodic solutions.

In the example presented in the previous section, we obtained long-period oscillations, which can be related to some periodic hematological diseases (in particular, to cyclical neutropenia [9]). This result is in keeping with previous analysis of blood cell dynamics models (as can be found in [20, 28, 29]). Periodic hematological diseases are particular diseases mostly originated from the hematopoietic stem cell compartment. The appearance of periodic solutions in our model with periods that can be related to the ones observed in some periodic hematological diseases stresses the interesting properties displayed by our model. Periods of oscillating solutions can for example be used to determine the length of cell cycles in hematopoietic stem cell populations that cannot be directly determined experimentally.

Moreover, stability switches have been observed, due to the structure of the equations (nonlinear equations with delay-dependent coefficients). Such a behavior had been noted in previous works dealing with blood cell production models (see [28, 29]), but it had never been mathematically explained.

We can note that our assumption, that proliferating and nonproliferating cells die at the same rate, may be too limitative, since Pujo-Menjouet et al. [28, 29]

already noticed that the apoptotic rate (the proliferating phase mortality rate $\gamma$) plays an important role in the appearance of oscillating solutions. However, by assuming that the two populations die with different rates, we are led to a second-order exponential polynomial characteristic equation, and the calculations are more difficult than the ones carried out in the present work. We leave it for further analysis.

## REFERENCES


[1] M. Adimy and F. Crauste, Global stability of a partial differential equation with distributed delay due to cellular replication, Nonlinear Analysis 54 (2003) 1469–1491.

[2] M. Adimy and F. Crauste, Existence, positivity and stability for a nonlinear model of cellular proliferation, Nonlinear Analysis: Real World Applications 6(2) (2005) 337–366.

[3] M. Adimy, F. Crauste and L. Pujo-Menjouet, On the stability of a maturity structured model of cellular proliferation, Discret. Cont. Dyn. Sys. Ser. A 12(3) (2005) 501–522.

[4] M. Adimy, F. Crauste and S. Ruan, A mathematical study of the hematopoiesis process with applications to chronic myelogenous leukemia, SIAM J. Appl. Math. 65(4) (2005) 1328–1352.

[5] M. Adimy, F. Crauste and S. Ruan, Stability and Hopf bifurcation in a mathematical model of pluripotent stem cell dynamics, Nonlinear Analysis: Real World Applications 6(4) (2005) 651–670.

[6] M. Adimy and L. Pujo-Menjouet, Asymptotic behaviour of a singular transport equation modelling cell division, Discret. Cont. Dyn. Syst. Ser. B 3 (2003) 439–456.

[7] J. Bélair, M.C. Mackey and J.M. Mahaffy, Age-structured and two-delay models for erythropoiesis, Math. Biosci. 128 (1995) 317–346.

[8] E. Beretta and Y. Kuang, Geometric stability switch criteria in delay differential systems with delay dependent parameters, SIAM J. Math. Anal. 33(5) (2002) 1144–1165.

[9] S. Bernard, J. Bélair and M.C. Mackey, Oscillations in cyclical neutropenia: New evidence based on mathematical modeling, J. Theor. Biol. 223 (2003) 283–298.

[10] F.J. Burns and I.F. Tannock, On the existence of a $G_0$ phase in the cell cycle, Cell Tissue Kinet. 19 (1970) 321–334.

[11] J. Dieudonné, Foundations of Modern Analysis, Academic Press, New-York, 1960.

[12] J. Dyson, R. Villella-Bressan and G.F. Webb, A nonlinear age and maturity structured model of population dynamics. I: Basic theory., J. Math. Anal. Appl. 242(1) (2000) 93–104.

[13] J. Dyson, R. Villella-Bressan and G.F. Webb, A nonlinear age and maturity structured model of population dynamics. II: Chaos., J. Math. Anal. Appl. 242(2) 255–270.

[14] J. Dyson, R. Villella-Bressan and G.F. Webb, Asynchronous exponential growth in an age structured population of proliferating and quiescent cells, Math. Biosci. 177–178 (2002) 73–83.

[15] P. Fortin and M.C. Mackey, Periodic chronic myelogenous leukemia: Spectral analysis of blood cell counts and etiological implications, Brit. J. Haematol. 104 (1999) 336–345.

[16] K. Gopalsamy, Stability and oscillations in delay differential equations of population dynamics, Mathematics and its Applications 74, Kluwer Academic Publishers Group, Dordrecht, 1992.

[17] J. Hale and S.M. Verduyn Lunel, Introduction to functional differential equations, Applied Mathematical Sciences 99, Springer-Verlag, New York, 1993.

[18] C. Haurie, D.C. Dale and M.C. Mackey, Cyclical neutropenia and other hematological disorders: A review of mechanisms and mathematical models, Blood 92(8) (1998) 2629–2640.

[19] Y. Kuang, Delay differential equations with applications in population dynamics, Mathematics in Science and Engineering 191, Academic Press, New York, 1993.

[20] M.C. Mackey, Unified hypothesis of the origin of aplastic anaemia and periodic hematopoiesis, Blood 51 (1978) 941–956.

[21] M.C. Mackey, Dynamic hematological disorders of stem cell origin, in J.G. Vassileva-Popova and E.V. Jensen (Eds), Biophysical and biochemical information transfer in recognition, Plenum Press, New York, 941–956, 1979.

[22] M.C. Mackey and A. Rey, Multistability and boundary layer development in a transport equation with retarded arguments, Can. Appl. Math. Quart. 1 (1993) 1–21.
[23] M.C. Mackey and A. Rey, Propagation of population pulses and fronts in a cell replication problem: non-locality and dependence on the initial function, Physica D 86 (1995) 373–395.
[24] M.C. Mackey and A. Rey, Transitions and kinematics of reaction-convection fronts in a cell population model, Physica D 80 (1995) 120–139.
[25] M.C. Mackey and R. Rudnicki, Global stability in a delayed partial differential equation describing cellular replication, J. Math. Biol. 33 (1994) 89–109.
[26] M.C. Mackey and R. Rudnicki, A new criterion for the global stability of simultaneous cell replication and maturation processes, J. Math. Biol. 38 (1999) 195–219.
[27] J.M. Mahaffy, J. Bélair and M.C. Mackey, Hematopoietic model with moving boundary condition and state dependent delay, J. Theor. Biol. 190 (1998) 135–146.
[28] L. Pujo-Menjouet, S. Bernard and M.C. Mackey, Long period oscillations in a $G_0$ model of hematopoietic stem cells, SIAM J. Appl. Dyn. Systems 4(2) (2005) 312–332.
[29] L. Pujo-Menjouet and M.C. Mackey, Contribution to the study of periodic chronic myelogenous leukemia, C. R. Biologies 327 (2004) 235–244.
[30] L.F. Shampine and S. Thompson, Solving DDEs in Matlab, Appl. Numer. Math. 37 (2001) 441–458. http://www.radford.edu/ thompson/webddes/

Received on October 11, 2005. Accepted on January 16, 2006.

*E-mail address*: fabien.crauste@univ-pau.fr

## 5.2 Crauste (2011)

Manuscrit de l'article : [54] F. Crauste, *A review on local asymptotic stability analysis for mathematical models of hematopoiesis with delay and delay-dependent coefficients*, Annals of the Tiberiu Popoviciu Seminar of functionnal equations, approximation and convexity, vol 9, 121–143 (2011).

**Annals of the Tiberiu Popoviciu Seminar**
of Functional Equations, Approximation and Convexity
ISSN 1584-4536, vol 9, 2011, pp. 121–143.

# A Review on Local Asymptotic Stability Analysis for Mathematical Models of Hematopoiesis with Delay and Delay-Dependent Coefficients

Fabien Crauste
(Lyon)

Abstract. Stability analysis of mathematical models of hematopoiesis (blood cell production process), described by differential equations with delay, needs to locate eigenvalues of characteristic equations that are usually exponential polynomial functions with delay-dependent coefficients. It is then more complicated than for ordinary differential equations to determine conditions for all roots to have negative real parts. We present, on three models of increasing complexity, the tools and method that can be used, with their advantages and their limitations. The method consists in the reduction of the problem to the localization of roots of a real function, these roots giving critical values of the delay for which stability possibly switches.

Key Words: Delay differential equations, delay-dependent coefficients, asymptotic stability, characteristic equation, exponential polynomial
MSC 2000: 34D20, 34K60, 92C37

◊Fabien Crauste, Université de Lyon, Université Lyon 1, CNRS UMR 5208, Institut Camille Jordan, 43 blvd du 11 novembre 1918, F-69622 Villeurbanne-Cedex, France, email: crauste@math.univ-lyon1.fr

## 1 Introduction

Mathematical modeling of hematopoiesis, the process of production and regulation of blood cells, has attracted a lot of attention since the end of the 1970's and the pioneering work of Mackey [23]. Based on Lajtha [22] and Burns and Tannock [11] works, Mackey proposed a system of two ordinary differential equations with delay to describe the dynamics of hematopoietic stem cell (HSC) populations, and applied his model to a blood disease, aplastic anemia. Mackey's model has been later studied, and improved by many authors, including Mackey and co-workers [12, 13, 18], see also Adimy et al [2, 3, 4, 5, 6, 7, 8], and the references therein. Such models are relevant due to their ability to describe some hematological diseases [18], like leukemia, through instabilities and oscillatory behaviors.

Analysis of Mackey's models, and subsequent related models based on delay differential systems, lies on the ability to determine conditions for the stability or the instability of steady states, and to characterize the change of stability. Global stability of steady states can sometimes be obtained with a Lyapunov function [5, 14, 15, 19], however for hematopoiesis models such conclusions can usually be reached only for the steady state describing cell extinction, which is consequently not the steady state expected to be asymptotically stable. For positive steady states, global stability is most of the time hard to establish, so determining local asymptotic stability represents a challenging work with potentially relevant results.

Local asymptotic stability of the steady state of a delay differential equation or system is obtained by studying a characteristic equation which is an exponential polynomial, and by locating eigenvalues with negative real parts. Loss of stability is obtained when eigenvalues cross on the imaginary axis [21]. Nevertheless, contrary to what happens with ordinary differential systems, the number of roots of an exponential polynomial is not finite, and determining explicitly its roots is usually impossible. In the case of hematopoiesis models, one difficulty is added: coefficients of the characteristic equations usually depend on the delay, either explicitly or implicitly through values of the steady states. Hence, analysis of the characteristic equations is often hard to perform.

We present here a review of some models of hematopoiesis dynamics for which exponential polynomial characteristic equations with delay-dependent

coefficients must be studied in order to determine asymptotic stability of the positive steady state. Three different cases are presented with increasing degree of the polynomial part of the characteristic equation, and difficulties are stressed out. A new model of erythropoiesis (red blood cell production), based on Adimy et al. [4] and Crauste et al. [17], is proposed to illustrate the case of a 3rd degree exponential polynomial characteristic equation. Analysis is allowed due to a method developed by Beretta and Kuang [9] for delay-dependent coefficient characteristic equations. We present the pros and cons of this method in the framework of hematopoiesis modeling.

## 2 Models of Quiescent and Proliferating cells

In 1978, Mackey [23] proposed a model of hematopoietic stem cell dynamics, based on two distinct populations: a quiescent one and a proliferating one. Both cell populations can die, with different death rates, and the main assumptions are the following: (a) quiescent cells are randomly introduced in the proliferating phase with a rate depending on their own amount, and (b) proliferating cells age and divide a fixed time $\tau$ after their introduction in the phase, to give two cells which immediately enter the quiescent phase. The model is illustrated in Figure 1.

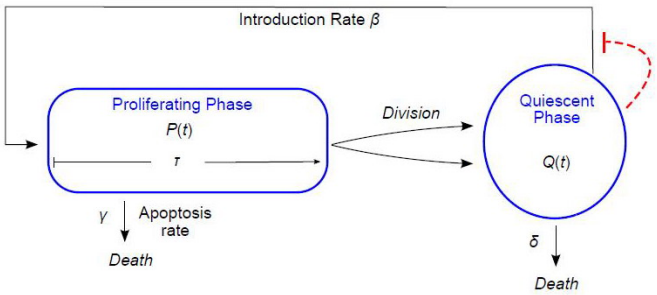


Figure 1: Schematic representation of HSC dynamics, from Mackey [23]. The dashed line represents the feedback control from quiescent cells on their own introduction in the proliferating phase.

The model has the form of a system of two differential equations with a discrete delay $\tau$,

$$\frac{dQ}{dt}(t) = -\delta Q(t) - \beta(Q(t))Q(t) + 2e^{-\gamma\tau}\beta(Q(t-\tau))Q(t-\tau), \tag{2.1}$$

$$\frac{dP}{dt}(t) = -\gamma P(t) + \beta(Q(t))Q(t) - e^{-\gamma\tau}\beta(Q(t-\tau))Q(t-\tau), \tag{2.2}$$

where $Q(t)$ denotes the number of quiescent cells at time $t$, $P(t)$ the number of proliferating cells at time $t$, $\delta$ and $\gamma$ the death rates, $\tau$ the length of the proliferating phase, and $\beta$ is the introduction rate of quiescent cells into the proliferating phase. The rate $\beta$ is assumed to depend on the number of quiescent cells $Q(t)$. The function $\beta$ is naturally assumed to be decreasing, bounded and positive with $\lim_{Q\to\infty}\beta(Q) = 0$ [23].

Existence and uniqueness of solutions of system (2.1)(2.2) can be deduced from Hale and Verduyn Lunel [19], by assuming the nonlinear term $\beta(Q)Q$ is a Lipschitz function. The same reasoning can be applied to examples considered in other Sections. Boundedness of solutions can also be rather easily obtained when death rates are supposed to be positive [5, 14, 15].

It is straightforward that equation (2.2) is decoupled from equation (2.1), so the analysis of (2.1)(2.2) reduces to the analysis of equation (2.1). A steady state of (2.1) is a solution $\overline{Q}$ satisfying

$$\frac{d\overline{Q}}{dt}(t) = 0 = (2e^{-\gamma\tau} - 1)\beta(\overline{Q})\overline{Q} - \delta\overline{Q}.$$

Hence, it is clear that (2.1) has one trivial steady state, $\overline{Q} = 0$, and a positive steady state $\overline{Q} = Q^*$, defined by

$$Q^* = \beta^{-1}\left(\frac{\delta}{2e^{-\gamma\tau} - 1}\right), \tag{2.3}$$

provided that

$$(2e^{-\gamma\tau} - 1)\beta(0) > \delta. \tag{2.4}$$

Inequality (2.4) describes a situation in which the maximum renewal rate ($2e^{-\gamma\tau}\beta(0)$) is larger than the disappearance rate ($\delta + \beta(0)$). Biologically, this condition is necessary for the survival of the cell population.

Global asymptotic stability of the trivial steady state may be obtained through a Lyapunov function [14, 19]. However, we are interested here in the stability of the positive steady state, and particularly in its local asymptotic stability, so we will not detail this point.

The characteristic equation of the linearized equation of (2.1) is

$$\Delta(\lambda,\tau) := \lambda + \delta + \beta^* - 2\beta^* e^{-\gamma\tau}e^{-\lambda\tau} = 0, \tag{2.5}$$

where $\beta^* = \beta(Q^*)+Q^*\beta'(Q^*)$. Contrary to an ordinary differential equation, the characteristic equation $\Delta$ defined in (2.5) is not a polynomial function but an exponential polynomial, of degree 1. Consequently, the characteristic equation has an infinite number of eigenvalues. Moreover, coefficients of the characteristic equation depend, explicitly or implicitly, on the delay $\tau$ (for instance, through the steady state value in $\beta^*$), and consequently locating the roots of $\Delta$ is not an easy task.

In order to analyze the stability of the positive steady state $Q^*$ with respect to values of the parameters, in particular of the value of the delay $\tau$, it is necessary to determine conditions for which stability can be ensured. To that aim, let's check whether the characteristic equation has roots with negative real parts when the delay $\tau$ equals zero. One gets

$$\Delta(\lambda,0) := \lambda + \delta - \beta^*,$$

so there is only one real root in this case, $\lambda = \beta^* - \delta$, that is with (2.3), $\lambda = Q^*\beta'(Q^*) < 0$. Hence, the steady state is locally asymptotically stable in the absence of delay.

Beretta and Kuang [9] proposed a method to determine critical values of $\tau$ for which eigenvalues cross the imaginary axis, and so stability is lost. We illustrate this method on the above example, and we determine conditions for local asymptotic stability of the positive steady state $Q^*$.

Consider a characteristic function in the form of an exponential polynomial function

$$\Delta(\lambda,\tau) = R_1(\lambda,\tau) + R_2(\lambda,\tau)e^{-\lambda\tau}, \tag{2.6}$$

where $R_1$ and $R_2$ are two polynomial functions of $\lambda$ with coefficients depending on the delay $\tau$, satisfying $\deg(R_1(\lambda,\cdot)) > \deg(R_2(\lambda,\cdot))$. The following properties must be verified

(i) $R_1(0,\tau) + R_2(0,\tau) \neq 0$;

(ii) $R_1(i\omega,\tau) + R_2(i\omega,\tau) \neq 0$;

(iii) $\limsup\left\{\left|\dfrac{R_2(\lambda,\tau)}{R_1(\lambda,\tau)}\right|;\ |\lambda|\to\infty,\ \mathrm{Re}\lambda \geq 0\right\} < 1$;

(iv) $F(\omega,\tau) := |R_1(i\omega,\tau)|^2 - |R_2(i\omega,\tau)|^2$ has a finite number of zeros,

in order to define a well-posed framework in which determining conditions on the parameters for the loss of stability (pure imaginary roots appear) is equivalent to locating a finite number of roots of an explicit function of the delay $\tau$. For instance, condition (i) ensures that $\lambda = 0$ is not a root of $\Delta$. Conditions (i) to (iv) must be verified for all $\tau \in [0, \tau_{\max})$ where $\tau_{\max}$ is, for instance, given by (2.4) (definition domain of the steady state).

Let us check that properties (i) to (iv) are satisfied on our example. First, one has, from (2.4),

$$R_1(0,\tau) + R_2(0,\tau) = \delta + \beta^* - 2\beta^* e^{-\gamma\tau} = -(2e^{-\gamma\tau} - 1)Q^*\beta'(Q^*) > 0. \tag{2.7}$$

Second,

$$R_1(i\omega,\tau) + R_2(i\omega,\tau) = -(2e^{-\gamma\tau} - 1)Q^*\beta'(Q^*) + i\omega \neq 0.$$

Third,

$$\limsup\left\{\left|\frac{R_2(\lambda,\tau)}{R_1(\lambda,\tau)}\right|;\ |\lambda|\to\infty,\ \mathrm{Re}\lambda \geq 0\right\} = 0 < 1.$$

Fourth,

$$F(\omega,\tau) := \omega^2 + (\delta + \beta^*)^2 - (2\beta^* e^{-\gamma\tau})^2.$$

It follows that $F(\omega,\tau)$ has a finite number of zeros,

$$\omega = \pm[(2\beta^* e^{-\gamma\tau})^2 - (\delta + \beta^*)^2]^{1/2}, \tag{2.8}$$

provided that

$$(2\beta^* e^{-\gamma\tau})^2 > (\delta + \beta^*)^2. \tag{2.9}$$

Thanks to (2.7), (2.9) is equivalent to

$$(2e^{-\gamma\tau}+1)\beta^*+\delta<0.$$

Condition (2.9) allows actually to define an interval $[0,\tau^*)$ in which one can search for critical values of $\tau$. Hence, positive roots $\omega$ defined in (2.8) are in fact functions of the delay $\tau$, so $\omega=\omega(\tau)$.

The method proposed by Beretta and Kuang [9] consists in determining critical values of $\tau$ using roots of $F(\cdot,\tau)$. Separating real and imaginary parts in (2.5) and searching for purely imaginary roots $\lambda=i\omega$ reduces to

$$\cos(\tau\omega(\tau))=\frac{\delta+\beta^*}{2\beta^*e^{-\gamma\tau}},\quad \sin(\tau\omega(\tau))=-\frac{\omega(\tau)}{2\beta^*e^{-\gamma\tau}}. \tag{2.10}$$

The problem now becomes to be able to find out values of $\tau$ satisfying (2.10). Indeed, by adding the squares of both equations in (2.10), one can check that values of $\omega$ and $\tau$ such that (2.10) is satisfied must verify $F(\omega,\tau)=0$. Setting, for $\tau\in[0,\tau^*)$,

$$\tau_k(\tau)=\frac{1}{\omega(\tau)}\left[\arccos\left(\frac{\delta+\beta^*}{2\beta^*e^{-\gamma\tau}}\right)+2k\pi\right],\quad k\in\mathbb{N}_0,$$

where $\omega(\tau)$ is given by (2.8), values of $\tau$ for which $(\omega(\tau),\tau)$ given by (2.8) and (2.9) is a solution of (2.10) are roots of the functions

$$Z_k(\tau):=\tau-\tau_k(\tau),\quad k\in\mathbb{N}_0,\ \tau\in[0,\tau^*). \tag{2.11}$$

Hence the problem of finding critical values of $\tau$ reduces to finding roots of a real function. The roots of $Z_k$ can be found using popular software, yet they are hard to determine with analytical tools [9]. The following lemma states some properties of the $Z_k$ functions [14], that are quite general in the kind of problems we focus on. We refer to [14] for the proof.

**Lemma 2.1** *For $k\in\mathbb{N}_0$,*

$$Z_k(0)<0\quad \textit{and}\quad \lim_{\tau\to\tau^*}Z_k(\tau)=-\infty.$$

*Therefore, provided that no root of $Z_k$ is a local extremum, the number of*

*positive roots of $Z_k$, $k \in \mathbb{N}_0$, on the interval $[0, \tau^*)$ is even. Moreover, if $Z_k$ has no root on the interval $[0, \tau^*)$, then $Z_j$, with $j > k$, does not have positive roots.*

The last statement in Lemma 2.1 implies, in particular, that, if $Z_0$ has no positive root, then (2.10) has no positive solution, and equation (2.5) does not have pure imaginary roots, so the steady state is always stable.

The analysis of functions $Z_k(\tau)$ allows determining values of the delay for which stability switches. An illustration is displayed in Figure 2, where functions $Z_0$, $Z_1$ and $Z_2$ have been drawn using Matlab, all defined by (2.11) with parameters from Crauste [14, 15].

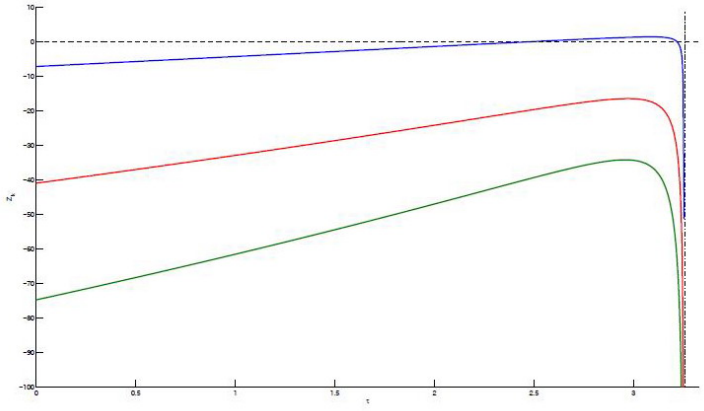

Figure 2: Functions $Z_k$, with $k = 1, 2, 3$, defined by (2.11). The above curve is $Z_0$, the middle one $Z_1$ and the bottom one $Z_2$. The vertical dashed curve on the right hand side indicates the value of $\tau^*$.

One can observe that $Z_0$ has two positive roots, hence there are two critical values of the delay $\tau$ for which stability switches, whereas $Z_1$, and consequently $Z_2$, has no positive root. In order to determine the nature of the instability (Hopf bifurcation, etc.) related to critical values of the delay, it is however necessary to go deeper in the analysis. We do not want to

focus on this point here, so we refer to [14, 21] for the interested reader. We can however mention that it is possible to show that stability of $Q^*$ switches through a Hopf bifurcation.

A modification of Mackey's model, proposed in 2006 [14], considering an introduction rate depending on the total population of hematopoietic stem cells, $S(t) := P(t) + Q(t)$ also reduces to the study of a characteristic equation in the form of (2.5), when assuming death rates of both quiescent and proliferating populations are the same. Considering different mortality rates leads to the following system [15],

$$\begin{cases} \dfrac{dQ}{dt}(t) = -[\delta + \beta(S(t))]Q(t) + 2e^{-\gamma\tau}\beta(S(t-\tau))Q(t-\tau), \\ \dfrac{dS}{dt}(t) = -\gamma S(t) + (\gamma - \delta)Q(t) + e^{-\gamma\tau}\beta(S(t-\tau))Q(t-\tau). \end{cases}$$

This system also exhibits a positive steady state $(\overline{Q}, \overline{S}) = (Q^*, S^*)$ with $Q^* < S^*$. Its local asymptotic stability depends on the sign of eigenvalues of the characteristic equation (2.6), where

$$R_1(\lambda, \tau) = \lambda^2 + [\delta + \gamma + \beta(S^*)]\lambda + \gamma(\delta + \beta(S^*)) + Q^*\beta'(S^*)(\gamma - \delta)$$

and

$$R_2(\lambda, \tau) = -[Q^*\beta'(S^*) + 2\beta(S^*)]e^{-\gamma\tau}\lambda + [Q^*\beta'(S^*)(\delta - 2\gamma) - 2\gamma\beta(S^*)]e^{-\gamma\tau}.$$

The characteristic equation is now a second degree exponential polynomial. We focus on such characteristic equations in the next section.

## 3 Models with 2 compartments

The method proposed by Beretta and Kuang [9], presented in the previous section, can be used to determine the appearance of pure imaginary roots for a priori any exponential polynomial characteristic equation, whatever the degree of the polynomial function. We focus here on a second degree exponential polynomial characteristic equation, arising from the local asymptotic stability analysis of the positive steady state of a model of

hematopoiesis incorporating both dynamics of hematopoietic stem cells (see previous section) and a population of mature cells (either red blood cells, white cells or platelets) [4], see Figure 3. In this case, properties (i) to (iii) are usually straightforwardly satisfied.

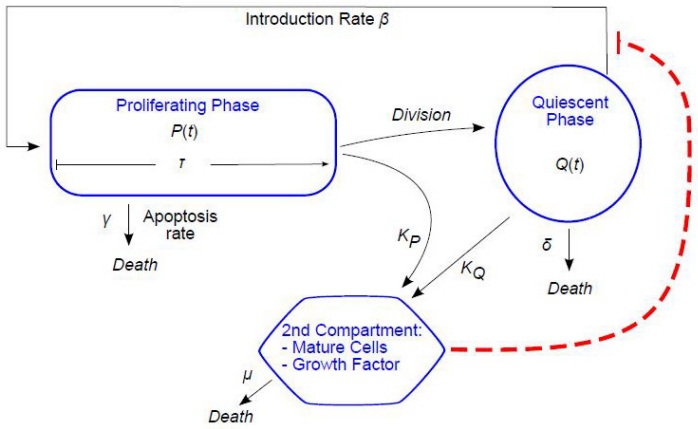


Figure 3: Schematic representation of a model of HSC dynamics with 2 compartments, from Adimy et al. [4], and one negative feedback control (dashed line).

As in the previous section, consider two populations of hematopoietic stem cells, a quiescent one, whose density is denoted by $Q(t)$, and a proliferating one, whose density is $P(t)$. In addition, consider a population of mature cells $M(t)$ which controls, through a negative feedback, the introduction of quiescent cells in the proliferating phase, so, according to the notations defined in the previous section, $\beta = \beta(M(t))$. Denoting by $K_Q$ (resp. $K_P$) the differentiation rate of quiescent (resp. proliferating) HSC

into mature cells, the system we consider is then

$$
(3.1)\quad \begin{cases} \dfrac{dP}{dt}(t) = \gamma P(t) + \beta(M(t))Q(t) - e^{-\gamma\tau}\beta(M(t-\tau))Q(t-\tau), \\ \dfrac{dQ}{dt}(t) = -[\delta + K_Q + \beta(M(t))]Q(t) \\ \qquad\qquad +2(1-K_P)e^{-\gamma\tau}\beta(M(t-\tau))Q(t-\tau), \\ \dfrac{dM}{dt}(t) = -\mu M(t) + K_Q Q(t) + 2K_P e^{-\gamma\tau}\beta(M(t-\tau))Q(t-\tau). \end{cases}
$$

Under the assumption

$$
[2(1-K_P)e^{-\gamma\tau} - 1]\beta(0) > \delta + K_Q,
$$

system (3.1) has a positive steady state $(P^*, Q^*, M^*)$, whose local asymptotic stability depends on the characteristic equation

$$
(3.2)\qquad \Delta(\lambda,\tau) := \lambda^2 + a_1(\tau)\lambda + a_2(\tau) + [a_3(\tau)\lambda + a_4(\tau)]e^{-\lambda\tau} = 0,
$$

with

$$
(3.3)\quad \begin{cases} a_1(\tau) = \mu + \delta + K_Q + \beta(M^*), \\ a_2(\tau) = \mu(\delta + K_Q + \beta(M^*)) + K_Q Q^* \beta'(M^*), \\ a_3(\tau) = -2e^{-\gamma\tau}[K_P Q^* \beta'(M^*) + (1-K_P)\beta(M^*)], \\ a_4(\tau) = -2e^{-\gamma\tau}[(\delta K_P + K_Q)Q^*\beta'(M^*) + \mu(1-K_P)\beta(M^*)]. \end{cases}
$$

We first check that

$$
\Delta(\lambda,0) = \lambda^2 + [a_1(0) + a_3(0)]\lambda + [a_2(0) + a_4(0)]
$$

has only roots with negative real parts. To that aim, one can use the Routh-Hurwitz criterion. Necessary and sufficient conditions for roots to have negative real parts are then

$$
a_1(0) + a_3(0) > 0 \quad \text{and} \quad a_2(0) + a_4(0) > 0.
$$

This is obtained from (3.3) and the definition of the steady state,

$$a_1(0) + a_3(0) = \mu - 2K_P R^* \beta'(M^*) > 0,$$

and

$$a_2(0) + a_4(0) = -2(\delta K_P + K_Q) Q^* \beta'(M^*) > 0.$$

Second, we check Beretta and Kuang's properties (i) to (iv). One has

$$P(0,\tau) + Q(0,\tau) = [-2K_P \delta e^{-\gamma\tau} - (2e^{-\gamma\tau} - 1)K_Q] Q^* \beta'(M^*) > 0.$$

Moreover,

$$R_1(i\omega,\tau) + R_2(i\omega,\tau) = -\omega^2 + a_2(\tau) + a_4(\tau) + i\omega[a_1(\tau) + a_3(\tau)] \neq 0.$$

Furthermore, it is straightforward that

$$\limsup \left\{ \left| \frac{a_3(\tau)\lambda + a_4(\tau)}{\lambda^2 + a_1(\tau)\lambda + a_2(\tau)} \right| ;\ |\lambda| \to \infty,\ \mathrm{Re}(\lambda) \geq 0 \right\} = 0 < 1.$$

Finally, let define the polynomial function

$$F(\omega,\tau) := |R_1(i\omega,\tau)|^2 - |R_2(i\omega,\tau)|^2,$$

that is

$$F(\omega,\tau) = \omega^4 + [a_1^2(\tau) - 2a_2(\tau) - a_3^2(\tau)]\omega^2 + a_2^2(\tau) - a_4^2(\tau).$$

It is clear that $F$ has a finite number of roots. However, contrary to the example developed in the previous section, it is not so trivial to exhibit explicit roots of function $F$. Assuming

$$\begin{cases} a_2^2(\tau) - a_4^2(\tau) < 0, \quad \text{or} \\ \dfrac{[a_1^2(\tau) - 2a_2(\tau) - a_3^2(\tau)]^2}{4} \geq a_2^2(\tau) - a_4^2(\tau) \geq 0 > a_1^2(\tau) - 2a_2(\tau) - a_3^2(\tau), \end{cases}$$

then $F(\cdot,\tau)$ has at least one positive root, and so there exists at least one $\omega = \omega(\tau) > 0$ such that $F(\omega(\tau),\tau) = 0$. One can assume there exists $\tau^* > 0$ such that $F(\cdot,\tau)$ has positive roots for $\tau \in [0,\tau^*)$ [4].

Now, searching for pure imaginary roots of (3.2), $\lambda = i\omega$, where $\omega = \omega(\tau)$ is a positive root of $F(\cdot, \tau)$ and $\tau \in [0, \tau^*)$ then it is possible, by separating real and imaginary parts in $\Delta(i\omega, \tau) = 0$ to define $\theta(\tau) \in [0, 2\pi]$, such that

$$\cos(\theta(\tau)) = \frac{[a_4(\tau) - a_1(\tau)a_3(\tau)]\omega^2(\tau) - a_2(\tau)a_4(\tau)}{a_4^2(\tau) + a_3^2(\tau)\omega^2(\tau)},$$

$$\sin(\theta(\tau)) = \frac{a_3(\tau)\omega^3(\tau) + [a_1(\tau)a_4(\tau) - a_2(\tau)a_3(\tau)]\omega(\tau)}{a_4^2(\tau) + a_3^2(\tau)\omega^2(\tau)}.$$

Then one can check that $i\omega(\tau)$ is a root of (3.2) if and only if

$$\tau\omega(\tau) = \theta(\tau) + 2k\pi, \quad k \in \mathbb{N}_0,$$

that is, if $\tau$ is a root of the function

$$Z_k(\tau) = \tau - \frac{1}{\omega(\tau)}[\theta(\tau) + 2k\pi], \quad \tau \in [0, \tau^*),\ k \in \mathbb{N}_0.$$

Stability of the positive steady state can then be deduced similarly to what has been presented in the previous section. It is however noticeable that obtaining conditions for the stability of the positive steady state has proved to be more difficult for a second degree exponential polynomial characteristic equation than for a first degree exponential polynomial characteristic equation. Indeed, the main difficulty lies in the ability to find conditions for the existence of positive roots (and potentially exact values of the positive roots) of a polynomial function, $F$, with the same degree (as a function of $\omega^2$) than the characteristic equation. It becomes clear then that increasing the complexity of the model, for instance by including cell compartments, or external factors involved in hematopoiesis, will increase difficulties to establish local asymptotic stability analytically due to the difficulty to identify roots of polynomial functions of high degree.

Similar examples may arise from the study of a model accounting for the influence of both quiescent and proliferating cells on the proliferation rate [15], as mentioned in the end of the previous section, a model including growth factor influence [1], a delay differential system with two delays [7] or from a system with a continuous distributed delay [17].

In the next section we focus on the stability of a third degree exponential

polynomial characteristic equation arising from the linearisation of a more complex model of hematopoiesis dynamics, considering different levels of cell maturity and feedback controls acting at different time scales.

## 4 Models with 3 compartments

Mathematical models of hematopoiesis dynamics leading to the study of a third degree exponential polynomial characteristic equation in order to determine the stability of a positive steady state have been developed to consider, in addition to a hematopoietic stem cell population made of quiescent and proliferating cells: both a growth factor concentration, acting on HSC fate, and a mature cell population controlling the release of growth factors [8]; the effect of a growth factor acting on a mortality rate [2]; the effect of two growth factors, with two different targets [3].

We consider here a new model, inspired by Adimy et al [4] and Crauste et al. [17] (see Figure 4). It consists in the coupling of a HSC dynamics model and a model of erythropoiesis (red blood cell production). This latter model considers two populations of erythroid cells, immature cells called progenitors and mature cells called erythrocytes (or red blood cells), interacting with each other. Mature red blood cells exert a positive feedback on erythroid progenitor apoptosis (this feedback control is in fact mediated by erythropoietin, a growth factor known to inhibit erythroid progenitor apoptosis [20], which is not explicitly considered here) and a negative feedback on their proliferation [17]. Erythroid progenitors exert a negative feedback on HSC proliferation. Hence this model couples two short-term negative feedback controls in order to describe erythropoiesis.

Similarly to the previous section, denote by $Q(t)$ and $P(t)$ the quiescent and proliferating HSC amounts at time $t$, with death rates given respectively by $\delta$ and $\gamma$, and denote by $\beta$ the introduction rate of quiescent cells in the proliferating phase. Moreover, denote by $Pr(t)$ the amount of erythroid progenitors at time $t$. These cells are produced by differentiation of quiescent HSC with a rate $K$, die by apoptosis with a rate $\alpha$ depending on the total number of circulating red blood cells, denoted by $E(t)$, and proliferate with a rate $\sigma$ depending also on $E(t)$. Erythroid progenitors also negatively influence introduction of quiescent cells in the proliferating phase,

so $\beta = \beta(Pr(t))$. Finally, red blood cells die with a constant rate $\mu$, and are produced from erythroid progenitors with a rate $\xi$. An amplification coefficient $A$ is also considered.

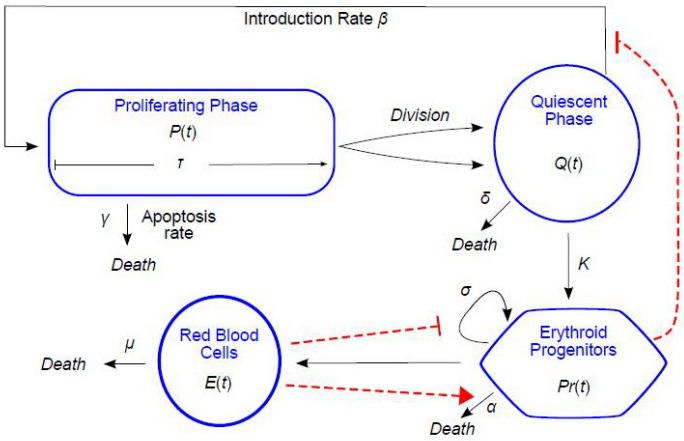


Figure 4: Schematic representation of a model of erythropoiesis including HSC dynamics, erythroid progenitor dynamics and red blood cell dynamics (3 compartments), as well as three short-term feedback controls, one positive and two negative (dashed lines).

All functions $\beta(Pr)$, $\sigma(E)$ and $\alpha(E)$ are supposed to be continuously differentiable, bounded and positive. The introduction rate $\beta$ is supposed to be a decreasing function of the variable $Pr(t)$, with $\lim_{r\to+\infty}\beta(Pr) = 0$. Similarly, the proliferation rate $\sigma$ is assumed to be a decreasing function of $E(t)$, with $\lim_{E\to+\infty}\sigma(E) = 0$. The apoptosis rate, on the contrary, is supposed to be an increasing function of $E(t)$ with $\alpha(0) = 0$ [17].

Variables $P(t)$, $Q(t)$, $Pr(t)$ and $E(t)$ satisfy the following system of delay

differential equations,

$$(4.1)\quad \begin{cases} \dfrac{dP}{dt}(t) = -\gamma P(t) + \beta(Pr(t))Q(t) - e^{-\gamma\tau}\beta(Pr(t-\tau))Q(t-\tau), \\ \dfrac{dQ}{dt}(t) = -[\delta + K + \beta(Pr(t))]Q(t) + 2e^{-\gamma\tau}\beta(Pr(t-\tau))Q(t-\tau), \\ \dfrac{dPr}{dt}(t) = [\sigma(E(t)) - \alpha(E(t)) - \xi]Pr(t) + KQ(t), \\ \dfrac{dE}{dt}(t) = -\mu E(t) + A\xi Pr(t). \end{cases}$$

Steady states of system (4.1) are solutions $(\overline{P}, \overline{Q}, \overline{Pr}, \overline{E})$ satisfying

$$(4.2)\quad \begin{cases} [(2e^{-\gamma\tau} - 1)\beta(\overline{Pr}) - \delta - K]\overline{Q} = 0, \\ [\alpha(\overline{E}) + \xi - \sigma(\overline{E})]\overline{Pr} = K\overline{Q}, \end{cases}$$

and $\gamma\overline{P} = (1 - e^{-\tau\tau})\beta(\overline{Pr})\overline{Q}$ and $\mu\overline{E} = A\xi\overline{Pr}$.

One steady state, $(P_0, Q_0, Pr_0, E_0) = (0, 0, 0, 0)$, always exists. It can be shown that this equilibrium is locally asymptotically stable when it is the only steady state. It describes extinction of all cell populations.

A second steady state is $(0, 0, Pr_1, E_1)$, where $\sigma(E_1) = \alpha(E_1) + \xi$ and $A\xi Pr_1 = \mu E_1$. This steady state exists provided that $\sigma(0) > \xi$ (see (4.2)). It corresponds to the extinction of HSCs and survival of more mature cells. This situation being biologically unrealistic, it is expected to be unstable.

Finally, the third steady state is $(P_2, Q_2, Pr_2, E_2)$, where

$$(2e^{-\gamma\tau} - 1)\beta(Pr_2) = \delta + K,$$

and positive values of $Q_2$, $P_2$ and $E_2$ follow from (4.2). This steady state exists provided that

$$(4.3)\quad (2e^{-\gamma\tau} - 1)\beta(0) > \delta + K$$

and

$$(4.4)\quad \alpha\left(\frac{A\xi}{\mu}Pr_2\right) + \xi > \sigma\left(\frac{A\xi}{\mu}Pr_2\right).$$

Linearization of system (4.1) about one of its steady states leads to the following characteristic equation,

$$\lambda^3 + a_1(\tau)\lambda^2 + a_2(\tau)\lambda + a_3(\tau) + [a_4(\tau)\lambda^2 + a_5(\tau)\lambda + a_6(\tau)]e^{-\lambda\tau} = 0, \tag{4.5}$$

with

$$\begin{aligned}
a_1(\tau) =& \mu + \delta + K + \beta(\overline{Pr}) + \alpha(\overline{E}) + \xi - \sigma(\overline{E}),\\
a_2(\tau) =& \mu(\delta + K + \beta(\overline{Pr})) + (\delta + K + \beta(\overline{Pr}))(\alpha(\overline{E}) + \xi - \alpha(\overline{E}))\\
&+ \mu(\alpha(\overline{E} + \xi - \alpha(\overline{E})) + K\overline{Q}\beta'(\overline{Pr}) + A\xi(\alpha'(\overline{E}) - \sigma'(\overline{E}))\overline{Pr},\\
a_3(\tau) =& \mu(\delta + K + \mu(\overline{Pr}))(\alpha(\overline{E}) + \xi - \sigma(\overline{E})) + \mu K\overline{Q}\beta'(\overline{Pr})\\
&+ A\xi(\alpha'(\overline{E}) - \sigma'(\overline{E}))\overline{Pr}(\delta + K + \beta(\overline{Pr})),\\
a_4(\tau) =& -2e^{-\gamma\tau}\beta(\overline{Pr}),\\
a_5(\tau) =& 2e^{-\gamma\tau}[-\mu\beta(\overline{Pr}) - \beta(\overline{Pr})(\alpha(\overline{E}) + \xi - \sigma(\overline{E})) - K\overline{Q}\beta'(\overline{Pr})],\\
a_6(\tau) =& 2e^{-\gamma\tau}[-\mu\beta(\overline{Pr})(\alpha(\overline{E}) + \xi - \sigma(\overline{E})) - \mu K\overline{Q}\beta'(\overline{Pr})\\
&- A\xi(\alpha'(\overline{E}) - \sigma'(\overline{E}))\overline{Pr}\beta(\overline{Pr})].
\end{aligned}$$

Let focus on the local asymptotic stability of $(P_2, Q_2, Pr_2, E_2)$. When $\tau = 0$, eigenvalues have negative real parts if and only if (Routh-Hurwitz criterion),

$$a_1(0) + a_4(0) > 0, \quad a_3(0) + a_6(0) > 0$$

and

$$[a_1(0) + a_4(0)][a_2(0) + a_5(0)] > a_3(0) + a_6(0).$$

One gets, from (4.4),

$$a_1(0) + a_4(0) = \mu + \alpha(E_2) + \xi - \sigma(E_2) > 0,$$

$$a_3(0) + a_6(0) = -\mu K Q_2 \beta'(Pr_2) > 0,$$

and

$$\begin{aligned}
a_2(0) + a_5(0) = \mu(\alpha(E_2) + \xi - \sigma(E_2)) + A\xi(\alpha'(E_2)\\
- \sigma'(E_2))Pr_2 - KQ_2\beta'(Pr_2) > 0.
\end{aligned}$$

Moreover, since

$$[\mu + \alpha(E_2) + \xi - \sigma(E_2)][\mu(\alpha(E_2) + \xi - \sigma(E_2)) + A\xi(\alpha'(E_2) - \sigma'(E_2))Pr_2] > Pr_2\beta'(Pr_2)[\alpha(E_2) + \xi - \sigma(E_2)]^2,$$

then the steady state $(P_2, Q_2, Pr_2, E_2)$ is locally asymptotically stable when $\tau = 0$. In order to determine whether or not an increase of the delay away from zero may lead to a loss of stability, we apply Beretta and Kuang criterion, presented in previous sections.

First, we already checked that $a_3(0) + a_6(0) > 0$, in fact one can easily get $a_3(\tau) + a_6(\tau) > 0$ for all satisfying (4.3). Hence, (i) is satisfied.

Second, it is straightforward that (ii) and (iii) are satisfied, since

$$-(a_1(\tau) + a_4(\tau))\omega^2 + a_3(\tau) + a_6(\tau) + i[-\omega^3 + (a_2(\tau) + a_5(\tau))\omega] \neq 0.$$

Finally, $F(\omega, \tau)$ is given by

$$F(\omega, \tau) = \omega^6 + b_1(\tau)\omega^4 + b_2(\tau)\omega^2 + b_3(\tau),$$

where

$$\begin{aligned} b_1(\tau) &= a_1^2(\tau) - 2a_2(\tau) - a_4^2(\tau), \\ b_2(\tau) &= a_2^2(\tau) + 2a_4(\tau)a_6(\tau) - 2a - 1(\tau)a_3(\tau) - a_5^2(\tau), \\ b_3(\tau) &= a_3^2(\tau) - a_6^2(\tau). \end{aligned}$$

Searching for pure imaginary roots of (4.5), $\lambda = i\omega$, as previously detailed one has to determine positive roots of $F(\omega, \tau)$. Since $F$ is a third degree polynomial in $\omega^2$, due to Ruan and Wei [25], one can exhibit conditions on the coefficients $b_i(\tau)$, $i = 1, 2, 3$, for existence of positive roots.

**Lemma 4.1** *Let $\tau$ satisfy (4.3). Then $F(\cdot, \tau)$ has positive roots if and only if*

$$\begin{aligned} &b_3(\tau) < 0 \quad \textit{or} \\ &b_3(\tau) \geq 0,\ b_1^2(\tau) - 3b_2(\tau) \geq 0,\ z(\tau) > 0 \textit{ and } F(z^2(\tau), \tau) < 0, \end{aligned} \tag{4.6}$$

*where*

$$z(\tau) = \frac{-b_1(\tau) + \sqrt{b_1^2(\tau) - 3b_2(\tau)}}{3}.$$

Thanks to condition (4.6), one can define an interval $[0, \tau^*)$ in which it makes sense to search for critical values of the delay $\tau$. For $\tau \in [0, \tau^*)$, let $\omega(\tau)$ be a positive root of $F(\cdot, \tau)$. Then, let $\theta(\tau) \in [0, 2\pi]$ be defined for $\tau \in [0, \tau^*)$ by

$$\cos(\theta(\tau)) = \frac{(a_5 - a_1a_4)\omega^4 + (a_1a_6 + a_3a_4 - a_2a_5)\omega^2 - a_3a_6}{a_4^2\omega^4 + (a_5^2 - 2a_4a_6)\omega^2 + a_6^2},$$

$$\sin(\theta(\tau)) = \frac{a_4\omega^5 + (a_1a_5 - a_2a_4 - a_6)\omega^3 + (a_2a_6 - a_3a_5)\omega}{a_4^2\omega^4 + (a_5^2 - 2a_4a_6)\omega^2 + a_6^2},$$

where $\omega = \omega(\tau)$, and we deliberately omit the dependence of the $a_i$ on $\tau$. Since $F(\omega(\tau), \tau) = 0$ for $\tau \in [0, \tau^*)$, it follows that $\tau$ is well and uniquely defined for all $\tau \in [0, \tau^*)$. One can check that $i\omega(\tau)$ is a root of (4.5) if and only if $\tau$ is a root of the function

$$Z_k(\tau) = \tau - \frac{1}{\omega(\tau)}[\theta(\tau) + 2k\pi], \quad \tau \in [0, \tau^*),\ k \in \mathbb{N}_0.$$

Once again, one can conclude to the stability of the steady state by searching for real roots of a $Z_k$ function.

One may note, however, that finding intervals of values of $\tau$ for which the polynomial function $F$ has positive roots $\omega$ is getting more and more difficult as the degree of the polynomial part of the characteristic equation increases. Moreover, determining stability of the steady state when the delay $\tau$ is zero also necessitates tedious computations in order to apply the Routh-Hurwitz criterion. Consequently, Beretta and Kuang's method to analyze stability of the steady state of a system with delay-dependent coefficients, although very useful for 2 or 3 dimensional systems, rapidly becomes useless from a theoretical point of view (it is always possible to perform numerical simulations in order to locate eigenvalues with positive real parts), unless properties of the steady state itself can lead to simplifications in the characteristic equation (simplifications leading to a decrease in the degree of the polynomial function).

## 5 Discussion and Remarks

The method presented in the previous section, which allows determining critical values of the delay associated with a loss of stability for the steady state of a system with delay-dependent coefficients, proved to be efficient for 'small' systems, that is with up to 3 variables. For higher order systems, tedious computations are necessary to determine the characteristic equations, and most of the time it is not possible to achieve interesting results on the stability of the steady state in the absence of delay (Routh-Hurwitz criterion) neither on the location of positive roots of a polynomial function with degree larger than 4.

For systems in low dimensions (up to 3), Beretta and Kuang method is nevertheless very useful and often easy to apply. Hematopoiesis models are in particular adapted to the use of this method, since usually they are stable in the absence of delay, which allows obtaining relevant results on stability (and the loss of stability) and gaining information on the appearance of oscillations in such systems [2, 8, 14, 15]. It appears that oscillations in blood cell counts may be associated with hematological diseases [12, 13, 18, 23].

Complexity of hematopoiesis leads to consider numerous feedback controls in the regulation of cell population dynamics. Apart from simple models, taking usually into account only one cell population (HSC, erythroid progenitors, etc.), it is often relevant to describe different controls, either short-term or long-term, of one population on an other one. A lot of delays may appear in such modelling, leading to either systems of ordinary differential equations with continuous distributed delay [5, 6] or with several discrete delays [3, 7]. In these cases, the stability analysis is usually much more complicated. There is, to our knowledge, no applicable theory equivalent to the one presented in this manuscript to investigate stability. One exception may be the case of a Gamma distribution for a distributed delay where, using the chain trick, one can reduce the initial system to an ordinary differential equation system [10]. Systems with distributed delays can sometimes reduce to systems with discrete delays, however $\lambda = 0$ may be an eigenvalue in this case (so Beretta and Kuang properties are not always satisfied), see [2, 3, 17].

For systems with continuous distributed delay, a state of the art can be

found in Crauste [16]. For systems with several discrete delays, the only option is often to deal with every particular case. Some examples can be found in Adimy et al [3, 7] or Niculescu et al [24], for instance. Biologists continuously asking for more complex models in order to consider the huge amount of information experiments can produce, developing theoretical approaches to deal with stability analysis of less classical delay models can become of strong relevance.

## References

[1] M. Adimy and F. Crauste, Stability and instability induced by time delay in an erythropoiesis model, *Monografias del Seminario Matematico Garcia de Galdeano*, **31** (2004), 312.

[2] M. Adimy and F. Crauste, Modelling and asymptotic stability of a growth factor-dependent stem cells dynamics model with distributed delay, *Discret. Cont. Dyn. Sys. Ser. B*, **8**(1) (2007), 1938.

[3] M. Adimy and F. Crauste, Mathematical model of hematopoiesis dynamics with growth factor-dependent apoptosis and proliferation regulation, *Mathematical and Computer Modelling*, **49** (2009), 21282137.

[4] M. Adimy, F. Crauste and C. Marquet, Asymptotic behavior and stability switch for a mature-immature model of cell differentiation, *Nonlinear Analysis: Real World Applications*, **11**(4) (2010), 29132929.

[5] M. Adimy, F. Crauste and S. Ruan, A mathematical study of the hematopoiesis process with applications to chronic myelogenous leukemia, *SIAM J. Appl. Math.*, **65**(4) (2005), 13281352.

[6] M. Adimy, F. Crauste and S. Ruan, Stability and Hopf bifurcation in a mathematical model of pluripotent stem cell dynamics, *Nonlinear Analysis Real World Applications*, **6**(4) (2005), 651670.

[7] M. Adimy, F. Crauste and S. Ruan, Periodic Oscillations in Leukopoiesis Models with Two Delays, *J. Theo. Biol.*, **242** (2006), 288299.

[8] M. Adimy, F. Crauste and S. Ruan, Modelling hematopoiesis mediated by growth factors with applications to periodic hematological diseases, *Bull. Math. Biol.*, **68**(8) (2006), 23212351.

[9] E. Beretta and Y. Kuang, Geometric stability switch criteria in delay differential systems with delay dependent parameters, *SIAM J. Math. Anal.*, **33**(5) (2002), 11441165.

[10] F. G. Boese, The stability chart for the linearized Cushing equation with a discrete delay and Gamma-distributed delays, *J. Math. Anal. Appl.*, **140** (1989), 510-536.

[11] F.J. Burns and I.F. Tannock, On the existence of a G0 phase in the cell cycle, *Cell Tissue Kinet.*, **19** (1970), 321334.

[12] C. Colijn and M. C. Mackey, A mathematical model of hematopoiesis, I, Periodic chronic myelogenous leukemia, *J. Theor. Biol.*, **237** (2006), 117132.

[13] C. Colijn and M. C. Mackey, A mathematical model of hematopoiesis, II. Cyclical neutropenia, *J. Theor. Biol.*, **237** (2006), 133146.

[14] F. Crauste, Global Asymptotic Stability and Hopf Bifurcation for a Blood Cell Production Model, *Math. Biosci. Eng.*, **3**(2) (2006), 325346.

[15] F. Crauste, Delay Model of Hematopoietic Stem Cell Dynamics: Asymptotic Stability and Stability Switch, *Math. Model. Nat. Phenom.*, **4**(2) (2009), 28-47.

[16] F. Crauste, *Stability and Hopf bifurcation for a first-order linear delay differential equation with distributed delay*, in Complex Time Delay Systems (Ed. F. Atay), Springer, 1st edition, 320 p. (2010).

[17] F. Crauste, L. Pujo-Menjouet, S. Génieys, C.Molina and O. Gandrillon, Adding Self-Renewal in Committed Erythroid Progenitors Improves the Biological Relevance of a Mathematical Model of Erythropoiesis, *Journal of Theoretical Biology*, **250** (2008), 322338.

[18] C. Foley and M.C. Mackey, *Dynamic hematological disease: a review,* J. Math. Biol., **58**(1-2) (2009), 285322.

[19] J. Hale and S.M. Verduyn Lunel, *Introduction to functional differential equations*, Applied Mathematical Sciences 99, Springer-Verlag, New York, 1993.

[20] M.J. Koury and M.C. Bondurant, Erythropoietin retards DNA breakdown and prevents programmed death in erythroid progenitor cells, *Science*, **248** (1990), 378381.

[21] Y. Kuang, *Delay differential equations with applications in population dynamics*, Mathematics in Science and Engineering 191, Academic Press, Boston, MA, 1993.

[22] L. G. Lajtha, On DNA labeling in the study of the dynamics of bone marrow cell populations, in: Stohlman, Jr., F. (Ed), *The Kinetics of Cellular Proliferation*, Grune and Stratton, New York (1959), 173182.

[23] M.C. Mackey, Unified hypothesis of the origin of aplastic anaemia and periodic hematopoiesis, *Blood*, **51** (1978), 941956.

[24] S. Niculescu, P.S. Kim, K. Gu, P.P. Lee, and D. Levy, Stability crossing boundaries of delay systems modeling immune dynamics in leukemia, *Discrete Contin. Dyn. Syst. Ser. B*, **13**(1) (2010), 129156.

[25] S. Ruan and J. Wei, On the zeros of a third degree exponential polynomial with applications to a delayed model for the control of testosterone secretion, *IMA J. Math. Appl. Med. Biol.*, **18** (2001), 4152.

## 5.3 Crauste (2010)

Manuscrit du chapitre de livre : [53] F. Crauste, *Stability and Hopf bifurcation for a first-order linear delay differential equation with distributed delay*, in Complex Time Delay Systems (Ed. F. Atay), Springer, 1st edition, 320 p., ISBN : 978-3-642-02328-6 (2010).

# 8

# Stability and Hopf Bifurcation for a First-Order Delay Differential Equation with Distributed Delay

Fabien Crauste

Université de Lyon ; Université Lyon 1
CNRS UMR5208 Institut Camille Jordan
INSA de Lyon, F-69621
Ecole Centrale de Lyon
43 blvd du 11 novembre 1918
F-69622 Villeurbanne-Cedex, France
crauste@math.univ-lyon1.fr

## 8.1 Introduction

The present chapter is devoted to the stability analysis of linear differential equations with continuous distributed delay

$$\frac{\mathrm{d}x}{\mathrm{d}t}(t) = -Ax(t) - B\int_0^\infty F(\theta)x(t-\theta)\,d\theta, \qquad t > 0, \tag{8.1}$$

where $A$ and $B$ are real coefficients and $F$ is an integrable function on $(0, +\infty)$, that can possibly have a compact support. Note that, except when it is mentioned, $F$ will not be supposed to be a density function.

This class of equations is widely used in many research fields—it can be obtained through the linearization of different nonlinear problems (see, for example, Section 8.5)—such as automatic, economic, and, for our purpose, in biological modelling because it can be associated with problems in which it is important to take into account some history of the state variable (e.g., gestation period, cell cycle durations or incubation time [23, 34]). When few data are available, this history is usually assumed to be discrete. Yet, in most cases very little is known about it, and how it is distributed; so, very abstract assumptions lead to equations in the form of (8.1).

We are interested in stability properties of (8.1), that is, under which conditions, on the parameters $A$ and $B$ or the function $F$, do all solutions of (8.1) converge toward zero? And, as a consequence, how can (8.1) be destabilized? Can oscillating or periodic solutions appear? All these questions arise from a need to understand how systems destabilize, or how can they stay stable for a long time. Partial answers are brought up in Section 8.4.

Many studies, as mentioned hereafter, tried to bring clear answers to these questions, yet only partial results have been proved up to now. Mainly, only sufficient conditions for stability – which are sometimes all one needs – have been obtained, or particular functions $F$ have been used so as to simplify in some way the study of the stability of (8.1).

To make this latter argument clearer, let us recall that the stability of (8.1) is related to the sign of the real parts of its eigenvalues (see Section 8.2, Proposition 1). Indeed, it is sufficient to determine the sign of real parts of all eigenvalues to deduce the stability or instability of (8.1). With well-chosen functions $F$, the integral term in (8.1), or in its characteristic equation, can be explicitly calculated and stability can be determined. For instance, when $F$ is the Dirac measure $\delta_\tau$, defined by

$$\delta_\tau(\theta) = \begin{cases} 1, & \text{if } \theta = \tau, \\ 0, & \text{otherwise,} \end{cases}$$

Eq. (8.1) reduces to the classical *linear discrete delay differential equation*

$$\frac{\mathrm{d}x}{\mathrm{d}t}(t) = -Ax(t) - Bx(t-\tau), \qquad t > 0. \tag{8.2}$$

This equation as been widely studied (see, for example, [18]) and its stability has been fully determined. This will be recalled in Section 8.3 where the importance of (8.2) is stressed. In particular, necessary and sufficient conditions for the existence of a Hopf bifurcation have been obtained.

When $F$ is a sum of Dirac measures, (8.1) is a differential equation with several discrete distributed delays. Such equations may display very interesting behavior, and their analysis is much more difficult than for (8.2). It is not the aim of this work to deal with such equations, but the interested reader is referred to the works in [3, 12, 35, 36, 39], and the numerous references therein.

Other types of density functions $F$ that have been often used, applied to different situations but mainly in biological modelling (e.g., to describe the distribution of cell cycle transit times [25]), are Gamma distributions. They consist in taking $F$ as

$$F(\theta) = \frac{\sigma^{k+1}}{\Gamma(k+1)}\theta^k e^{-\sigma\theta}, \tag{8.3}$$

the parameters $\sigma$ and $k$ being related to experimental data. One can also consider that $\sigma$ and $k$ are defined by the following relations,

$$E = \frac{k+1}{\sigma} \qquad \text{and} \qquad V = \frac{k+1}{\sigma^2},$$

$E$ and $V$ defining respectively the expectation and variance of $F$. In the stability analysis of (8.1), Gamma distributions have a technical advantage: they

allow to 'transform' a transcendental characteristic equation into a polynomial equation, then facilitating the analysis.

Studies for more general functions $F$ have been done during the last twenty years, and different achieved results may be mentioned. These results will be explained in more details in Section 8.3. Anderson [4, 5], between 1991 and 1992, considered a different form for (8.1), where $F$ is a density function, and he obtained stability results related to the different moments (especially the expectation and the variance) of the distribution. These results stress the importance of the shape of the function $F$ in the stability of (8.1). Kuang [24], in 1994, also obtained general stability results for systems of delay differential equations. More recently, sufficient conditions for the stability of delay differential equations with distributed delay have been obtained by Bernard et al [8], when $F$ is a probability density. The authors used some properties of the distribution to prove these results. However, it is noticeable to mention that in all the cited works the authors only focused on sufficient conditions for the stability, and no necessary condition has yet been proved.

In the next section we present some useful and important definitions for the stability of differential equations that will make the reading of this chapter easier. Then, in Section 8.3, we briefly summarize the state of the art in the stability of differential equations with distributed delay, starting with the case of the stability of (8.2) which, without falling in the framework of this chapter, is very useful in determining strategies to analyze the stability of (8.1). In Section 8.4, we present the main result of this chapter which consists in finding a critical value of the parameters that would destabilize (8.1). We show that this destabilization occurs through a Hopf bifurcation. We conclude with an application of the results of Section 8.4 to a model of hematopoietic stem cells dynamics, pointing out how the mathematical study allows to determine the existence of oscillating solutions in this model that can be related to chronic myelogenous leukemia, a severe blood disease.

## 8.2 Definitions and Hopf Bifurcation Theorem

Let consider the delay differential equation

$$y'(t) = f(y_t), \quad t > 0, \tag{8.4}$$

where $f : \varphi \in \mathcal{C}((-\infty, 0], \mathbb{R}^n) \mapsto f(\varphi) \in \mathbb{R}^n$ has continuous first and second derivatives for all $\varphi \in \mathcal{C}((-\infty, 0], \mathbb{R}^n)$, the space of continuous functions mapping $(-\infty, 0]$ into $\mathbb{R}^n$, $f(0) = 0$, and $y_t$ is a continuous function defined, for $\theta \leq 0$, by

$$y_t(\theta) = y(t + \theta).$$

Define $L : \mathcal{C}((-\infty, 0], \mathbb{R}^n) \to \mathbb{R}^n$ by

$$L\varphi = \frac{\mathrm{d}f}{\mathrm{d}\phi}(0)\varphi,$$

and consider the linear differential equation with delay

$$y'(t) = Ly_t, \quad t > 0. \tag{8.5}$$

Eq. (8.5) is the linearized equation of (8.4) at $\varphi = 0$.

*Example 1.* If, for continuous functions $\varphi : (-\infty, 0] \mapsto \mathbb{R}$,

$$L\varphi = -A\varphi(0) - B\int_0^\infty F(\theta)\varphi(-\theta)\,d\theta,$$

then (8.5) is (8.1).

**Definition 1.** *The trivial solution $y \equiv 0$ of (8.5) is said to be* asymptotically stable *if all solutions of (8.5) converge toward zero when $t$ tends to infinity.*

Instead of "The trivial solution of (8.5) is stable or unstable", one may find the expression "Eq. (8.5) is stable or unstable".

One must note that asymptotic stability of (8.5) implies *local* asymptotic stability of (8.4), and instability of (8.5) implies instability of (8.4).

Different techniques may be used to determine the asymptotic stability of (8.5), although two approaches are usually privileged. The first technique, which is usually applied to nonlinear delay differential equations, aims to determine global asymptotic stability (the distinction vanishes for linear equations) and is based on the use of Lyapunov functions (see Hale [18]). Without giving too much details (we invite the interested reader to look through the book of Hale [18] for the application of Lyapunov functions to delay differential equations), the main difficulty lies in finding a good function, which is not an easy task. The second way of finding the stability properties of (8.5) is to study its eigenvalues.

Consider the equation

$$\det\left(\lambda - Le^{\lambda\cdot}\right) = 0, \quad \lambda \in \mathbb{C}. \tag{8.6}$$

This equation is called the *characteristic equation* of (8.5). When the linear function $L$ is known, (8.6) is obtained by searching for solutions of (8.5) in the form $y(t) = Ce^{\lambda t}$, $C \in \mathbb{R}^n$. The solutions $\lambda$ of (8.6) are called the *characteristic roots*, and they are the *eigenvalues* of (8.5).

**Proposition 1.** *The trivial solution of (8.5) is asymptotically stable if all characteristic roots of (8.6) have negative real parts, and unstable if (8.6) has a characteristic root with positive real part.*

Note that when $\lambda = 0$ is an eigenvalue of (8.5) and all other eigenvalues have negative real parts, then one cannot immediately conclude the stability or instability of (8.5). A more detailed analysis is then necessary. It is also important to note that the stability of (8.5) can only be lost if eigenvalues cross the imaginary axis from left to right. That is, if purely imaginary eigenvalues

appear (see Cooke and Grossman [14], and the numerous generalizations of their result, based on Rouché's Theorem [16, p.248]).

Stated in the next theorem, the Hopf bifurcation theorem describes the instability of (8.4) through the appearance of periodic solutions, related to the existence of purely imaginary eigenvalues of (8.5). As mentioned in Hale [18], the Hopf bifurcation is one of the simplest way for (nonconstant) periodic solutions to arise in delay differential equations.

Let us suppose that the function $f$ in (8.4) depends on a real parameter, say $\alpha \in \mathbb{R}$, and $f$ has continuous first and second derivatives in $\alpha$ and $\varphi$ for all $\alpha \in \mathbb{R}$ and $\varphi \in \mathcal{C}((-\infty, 0], \mathbb{R}^n)$. Then the linear function $L$ in (8.5) also depends on $\alpha$ and (8.5) can be written

$$y'(t) = L(\alpha)y_t, \quad t > 0. \tag{8.7}$$

If $\lambda$ is an eigenvalue of (8.7), we denote by $\Re(\lambda)$ and $\Im(\lambda)$ the real and imaginary parts of $\lambda$ respectively.

**Theorem 1 (Hopf Bifurcation Theorem for DDEs, Hale [18]).** *Suppose that (8.7) has a simple nonzero purely imaginary eigenvalue $\lambda_0$ for $\alpha = 0$, and that all other eigenvalues are not integer multiples of $\lambda_0$. In addition, suppose that the branch of eigenvalues $\lambda(\alpha)$ which satisfies $\lambda(0) = \lambda_0$ is such that $\Re(\lambda'(0)) \neq 0$. Then, for $\alpha$ close to zero, (8.4) has nontrivial periodic solutions, with period close to $2\pi/\Im(\lambda_0)$.*

The assumption $\Re(\lambda'(0)) \neq 0$ in the above theorem is called the *transversality condition*, and $\alpha$ is called the *bifurcation parameter*. When all assumptions of Theorem 1 are fulfilled, one says that (8.4) undergoes a Hopf bifurcation for $\alpha = 0$.

*Example 2.* Through this example, we illustrate the results stated in Proposition 1 as well as in Theorem 1, on a differential equation with discrete delay.

Consider the delay differential equation

$$y'(t) = -\alpha \frac{y(t-1)}{1 + y(t-1)}, \quad \alpha > 0,\ t > 0. \tag{8.8}$$

The linearization of (8.8) around $y \equiv 0$ gives the linear DDE

$$y'(t) = -\alpha y(t-1), \quad \alpha > 0. \tag{8.9}$$

This equation can be written as (8.7) with $L(\alpha)$ given by $L(\alpha)\varphi = -\alpha\varphi(-1)$. Looking for solutions of (8.9) in the form $y(t) = Ce^{\lambda t}$, we deduce the characteristic equation

$$\lambda + \alpha e^{-\lambda} = 0. \tag{8.10}$$

For the sake of simplicity, we write $\lambda = \mu + \mathrm{i}\omega$, and we separate real and imaginary parts in the above equation, to obtain

$$\mu + \alpha e^{-\mu}\cos(\omega) = 0 \qquad \text{and} \qquad \omega - \alpha e^{-\mu}\sin(\omega) = 0. \tag{8.11}$$

One can notice that if $(\mu, \omega)$ is a solution, then so is $(\mu, -\omega)$. Consequently, we will only consider $\omega > 0$.

Let us suppose that there exists a positive value of $\alpha$, say $\alpha^*$, for which $\mu = 0$. Then, from (8.11),

$$\alpha^*\cos(\omega) = 0 \qquad \text{and} \qquad \omega = \alpha^*\sin(\omega).$$

Since $\alpha^* > 0$, it follows that $\cos(\omega) = 0$, and so $\omega = \pi/2 + k\pi$. Using the second equation, we deduce that for $\alpha^* = \pi/2$, (8.9) has purely imaginary eigenvalues; these eigenvalues are $\pm\pi/2$.

Let us check first that (8.8) is locally asymptotically stable for $0 < \alpha < \pi/2$, and, second, that (8.8) undergoes a Hopf bifurcation when $\alpha = \pi/2$.

Suppose that $0 < \alpha < \pi/2$ and that $\lambda = \mu + \mathrm{i}\omega$ is an eigenvalue of (8.9). By contradiction, assume $\mu > 0$. Then $e^{-\mu} < 1$ and we deduce, from (8.11), that $\omega = \alpha e^{-\mu}\sin(\omega) < \pi/2$. Consequently, with $\omega > 0$, we obtain that $\cos(\omega) > 0$ and, still from (8.11), that $\mu < 0$. There is a contradiction, so $\mu \leq 0$. Since $\alpha < \pi/2$, $\mu$ cannot be zero, so $\mu < 0$ and all characteristic roots have negative real parts. From Proposition 1, we conclude that (8.9) is asymptotically stable when $0 < \alpha < \pi/2$, and consequently (8.8) is locally asymptotically stable for $0 < \alpha < \pi/2$.

Now let $\alpha = \pi/2$. We are going to check that all assumptions of Theorem 1 are satisfied, in particular that (8.9) has a periodic solution, so that (8.8) undergoes a Hopf bifurcation when $\alpha = \pi/2$.

First, we already checked that, when $\alpha = \pi/2$, (8.9) has a pair of purely imaginary eigenvalues, and that they are the only imaginary eigenvalues. Let us consider the branch of eigenvalues $\lambda(\alpha) = \mu(\alpha) + \mathrm{i}\omega(\alpha)$, solutions of (8.10), such that $\lambda(\pi/2) = \mathrm{i}\pi/2$. Differentiating (8.10) with respect to $\alpha$, we obtain

$$\left(\alpha e^{-\lambda(\alpha)} - 1\right)\lambda'(\alpha) = e^{-\lambda(\alpha)}.$$

It is straightforward to check that $\pm\mathrm{i}\pi/2$ are simple eigenvalues. Indeed, if $\lambda'(\pi/2) = 0$ then $e^{-\lambda(\pi/2)} = 0$, which is impossible. Thus the first assumption in Theorem 1 is satisfied. Moreover, using the fact that $e^{-\lambda(\alpha)} = -\lambda(\alpha)/\alpha$, we deduce that

$$\lambda'(\alpha) = \frac{e^{-\lambda(\alpha)}}{\alpha e^{-\lambda(\alpha)} - 1} = \frac{\lambda(\alpha)}{\alpha(\lambda(\alpha) + 1)}.$$

Consequently,

$$\lambda'\left(\frac{\pi}{2}\right) = \frac{\mathrm{i}\dfrac{\pi}{2}}{\dfrac{\pi}{2}(\mathrm{i}\dfrac{\pi}{2} + 1)} = \frac{\dfrac{\pi}{2} + \mathrm{i}}{\dfrac{\pi^2}{4} + 1},$$

and $\Re(\lambda'(\pi/2)) \neq 0$. The second assumption of Theorem 1 is then satisfied. It follows that (8.8) undergoes a Hopf bifurcation when $\alpha = \pi/2$, and periodic solutions with periods close to 4 exist.

## 8.3 State of the Art and Objectives

Differential equations with continuous distributed delay such as (8.1), or in a modified form, have not been the object of much attention, at least when one is interested in necessary and sufficient conditions for asymptotic stability. Mainly, particular cases have been investigated (when $F$ is a Gamma distribution (8.3)), and sufficient stability conditions have been obtained.

Yet, to understand the lack of results concerning the asymptotic stability of (8.1), one has to have in mind the known results about the stability of the classical discrete delay differential equation (8.2) – which can logically be considered as the simplest delay differential equation – and the techniques used to obtain these results. In the next subsection, we recall stability results for (8.2). Then, we will focus on actual known results of stability for (8.1) and their limitations.

### 8.3.1 The Classical Linear Discrete Delay Differential Equation

Let us focus, for a while, on stability properties of (8.2), which is a particular case of (8.1), known as the *discrete delay differential equation*. Asymptotic properties of this equation, in terms of the coefficients $A$ and $B$, and of the time delay $\tau$, have been established in [14, 18], using a well-known result by Hayes [20]. We state and prove these results, using an alternative proof, based on the one given in [14], which will be useful later in this chapter.

Stability of differential equations is related to the sign of the real parts of their eigenvalues (Proposition 1). The equation is *asymptotically stable* if all eigenvalues have negative real parts, and *unstable* if eigenvalues with positive real parts exist. The stability can be lost only if purely imaginary eigenvalues appear. In the case of ordinary differential equations, the characteristic equation is a polynomial function; so, easy-to-find criteria can be used to locate the eigenvalues. In the case of delay differential equations, the characteristic equation is transcendental, making it difficult to locate the characteristic roots. In particular, the characteristic equation associated with (8.2), obtained by searching for solutions $x(t) = Ce^{\lambda t}$, $C \in \mathbb{R}$, is

$$\lambda + A + Be^{-\lambda\tau} = 0. \tag{8.12}$$

Let us set

$$\Delta(\lambda, \tau) = \lambda + A + Be^{-\lambda\tau}.$$

In the next theorem, we state and prove stability conditions for equation (8.2). We make a difference between delay-independent stability conditions (in *(a)* and *(b)*), and delay-dependent ones (in *(c)*). The latter are related to the existence of a Hopf bifurcation.

**Theorem 2.** *The stability properties of (8.2) are as follows:*
*(a) If $B \leq 0$, (8.2) is asymptotically stable for all $\tau \geq 0$ when $A + B > 0$, and*

*unstable for all $\tau \geq 0$ when $A + B < 0$;*
*(b) If $B > 0$, (8.2) is asymptotically stable for all $\tau \geq 0$ when $A > B$, and unstable for all $\tau \geq 0$ when $A + B < 0$;*
*(c) If $B > 0$ and $B > |A|$, then (8.2) is asymptotically stable for $\tau \in [0, \tau^*)$ and unstable for $\tau \geq \tau^*$, where*

$$\tau^* = \frac{\arccos\left(-\dfrac{A}{B}\right)}{\sqrt{B^2 - A^2}}.$$

*When $\tau = \tau^*$, a Hopf bifurcation occurs and periodic solutions appear.*

*Proof.* Assertions in *(a)* and *(b)* follow immediately from Theorem 6, with $F = \delta_\tau$, the Dirac measure in $\tau$. We refer to the proof of Theorem 6.

Let us focus on the case $B > |A|$ (that is $A + B > 0$ and $A < B$). The stability in this case will depend on the delay. Indeed, we are going to prove the existence of a unique Hopf bifurcation that can destabilize the equation for some value of the delay.

Firstly notice that $\Delta(\lambda, 0) = \lambda + A + B$, so, when $\tau = 0$, $\overline{\lambda} = -(A + B)$ is the only eigenvalue of (8.2). Since $A + B > 0$, $\overline{\lambda} < 0$ and the equation is then asymptotically stable when $\tau = 0$.

Suppose $\tau > 0$, and search for purely imaginary eigenvalues $\lambda = \mathrm{i}\omega$. Separating real and imaginary parts of $\Delta(\mathrm{i}\omega, \tau)$, one finds that $\omega$ and $\tau$ must satisfy

$$\begin{cases} A + B\cos(\omega\tau) = 0, \\ \omega - B\sin(\omega\tau) = 0. \end{cases} \tag{8.13}$$

One can easily check that $\omega = 0$ cannot be a solution, since $A + B > 0$, and if $(\omega, \tau)$ is a solution of (8.13), then so is $(-\omega, \tau)$. Hence, we only focus on positive values of $\omega$.

Since $B > 0$, we rewrite (8.13) as

$$\cos(\omega\tau) = -\frac{A}{B} \quad \text{and} \quad \sin(\omega\tau) = \frac{\omega}{B}.$$

Then one easily checks that the only $\omega$ that can satisfy these conditions is given by

$$\omega^2 = B^2 - A^2.$$

Of course, this definition of $\omega$ is valid only if $B > |A|$, which is the case here.

We then deduce that

$$\tau\sqrt{B^2 - A^2} = \arccos\left(-\frac{A}{B}\right),$$

and the value of $\tau$ for which $\mathrm{i}\omega$ is a root of $\Delta$ must be

$$\tau = \tau^* := \frac{\arccos\left(-\dfrac{A}{B}\right)}{\sqrt{B^2 - A^2}}.$$

The converse is straightforward: If $\tau = \tau^*$, then $\pm \mathrm{i}\sqrt{B^2 - A^2}$ are purely imaginary eigenvalues of (8.2). And indeed they are the only ones. So there is only one change of stability and it occurs for $\tau = \tau^*$. Let us check that this change of stability occurs through a Hopf bifurcation.

Let us set $\omega^* = \sqrt{B^2 - A^2}$. In order to show that a Hopf bifurcation occurs when $\tau = \tau^*$, we must verify that $\pm \mathrm{i}\omega^*$ are simple eigenvalues and

$$\frac{\mathrm{d}}{\mathrm{d}\tau} \Re(\lambda(\tau)) \bigg|_{\tau=\tau^*} > 0.$$

Consider a branch of eigenvalues $\lambda(\tau) = \mu(\tau) + \mathrm{i}\omega(\tau)$ such that

$$\mu(\tau^*) = 0 \quad \text{and} \quad \omega(\tau^*) = \omega^*.$$

Then, for all $\tau \geq 0$, $\Delta(\lambda(\tau), \tau) = 0$. Hence,

$$\frac{\mathrm{d}\Delta}{\mathrm{d}\tau}(\lambda(\tau), \tau) := \frac{\mathrm{d}\lambda}{\mathrm{d}\tau}(\tau) \frac{\partial \Delta}{\partial \lambda}(\lambda(\tau), \tau) + \frac{\partial \Delta}{\partial \tau}(\lambda(\tau), \tau) = 0. \tag{8.14}$$

First notice that

$$\frac{\partial \Delta}{\partial \lambda}(\lambda(\tau), \tau) = 1 - B\tau e^{-\lambda(\tau)\tau}.$$

Therefore, using (8.13), we obtain

$$\frac{\partial \Delta}{\partial \lambda}(\lambda(\tau^*), \tau^*) = 1 - B\tau^* \cos(\omega^* \tau^*) + \mathrm{i} B\tau^* \sin(\omega^* \tau^*) = 1 + A\tau^* + \mathrm{i}\omega^* \tau^*.$$

Since $\omega^*$ and $\tau^*$ are strictly positive, it follows that $\partial \Delta(\lambda(\tau^*), \tau^*)/\partial \lambda \neq 0$, and $\pm \mathrm{i}\omega^*$ are simple eigenvalues of (8.2).

Now, from (8.14), we deduce that

$$\frac{\mathrm{d}\lambda}{\mathrm{d}\tau}(\tau^*) = \frac{\dfrac{\partial \Delta}{\partial \tau}(\mathrm{i}\omega^*, \tau^*)}{\dfrac{\partial \Delta}{\partial \lambda}(\mathrm{i}\omega^*, \tau^*)} = \frac{\mathrm{i} B\omega^* e^{-\mathrm{i}\omega^* \tau^*}}{1 + A\tau^* + \mathrm{i}\omega^* \tau^*}.$$

This yields

$$\frac{\mathrm{d}}{\mathrm{d}\tau} \Re(\lambda(\tau)) \bigg|_{\tau=\tau^*} = \Re\left( \frac{\mathrm{d}\lambda}{\mathrm{d}\tau}(\tau^*) \right) = \frac{B\omega^* \sin(\omega^* \tau^*)}{(1 + A\tau^*)^2 + (\omega^* \tau^*)^2}.$$

Using the fact that $(\omega^*, \tau^*)$ satisfies (8.13), we deduce

$$\frac{\mathrm{d}}{\mathrm{d}\tau} \Re(\lambda(\tau)) \bigg|_{\tau=\tau^*} = \frac{(\omega^*)^2}{(1 + A\tau^*)^2 + (\omega^* \tau^*)^2} > 0.$$

Hence the branch of eigenvalues crosses the imaginary axis from left to right, and the transversality condition (see Theorem 1) is satisfied: a Hopf bifurcation occurs when $\tau = \tau^*$. This completes the proof of *(c)* and ends the proof of the theorem. □

*Remark 1.* In statement *(c)* of Theorem 2, and more particularly in the proof of *(c)*, the critical value $\tau^*$ of the time delay appears to be unique, implying that a unique bifurcation can change the stability of (8.2). It is however important to notice that in practical cases the linear delay differential equation (8.2) is obtained through the linearization of a nonlinear delay differential equation about one of its steady states, and coefficients $A$ and $B$ may depend, explicitly or not, on the time delay. Then the critical values of $\tau$ (here $\tau^*$) for which a stability switch may occur may not be unique, but can be the solutions of a fixed point problem,

$$\tau = \frac{\arccos\left(-\dfrac{A(\tau)}{B(\tau)}\right)}{\sqrt{B(\tau)^2 - A(\tau)^2}}.$$

Consequently stability switches may occur (see Beretta and Kuang [7]).

*Remark 2.* Hayes [20] proved the following result (whose proof can be found in [14] or [18]), which enables to locate the roots of (8.12), and thus allows to draw the stability diagram for equation (8.2). Yet in contrast to Theorem 2, this result does not explain how the equation becomes unstable (e.g. whether through a Hopf bifurcation).

**Theorem 3.** *All roots of (8.12) have negative real parts if and only if* $A\tau > -1$, $A + B > 0$ *and* $B\tau < \zeta\sin(\zeta) - A\tau\cos(\zeta)$, *where* $\zeta \in [0, \pi]$ *is the root of* $\zeta = -A\tau\tan(\zeta)$ *if* $A \neq 0$ *and* $\zeta = \pi/2$ *if* $A = 0$.

When comparing results about distributed delay differential equations with the ones obtained in Theorem 2 for the discrete delay differential equations (see Section 8.4), it will be important to notice that the main difficulty lies inn the existence of purely imaginary eigenvalues. Most of other properties, such as the transversality condition, will be obtained without too much difficulty, in a similar manner to Theorem 2.

In the case of discrete delay, it is possible to obtain necessary and sufficient conditions for the stability (see Theorem 2) because, in the proof of the theorem, usual properties of cosine and sine functions (precisely, that $\cos^2 + \sin^2 = 1$) have been used to determine the exact values of the purely imaginary eigenvalues. This will be impossible for the case with distributed delay, due to the presence of weighed integrals of cosine and sine functions. One can see that the so-called delay-independent stability results in Theorem 2 will hold for the distributed delay case, but as soon as stability results depend on the delay difficulties appear and we are obliged to develop new techniques to obtain stability or bifurcation conditions. A brief but wide summary of known results dealing with the stability of some distributed delay differential equations is presented in the following subsection.

### 8.3.2 Known Results about Stability of Distributed Delay Differential Equations

As mentioned in the introduction, the stability analysis of DDEs with distributed delay has not received so much attention in the literature, except for some particular cases, when $F$, in (8.1), is a Gamma distribution for instance. In 1989, Boese [11] analyzed the stability of (8.1) when $F$ is a Gamma distribution, given by (8.3). The characteristic function of (8.1) is then a $(k+1)$-th degree polynomial function. The author determines sufficient conditions for the asymptotic stability of the trivial solution of (8.1), which are rather technical.

Kuang [24], in 1994, considered a system of two differential equations with continuous distributed delay, possibly infinite. He concentrates on purely imaginary eigenvalues, and determines conditions for their nonexistence, obtaining sufficient conditions for the asymptotic stability of his system.

One particularly interesting result has been published in 2001 by Bernard et al. [8], where the authors considered (8.1) and determined sufficient conditions for its stability. Their main result is stated hereafter.

**Theorem 4 (Bernard et al., 2001 [8]).** *Suppose $B > |A|$, $F$ is a density function, so that $F$ is nonnegative and $\int_0^\infty F(\theta)\,d\theta = 1$, and let $E$ be the expectation of $F$, defined by $\int_0^\infty \theta F(\theta)\,d\theta = E$. The following assertions hold:*
*(a) Eq. (8.1) is asymptotically stable if*

$$E < \frac{\pi\left(1+\dfrac{A}{B}\right)}{c\sqrt{B^2-A^2}},$$

*where $c := \sup\{\bar{c} \mid \cos(x) = 1 - \bar{c}x/\pi, x > 0\} \approx 2.2704$.*
*(b) If $F$ is symmetric, that is $F(E+\theta) = F(E-\theta)$, then (8.1) is asymptotically stable if*

$$E < \frac{\arccos\left(-\dfrac{A}{B}\right)}{\sqrt{B^2-A^2}}. \tag{8.15}$$

The more interesting result in Theorem 4 is cited in *(b)*. One can note that (8.15) corresponds to the necessary and sufficient condition that gives the stability in Theorem 2, in the case when $F$ is a Dirac measure $\delta_\tau$. It is noticeable to mention that Bernard et al. [8] suggest, as a conjecture, that the single Dirac measure $\delta_\tau$ would be the most destabilizing distribution of delays for (8.1). This conjecture is still unproved, yet a recent result (Atay [6]) gave arguments in its favor.

In [6], Atay focuses on the stability of delay differential equations near a Hopf bifurcation, and particularly on the respective influence of discrete and distributed delays on the stability of such equations. For linear delay differential equations, he shows that if the delay has a destabilizing effect,

then the discrete delay is locally the most destabilizing delay distribution (one may note that when the delay has a stabilizing effect, then the discrete delay is locally the most stabilizing delay distribution). When the distribution is symmetric, as in Theorem 4.*(b)*, he shows that the result is global: the discrete delay is the most destabilizing delay distribution.

When one deals with a nonsymmetric distribution $F$, the sufficient condition for the stability of (8.1) provided by Theorem 4 reveals bad results: the limit given for the stability is far from the exact stability boundary, that can be obtained through numerical simulations on some easy-to-handle examples. Up to now, however, these results are probably the best obtained for the stability of a large class of differential equations with distributed delay.

More recently, Huang and Vandewalle [21] and Tang [38] analyzed the stability of equations similar to (8.1). The first authors were interested in the numerical stability of differential equations with distributed delay, but they proposed an interesting geometrical approach to determine conditions for the stability of (8.1) when $F$ is defined by

$$F(\theta) = \begin{cases} 1, & \text{if } 0 < \theta < \tau, \\ 0, & \text{otherwise.} \end{cases}$$

Unfortunately, the way they proceed to obtain their stability conditions cannot be extended to general functions $F$.

In [38], Tang determines sufficient stability conditions for very general differential equations with distributed delay, but his results, that can be seen as a generalization of the works of Boese [11], are very technical and not easy to handle in particular nontrivial examples.

In [31], Ozbay et al. investigate the stability of linear systems of equations with distributed delays, and apply their results to a model of hematopoietic stem cell dynamics. Considering an exponential distribution of delays, they obtain necessary and sufficient conditions for the stability using the small gain theorem and Nyquist stability criterion.

In the above mentioned works, either particular functions $F$ have been used to obtain stability conditions (usually Gamma distributions), or only sufficient stability conditions have been obtained. In the next section, we are going to present a way to obtain stability conditions and, more particularly, conditions for the loss of the stability. These conditions will not be, however, necessary and sufficient ones. But they will allow to describe, through a Hopf bifurcation, the appearance of periodic solutions for (8.1), and may lead to interesting results in practical cases. This will be detailed in Section 8.5.

Before turning to the main point of this chapter, let us mention a last contribution to the study of the stability for differential equations with distributed delay. In 1991 and 1992, Anderson [4, 5] focused on the stability of delay differential equations, called *regulator models*, in the form

$$\frac{\mathrm{d}x}{\mathrm{d}t}(t) = -h \int_0^\infty x(t-u)\,\mu(du), \tag{8.16}$$

where $h$ is a parameter, known as the *amplitude of the regulation*, and $\mu(du)$ is a probability measure supported on $[0, \infty)$. By taking

$$h = A + B \int_0^\infty F(\theta)\, d\theta \quad \text{and} \quad \mu(du) = A\delta_0 + BF(u)\, du,$$

it is easy to check that (8.16) becomes (8.1). The theory developed by Anderson [4, 5] focuses on the properties of the probability measure $\mu(du)$, related to its expectation $E_\mu$ and its relative variance $R_\mu$, defined by $R_\mu = V_\mu/E_\mu^2$, $V_\mu$ being the variance of $\mu(du)$.

Results established by Anderson in [4] and [5] are stated in the next theorem. Suppose that $h_0$ is the largest number such that for $0 \leq h < h_0$ the trivial solution of (8.16) is asymptotically stable. This number is called the *threshold amplitude of the probability delay measure* $\mu(du)$. Note that $h_0$ may be infinite, and in this case (8.16) is always stable.

**Theorem 5.** *Suppose $\mu(du)$ is a probability measure of finite expectation $E_\mu$. Denote by $R_\mu$ its relative variance.*

*If $R_\mu$ satisfies*

$$R_\mu < \frac{2}{\pi^2},$$

*then $h_0$ is finite, and there is a change of stability for (8.16).*

*If $\mu(du) = k(u)\, du$ where $k$ is continuous, convex and not everywhere piecewise linear on $[0, +\infty)$, then $h_0 = +\infty$, and the stability of (8.16) never changes.*

Although the results of Anderson are only valid for some class of probability measures (in particular the second result in Theorem 5), they stress the importance of the shape of the delay distribution. This is an idea that can be found in [8], as stated in Theorem 4. Moreover, Anderson mentions that "the more concentrated the probability measure, the worse the stability property of the model" [5]. This goes in the sense of Bernard et al.'s conjecture [6, 8].

However, despite the interest of Theorem 5, in order to apply the theory of Anderson one needs to know a lot about the probability measure properties, what is rarely the case, for example in biological modelling. I would quote MacDonald [25] writing that, in the case of maturation times for some cells, too little is known to fix a form for their distribution. This was true in 1989, and it is unfortunately usually still true.

## 8.4 Stability Analysis and Hopf Bifurcation for a Delay Differential Equation with Distributed Delay

We now focus on the main objective of this chapter: the stability analysis of (8.1), and the existence of a Hopf bifurcation that would destabilize (8.1). Let us recall that (8.1) is

$$\frac{\mathrm{d}x}{\mathrm{d}t}(t) = -Ax(t) - B\int_0^\infty F(\theta)x(t-\theta)\,d\theta, \qquad t > 0,$$

where $A$ and $B$ are real coefficients, with $A \neq 0$ and $B \neq 0$, and $F$ is a nonnegative integrable function on $(0, +\infty)$. We do not suppose that $F$ is a density function. Without loss of generality one could assume $F$ is a density function, yet to avoid introduction of more notations in the following section and to stay close to applications (where kernel functions are not necessarily density functions, see Section 8.5), this assumption will not be made.

Looking for solutions of (8.1) in the form $Ce^{\lambda t}$, $C \in \mathbb{R}$ and $\lambda$ a complex number, we find the characteristic equation associated with (8.1),

$$\lambda + A + B\int_0^\infty F(\theta)e^{-\lambda\theta}\,d\theta = 0. \tag{8.17}$$

In the following, we denote by $\Delta(\lambda)$ the complex function

$$\Delta(\lambda) := \lambda + A + B\int_0^\infty F(\theta)e^{-\lambda\theta}\,d\theta. \tag{8.18}$$

If $\lambda = \mu + \mathrm{i}\omega$ is an eigenvalue of (8.1), then separating real and imaginary parts in (8.17) leads to

$$\begin{cases} \mu + A + B\displaystyle\int_0^\infty F(\theta)e^{-\mu\theta}\cos(\omega\theta)\,d\theta = 0, \\ \omega - B\displaystyle\int_0^\infty F(\theta)e^{-\mu\theta}\sin(\omega\theta)\,d\theta = 0. \end{cases} \tag{8.19}$$

We can state and prove the following theorem on the stability of (8.1).

**Theorem 6.** *Eq. (8.1) is unstable if*

$$A + B\int_0^\infty F(\theta)\,d\theta < 0, \tag{8.20}$$

*and asymptotically stable if*

$$B \leq 0 \quad \textit{and} \quad A + B\int_0^\infty F(\theta)\,d\theta > 0, \tag{8.21}$$

*or*

$$B > 0 \quad \textit{and} \quad A > B\int_0^\infty F(\theta)\,d\theta. \tag{8.22}$$

*Proof.* Consider $\Delta$, given by (8.18), as a function of real $\lambda$. Then $\Delta$ is differentiable and

$$\frac{\mathrm{d}\Delta}{\mathrm{d}\lambda}(\lambda) = 1 - B\int_0^\infty \theta F(\theta)e^{-\lambda\theta}\,d\theta. \tag{8.23}$$

Moreover,

$$\lim_{\lambda\to+\infty} \Delta(\lambda) = +\infty.$$

First assume (8.20) holds. Then

$$\Delta(0) = A + B\int_0^\infty F(\theta)\,d\theta < 0.$$

Since $\Delta$ is a continuous function which tends to infinity when $\lambda$ tends to infinity, there exists at least one $\lambda_0 \in \mathbb{R}$, $\lambda_0 > 0$, such that $\Delta(\lambda_0) = 0$. Consequently, (8.1) has at least one eigenvalue with positive real part, and is unstable.

Suppose now that (8.21) holds. Since $B \le 0$, it follows from (8.23) that $\Delta$ is increasing. Moreover, since

$$\lim_{\lambda\to-\infty} \Delta(\lambda) = -\infty \quad \text{and} \quad \lim_{\lambda\to+\infty} \Delta(\lambda) = +\infty,$$

we deduce that there exists a unique $\lambda_0 \in \mathbb{R}$ such that $\Delta(\lambda_0) = 0$. In addition,

$$\Delta(0) = A + B\int_0^\infty F(\theta)\,d\theta > 0,$$

so $\lambda_0 < 0$.

Moreover, if $\lambda = \mu + \mathrm{i}\omega$ is a root of $\Delta$, $\lambda \neq \lambda_0$, then from (8.19) we obtain

$$\mu + A + B\int_0^\infty F(\theta)e^{-\mu\theta}\cos(\omega\theta)\,d\theta = 0.$$

Hence

$$\begin{aligned}\lambda_0 - \mu &= -B\int_0^\infty F(\theta)\left[e^{-\lambda_0\theta} - e^{-\mu\theta}\cos(\omega\theta)\right]\,d\theta,\\ &\ge -B\int_0^\infty F(\theta)\left[e^{-\lambda_0\theta} - e^{-\mu\theta}\right]\,d\theta.\end{aligned}$$

If one supposes that $\lambda_0 < \mu$, then one obtains a contradiction. Consequently, $\mu \le \lambda_0$.

Since $\lambda_0 < 0$, we deduce that all roots of $\Delta$ have negative real parts. Hence all eigenvalues of (8.1) have negative real parts and (8.1) is asymptotically stable.

Eventually, assume condition (8.22) is fulfilled. By contradiction, let us suppose that $\Delta$ has a root $\lambda = \mu + \mathrm{i}\omega$ with $\mu > 0$. Then, from (8.19),

$$\mu = -A - B\int_0^\infty F(\theta)e^{-\mu\theta}\cos(\omega\theta)\,d\theta.$$

Since

$$\begin{aligned}-B\int_0^\infty F(\theta)e^{-\mu\theta}\cos(\omega\theta)\,d\theta &\le \left|-B\int_0^\infty F(\theta)e^{-\mu\theta}\cos(\omega\theta)\,d\theta\right|,\\ &\le B\int_0^\infty F(\theta)e^{-\mu\theta}|\cos(\omega\theta)|\,d\theta,\\ &\le B\int_0^\infty F(\theta)\,d\theta,\end{aligned}$$

then, with (8.22), one finds that

$$\mu \leq -A + B \int_0^\infty F(\theta)\, d\theta < 0.$$

This gives a contradiction. Therefore we deduce that $\mu \leq 0$. Let us show that $\mu \neq 0$.

Assume $\mu = 0$. Then, from (8.19), $\omega$ must satisfy

$$\begin{cases} A + B \displaystyle\int_0^\infty F(\theta)\cos(\omega\theta)\, d\theta = 0, \\ \omega - B \displaystyle\int_0^\infty F(\theta)\sin(\omega\theta)\, d\theta = 0. \end{cases} \tag{8.24}$$

Note that for all $\omega \in \mathbb{R}$

$$-\int_0^\infty F(\theta)\, d\theta \leq \int_0^\infty F(\theta)\cos(\omega\theta)\, d\theta \leq \int_0^\infty F(\theta)\, d\theta,$$

so a necessary condition for the existence of purely imaginary roots of $\Delta$ is

$$-\int_0^\infty F(\theta)\, d\theta \leq -\frac{A}{B} \leq \int_0^\infty F(\theta)\, d\theta.$$

Note that (8.22) implies that

$$-\frac{A}{B} < -\int_0^\infty F(\theta)\, d\theta.$$

Consequently, system (8.24) cannot have solutions, and $\mu \neq 0$. This yields that $\mu < 0$. Hence all eigenvalues of (8.1) have negative real parts and (8.1) is asymptotically stable. This ends the proof. □

*Remark 3.* If $F$ is a density function then $\int_0^\infty F(\theta)\, d\theta = 1$ and all conditions for the stability or instability of (8.1) in Theorem 6 are expressed in terms of $A$ and $B$. Moreover, if $F$ is the Dirac measure in $\tau$, denoted by $\delta_\tau$, with $\tau > 0$, then Theorem 6 reduces to Theorem 2.*(a)* and *(b)*.

From the results established in Theorem 6, one can notice that the only parameter region for which the behavior of (8.1) is unknown is

$$B \int_0^\infty F(\theta)\, d\theta > |A|. \tag{8.25}$$

In this case, different behavior can be observed depending on the properties of the function $F$. Yet, no necessary and sufficient condition have been proved for the stability of (8.1). Most results only give sufficient conditions for the stability of (8.1) by finding conditions for the nonexistence of purely imaginary eigenvalues (see for instance Bernard et al. [8], or Theorem 4 in Section 8.3.2).

We investigate, in the following, the existence of purely imaginary eigenvalues of (8.1). We follow the idea developed in [1].

Assume (8.25) holds. Let $\lambda = \mathrm{i}\omega$, with $\omega \in \mathbb{R}$, be a purely imaginary eigenvalue of (8.1). Then $\mathrm{i}\omega$ is a root of $\Delta$, and separating real and imaginary parts of $\Delta(\mathrm{i}\omega)$ one obtains system (8.24), which we rewrite as

$$\begin{cases} A + BC(\omega) = 0, \\ \omega - BS(\omega) = 0, \end{cases} \tag{8.26}$$

where

$$C(\omega) = \int_0^\infty F(\theta)\cos(\omega\theta)\,d\theta \quad \text{and} \quad S(\omega) = \int_0^\infty F(\theta)\sin(\omega\theta)\,d\theta. \tag{8.27}$$

First, one can notice that $\omega = 0$ is not a solution of (8.26) under assumption (8.25), since

$$A + BC(0) = A + B\int_0^\infty F(\theta)d\theta > 0.$$

Moreover, if $\omega$ satisfies (8.26) then so does $-\omega$. Hence we only focus, in the following, on positive solutions of (8.26).

The main issue here is to prove the *existence* of purely imaginary eigenvalues. We will prove in Lemma 3 that a pair of purely imaginary eigenvalues is simple, and it is easy to determine conditions for the transversality condition to hold, in order to verify the Hopf Theorem (see Theorem 1).

To obtain the existence of purely imaginary eigenvalues one must be able to solve system (8.26). To do that, and to determine a stability region, we have to choose a parameter that will be used as the *bifurcation parameter*. One can choose a quantity related to the function $F$ (its expectation or its relative variance, as used by Anderson [4, 5]), or one of the parameters $A$ or $B$. We study the loss of stability of (8.1) with respect to the parameter $B$. Hence, we look for $(\omega, B)$ solution of (8.26), with $\omega > 0$ and $B\int_0^\infty F(\theta)d\theta > |A|$.

In order to solve (8.26), we want to eliminate the parameter $B$, to obtain an equation on $\omega$. Thus we would find successively critical values of $\omega$ and $B$ that would destabilize (8.1). The parameter $B$ could be expressed, from (8.26), as $\omega/S(\omega)$, provided that the division by $S(\omega)$ is allowed. We prove the next lemma.

**Lemma 1.** *Suppose that $F$ is decreasing. Then, for $\omega > 0$,*

$$S(\omega) \geq \chi(\omega) > 0, \tag{8.28}$$

*where*

$$\chi(\omega) := \int_0^{\frac{2\pi}{\omega}} F(\theta)\sin(\omega\theta)\,d\theta, \quad \omega > 0. \tag{8.29}$$

*Proof.* Let $N > 0$ be fixed. Define the truncated functions $F_N$ by

$$F_N(\theta) = \begin{cases} F(\theta), & \text{if } \theta < N, \\ 0, & \text{if } \theta \geq N, \end{cases} \tag{8.30}$$

and the functions $S_N$ and $\chi_N$, for $\omega > 0$, by

$$S_N(\omega) = \int_0^N F_N(\theta)\sin(\omega\theta)\,d\theta \quad \text{and} \quad \chi_N(\omega) = \int_0^{\frac{2\pi}{\omega}} F_N(\theta)\sin(\omega\theta)\,d\theta. \tag{8.31}$$

Note that

$$\chi_N(\omega) = \begin{cases} S_N(\omega), & \text{if } \omega N \leq 2\pi, \\ \chi(\omega), & \text{if } \omega N > 2\pi. \end{cases} \tag{8.32}$$

Indeed, if $\omega N < 2\pi$, then from (8.30) one obtains

$$F_N(\theta) = 0 \quad \text{for } N < \theta < \frac{2\pi}{\omega},$$

so,

$$\chi_N(\omega) = \int_0^N F_N(\theta)\sin(\omega\theta)\,d\theta = S_N(\omega).$$

If $\omega N = 2\pi$, then obviously $\chi_N(\omega) = S_N(\omega)$.

If $\omega N > 2\pi$, then, for all $\theta < 2\pi/\omega$, $\theta < N$ and $F_N(\theta) = F(\theta)$, so

$$\chi_N(\omega) = \int_0^{\frac{2\pi}{\omega}} F(\theta)\sin(\omega\theta)\,d\theta = \chi(\omega).$$

Let us check that $\chi_N(\omega)$ is positive for all $\omega > 0$. Let $\omega > 0$ and $N > 0$ be fixed. Then, using a simple change of variables,

$$\begin{aligned} \chi_N(\omega) &= \int_0^{\frac{2\pi}{\omega}} F_N(\theta)\sin(\omega\theta)\,d\theta, \\ &= \frac{1}{\omega}\int_0^{2\pi} F_N\left(\frac{\sigma}{\omega}\right)\sin(\sigma)d\sigma, \\ &= \frac{1}{\omega}\int_0^{\pi} F_N\left(\frac{\sigma}{\omega}\right)\sin(\sigma)d\sigma + \frac{1}{\omega}\int_{\pi}^{2\pi} F_N\left(\frac{\sigma}{\omega}\right)\sin(\sigma)d\sigma, \\ &= \frac{1}{\omega}\int_0^{\pi}\left[F_N\left(\frac{\sigma}{\omega}\right) - F_N\left(\frac{\sigma+\pi}{\omega}\right)\right]\sin(\sigma)d\sigma. \end{aligned}$$

Since $F$ is supposed to be decreasing, then so is $F_N$. Consequently, for $\sigma \in (0,\pi)$,

$$F_N\left(\frac{\sigma}{\omega}\right) - F_N\left(\frac{\sigma+\pi}{\omega}\right) > 0,$$

and

$$\chi_N(\omega) > 0.$$

It follows, from (8.32), that $S_N(\omega) > 0$ for $0 < \omega N < 2\pi$.

Let us show that $S_N(\omega) > \chi_N(\omega)$ for $\omega N > 2\pi$.
Assume $2\pi < \omega N \leq 3\pi$. From (8.31),

$$S_N(\omega) - \chi_N(\omega) = \int_{\frac{2\pi}{\omega}}^{N} F_N(\theta)\sin(\omega\theta)\,d\theta.$$

Using a simple change of variables ($\sigma = \omega\theta$), we obtain

$$S_N(\omega) - \chi_N(\omega) = \frac{1}{\omega}\int_{2\pi}^{\omega N} F_N\left(\frac{\sigma}{\omega}\right)\sin(\sigma)d\sigma.$$

Since $2\pi < \omega N \leq 3\pi$ and $2\pi < \sigma < \omega N$, then $\sin(\sigma) > 0$ and $S_N(\omega) - \chi_N(\omega) > 0$.

Assume now $3\pi < \omega N \leq 4\pi$. Then, similarly,

$$\begin{aligned} S_N(\omega) - \chi_N(\omega) &= \int_{\frac{2\pi}{\omega}}^{N} F_N(\theta)\sin(\omega\theta)\,d\theta, \\ &= \frac{1}{\omega}\int_{2\pi}^{\omega N} F_N\left(\frac{\sigma}{\omega}\right)\sin(\sigma)d\sigma, \\ &= \frac{1}{\omega}\int_{2\pi}^{3\pi} F_N\left(\frac{\sigma}{\omega}\right)\sin(\sigma)d\sigma + \frac{1}{\omega}\int_{3\pi}^{\omega N} F_N\left(\frac{\sigma}{\omega}\right)\sin(\sigma)d\sigma. \end{aligned}$$

Noting that, from (8.30), $F_N(\theta) = 0$ for $\theta \geq N$, then

$$\int_{3\pi}^{\omega N} F_N\left(\frac{\sigma}{\omega}\right)\sin(\sigma)d\sigma = \int_{3\pi}^{4\pi} F_N\left(\frac{\sigma}{\omega}\right)\sin(\sigma)d\sigma.$$

Thus,

$$\begin{aligned} S_N(\omega) - \chi_N(\omega) &= \frac{1}{\omega}\int_{2\pi}^{3\pi} F_N\left(\frac{\sigma}{\omega}\right)\sin(\sigma)d\sigma + \frac{1}{\omega}\int_{3\pi}^{4\pi} F_N\left(\frac{\sigma}{\omega}\right)\sin(\sigma)d\sigma, \\ &= \frac{1}{\omega}\int_{2\pi}^{3\pi}\left[F_N\left(\frac{\sigma}{\omega}\right) - F_N\left(\frac{\sigma+\pi}{\omega}\right)\right]\sin(\sigma)d\sigma. \end{aligned}$$

Since $F$ is supposed to be decreasing, we deduce that

$$S_N(\omega) - \chi_N(\omega) > 0.$$

By induction, we can prove that, for $\omega N \in (k\pi, (k+1)\pi]$, $k \geq 2$, $S_N(\omega) > \chi_N(\omega)$. Therefore, $S_N(\omega) > \chi_N(\omega)$ for $\omega N > 2\pi$.

Now let $\omega > 0$ be fixed. There exists $N > 0$ large enough such that $\omega N > 2\pi$. Consequently, from the above result, $S_N(\omega) > \chi_N(\omega) > 0$.

Since $\omega N > 2\pi$, then (8.32) implies that $\chi_N(\omega) = \chi(\omega)$, where $\chi(\omega)$ is given by (8.29), and $\chi_N(\omega)$ is then independent of $N$. Thus

$$S_N(\omega) > \chi(\omega) > 0.$$

Taking the limit when $N$ tends to infinity in the above inequality, one obtains

$$S(\omega) \geq \chi(\omega) > 0.$$

This concludes the proof. □

Under the assumption of Lemma 1, $S(\omega) > 0$ for $\omega > 0$. Thus, we can rewrite the second equation of (8.26)

$$B = \frac{\omega}{S(\omega)}.$$

Then this expression of $B$ can be used in the first equation of (8.26) to obtain an equation satisfied only by $\omega$. This equation would be

$$\omega \frac{C(\omega)}{S(\omega)} = -A. \tag{8.33}$$

However, it is not easy to solve (8.33) and neither it is to determine properties of the function $\omega C(\omega)/S(\omega)$. That is why we introduce a new variable, $\overline{A}$, defined by

$$\overline{A} = A + B \int_0^\infty F(\theta)\, d\theta. \tag{8.34}$$

For the sake of simplicity, we denote, in the following, by $\overline{F}$ the integral of the function $F$, so that

$$\overline{A} = A + B\overline{F}.$$

Assumption (8.25) is then equivalent to $2B\overline{F} > \overline{A} > 0$.

Writing $A = \overline{A} - B\overline{F}$ in (8.26), we obtain

$$B = \frac{\omega}{S(\omega)} \quad \text{and} \quad \omega \frac{\overline{F} - C(\omega)}{S(\omega)} = \overline{A}. \tag{8.35}$$

By solving (8.35), we will obtain a solution $(\omega^*, B^*)$ for which $\pm \mathrm{i}\omega^*$ is a pair of purely imaginary eigenvalues of (8.1) when $B = B^*$.

**Lemma 2.** *Suppose $S(\omega) > 0$ for $\omega > 0$. Then there exists $B^* > 0$ satisfying (8.25) such that, when $B = B^*$, (8.1) has a pair of purely imaginary eigenvalues $\pm \mathrm{i}\omega^*$, where $B^* = \overline{A}/(\overline{F} - C(\omega^*))$ and $\omega^*$ satisfies (8.35).*

*Proof.* Define the function $\xi : (0, +\infty) \to \mathbb{R}$ by

$$\xi(\omega) = \omega \frac{\overline{F} - C(\omega)}{S(\omega)}, \quad \omega > 0,$$

where $C$ and $S$ are given by (8.27).

Since

$$\lim_{\omega\to 0}\frac{S(\omega)}{\omega}=\lim_{\omega\to 0}\int_0^\infty \theta F(\theta)\frac{\sin(\omega\theta)}{\omega\theta}\,d\theta=\int_0^\infty \theta F(\theta)\,d\theta,$$

and $C(0)=\overline{F}$, we deduce

$$\lim_{\omega\to 0}\xi(\omega)=0.$$

In addition, from Riemann-Lebesgue's Lemma,

$$\lim_{\omega\to+\infty}S(\omega)=\lim_{\omega\to+\infty}C(\omega)=0,$$

so

$$\lim_{\omega\to+\infty}\xi(\omega)=+\infty.$$

Since $\xi$ is a continuous function on $(0,+\infty)$, we obtain the existence of at least one $\omega>0$, denoted by $\omega^*$, such that

$$\xi(\omega^*)=\overline{A}, \tag{8.36}$$

where we recall that $\overline{A}>0$.

Note that $C(\omega^*)\neq\overline{F}$, otherwise $\xi(\omega^*)=0<\overline{A}$. Then, we set

$$B^*=\frac{\omega^*}{S(\omega^*)}=\frac{\overline{A}}{\overline{F}-C(\omega^*)}>0.$$

Since $|C(\omega)|\leq\overline{F}$, then

$$B^*>\frac{\overline{A}}{2\overline{F}},$$

and $2B^*\overline{F}>\overline{A}$. Therefore $B^*$ satisfies (8.25). Moreover, $(\omega^*,B^*)$ satisfies (8.35), which is equivalent to (8.26), so $\pm\mathrm{i}\omega^*$ is a pair of purely imaginary eigenvalues of (8.1) when $B=B^*$. This ends the proof. □

Lemma 2 gives a condition for the existence of purely imaginary eigenvalues of (8.1). In the next lemma, we show that purely imaginary eigenvalues of (8.1) are always simple and we determine a condition for the transversality condition to hold.

**Lemma 3.** *Suppose $\pm\mathrm{i}\omega^*$, with $\omega^*>0$, is a pair of purely imaginary eigenvalues of (8.1) that appears when $B=B^*$. Then $\pm\mathrm{i}\omega^*$ is a simple pair of characteristic roots such that*

$$\Re\left(\frac{\mathrm{d}\lambda}{\mathrm{d}B}(B^*)\right)>0 \quad \textit{if and only if} \quad \frac{\omega^*S'(\omega^*)}{C(\omega^*)S(\omega^*)}>\frac{\mathrm{d}}{\mathrm{d}\omega}\left(\frac{\omega}{C(\omega)}\right)\Big|_{\omega=\omega^*}. \tag{8.37}$$

*Proof.* Consider a branch $\lambda(B)$ of eigenvalues of (8.1), given by $\lambda(B)=\mu(B)+\mathrm{i}\omega(B)$, such that

$$\mu(B^*)=0 \quad \text{and} \quad \omega(B^*)=\omega^*,\ \omega^*>0.$$

From now on, we explicitly write the dependence of the characteristic equation (8.17) on the bifurcation parameter $B$, so we write $\Delta(\lambda, B)$ instead of $\Delta(\lambda)$, as defined in (8.18). Since $\Delta(\lambda(B), B) = 0$, then differentiating $\Delta(\lambda(B), B)$ with respect to $B$ gives

$$\frac{\mathrm{d}\lambda}{\mathrm{d}B}(B)\frac{\partial\Delta}{\partial\lambda}(\lambda(B), B) + \frac{\partial\Delta}{\partial B}(\lambda(B), B) = 0. \tag{8.38}$$

One can check that

$$\frac{\partial\Delta}{\partial\lambda}(\lambda(B), B) = 1 - B\int_0^\infty \theta F(\theta)e^{-\lambda(B)\theta}\,d\theta, \tag{8.39}$$

and

$$\frac{\partial\Delta}{\partial B}(\lambda(B), B) = \int_0^\infty F(\theta)e^{-\lambda(B)\theta}\,d\theta.$$

Since $\lambda(B)$ is an eigenvalue of (8.1), it satisfies (8.17) and so

$$\int_0^\infty F(\theta)e^{-\lambda(B)\theta}\,d\theta = -\frac{\lambda(B) + A}{B}.$$

Hence,

$$\frac{\partial\Delta}{\partial B}(\lambda(B), B) = -\frac{\lambda(B) + A}{B}. \tag{8.40}$$

Suppose, by contradiction, that $\pm\mathrm{i}\omega^*$ are not simple eigenvalues of (8.1). Then

$$\frac{\partial\Delta}{\partial\lambda}(\lambda(B^*), B^*) = 0.$$

From (8.38), we deduce that

$$\frac{\partial\Delta}{\partial B}(\lambda(B^*), B^*) = 0,$$

that is, from (8.40),

$$\frac{\lambda(B^*) + A}{B^*} = 0.$$

Separating real and imaginary parts and taking into account that $B^* > 0$, this yields

$$\omega^* = 0 \quad \text{and} \quad A = 0.$$

This is impossible since $\omega^* > 0$ and we assumed, at the beginning of this section, that $A \neq 0$, so a contradiction holds. We conclude that $\pm\mathrm{i}\omega^*$ are simple eigenvalues of (8.1).

From (8.38), (8.39) and (8.40), we obtain

$$\left(\frac{\mathrm{d}\lambda}{\mathrm{d}B}(B)\right)^{-1} = -\frac{\dfrac{\partial\Delta}{\partial\lambda}(\lambda(B), B)}{\dfrac{\partial\Delta}{\partial B}(\lambda(B), B)} = B\frac{1 - B\displaystyle\int_0^\infty \theta F(\theta)e^{-\lambda(B)\theta}\,d\theta}{\lambda(B) + A}.$$

Therefore,

$$\left(\frac{\mathrm{d}\lambda}{\mathrm{d}B}(B^*)\right)^{-1} = B^* \frac{1 - B^* S'(\omega^*) + \mathrm{i}B^* C'(\omega^*)}{A + \mathrm{i}\omega^*},$$

where $C$ and $S$ are defined by (8.27). Hence,

$$\Re\left(\frac{\mathrm{d}\lambda}{\mathrm{d}B}(B^*)\right)^{-1} = \frac{B^*}{A^2 + (\omega^*)^2}\left[A(1 - B^* S'(\omega^*)) + \omega^* B^* C'(\omega^*)\right].$$

Remembering that $\omega^*$ and $B^*$ satisfy (8.26), we have

$$B^* = \frac{\omega^*}{S(\omega^*)} \quad \text{and} \quad A = -B^* C(\omega^*).$$

Using these expressions, we obtain

$$\Re\left(\frac{\mathrm{d}\lambda}{\mathrm{d}B}(B^*)\right)^{-1} = \frac{(B^*)^2}{A^2 + (\omega^*)^2}\left[-C(\omega^*) + \frac{\omega^* C(\omega^*) S'(\omega^*)}{S(\omega^*)} + \omega^* C'(\omega^*)\right],$$

that we rewrite

$$\begin{aligned}\Re\left(\frac{\mathrm{d}\lambda}{\mathrm{d}B}(B^*)\right)^{-1} &= \frac{(B^*)^2 C^2(\omega^*)}{A^2 + (\omega^*)^2}\left[\frac{\omega^* S'(\omega^*)}{C(\omega^*)S(\omega^*)} - \frac{C(\omega^*) - \omega^* C'(\omega^*)}{C^2(\omega^*)}\right], \\ &= \frac{A^2}{A^2 + (\omega^*)^2}\left[\frac{\omega^* S'(\omega^*)}{C(\omega^*)S(\omega^*)} - \frac{\mathrm{d}}{\mathrm{d}\omega}\left(\frac{\omega}{C(\omega)}\right)\Big|_{\omega=\omega^*}\right].\end{aligned}$$

Since

$$\operatorname{sign}\left\{\frac{\mathrm{d}\Re(\lambda)}{\mathrm{d}B}(B^*)\right\} = \operatorname{sign}\left\{\Re\left(\frac{\mathrm{d}\lambda}{\mathrm{d}B}(B^*)\right)^{-1}\right\},$$

we conclude to (8.37). This concludes the proof. □

From the results established in Lemmas 1, 2 and 3, we are able to prove the existence of a Hopf bifurcation that would destabilize (8.1) for a certain value of the parameter $B$. This is proved in the next theorem.

**Theorem 7.** *Assume*

$$B\int_0^\infty F(\theta)\,d\theta > |A|,$$

*and $F$ is a decreasing function. Then there exists $B^* > 0$ satisfying (8.25) such that (8.1) is asymptotically stable for*

$$\frac{|A|}{\int_0^\infty F(\theta)\,d\theta} < B < B^*, \tag{8.41}$$

*and (8.1) becomes unstable for $B \geq B^*$, with a Hopf bifurcation occurring when $B = B^*$, provided that*

$$\frac{\omega^* S'(\omega^*)}{C(\omega^*)S(\omega^*)} \neq \frac{\mathrm{d}}{\mathrm{d}\omega}\left(\frac{\omega}{C(\omega)}\right)\Big|_{\omega=\omega^*}, \tag{8.42}$$

*where $\pm\mathrm{i}\omega^*$ are purely imaginary eigenvalues of (8.1) when $B = B^*$.*

*Proof.* Since $F$ is supposed to be decreasing, $S(\omega) > 0$ for all $\omega > 0$ from Lemma 1. Thus, Lemma 2 gives the existence of $(\omega^*, B^*)$, with $\omega^* > 0$ and $B^*$ satisfying (8.25), such that a pair of simple (see Lemma 3) purely imaginary eigenvalues $\pm i\omega^*$ of (8.1) exists when $B = B^*$. As a consequence of the proof of Lemma 2, (8.1) does not have purely imaginary eigenvalues when $B < B^*$.

From Rouché's Theorem [16, p.248], it follows that (8.1) is asymptotically stable when $B$ satisfies (8.41).

Assume (8.42) holds. Then, from Lemma 3, either

$$\Re\left(\frac{\mathrm{d}\lambda}{\mathrm{d}B}(B^*)\right) > 0 \quad \text{or} \quad \Re\left(\frac{\mathrm{d}\lambda}{\mathrm{d}B}(B^*)\right) < 0.$$

Suppose, by contradiction, that

$$\Re\left(\frac{\mathrm{d}\lambda}{\mathrm{d}B}\right) < 0$$

for $B < B^*$, $B$ close to $B^*$. Then there exists an eigenvalue $\lambda(B)$ of (8.1) such that $\Re(\lambda(B)) > 0$ and $B < B^*$. This contradicts the stability of (8.1) for $B < B^*$. Thus,

$$\Re\left(\frac{\mathrm{d}\lambda}{\mathrm{d}B}(B^*)\right) > 0.$$

This implies the existence of a Hopf bifurcation when $B = B^*$ (see Theorem 1). □

Theorem 7 gives a condition for the existence of a Hopf bifurcation, which leads to the appearance of periodic solutions. This condition that the function $F$ is decreasing can be relaxed to the condition that $F$ is such that $S(\omega) > 0$ for $\omega > 0$, where $S$ is defined by (8.27). However, up to now, no better condition has been found.

If $F$ is a density function, it can be decreasing if it is piecewise constant, or if $F$ is an exponential law for example. If $F$ is a Gamma distribution with parameters $k$ and $\sigma$, given by (8.3), then it is a decreasing function if and only if $k = 0$, that is, if $F$ is a *weak kernel*, which is an exponential distribution. However, given the fact that Gamma distributions are the more used density functions in the literature, it is not so worrying that Theorem 7 only works for the weak kernel, because if $F$ has a Gamma distribution the characteristic equation can be reduced to a polynomial function and so other methods, that are more interesting, can be used to determine the stability of (8.1).

Eventually, the interest of Theorem 7 relies on the fact that it can be applied to functions $F$ that are not *necessarily* density functions, but rather the product of a density function and a more general term (see the next section).

Another important point that deserves to be stressed, is that Theorem 7 does not give information on an eventual bifurcation that could occur for larger values of the parameter $B$, and lead to a stability switch. This can

be observed for equations with delay-dependent coefficients (see [7]), and it can be assumed that, maybe under particular assumptions, the same behavior could be observed in differential equations with distributed delay.

In the next section, we consider a problem from population dynamics, the evolution of a stem cell population, modelled by a nonlinear delay differential equation with distributed delay, and we show that the existence of a Hopf bifurcation, given by Theorem 7, leads to interesting results related to some blood diseases, in particular to leukemias.

## 8.5 Application: Periodic Oscillations in a Stem Cell Population

Let consider a population of hematopoietic stem cells (HSC), denoted by $S(t)$. These cells are at the root of the blood production process. They are located in the bone marrow, where they mature and differentiate through successive divisions to produce more and more differentiated cells, which will eventually give birth to blood cells. HSC can be divided in actively proliferating cells (which are in cell cycle where they synthesize DNA and divide at mitosis) and quiescent cells. The cell population $S(t)$ denotes the quiescent HSC population. It satisfies the nonlinear delay differential equation (see Adimy et al [1, 2])

$$S'(t) = -\left[\alpha + \beta(S(t))\right] S(t) + 2\int_0^\infty e^{-\gamma a} f(a)\beta(S(t-a))S(t-a)\, da. \quad (8.43)$$

In this model, HSC are assumed to differentiate with a constant rate $\alpha > 0$. Moreover, they can be introduced in the cell cycle whenever during their life with a rate $\beta$, depending on the HSC population itself. Typically, and from now on, $\beta$ is chosen to be a Hill function,

$$\beta(S) = \beta_0 \frac{\theta^n}{\theta^n + S^n}, \quad \beta_0, \theta, n > 0. \quad (8.44)$$

It is a decreasing and bounded function of the HSC population, which tends to zero at infinity. The coefficient $\beta_0$ represents the maximum introduction rate, $\theta$ is the HSC population for which the introduction rate reaches half of its maximum, and $n$ is the sensitivity of the introduction rate.

A proportion of cells that have been introduced in the cell cycle returns in the HSC population after division. The division occurs a certain time $a$ after the introduction of cells in cycle. The time of division is distributed according to a density function $f$, which can usually be considered to have a compact support $[0, \tau]$, where $\tau > 0$ is the maximum age of division. Moreover, while in cycle, cells can die by apoptosis (a programmed cell death) with a rate $\gamma > 0$. The term $e^{-\gamma a}$ must then be understood as a survival rate of cells that have spent a time $a$ in the cell cycle. Hence, the integral term in the

right hand side of (8.43) describes the amount of cells corresponding to cells introduced a time $a$ earlier in cycle, that have survived, and divide according to the density $f$. Finally, the coefficient 2 in the last term of the right hand side of (8.43) takes into account the division of each cell in two daughter cells. The reader interested in the mathematical modelling of hematopoiesis and stem cells dynamics is invited to study the works of Mackey [26, 27], Mackey and Rudnicki [29, 30], Bernard et al [9, 10], Pujo et al [33, 32], Adimy et al [1, 2], Crauste [15], and the references therein.

Eq. (8.43) is a nonlinear differential equation with distributed delay. From Hale and Verduyn Lunel [19], for every nonnegative and continuous initial condition $\varphi$, defined on $(-\infty, 0]$ (or $[-\tau, 0]$ if $f$ is supported on $[0, \tau]$), (8.43) has a unique nonnegative and continuous solution $S = S^{\varphi}$, defined for $t > 0$. In addition, if $\alpha > 0$, all solutions of (8.43) are bounded, and, if $\alpha = 0$, (8.43) may admit unbounded solutions. We refer to [1] for a detailed proof of these boundedness results.

We are going to apply the results obtained in Section 8.4, Theorems 6 and 7, to the linearized equation of (8.43) in order to determine the stability of the unique positive steady state of (8.43). We recall that a steady state of (8.43) is said to be *locally asymptotically stable*, or LAS, if the linearized equation of (8.43) about this steady state is asymptotically stable. The steady state is unstable if the linearized equation is unstable.

A steady state of (8.43) is a solution $\overline{S}$ satisfying $\overline{S}\,'(t) = 0$ for all $t > 0$. That is

$$\left[\alpha + \beta(\overline{S})\right] \overline{S} = 2 \left( \int_0^{\infty} e^{-\gamma a} f(a)\, da \right) \beta(\overline{S}) \overline{S}. \tag{8.45}$$

One easily checks that $\overline{S} = 0$ is always a steady state of (8.43). It describes the cell population extinction and, therefore, its study is not really biologically relevant.

Searching for nontrivial steady states of (8.43), one can see that (8.45) has a unique positive solution, denoted by $S^*$, satisfying

$$\left( 2 \int_0^{\infty} e^{-\gamma a} f(a)\, da - 1 \right) \beta(S^*) = \alpha, \tag{8.46}$$

provided that

$$\left( 2 \int_0^{\infty} e^{-\gamma a} f(a)\, da - 1 \right) \beta_0 > \alpha > 0. \tag{8.47}$$

From (8.46), using (8.44), we obtain

$$S^* = \theta \left( \frac{\kappa \beta_0 - \alpha}{\alpha} \right)^{\frac{1}{n}}, \tag{8.48}$$

where we have set, for the sake of simplicity,

$$\kappa = 2 \int_0^{\infty} e^{-\gamma a} f(a)\, da - 1.$$

Under assumption (8.47), $\kappa > 0$.

To analyze the behavior of the nontrivial steady state $S^*$, let us linearize (8.43) about $S^*$ and study the eigenvalues of (8.43). We set

$$\beta^* := \frac{\mathrm{d}}{\mathrm{d}S}\left(S\beta(S)\right)_{S=S^*} = \frac{\alpha}{\kappa^2\beta_0}\left[\kappa\beta_0 - (\kappa\beta_0 - \alpha)n\right]. \tag{8.49}$$

Let $x(t) = S(t) - S^*$. The linearized equation of (8.43) about $S^*$ is then given by

$$x'(t) = -(\alpha + \beta^*)x(t) + 2\beta^* \int_0^\infty e^{-\gamma a} f(a)x(t-a)\,da. \tag{8.50}$$

Setting

$$A = \alpha + \beta^*, \quad B = -\beta^*, \quad F(\theta) = 2e^{-\gamma\theta} f(\theta),$$

Eq. (8.50) can be written in the form of (8.1). Moreover, the variable $\overline{A}$, defined by (8.34), is here given by

$$\overline{A} = \alpha - \kappa\beta^* = \alpha\frac{\kappa\beta_0 - \alpha}{\kappa\beta_0}n,$$

which is positive, thanks to (8.47). Note that $B > 0$ if and only if $\beta^* < 0$. Hence, we can state and prove the next proposition, using Theorems 6 and 7.

**Proposition 2.** *The nontrivial steady state $S^*$ of (8.43) is locally asymptotically stable when*

$$0 < n \leq \left[1 + \frac{\kappa}{\kappa + 2}\right]\frac{\kappa\beta_0}{\kappa\beta_0 - \alpha}. \tag{8.51}$$

*In addition, assuming the function $a \mapsto e^{-\gamma a} f(a)$ is decreasing, there exists $n^*$, satisfying*

$$\left[1 + \frac{\kappa}{\kappa + 2}\right]\frac{\kappa\beta_0}{\kappa\beta_0 - \alpha} < n^*, \tag{8.52}$$

*such that $S^*$ is locally asymptotically stable for $0 < n < n^*$ and unstable for $n \geq n^*$, with a Hopf bifurcation occurring when $n = n^*$ provided that (8.42) holds.*

*Proof.* As recalled above, $S^*$ is locally asymptotically stable if (8.50) is asymptotically stable. Then we use Theorem 6.

We already noticed that $\overline{A} = A + B\int_0^\infty F(\theta)\,d\theta > 0$, so $S^*$ is LAS if $B \leq 0$ (see Theorem 6), that is if $\beta^* \geq 0$. Using (8.44), this corresponds to

$$0 < n \leq \frac{\kappa\beta_0}{\kappa\beta_0 - \alpha}.$$

In addition, Theorem 6 says that $S^*$ is LAS if $B > 0$ and $A > B\int_0^\infty F(\theta)\,d\theta$. After easy computations, it comes that these conditions are equivalent to

$$\frac{\kappa\beta_0}{\kappa\beta_0 - \alpha} < n \leq \left[1 + \frac{\kappa}{\kappa + 2}\right]\frac{\kappa\beta_0}{\kappa\beta_0 - \alpha}.$$

This proves (8.51) and the first point of this proposition.

Since finding a critical value of $B$ is equivalent to finding a critical value of $n$, the second point of Proposition 2 is a trivial application of Theorem 7. □

The following corollaries are straightforward.

**Corollary 1.** *Suppose $f$ has a uniform distribution on the interval $[0,\tau]$, $\tau > 0$. Then there exists $n^*$ satisfying (8.52) such that $S^*$ is locally asymptotically stable for $0 < n < n^*$ and unstable for $n \geq n^*$.*

**Corollary 2.** *Suppose $f$ has an exponential distribution, as in (8.3) with $k = 0$ and $\sigma \in \mathbb{R}$. Then, if $\gamma + \sigma \geq 0$, there exists $n^*$ satisfying (8.52) such that $S^*$ is locally asymptotically stable for $0 < n < n^*$ and unstable for $n \geq n^*$.*

In order to numerically compute the solutions of (8.43), let us fix the values of the parameters $\beta_0$, $\theta$, $\alpha$ and $\gamma$, as given by Mackey [26],

$$\beta_0 = 1.77 \text{ d}^{-1}, \quad \theta = 1.68 \times 10^8 \text{ cells/kg}, \quad \alpha = 0.05 \text{ d}^{-1}, \quad \gamma = 0.2 \text{ d}^{-1}. \tag{8.53}$$

Using the MATLAB solver dde23 [37], we can compute the solutions of (8.43). We use the values of the parameters given by (8.53) and we consider two different types of density functions $f$, a first case when $f$ has a uniform law on the interval $[0,\tau]$, with $\tau = 7$ days, and a second case when $f$ is a *weak kernel*, that is, an exponential distribution (as in (8.3) with $k = 0$). The value of $\sigma$, in this latter case, is chosen as $\sigma = 2/7$ so that the expectation of $f$ equals 3.5 days, similar to the uniform law case. Both distributions are depicted in Figure 8.1.

When $f$ has a uniform law on the interval $[0,7]$, the Hopf bifurcation determined in Corollary 1 occurs when $n^* = 2.53$, whereas when $f$ has an

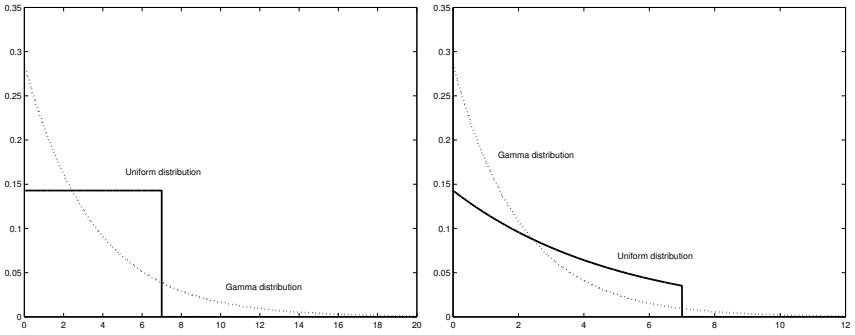


**Fig. 8.1.** Left: Density functions used in the simulations displayed in Fig. 8.2 to 8.5, a uniform distribution on the interval $[0,7]$ and an exponential distribution, as defined in (8.3), with $\sigma = 2/7$ and $k = 0$. Right: One can observe shapes of the density functions multiplied by the survival rate $e^{-\gamma a}$, with $\gamma = 0.2$ days$^{-1}$.

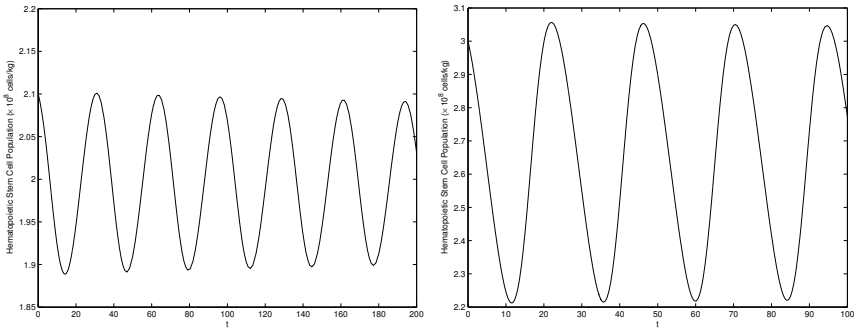


**Fig. 8.2.** Solutions $S(t)$ of (8.43) are drawn for parameters given by (8.53). For a critical value $n^*$ of the parameter $n$, the steady state $S^*$ undergoes a Hopf bifurcation and periodic solutions appear, with different periods and amplitudes depending on the density function. When division times are distributed uniformly on the interval $[0, 7]$ (left), the Hopf bifurcation occurs for $n^* = 2.53$. Oscillating solutions have periods about 33 days. When the density function is an exponential distribution (right), the Hopf bifurcation occurs for $n^* = 3.44$ and periods of the oscillations are in the order of 24 days.

exponential distribution with $\sigma = 2/7$ the Hopf bifurcation occurs for $n^* = 3.44$ (see Fig. 8.2).

A bifurcation diagram showing values of the steady state $S^*$, explicitly given by (8.48), for both types of distributions is presented in Fig. 8.3. One can observe that values of the steady state are different depending on the choice of the density function, especially for small values of $n$ (that is when the steady state is asymptotically stable). For large values of $n$, this phenomenon disappears.

When $n$ increases away from the critical value $n^*$, oscillating solutions can be observed, with increasing periods. This is displayed in Fig. 8.4 and 8.5. However, it is noticeable that amplitudes and periods of the oscillations are different depending on the choice of the density function $f$. With a uniform distribution of cell cycle durations, long period oscillations, in the order of 40 to 70 days, can be observed for values of $n$ between 3 and 5 (see Fig. 8.4). In the case of exponential distribution, periods and amplitudes of the oscillations are shorter, in the order of 26 to 40 days, for larger values of the parameter $n$ (see Fig. 8.5).

Periods of the oscillations for the uniform distribution increase rapidly with $n$, to reach very long periods, whereas the exponential distribution slows down the increase of the periods, which quickly reach some limit value. The same effect is observed for amplitudes of the oscillations. Thus the shape of the density function – more particularly in this case the shape of the density function multiplied by the exponential survival rate – plays an important role

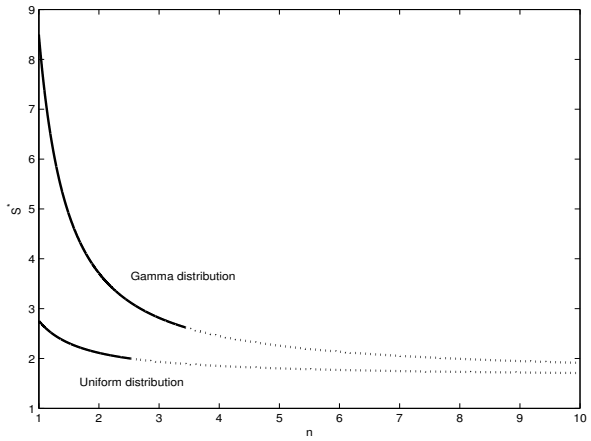


**Fig. 8.3.** Bifurcation diagram for the steady state $S^*$ given by (8.48). All parameters are given by (8.53). The upper curve corresponds to an exponential distribution (8.3) with $\sigma = 2/7$. The steady state is asymptotically stable for $n < 3.44$, and unstable for $n \geq 3.44$. The lower curve corresponds to a uniform distribution of cell cycle times on $[0, 7]$. The steady state is asymptotically stable for $n < 2.53$, and unstable for $n \geq 2.53$.

not only in the appearance of oscillating solutions but also in the length of the periods and the range of the amplitudes (see Fig. 8.1).

Oscillating solutions in blood cell populations have been observed in some patients with blood diseases [22]. For example, experimental studies report cases of oscillations of all blood cell counts with average periods of 70-80 days in some patients with chronic myelogenous leukemia (see [17]), a widespread form of blood cancer. Cyclical neutropenia [22], another blood disease, characterized by a fall of blood cell counts every three weeks in human, may also exhibit stressed oscillations, with periods in the range of 20 to 30 days. Oscillations obtained in Fig. 8.4 and 8.5 by simulating the differential equation with distributed delay (8.43) for different density functions may contribute to the study of blood diseases characterized by oscillations of blood cell counts (such diseases are known as *periodic hematological diseases*). This can be found, for example, in [9] or [1, 2], where the results obtained by the authors stress the localization of these diseases in the pluripotent HSC compartment. This explains why oscillations are observed in all cell types (red blood cells, white cells and platelets) though these diseases are associated with only one blood cell type (white cells for leukemia for example).

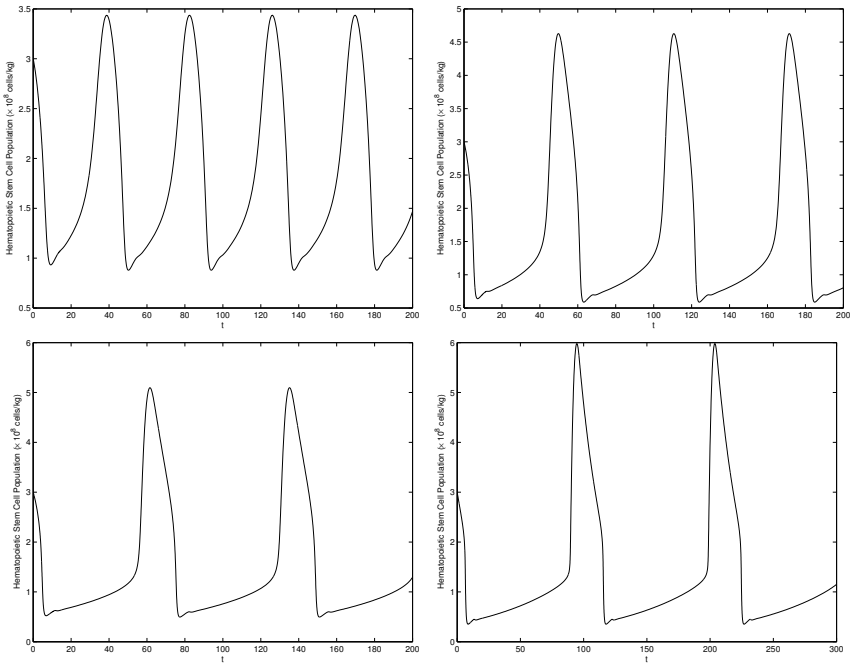


**Fig. 8.4.** Solutions of (8.43) are drawn for $n$ larger than the critical value $n^*$ given by Corollary 1, when the density function has a uniform distribution on the interval $[0, 7]$. From left to right and top to bottom $n$ successively equals 3, 4, 5 and 10. Periods of the oscillations range from 40 days to 110 days, with periods about 60-70 days when $n = 4$ or 5. Amplitudes increase as $n$ increases, with very low values reached by the population when $n$ is large enough.

## References

1. Adimy, M., Crauste, F., Ruan, S.: A Mathematical Study of the Hematopoiesis Process with Applications to Chronic Myelogenous Leukemia. SIAM J. Appl. Math., **65** (4), 1328–1352 (2005)
2. Adimy, M., Crauste, F., Ruan, S.: Stability and Hopf Bifurcation in a Mathematical Model of Pluripotent Stem Cell Dynamics. Nonlinear Analysis: Real World Applications, **6**, 651–670 (2005)
3. Adimy, M., Crauste, F., Ruan, S.: Periodic Oscillations in Leukopoiesis Models with Two Delays. J. Theor. Biol., **242**, 288–299 (2006)
4. Anderson, R.F.V.: Geometric and Probabilistic Stability Criteria for Delay Systems. Math. Biosci. **105**, 81–96 (1991)
5. Anderson, R.F.V.: Intrinsic Parameters and Stability of Differential-Delay Equations. J. Math. Anal. Appl. **163**, 184–199 (1992)
6. Atay, F.M.: Delayed Feedback Control near Hopf Bifurcation. Disc. Cont. Dyn. Syst. Ser. S **1** (2), 197–205 (2008).

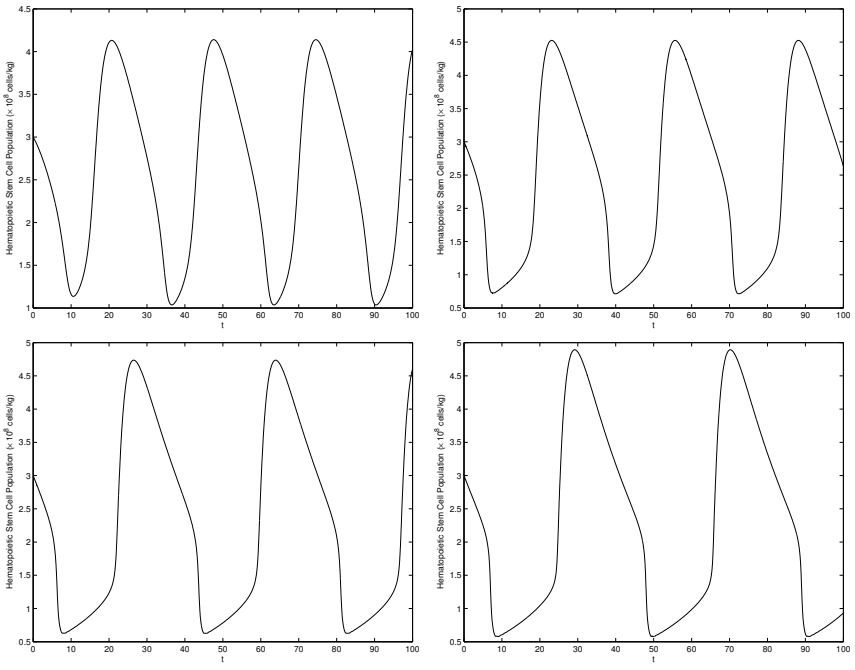


**Fig. 8.5.** Solutions of (8.43) are drawn for $n$ larger than the critical value $n^*$ given by Corollary 2, when the density function has an exponential distribution with parameter $\sigma = 2/7$. From left to right and top to bottom $n$ successively equals 4, 6, 8 and 10. Periods of the oscillations range from 26 to 40 days. Amplitudes increase as $n$ increases, with very low values reached by the population when $n$ is large enough, yet the increase is less drastic than in the case of the uniform distribution.


7. Beretta, E., Kuang, Y.: Geometric Stability Switch Criteria in Delay Differential Systems with Delay Dependent Parameters. SIAM J. Math. Anal. **33** (5), 1144-1165 (2002)
8. Bernard, S., Bélair, J., Mackey, M.C.: Sufficient Conditions for Stability of Linear Differential Equations with Distributed Delay. Disc. Cont. Dyn. Syst. Ser. B **1**, 233–256 (2001)
9. Bernard, S., Bélair, J., Mackey, M.C.: Oscillations in Cyclical Neutropenia: New Evidence for Origins Based on Mathematical Modeling. J. Theor. Biol. **223**, 283–298 (2003)
10. Bernard, S., Bélair, J., Mackey, M.C.: Bifurcations in a White Blood Cell Production Model. Comptes Rendus Biologies **327**, 201-ñ210 (2004)
11. Boese, F.G.: The Stability Chart for the Linearized Cushing Equation with a Discrete Delay and Gamma-Distributed Delays. J. Math. Anal. Appl. **140**, 510–536 (1989)
12. Boese, F.G.: Stability Criteria for Second-Order Dynamical Systems Involving Several Time Delays. SIAM J. Math. Anal. **26**, 1306–1330 (1995)

13. Burns, F.J., Tannock, I.F.: On the Existence of a $G_0$ Phase in the Cell Cycle. Cell. Tissue Kinet, **19**, 321–334 (1970)
14. Cooke, K.L., Grossman, Z.: Discrete Delay, Distributed Delay and Stability Switches. J. Math. Anal. Appl. **86**, 592–627 (1982)
15. Crauste, F.: Global Asymptotic Stability and Hopf Bifurcation for a Blood Cell Production Model. Mathematical Biosciences and Engineering, **3** (2), 325–346 (2006)
16. Dieudonné, J.: Foundations of Modern Analysis. Academic Press, New-York, 1960
17. Fortin, P., Mackey, M.C.: Periodic Chronic Myelogenous Leukemia: Spectral Analysis of Blood Cell Counts and Etiological Implications. Brit. J. Haematol. **104**, 336–345 (1999)
18. Hale, J.: Theory of Functional Differential Equations. Springer, New York, 1977
19. Hale, J.K., Verduyn Lunel, S.M.: Introduction to Functional Differential Equations. Applied Mathematical Sciences **99**, Springer-Verlag, New York, 1993
20. Hayes, N.D.: Roots of the Transcendental Equation Associated with a Certain Differential Difference Equation. J. London Math. Society. **25**, 226–232 (1950)
21. Huang, C., Vandewalle, S.: An Analysis of Delay-Dependent Stability for Ordinary and Partial Differential Equations with Fixed and Distributed Delays. SIAM J. Sci. Comput. **25** (5), 1608–1632 (2004)
22. Haurie, C., Dale, D.C., Mackey, M.C.: Cyclical Neutropenia and Other Periodic Hematological Diseases: A Review of Mechanisms and Mathematical Models. Blood, **92**, 2629–2640 (1998)
23. Kuang, Y.: Delay Differential Equations with Applications in Population Dynamics. Mathematics in Science and Engineering **191**, Academic Press, 1993
24. Kuang, Y.: Nonoccurrence of Stability Switching in Systems of Differential Equations with Distributed Delays. Quart. Appl. Math. **LII** (3), 569–578 (1994)
25. MacDonalds, N.: Biological Delay Systems: Linear Stability Theory. Cambridge Studies Math. Biol. **8**, Cambridge University Press, Cambridge, 1989
26. Mackey, M.C.: A Unified Hypothesis on the Origin of Aplastic Anaemia and Periodic Hematopoiesis. Blood, **51**, 946–956 (1978)
27. Mackey, M.C.: Dynamic Hematological Disorders of Stem Cell Origin. In: Vassileva-Popova, J.G., Jensen, E.V. (eds) Biophysical and Biochemical Information Transfer in Recognition. Plenum Press, New York (1979)
28. Mackey, M.C., Haurie, C., Bélair, J.: Cell Replication and Control. In: Beuter, A., Glass, L., Mackey, M.C., Titcombe, M.S. (eds) Nonlinear Dynamics in Physiology and Medicine. Springer, New York (2003)
29. Mackey, M.C., Rudnicki, R.: Global Stability in a Delayed Partial Differential Equation Describing Cellular Replication. J. Math. Biol. **33**, 89–109 (1994)
30. Mackey, M.C., Rudnicki, R.: A New Criterion for the Global Stability of Simultaneous Cell Replication and Maturation Processes. J. Math. Biol. **38**, 195–219 (1999)

31. Ozbay, H., Bonnet, C., Clairambault, J.: Stability Analysis of Systems with Distributed Delays and Application to Hematopoietic Cell Maturation Dynamics. Proceedings of the 47th IEEE Conference on Decision and Control, Cancun, Mexico, December 2008 (to appear)
32. Pujo-Menjouet, L., Bernard, S., Mackey, M.C.: Long Period Oscillations in a $G_0$ Model of Hematopoietic Stem Cells. SIAM J. Appl. Dynam. Sys. **4** (2), 312–332 (2005)
33. Pujo-Menjouet, L., Mackey, M.C.: Contribution to the Study of Periodic Chronic Myelogenous Leukemia. C. R. Biologies **327**, 235–244 (2004)
34. Ruan, S.: Delay Differential Equations in Single Species Dynamics. In: Arino, O., Hbid, M., Aitdads, E. (eds) Delay Differential Equations with Applications. Springer, Berlin (2006)
35. Ruan, S., Wei, J.: Periodic Solutions of Planar Systems with two Delays. Proc. Royal Soc. Edinburgh Ser. **129A**, 1017–1032 (1999)
36. Ruan, S., Wei, J.: On the Zeros of Transcendental Functions with Applications to Stability of Delay Differential Equations with Two Delays. Dyn. Contin. Discrete Impuls. Syst. Ser. A Math. Anal. **10**, 863–874 (2003)
37. Shampine, L.F., Thompson, S.: Solving DDEs in MATLAB. Appl. Numer. Math. **37**, 441–458 (2001)
http://www.radford.edu/~thompson/webddes/.
38. Tang, X.H.: Asymptotic Behavior of a Differential Equation with Distributed Delays. J. Math. Anal. Appl. **301**, 313–335 (2005)
39. Wei, J., Ruan, S.: Stability and Bifurcation in a Neural Network Model with Two Delays. Physica D **130**, 255–272 (1999)

## 5.4 Adimy et al. (2010)

Manuscrit de l'article : [10] M. Adimy, F. Crauste, My L. Hbid, R. Qesmi, *Stability and Hopf bifurcation for a cell population model with state-dependent delay*, SIAM J. Appl. Math, 70 (5), 1611–1633 (2010).

SIAM J. APPL. MATH.
Vol. 70, No. 5, pp. 1611–1633



# STABILITY AND HOPF BIFURCATION FOR A CELL POPULATION MODEL WITH STATE-DEPENDENT DELAY*

MOSTAFA ADIMY†, FABIEN CRAUSTE‡, MY LHASSAN HBID§, AND REDOUANE QESMI¶

**Abstract.** We propose a mathematical model describing the dynamics of a hematopoietic stem cell population. The method of characteristics reduces the age-structured model to a system of differential equations with a state-dependent delay. A detailed stability analysis is performed. A sufficient condition for the global asymptotic stability of the trivial steady state is obtained using a Lyapunov–Razumikhin function. A unique positive steady state is shown to appear through a transcritical bifurcation of the trivial steady state. The analysis of the positive steady state behavior, through the study of a first order exponential polynomial characteristic equation, concludes the existence of a Hopf bifurcation and gives criteria for stability switches. A numerical analysis confirms the results and stresses the role of each parameter involved in the system on the stability of the positive steady state.

**Key words.** hematopoietic stem cells, functional differential equation, state-dependent delay, Lyapunov–Razumikhin function, Hopf bifurcation

**AMS subject classifications.** 34D20, 34K20, 34K99, 92C37

**DOI.** 10.1137/080742713

## 1. Introduction.

The production and regulation of blood cells is a very complex process, called hematopoiesis. It involves a population of hematopoietic stem cells (HSCs), able to differentiate and self-renew, in order to maintain an HSC population. These cells produce by differentiation all blood cell lineages (white cells, red blood cells, platelets) that mature within several generations and finally give birth to blood cells that enter the circulating blood.

HSCs are either proliferating or nonproliferating cells. A majority of HSCs is actually in a quiescent stage [18]. Nonproliferating (or resting) HSCs represent a pool of stem cells that is used to produce new blood cells. Proliferating HSCs are actively involved in cell division (growth, DNA synthesis, etc.). The dynamics of HSCs have attracted the attention of modelers for forty years now, due to their involvement in major blood diseases, such as leukemias, that originate at the stem cell level [27, 33].

To our knowledge, the first mathematical model of HSC dynamics has been proposed by Mackey [43] in 1978, inspired by Lajtha [40] and Burns and Tannock [17]. Mackey's model consists in a system of two nonlinear delay differential equations, describing the dynamics of proliferating and nonproliferating HSCs. The delay, which is constant, accounts for an average cell cycle duration. Since then, many authors have tried to improve Mackey's model, particularly to better take into account cell

*Received by the editors December 4, 2008; accepted for publication (in revised form) October 15, 2009; published electronically January 13, 2010.
http://www.siam.org/journals/siap/70-5/74271.html

†INRIA Rhône-Alpes, Institut Camille Jordan UMR 5208, 43 blvd du 11 novembre 1918, F-69622 Villeurbanne Cedex, France (mostafa.adimy@inria.fr).

‡Université de Lyon, CNRS, Université Lyon 1, Institut Camille Jordan UMR 5208, Batiment du Doyen Jean Braconnier, 43 blvd du 11 novembre 1918, F-69222 Villeurbanne Cedex, France (crauste@math.univ-lyon1.fr).

§Department of Mathematics, Semlalia Faculty of Sciences, Cadi Ayyad University, P.O. 2390 Marrakesh, Morocco (hbid@ucam.ac.ma).

¶Department of Mathematics and Statistics, York University, 4700 Keele Street, Toronto, ON, M3J 1P3, Canada (rqesm@mathstat.yorku.ca).

maturity and cell cycle duration's control in HSC dynamics [1, 8, 46, 47]. This latter point is of particular interest. Cell cycle durations may vary a lot, and the nature of the signal that triggers cell division remains mainly unknown.

In 1978, MacDonald [42] focused on this problem and proposed that cell cycle division times are distributed according to a density function, for instance, a Gamma distribution. In 1993, Mackey and Rey [45] considered a distribution of cell cycle durations according to a density function, but their analysis took into account only a particular case (when the density is a Dirac measure), and then their system exhibited a discrete time delay. For many years, only discrete time delay systems of HSC dynamics were studied; see, for instance, [7, 25, 46, 47] and the references therein. Recently, Adimy and Crauste [1], Adimy, Crauste, and Ruan [5, 6], and Bernard, Bélair, and Mackey [16] analyzed modified versions of Mackey's model [43] by assuming a distribution of cell division times. They stressed the influence of the distribution (some properties of the density function) on solution's behavior. However, this approach is not always satisfactory, especially because no biological data can allow us to precisely determine the nature—the shape—of the age distribution. In 2005, Adimy and Crauste [2] and Adimy, Crauste, and Pujo-Menjouet [4] proposed a model of HSC dynamics in which the cell cycle duration depends on the cell maturity. This is a way of indicating that cell cycles can be shortened for some types of cells, or in particular situations such as diseases or anemias.

In this paper, we focus on the influence of the number of cells on cell cycle durations. Low cell counts lead to quick reactions of the organism, in order to produce enough cells to return to a normal state, and this can then induce shorter cell cycles (this is observed for red cells, where, following an anemia, immature cells enter the bloodstream and replace mature cells very quickly [22]). Moreover, cell cycle duration variability has been the subject of numerous modeling works (see, for instance, Alarcon and Tindall [12], Fuss et al. [28], and Tyson and Novak [58]) based on the control of progression through the different phases of the cell cycle by protein concentration. In [12], the authors consider in particular the influence of extracellular factors (nutrients) in the regulation of cell cycle duration in budding yeast. These nutrients are consumed by cells, and this triggers the progression through the cell cycle phases. Considering that nutrient consumption causes progression through cell cycle likely leads to delay differential equations of threshold type (see Kuang [38, Chapter 5.4] or Smith and Kuang [57]) that are close to state-dependent delay equations. Another approach consists in avoiding introduction of new variables (nutrient concentration, for instance) and describing cell cycle duration control by means of cell population counts.

A natural way of doing this is to consider that cell cycle durations depend either on the total population of HSCs or on the population of proliferating HSCs. Yet, proliferating cells are indeed cells committed to divide (once they have passed the $G_1/S$ transition) and consequently one can assume that they no longer consume nutrients. Hence, they would have no action on factors responsible for durations of cell cycles. On the contrary, the total population of HSCs, that is, both proliferating and nonproliferating cells, seems to be appropriate for controlling cell cycle lengths. However, proliferating HSCs represent only about 5% of all HSCs [18], so their role in cell cycle regulation can be neglected, and we will assume in this work, for simplicity, that only nonproliferating cells control cell cycle durations. The control of cell cycle durations by the total number of HSCs, although more natural and certainly appropriate, will not be considered in this work. This assumption is comforted by recent works [20, 21] in which a modified version of Mackey's model [43], in which the total number of HSCs negatively controls HSC proliferation (in Mackey's model [43], only nonprolif-

erating cells act on HSC proliferation), was studied, and both models were found to be qualitatively and quantitatively similar. Assuming the number of nonproliferating cells influences cell cycle durations modifies the nature of the time delay in Mackey's model [43] and transforms his system into a state-dependent delay system.

The theory of state-dependent delay differential equations has attracted a lot of attention over the last twenty years and started earlier in the 1960s. Driver [24], in 1963, studied existence of solutions, uniqueness, and continuous dependence on initial conditions for state-dependent delay differential equations, and his work has been developed and completed by various authors [9, 10, 37, 39, 48, 50, 51, 54, 59] while investigating periodic solutions for state-dependent delay equations. Nonlinear semigroups for some class of equations have been analyzed by Louihi, Hbid, and Arino [41]. The linearization of state-dependent delay equations has been studied by Cooke and Huang [19], Arino and Sanchez [11], Hartung [30], Hartung and Turi [31], Hartung et al. [32], and Walther [60]. A Hopf bifurcation theorem for state-dependent delay differential equations has been recently obtained by Eichmann [26]. Numerical methods for solving state-dependent delay differential equations have been investigated by Hofer, Tibken, and Lehn [35], Shampine [56], and the references therein. Despite the difficulty related to the analysis of state-dependent delay differential equations, they have been used in some applied works—in cell biology, for instance, by Bélair [13], Bélair, Mackey, and Mahaffy [14], Hbid, Sanchez, and Bravo de la Parra [34], Hofer, Tibken, and Lehn [36], and Mahaffy, Bélair, and Mackey [49], but also in automatic [61].

We propose a complete stability analysis of a nonlinear model of HSC dynamics, with state-dependent delay. The next section is devoted to the presentation of the model, which originally takes the form of an age-structured system. This system is reduced to a system of state-dependent delay equations in section 3. Properties of the resulting system, such as positivity and existence of steady states, are established in section 4. We then focus on the stability of the trivial steady state and prove a sufficient condition for its global asymptotic stability using a Lyapunov–Razumikhin function in section 5. Next, we linearize the system about the unique positive steady state, which is shown to appear through a transcritical bifurcation of the trivial steady state, and perform the analysis of the Hopf bifurcation in section 6. A detailed numerical analysis, in section 7, allows us to identify the role of each parameter and the influence of the state-dependent delay in stability switch of the positive steady state.

**2. The model of HSC dynamics.** Let us consider a population of HSCs, divided into two compartments: proliferating and resting (nonproliferating) cells. Denote by $n(t,a)$ and $p(t,a)$ the population densities of resting and proliferating cells, respectively, which have spent a time $a \geq 0$ in their phase at time $t \geq 0$.

As soon as a cell enters the proliferating phase, it is committed to divide a time $\tau$ later. We assume that the duration of the proliferating phase depends on the total population of nonproliferating cells

$$N(t) = \int_0^\infty n(t,a)da, \tag{2.1}$$

that is, $\tau = \tau(N(t))$. This choice (considering cell cycle durations are controlled only by nonproliferating cells) is justified above, in the introduction (paragraphs 5 and 6).

In [12], nutrients are considered as cell cycle duration regulators. These nutrients bind to cells and modify intracellular protein concentrations that decide on progres-

sion through cell cycle phases. Assuming a constant concentration of nutrients, the cell cycle duration appears as a decreasing function of the available quantity of nutrients for each nonproliferating cell [12, 55] and consequently as an increasing function of $N(t)$. Hence the function $\tau$ is supposed to be bounded, positive, continuously differentiable, and increasing (a lack of HSCs is supposed to shorten cell cycles). We define

$$\tau_0 := \inf_{x\geq 0} \tau(x) = \tau(0) \qquad \text{and} \qquad \tau_{\max} = \sup_{x\geq 0} \tau(x).$$

Proliferating cells can be lost by apoptosis (a programmed cell death) at a rate $\gamma \geq 0$, and, at mitosis, cells with age $\tau$ divide into two daughter cells which immediately enter the resting phase.

Nonproliferating cells are assumed to differentiate at a constant rate $\delta > 0$, which can also take some natural mortality into account. They are introduced in the proliferating phase with a rate $\beta$, which is supposed to depend on the total population of nonproliferating cells (see Mackey [43, 44], Mackey and Rudnicki [46, 47], or Pujo-Menjouet et al. [52, 53]), given by (2.1). The function $\beta$ is supposed to be continuously differentiable, bounded, and positive. Furthermore, from a reasonable biological point of view, we assume $\beta$ is decreasing with $\lim_{x\to+\infty} \beta(x) = 0$. Usually, it is believed that the function $\beta$ is a monotone decreasing Hill function (see [43]), given by

$$\beta(x) = \frac{\beta_0 \theta^r}{\theta^r + x^r}, \quad x \geq 0, \tag{2.2}$$

with $\beta_0 > 0$, $\theta \geq 0$, and $r > 0$. The parameter $\beta_0$ is the maximal rate of reentry in the proliferating phase, $\theta$ is the number of resting cells for which $\beta$ has its maximum rate of change with respect to the resting phase population, and $r$ describes the sensitivity of the reintroduction rate with changes in the population.

The evolution of HSC dynamics is described by the following system of age-structured partial differential equations:

$$\frac{\partial n}{\partial t} + \frac{\partial n}{\partial a} = -\left(\delta + \beta(N(t))\right) n, \qquad a > 0,\ t > 0, \tag{2.3}$$

$$\frac{\partial p}{\partial t} + \frac{\partial p}{\partial a} = -\gamma p, \qquad 0 < a < \tau(N(t)),\ t > 0, \tag{2.4}$$

where $N(t)$ denotes the total population of resting cells, defined by (2.1).

System (2.3)–(2.4) is completed by boundary conditions and initial conditions. The first ones describe the flux of cells entering each phase: new proliferating cells are nonproliferating cells introduced with a rate $\beta$, and new resting cells come from the division of proliferating cells that have spent a time $\tau(N(t))$ in the proliferating phase. Then the boundary conditions of (2.3)–(2.4) are

$$n(t,0) = 2p(t, \tau(N(t))), \tag{2.5}$$

$$p(t,0) = \beta(N(t))N(t). \tag{2.6}$$

Moreover, we suppose that $\lim_{a\to+\infty} n(t,a) = 0$.

Initial conditions of (2.3)–(2.4) are given by nonnegative $L^1$ functions $n_0$ and $p_0$ such that

$$n(0,a) = n_0(a),\ a \geq 0, \quad \text{and} \quad p(0,a) = p_0(a),\ a \in [0, \tau(N(0))]. \tag{2.7}$$

We are now going to check that system (2.3)–(2.4) reduces to a system of differential equations with state-dependent delay.

**3. Reduction to a state-dependent delay equation.** First, we see that using the method of characteristics (see Webb [62]), the solution $p(t,a)$ of (2.4), (2.6), and (2.7) is given, for $t>0$ and $0<a<\tau(N(t))$, by

$$p(t,a)=\begin{cases} p_0(a-t)e^{-\gamma t} & \text{if } 0\le t<a,\\ \beta(N(t-a))N(t-a)e^{-\gamma a} & \text{if } 0\le a\le t.\end{cases} \tag{3.1}$$

Since resting cells are introduced in the proliferating phase with a rate $\beta$, then $p_0(0)$, the population of cells introduced at time $t=0$ in the cycle, should satisfy the classical compatibility condition

$$p_0(0)=\beta(N(0))N(0). \tag{3.2}$$

This condition ensures the continuity of $p(t,a)$ on the line $t=a$.

Denote by $P(t)$ the total population of proliferating stem cells,

$$P(t)=\int_0^{\tau(N(t))} p(t,a)da, \qquad t\ge 0.$$

Then, using (3.1), we deduce

$$P(t)=\begin{cases} e^{-\gamma t}\left(\displaystyle\int_0^t e^{\gamma\theta}\beta(N(\theta))N(\theta)d\theta+\int_0^{\tau(N(t))-t} p_0(\theta)d\theta\right), & t<\tau(N(t)),\\ e^{-\gamma t}\displaystyle\int_{t-\tau(N(t))}^t e^{\gamma\theta}\beta(N(\theta))N(\theta)d\theta, & t\ge\tau(N(t)).\end{cases} \tag{3.3}$$

The variable $P(t)$ is straightforwardly continuous for $t\ge 0$, and since $\tau$ is continuously differentiable, $P(t)$ is also continuously differentiable provided that (3.2) holds true.

Integrating (2.3) with respect to the age variable, and using (2.5), we obtain

$$N'(t)=-\delta N(t)-\beta(N(t))N(t)+2p(t,\tau(N(t))) \qquad \text{for } t\ge 0.$$

Using (3.1), we finally obtain, for $0\le t\le\tau(N(t))$,

$$N'(t)=-\delta N(t)-\beta(N(t))N(t)+2p_0(\tau(N(t))-t)e^{-\gamma t}, \tag{3.4}$$

and, for $t>\tau(N(t))$,

$$N'(t)=-\delta N(t)-\beta(N(t))\,N(t)+2e^{-\gamma\tau(N(t))}\beta(N(t-\tau(N(t))))\,N(t-\tau(N(t))). \tag{3.5}$$

Moreover, $N(0)=\int_0^\infty n_0(a)da$.

One can notice that problem (3.4)–(3.5) is a nonlinear nonautonomous ordinary differential equation for $t<\tau(N(t))$, whereas, for $t\ge\tau(N(t))$, it is a system of differential equations with state-dependent delay. Let us concentrate on system (3.4)–(3.5) for $t\in[0,\tau_{\max}]$.

Consider the differential equation

$$\begin{aligned}\frac{dx}{dt}(t)&=\begin{cases}-\delta x(t)-\beta(x(t))x(t)+2p_0(\tau(x(t))-t)e^{-\gamma t}, & 0\le t\le\tau(x(t)),\\ -\delta x(t)-\beta(x(t))x(t)\\ \quad +2\beta(x(t-\tau(x(t))))x(t-\tau(x(t)))e^{-\gamma\tau(x(t))}, & \tau(x(t))<t\le\tau_{\max},\end{cases}\\ x(0)&=\int_0^\infty n_0(a)da.\end{aligned} \tag{3.6}$$

For a smooth enough function $p_0$ satisfying (3.2), (3.6) has a unique continuously differentiable solution $\phi$ defined on $[0, \tau_{\max}]$ (see Walther [60]). Then (3.5) becomes the following delay differential equation for $t \geq \tau_{\max}$:

$$\begin{cases} \dfrac{dy}{dt}(t) &= -\delta y(t) - \beta(y(t))y(t) + 2\beta(y(t-\tau(y(t))))y(t-\tau(y(t)))e^{-\gamma\tau(y(t))}, \\ y(\theta) &= \phi(\theta), \qquad 0 \leq \theta \leq \tau_{\max}. \end{cases}$$

Thus, by making a change of variable $N(t) := y(t + \tau_{\max})$, system (3.4)–(3.5) can be written as a state-dependent delay differential equation for $t \geq 0$,

$$N'(t) = -(\delta + \beta(N(t)))\, N(t) + 2e^{-\gamma\tau(N(t))}\beta(N(t-\tau(N(t))))\, N(t-\tau(N(t))), \tag{3.7}$$

with, for $\theta \in [-\tau_{\max}, 0]$, $N(\theta) = \phi(\theta + \tau_{\max})$.

Existence and uniqueness of solutions of (3.7) cannot be easily deduced. Equation (3.7) writes $x'(t) = g(x(t), x(t-\tau(x(t))))$ for $t \geq 0$, where the function $g : (\mathbb{R}^+)^2 \to \mathbb{R}$ is given by

$$g(x, y) = -(\delta + \beta(x))\, x + 2e^{-\gamma\tau(x)}\beta(y)\, y, \qquad (x, y) \in (\mathbb{R}^+)^2.$$

This equation can also be written in the general form

$$x'(t) = f(x_t) \qquad \text{for } t \geq 0, \tag{3.8}$$

where $x_t$ is defined by $x_t(\theta) = x(t+\theta)$ for $\theta \in [-\tau_{\max}, 0]$, and the function $f : C \to \mathbb{R}$ is given, for $\phi \in C$, the space of continuous functions on $[-\tau_{\max}, 0]$, by

$$f(\phi) = g(\phi(0), \phi(-\tau(\phi(0)))).$$

Since the functions $\beta(x)$ and $\tau(x)$ are continuously differentiable on $[0, +\infty)$, then $g$ is also continuously differentiable on $(\mathbb{R}^+)^2$. Therefore, existence and uniqueness of a solution of (3.7) defined on $[0, +\infty)$ for an initial condition belonging to $C^1$, the space of continuously differentiable functions on $[-\tau_{\max}, 0]$, follow from Mallet-Paret, Nussbaum, and Paraskevopoulos [50]. One may note that it is not reasonable to expect a well-posed state-dependent delay differential problem from searching for solutions in $C$ (see Walther [60]).

One can notice that (3.7) does not depend on the proliferating cell population $P$, whereas the converse is not true.

In the next section, we focus on some properties of (3.7), such as positivity and boundedness of solutions, as well as the existence of steady states.

**4. Properties of the model and existence of steady states.** In this section we focus on basic properties of solutions of (3.7), such as positivity and boundedness. We also concentrate on the existence of steady states. We suppose from now on that existence and uniqueness of solutions of (3.7) hold for $t \in [-\tau_{\max}, +\infty)$.

The solutions of (3.7) represent cell numbers; therefore, it is essential to show positivity and boundedness. Such properties are straightforwardly obtained (for instance, using a method similar to the one presented in Adimy, Crauste, and Ruan [5]). They are stated in the following proposition.

PROPOSITION 4.1. *The solutions of* (3.7) *are nonnegative, and, provided that* $\delta > 0$*, they are bounded.*

The expression of $P(t)$ in (3.3) gives more precise information on the influence of the behavior of $N(t)$ on the stability and periodicity of the solutions $P(t)$. The following lemma, which states these results, is immediately obtained by using (3.3).

LEMMA 4.2. *Let* $(P(t), N(t))$ *be a solution of* (3.3) *and* (3.7). *If* $N_\infty := \lim_{t\to\infty} N(t)$ *exists, then*

$$\lim_{t\to\infty} P(t) = \begin{cases} N_\infty \beta(N_\infty)\left(\dfrac{1-e^{-\gamma\tau(N_\infty)}}{\gamma}\right) & \text{if } \gamma > 0, \\ N_\infty \beta(N_\infty)\,\tau(N_\infty) & \text{if } \gamma = 0. \end{cases}$$

*If* $N(t)$ *is* $T$*-periodic, then* $P(t)$ *is also* $T$*-periodic.*

In particular, Lemma 4.2 shows the influence of (3.7) on the stability of the entire system. We now focus on the existence of steady states of (3.7).

PROPOSITION 4.3. *Assume* $\delta > 0$ *and*

$$\tau_0 < \frac{1}{\gamma}\ln\left(\frac{2\beta(0)}{\beta(0)+\delta}\right). \tag{4.1}$$

*Then equation* (3.7) *has two steady states* $N \equiv 0$ *and* $N \equiv N^* > 0$, *where*

$$(2e^{-\gamma\tau(N^*)} - 1)\beta(N^*) = \delta. \tag{4.2}$$

*If* (4.1) *does not hold, then* $N \equiv 0$ *is the only steady state of* (3.7).

*Proof.* Define, for $N \geq 0$, the function $\chi(N) := (2e^{-\gamma\tau(N)} - 1)\beta(N)$. Then

$$\chi(0) = (2e^{-\gamma\tau_0} - 1)\beta(0) > \delta \qquad \text{and} \qquad \lim_{N\to+\infty} \chi(N) = 0.$$

Consequently, (4.2) has at least one positive solution $N^*$. Moreover, since $\tau$ is increasing, then $\chi$ is decreasing, and, provided that $\chi(N) > 0$, $N^*$ is unique. □

In the next section, we concentrate on the asymptotic stability of the trivial steady state of (3.7).

**5. Asymptotic stability of the trivial steady state.** In the next theorem, we give a necessary and sufficient condition for the trivial steady state of (3.7), when it is unique, to be globally asymptotically stable using a Lyapunov–Razumikhin function presented in [29].

We recall that $\delta > 0$. From Proposition 4.1 all solutions of (3.7) are then bounded.

THEOREM 5.1. *Assume*

$$\frac{1}{\gamma}\ln\left(\frac{2\beta(0)}{\delta}\right) < \tau_0. \tag{5.1}$$

*Then the trivial steady state of* (3.7) *is globally asymptotically stable.*

*Proof.* Consider the Lyapunov function $V : \mathbb{R}^+ \to \mathbb{R}^+$ given by $V(x) = x^2/2$. We have, for $x \in \mathbb{R}^+$, $u(x) \leq V(x) \leq v(x)$, with $u(x) = x^2/2$ and $v(x) = x^2$.

Define $p : \mathbb{R}^+ \to \mathbb{R}^+$ by $p(x) = xe^{2\alpha\tau(\sqrt{2x})}$, $x \in \mathbb{R}^+$, with $0 < \alpha < \min\{\gamma, \gamma - \ln(2\beta(0)/\delta)/\tau_0\}$. Let $N$ be a solution of (3.7) such that, for $t \geq 0$, $\theta \in [-\tau_{\max}, 0]$,

$$V(N(t+\theta)) < p\left(V(N(t))\right). \tag{5.2}$$

Then, for $t \geq 0$, $N(t - \tau(N(t))) \leq e^{\alpha\tau(N(t))}N(t)$. It follows that, for $t \geq 0$,

$$\begin{aligned} \dot V(N(t)) &= -\left(\delta + \beta(N(t))\right)N(t)^2 \\ &\quad +2e^{-\gamma\tau(N(t))}\beta\left(N(t-\tau(N(t)))\right)N(t-\tau(N(t)))N(t) \\ &\leq -\delta N(t)^2 + 2e^{-\gamma\tau(N(t))}\beta(0)e^{\alpha\tau(N(t))}N(t)^2 \\ &= -\left[\delta - 2e^{-(\gamma-\alpha)\tau(N(t))}\beta(0)\right]N(t)^2. \end{aligned} \tag{5.3}$$

Let $W : \mathbb{R}^+ \to \mathbb{R}$ be the map defined, for $x \in \mathbb{R}^+$, by $W(x) = \left[\delta - 2e^{-(\gamma-\alpha)\tau(x)}\beta(0)\right] x^2$. From (5.1), $W$ is a positive nondecreasing function. Moreover, (5.3) gives $\dot{V}(N(t)) \leq -W(N(t))$ whenever (5.2) holds true. Since $u(r) \to \infty$ as $r \to \infty$, conditions of [29, Theorem 5.2] hold, and so does the conclusion. ∎

The global asymptotic stability of $N \equiv 0$ is obtained in Theorem 5.1 with an assumption, condition (5.1), that corresponds only to a part of the domain where $N \equiv 0$ is the only steady state of (3.7), contrary to what can be noted for a constant time delay (see, for instance, Adimy, Crauste, and Ruan [5]). We can, however, complete this result by studying the local asymptotic stability of the steady states.

Next, we analyze the local asymptotic stability of the two steady states of system (3.7), $N \equiv 0$ and $N \equiv N^*$, by studying the sign of the real parts of eigenvalues of the associated characteristic equations (see [32, 60] for more details about linearization and stability of state-dependent delay differential equations).

Let $J : C^1 \to \mathbb{R}$ be the map defined, for $\phi \in C^1$, by $J(\phi) = \phi(-\tau(\phi(0)))$. The derivatives of $J$ have the form

$$\frac{d}{d\phi} J(\phi)\psi = -\tau'(\phi(0))\phi'(-\tau(\phi(0)))\psi(0) + \psi(-\tau(\phi(0))), \qquad \phi, \psi \in C^1.$$

Then, for a steady state $x^* \in \{0, N^*\}$ of (3.7), the linearized function $f$ of (3.8) around $x^*$ is, for $\psi \in C^1$,

$$\begin{aligned} Df(x^*)\psi = &-[\delta + \beta(x^*) + \beta'(x^*)x^*]\psi(0) - 2\gamma e^{-\gamma\tau(x^*)}\tau'(x^*)\beta(x^*)x^*\psi(0) \\ &+ 2e^{-\gamma\tau(x^*)}[\beta'(x^*)x^* + \beta(x^*)]\psi(-\tau(x^*)). \end{aligned}$$

It follows that the characteristic equation associated with the linearization of (3.7) around $x^*$ is

$$\Delta(\lambda) = \lambda + \delta + \overline{\beta} + \tau'(x^*)\overline{\alpha}e^{-\gamma\tau(x^*)} - 2\overline{\beta}e^{-\gamma\tau(x^*)}e^{-\lambda\tau(x^*)}, \tag{5.4}$$

where

$$\overline{\alpha} = 2\gamma\beta(x^*)x^*, \qquad \overline{\beta} = \beta(x^*) + \beta'(x^*)x^*.$$

We easily obtain the following theorem.

THEOREM 5.2. *The trivial steady state of* (3.7) *is unstable when* (4.1) *holds true and locally asymptotically stable when* (4.1) *does not hold.*

*Proof.* The characteristic equation (5.4), when $x^* = 0$, is given by

$$\Delta(\lambda) = \lambda + \delta + \beta(0) - 2\beta(0)e^{-\gamma\tau_0}e^{-\lambda\tau_0}.$$

Let $\lambda \in \mathbb{R}$. We have

$$\frac{d\Delta}{d\lambda}(\lambda) = 1 + 2\tau_0 e^{-\gamma\tau_0}\beta(0)e^{-\lambda\tau_0} > 0,$$

$$\Delta(0) = \delta + \beta(0) - 2\beta(0)e^{-\gamma\tau_0} = \delta - \left(2e^{-\gamma\tau_0} - 1\right)\beta(0),$$

and $\lim_{\lambda\to\infty} \Delta(\lambda) = +\infty$. Then there exists $\lambda_0 \in \mathbb{R}$, which is unique, such that $\Delta(\lambda_0) = 0$. When (4.1) holds, then $\Delta(0) < 0$, so $\lambda_0 > 0$, which proves the instability of the trivial steady state.

Conversely, when (4.1) does not hold, $\Delta(0) \geq 0$ and $\lambda_0 \leq 0$. One can show (see [20], for instance) that all roots $\lambda \neq \lambda_0$ of $\Delta$ satisfy $\mathrm{Re}(\lambda) < \lambda_0$. Consequently, the local asymptotic stability straightforwardly follows when (4.1) does not hold. ∎

From Theorems 5.1 and 5.2, we obtain that the trivial steady state $N \equiv 0$ of (3.7) is globally asymptotically stable when

$$\frac{1}{\gamma}\ln\left(\frac{2\beta(0)}{\delta}\right) < \tau_0,$$

locally asymptotically stable when

$$\frac{1}{\gamma}\ln\left(\frac{2\beta(0)}{\beta(0)+\delta}\right) < \tau_0 \leq \frac{1}{\gamma}\ln\left(\frac{2\beta(0)}{\delta}\right),$$

and unstable when

$$\tau_0 < \frac{1}{\gamma}\ln\left(\frac{2\beta(0)}{\beta(0)+\delta}\right).$$

In the next section we focus on the local asymptotic stability of the steady state $N^*$ of (3.7). In particular, we study the existence of a Hopf bifurcation that would destabilize the steady state and create periodic solutions.

**6. Transcritical bifurcation, Hopf bifurcation, and periodic solutions.** This section is devoted to the local asymptotic stability analysis of the positive steady state $N \equiv N^*$ of (3.7). We are going to investigate the sign of real parts of eigenvalues of (5.4) to obtain the existence of a local Hopf bifurcation (see [26]).

Throughout this section, we assume the function $\tau$ is given by $\tau(x) = \mu\tilde{\tau}(x)$, where $\mu$ is a positive parameter and $\tilde{\tau} : \mathbb{R}^+ \to \mathbb{R}^+$ is a positive, increasing, bounded, and differentiable function. Equation (3.7) reads

(6.1)
$$N'(t) = -\left(\delta + \beta(N(t))\right)N(t) + 2e^{-\gamma\mu\tilde{\tau}(N(t))}\beta(N(t-\mu\tilde{\tau}(N(t))))N(t-\mu\tilde{\tau}(N(t))).$$

Moreover, we assume that condition (4.1) holds to ensure the existence of the positive steady state $N^*$ of (3.7). Condition (4.1) is equivalent to

$$\beta(0) > \delta \qquad \text{and} \qquad 0 \leq \mu < \frac{1}{\tilde{\tau}(0)\gamma}\ln\left(\frac{2\beta(0)}{\delta+\beta(0)}\right) := \overline{\mu}. \tag{6.2}$$

This describes the fact that the maximal introduction rate $\beta(0)$ has to be larger than the mortality rate $\delta$, and the cell cycle duration $\tau$ cannot be too long for system (6.1) to exhibit a steady state other than the one describing the cell's dying out.

The positive steady state $N^*$ depends then on the parameter $\mu$ and is given implicitly by

$$\left(2e^{-\gamma\mu\tilde{\tau}(N^*(\mu))} - 1\right)\beta\left(N^*(\mu)\right) = \delta, \qquad \mu \in [0, \overline{\mu}). \tag{6.3}$$

Thus, by using the implicit function theorem, $N^*$ is a decreasing continuously differentiable function of $\mu$. Furthermore, using (6.2) and (6.3), one obtains

$$N^*(\mu = 0) = \beta^{-1}(\delta) \qquad \text{and} \qquad \lim_{\mu\to\overline{\mu}} N^*(\mu) = 0. \tag{6.4}$$

Taking $\mu$ as a parameter, our purpose is to prove the existence of the local Hopf bifurcation of (6.1).

From (5.4), the characteristic equation associated with $N^*(\mu)$ is written as

$$\Delta(\lambda,\mu) = \lambda + \delta + \overline{\beta}(\mu) + \mu\tilde{\tau}'(N^*(\mu))\overline{\alpha}(\mu)e^{-\gamma\mu\tilde{\tau}(N^*(\mu))} - 2\overline{\beta}(\mu)e^{-\gamma\mu\tilde{\tau}(N^*(\mu))}e^{-\lambda\mu\tilde{\tau}(N^*(\mu))}, \tag{6.5}$$

where

$$\overline{\alpha}(\mu) = 2\gamma\beta(N^*(\mu))N^*(\mu) \quad \text{and} \quad \overline{\beta}(\mu) = \beta(N^*(\mu)) + \beta'(N^*(\mu))N^*(\mu).$$

The next result states the existence of a transcritical bifurcation of the positive steady state when $\mu = \overline{\mu}$.

THEOREM 6.1. *When $\mu = \overline{\mu}$, the positive steady state undergoes a transcritical bifurcation, that is, for $\mu < \overline{\mu}$, $\mu$ close to $\overline{\mu}$, the positive steady state is locally asymptotically stable, whereas the trivial steady state is unstable, and for $\mu > \overline{\mu}$ the trivial steady state is locally asymptotically stable and is the only steady state of* (6.1).

*Proof.* The stability of the trivial steady state follows from Theorem 5.2. We investigate local asymptotic stability of $N^*(\mu)$ in a neighborhood of $\overline{\mu}$.

First, notice that when $\overline{\beta}(\mu) > 0$, characteristic roots of (6.5) have negative real parts. Indeed, assume $\overline{\beta}(\mu) > 0$, and consider $\Delta(\lambda,\mu)$ as a function of real $\lambda$. Then $\lambda \mapsto \Delta(\lambda,\mu)$ is an increasing function such that $\lim_{\lambda\to+\infty}\Delta(\lambda,\mu) = +\infty$ and, using the above definition of $\overline{\beta}(\mu)$,

$$\Delta(0,\mu) = -(2e^{-\gamma\mu\tilde{\tau}(N^*(\mu))} - 1)N^*(\mu)\beta'(N^*(\mu)) + \mu\tilde{\tau}'(N^*(\mu))\overline{\alpha}(\mu)e^{-\gamma\mu\tilde{\tau}(N^*(\mu))} > 0.$$

Thus, there exists a unique $\lambda^* < 0$ such that $\Delta(\lambda^*,\mu) = 0$. Separating real and imaginary parts in (6.5), one can easily show that all characteristic roots $\lambda \neq \lambda^*$ satisfy $\mathrm{Re}(\lambda) < \lambda^*$. The local asymptotic stability of the positive steady state when $\overline{\beta}(\mu) > 0$ immediately follows.

Finally, one has to note that when $\mu$ is close to $\overline{\mu}$, $\mu < \overline{\mu}$, then $N^*(\mu)$ is close to zero (see (6.4)); therefore, $\overline{\beta}(\mu) \approx \beta(0) > 0$. The conclusion follows. □

Local asymptotic stability of the positive steady state when $\mu = 0$ is established in the following lemma.

LEMMA 6.2. *Assume $\beta(0) > \delta$ and $\mu = 0$. Then the steady state $N^*$ of system* (6.1) *is locally asymptotically stable.*

*Proof.* Let $\mu = 0$. From (6.5), $\Delta(\lambda,0) = \lambda + \delta - \overline{\beta}(0)$. Then, $\lambda = \overline{\beta}(0) - \delta$ is the unique eigenvalue associated with the characteristic equation. On the other hand, $N^*(0) = \beta^{-1}(\delta) > 0$, so $\lambda = \beta'(N^*(0))N^*(0) < 0$. This concludes the proof. □

Thus, $N^*(\mu)$ is locally asymptotically stable for $\mu = 0$ and the stability can be lost as $\mu$ increases away from 0, with $\mu < \overline{\mu}$, only if purely imaginary characteristic roots appear. One may note that $N^*(\mu)$ is locally asymptotically stable for $\mu < \overline{\mu}$, $\mu$ close to $\overline{\mu}$ (see Theorem 6.1), and so if stability is lost as $\mu$ increases away from zero, a second switch must be observed as $\mu$ keeps increasing and reaches $\overline{\mu}$.

Define, for $\mu \in [0,\overline{\mu})$,

$$b(\mu) = \delta + \overline{\beta}(\mu) + \mu\tilde{\tau}'(N^*(\mu))\overline{\alpha}(\mu)e^{-\gamma\mu\tilde{\tau}(N^*(\mu))} \quad \text{and} \quad c(\mu) = -2\overline{\beta}(\mu)e^{-\gamma\mu\tilde{\tau}(N^*(\mu))}.$$

Then (6.5) becomes

$$\Delta(\lambda,\mu) = \lambda + b(\mu) + c(\mu)e^{-\lambda\mu\tilde{\tau}(N^*(\mu))}. \tag{6.6}$$

In the following, we investigate the existence of purely imaginary roots of (6.6). It is obvious that $\lambda = 0$ is not a characteristic root of (6.6). Indeed,

$$\begin{aligned} b(\mu) + c(\mu) = \delta &+ \beta(N^*(\mu))\left(1 - 2e^{-\gamma\mu\tilde{\tau}(N^*(\mu))}\right) \\ &+ \beta'(N^*(\mu))\left(1 - 2e^{-\gamma\mu\tilde{\tau}(N^*(\mu))}\right) N^*(\mu) \\ &+ 2\gamma\mu\tilde{\tau}'(N^*(\mu))\beta(N^*(\mu))N^*(\mu)e^{-\gamma\mu\tilde{\tau}(N^*(\mu))}. \end{aligned}$$

Since $\delta - (2e^{-\gamma\mu\tilde{\tau}(N^*(\mu))} - 1)\beta(N^*(\mu)) = 0$, we obtain $1 - 2e^{-\gamma\mu\tilde{\tau}(N^*(\mu))} < 0$ and

$$\Delta(0, \mu) = b(\mu) + c(\mu) > 0.$$

It follows that $\lambda = 0$ is not an eigenvalue.

Let $\omega > 0$. Separating real and imaginary parts, equality $\Delta(i\omega, \mu) = 0$ is equivalent to

$$\left\{ \begin{array}{rcl} \omega & = & c(\mu)\sin(\omega\mu\tilde{\tau}\,(N^*(\mu))), \\ b(\mu) & = & -c(\mu)\cos(\omega\mu\tilde{\tau}\,(N^*(\mu))). \end{array} \right. \tag{6.7}$$

One can note that if $i\omega$ is a purely imaginary root of (6.6) then so is $-i\omega$. A necessary condition for (6.6) to have purely imaginary roots is

$$|\, c(\mu)\,| > |\, b(\mu)\,|\,. \tag{6.8}$$

If no $\mu \in [0, \overline{\mu})$ fulfills condition (6.8), then the characteristic equation (6.6) has no purely imaginary root. Consequently, from Lemma 6.2, all eigenvalues of (6.6) have negative real parts and the steady state $N^*(\mu)$ is locally asymptotically stable for all $\mu \in [0, \overline{\mu})$.

We have already checked that $b(\mu) + c(\mu) > 0$. Then, for (6.8) to hold true, it is necessary that $c(\mu) > 0$, that is, $\overline{\beta}(\mu) < 0$. A sufficient condition for (6.8) is then $b(\mu) < 0$, which is equivalent to

$$\begin{array}{l} \delta + \beta(N^*(\mu)) + \beta'(N^*(\mu))N^*(\mu) \\ + 2\gamma\mu\tilde{\tau}'(N^*(\mu))\beta(N^*(\mu))N^*(\mu)e^{-\gamma\mu\tilde{\tau}(N^*(\mu))} \quad < \quad 0. \end{array} \tag{6.9}$$

We have the following lemma.

LEMMA 6.3. *Let $\eta : [0, +\infty) \to (-\infty, 0]$ and $\sigma : [0, +\infty) \to [0, +\infty)$ be defined, for $y \geq 0$, by $\eta(y) = y\beta'(y)$ and $\sigma(y) = y\tilde{\tau}'(y)$. Assume the following:*

(R1) *$\eta$ and $\sigma$ are decreasing on the interval $[0, \beta^{-1}(\delta)]$.*

(R2) *$\eta\left(\beta^{-1}(\delta)\right) < -2\delta$.*

*Then there exists a unique $\mu^* \in (0, \overline{\mu})$ such that condition (6.9) is satisfied if and only if $\mu \in [0, \mu^*)$.*

*Proof.* Let $h_1$ and $h_2$ be the negative functions defined, for $\mu \in [0, \overline{\mu})$, by

$$h_1(\mu) = \eta\left(N^*(\mu)\right) \qquad \text{and} \qquad h_2(\mu) = -\left(\delta + \beta\left(N^*(\mu)\right)\right)\left(1 + 2\gamma\mu\sigma\left(N^*(\mu)\right)\right).$$

Then, from (6.3), $\{\mu \in [0, \overline{\mu}) : \text{condition (6.9) is satisfied}\} = \{\mu \in [0, \overline{\mu}) : h_1(\mu) < h_2(\mu)\}$. Since $\beta$ is decreasing on $[0, +\infty)$, $N^*$ is decreasing on $[0, \overline{\mu})$, and, from (R1), $\eta$ and $\sigma$ are decreasing on $[0, \beta^{-1}(\delta)]$, we deduce that $h_1$ is increasing and $h_2$ is decreasing. Moreover, from (6.4), $\lim_{\mu \to \overline{\mu}} N^*(\mu) = 0$. It follows that

$$\begin{array}{ll} h_1(0) = \eta(\beta^{-1}(\delta)) < 0, & \lim_{\mu \to \overline{\mu}} h_1(\mu) = \eta(0) = 0, \\ h_2(0) = -2\delta, & \lim_{\mu \to \overline{\mu}} h_2(\mu) = -(\delta + \beta(0)). \end{array}$$

From (R2), it follows that $h_1(0) < h_2(0)$. Consequently there exists a unique $\mu^* \in (0, \overline{\mu})$ such that $\{\mu \in [0, \overline{\mu}) : h_1(\mu) < h_2(\mu)\} = [0, \mu^*)$. This achieves the proof. □

In what follows, we assume there exists $\mu^* \in (0, \overline{\mu})$ such that (6.8) is fulfilled for $\mu \in [0, \mu^*)$.

System (6.7) is equivalent to

$$\cos(\omega\mu\tau^*(\mu)) = -\frac{b(\mu)}{c(\mu)}, \qquad \sin(\omega\mu\tau^*(\mu)) = \frac{\omega}{c(\mu)}, \tag{6.10}$$

where $\tau^*(\mu) = \tilde{\tau}(N^*(\mu))$. Therefore, adding the squares of both sides of (6.10), purely imaginary eigenvalues $i\omega$ of (6.6), with $\omega > 0$, must satisfy

$$\omega = \left(c^2(\mu) - b^2(\mu)\right)^{\frac{1}{2}}. \tag{6.11}$$

Thus, in the following, we will think of $\omega$ as $\omega(\mu)$, $\mu \in [0, \mu^*)$. Substituting expression (6.11) for $\omega$ in (6.10), we obtain

$$\begin{cases} \cos\left(\mu\tau^*(\mu)\left(c^2(\mu) - b^2(\mu)\right)^{\frac{1}{2}}\right) &= -\dfrac{b(\mu)}{c(\mu)}, \\ \sin\left(\mu\tau^*(\mu)\left(c^2(\mu) - b^2(\mu)\right)^{\frac{1}{2}}\right) &= \dfrac{\left(c^2(\mu) - b^2(\mu)\right)^{\frac{1}{2}}}{c(\mu)}. \end{cases} \tag{6.12}$$

From the above reasoning, values of $\mu \in [0, \mu^*)$ solutions of system (6.12) generate positive $\omega(\mu)$ given by (6.11) and hence yield imaginary eigenvalues of (6.6). Consequently, we look for positive solutions $\mu$ of (6.12) in the interval $[0, \mu^*)$. They satisfy

$$\mu\tau^*(\mu)\left(c^2(\mu) - b^2(\mu)\right)^{\frac{1}{2}} = \arccos\left(-\frac{b(\mu)}{c(\mu)}\right) + 2k\pi, \quad k \in \mathbb{N}_0,$$

where $\mathbb{N}_0$ denotes the set of all nonnegative integers. We set

$$\mu^k(\mu) := \frac{\arccos\left(-\frac{b(\mu)}{c(\mu)}\right) + 2k\pi}{\tau^*(\mu)\left(c^2(\mu) - b^2(\mu)\right)^{\frac{1}{2}}}, \qquad k \in \mathbb{N}_0,\ \mu \in [0, \mu^*).$$

Values of $\mu$ for which $\omega(\mu) = \left(c^2(\mu) - b^2(\mu)\right)^{\frac{1}{2}}$ is a solution of (6.7) are roots of the functions

$$Z_k(\mu) = \mu - \mu^k(\mu), \quad k \in \mathbb{N}_0,\ \mu \in [0, \mu^*). \tag{6.13}$$

The roots of $Z_k$ can be found using popular software but are hard to determine with analytical tools [15]. The following lemma states some straightforward properties of the $Z_k$ functions.

LEMMA 6.4. *For $k \in \mathbb{N}_0$,*

$$Z_k(0) < 0 \quad \text{and} \quad \lim_{\mu \to \mu^*} Z_k(\mu) = -\infty.$$

*Therefore, provided that no root of $Z_k$ is a local extremum, the number of positive roots of $Z_k$, $k \in \mathbb{N}_0$, on the interval $[0, \mu^*)$ is even. Moreover, if $Z_k$ has no root on the interval $[0, \mu^*)$, then $Z_j$, with $j > k$, does not have positive roots.*

*Remark* 1. The last statement in Lemma 6.4 implies, in particular, that, if $Z_0$ has no positive root, then (6.7) has no positive solution, and (6.6) does not have purely imaginary roots.

The search for purely imaginary roots ends up finding positive real roots of real functions $Z_k$ that can mostly be handled numerically. In the following proposition, however, we establish some properties of purely imaginary roots of (6.6) using a method described in [38].

PROPOSITION 6.5. *Let $\pm i\omega(\mu_c)$, with $\omega(\mu_c) > 0$ and $\mu_c \in (0, \mu^*)$, be a pair of purely imaginary roots of* (6.6) *when $\mu = \mu_c$. Then $\pm i\omega(\mu_c)$ are simple roots of* (6.6) *such that*

$$\begin{aligned} &sign\left\{\frac{d\mathcal{R}e(\lambda(\mu))}{d\mu}\right\}_{\mu=\mu_c} \\ &= sign\left\{c^3\left(\mu_c\hat{\tau}_c' + \tau_c^*\right) + c^2c'\mu_c\tau^* - c(b^2\left(\mu_c\hat{\tau}_c' + \tau_c^*\right) + b' + bb'\mu_c\tau_c^*) + c'b\right\}, \end{aligned} \tag{6.14}$$

*with $\tau_c^* = \tau^*(\mu_c)$, $\hat{\tau}_c' = d\tau^*(\mu_c)/d\mu$, $b = b(\mu_c)$, $c = c(\mu_c)$, $b' = b'(\mu_c)$, and $c' = c'(\mu_c)$.*

*Proof.* Let $\lambda(\mu)$ be a branch of roots of (6.6), so $\Delta(\lambda(\mu), \mu) = 0$, such that $\lambda(\mu_c) = i\omega(\mu_c)$. Then,

$$\frac{d\lambda}{d\mu}(\mu)\Delta_\lambda(\lambda, \mu) + \Delta_\mu(\lambda, \mu) = 0, \tag{6.15}$$

where

$$\Delta_\lambda(\lambda, \mu) := \frac{d\Delta}{d\lambda}(\lambda, \mu) = 1 - c(\mu)\mu\tau^*(\mu)e^{-\lambda\mu\tau^*(\mu)},$$

and

$$\Delta_\mu(\lambda, \mu) := \frac{d\Delta}{d\mu}(\lambda, \mu) = b'(\mu) - [c(\mu)\left(\mu\hat{\tau}'(\mu) + \tau^*(\mu)\right)\lambda - c'(\mu)]e^{-\lambda\mu\tau^*(\mu)},$$

with $\hat{\tau}'(\mu) = d\tilde{\tau}(N^*(\mu))/d\mu$.

Assume, by contradiction, that $\lambda(\mu_c) = i\omega(\mu_c)$ is not a simple root of (6.6). Then

$$\Delta_\lambda(i\omega(\mu_c), \mu_c) = 1 - \mu_c\tau_c^*c(\mu_c)e^{-i\omega(\mu_c)\mu_c\tau_c^*} = 0.$$

Using (6.6) for $\mu = \mu_c$, we then deduce $b(\mu_c)+1/(\mu_c\tau_c^*)+i\omega(\mu_c) = 0$, and consequently $\omega(\mu_c) = 0$, which gives a contradiction. It follows that all purely imaginary roots of (6.6) are simple.

In the following, we do not mention the dependence of the coefficients $\tau^*$, $\hat{\tau}'$, $b$, and $c$ (and their derivatives) with respect to $\mu$.

Since $\Delta(\lambda, \mu) = 0$, we deduce $e^{\lambda\mu\tau^*} = -c/(\lambda + b)$. Therefore, from (6.15) we obtain

$$\left(\frac{d\lambda}{d\mu}\right)^{-1} = \frac{c + c\mu\tau^*(\lambda + b)}{\left[c' - c\lambda\left(\mu\hat{\tau}' + \tau^*\right)\right](\lambda + b) - b'c}.$$

Taking the real part of the above equality for $\mu = \mu_c$, we obtain

$$\begin{aligned} &\mathcal{R}e\left(\tfrac{d\lambda}{d\mu}\right)^{-1}\Big|_{\mu=\mu_c} \\ &= \tfrac{[c^2(1+b\mu_c\tau_c^*)(\mu_c\hat{\tau}_c'+\tau_c^*)+\mu_c\tau_c^*c(c'-bc(\mu_c\hat{\tau}_c'+\tau_c^*))]\omega(\mu_c)^2+c(1+b\mu_c\tau_c^*)(c'b-b'c)}{(b'c-c'b-c(\mu_c\hat{\tau}_c'+\tau_c^*)\omega(\mu_c)^2)^2+(c'-bc(\mu_c\hat{\tau}_c'+\tau_c^*))\omega(\mu_c)^2}. \end{aligned}$$

Notice that $\operatorname{sign}\{d\mathcal{R}e(\lambda)/d\mu\} = \operatorname{sign}\{\mathcal{R}e\,(d\lambda/d\mu)^{-1}\}$. Since $i\omega(\mu_c)$ is a purely imaginary root of (6.5), then, from (6.11), $\omega(\mu_c)^2 = c^2 - b^2$, and we obtain

$$\operatorname{sign}\left\{\left.\frac{d\mathcal{R}e(\lambda)}{d\mu}\right|_{\mu=\mu_c}\right\}$$
$$= \operatorname{sign}\left\{c[c^3\left(\mu_c\hat{\tau}_c' + \tau_c^*\right) + c^2c'\mu_c\tau^* - c(b^2\left(\mu_c\hat{\tau}_c' + \tau_c^*\right) + b' + bb'\mu_c\tau_c^*) + c'b]\right\}.$$

As we already noticed, if (6.5) has pure imaginary roots, then necessarily $c > 0$. We deduce (6.14), and the proof is complete. □

In the next theorem we summarize and prove our results dealing with the asymptotic stability of the positive steady state $N^*$.

THEOREM 6.6. *Assume* (6.2) *holds true; $\beta$ and $\tau$ are $C^2$ functions. If no $\mu \in [0, \overline{\mu})$ satisfies* (6.8)*, then the positive steady state $N^*$ of* (3.7) *is locally asymptotically stable for $\mu \in [0, \overline{\mu})$.*

*Assume there exists $\mu^* \in (0, \overline{\mu})$ such that* (6.8) *is fulfilled for $\mu \in [0, \mu^*)$ (for instance, if* (R1) *and* (R2) *are fulfilled). Then, the following hold true:*

(i) *If $Z_0$, defined in* (6.13)*, has no root on the interval $[0, \mu^*)$, then the positive steady state $N^*$ of* (3.7) *is locally asymptotically stable for $\mu \in [0, \mu^*)$.*

(ii) *If $Z_0$ has at least one positive root $\mu_c \in (0, \mu^*)$, then $N^*$ is locally asymptotically stable for $\mu \in [0, \mu_c)$ and unstable for $\mu \geq \mu_c$, $\mu$ in a neighborhood of $\mu_c$, and a Hopf bifurcation occurs at $N^*$ for $\mu = \mu_c$ if*

$$\begin{aligned} &c^3\left(\mu_c\hat{\tau}_c' + \tau_c^*\right) + c^2c'\mu_c\tau_c^* \\ &- c(b^2\left(\mu_c\hat{\tau}_c' + \tau_c^*\right) + b' + bb'\mu_c\tau_c^*) + c'b \neq 0. \end{aligned} \tag{6.16}$$

*When* (ii) *holds true, several stability switches can potentially occur for every $\tau = \tau_c$, roots of $Z_k$ functions.*

*Proof.* From Lemma 6.3 we know that $N^*$ is locally asymptotically stable when $\mu = 0$. The first statement is straightforwardly satisfied.

Assume there exists $\mu^* \in (0, \overline{\mu})$ such that (6.8) is fulfilled for $\mu \in [0, \mu^*)$. If $Z_0$ has no positive root on the interval $(0, \mu^*)$, then the characteristic equation (6.5) has no pure imaginary root (see Remark 1 and Lemma 6.4). Consequently, the stability of $N^*$ cannot be lost when $\mu$ increases. We obtain the statement in (i).

Now, if $Z_0$ has at least one positive root, say, $\mu_c \in (0, \mu^*)$, then (6.5) has a pair of simple conjugate pure imaginary roots $\pm i\omega_c$ for $\mu = \mu_c$. From (6.16) together with Proposition 6.5, we have either $d\mathcal{R}e(\lambda)/d\mu(\mu = \mu_c) > 0$ or $d\mathcal{R}e(\lambda)/d\mu(\mu = \mu_c) < 0$. By contradiction, we assume there exists a branch of characteristic roots $\lambda(\mu)$ such that $\lambda(\mu_c) = i\omega_c$ and $d\mathcal{R}e(\lambda(\mu))/d\mu < 0$ for $\mu < \mu_c$, $\mu$ close to $\mu_c$. Then there exists a characteristic root $\lambda(\mu)$ such that $\mathcal{R}e(\lambda(\mu)) > 0$ and $\mu < \mu_c$. Since $N^*$ is locally asymptotically stable when $\mu = 0$, applying Rouché's theorem [23], we obtain that all characteristic roots of (6.5) have negative real parts when $\mu \in [0, \mu_c)$, and we obtain a contradiction. Thus,

$$\left.\frac{d\mathcal{R}e(\lambda)}{d\mu}\right|_{\mu=\mu_c} > 0. \tag{6.17}$$

Now, let $N$ be a solution of (3.7). Then the function $x$, defined, for $t \geq 0$, by

$$x(t) := N(\mu t), \tag{6.18}$$

satisfies

$$\dot{x}(t) = \zeta(\mu, x_t), \tag{6.19}$$

where $\zeta : \mathbb{R}^+ \times C \to \mathbb{R}$ is given by

$$\zeta(\mu, \phi) = -\mu\left(\delta + \beta(\phi(0))\right)\phi(0) + 2\mu e^{-\gamma\mu\tilde{\tau}(\phi(0))}\beta\left(\phi(-\tilde{\tau}(\phi(0)))\right)\phi(-\tilde{\tau}(\phi(0))).$$

In order to prove the Hopf bifurcation for (3.7), from the change of variable in (6.18), it suffices to prove the Hopf bifurcation for (6.19). In [26], Eichmann stated some conditions on the function $\zeta$ allowing a Hopf bifurcation to occur at the positive steady state of (6.19). The function $\zeta$ defined above satisfies in particular the assumptions in [26], which are not recalled here for the sake of clarity.

The characteristic equation associated with the equilibrium $N^*$ of (6.19) is

$$\begin{aligned}\tilde{\Delta}(\lambda, \mu) = \lambda + \mu\left(\delta + \overline{\beta}\right) + \mu^2\tilde{\tau}'(N^*(\mu))\overline{\alpha}e^{-\gamma\mu\tilde{\tau}(N^*(\mu))} \\ - 2\mu\overline{\beta}e^{-\gamma\mu\tilde{\tau}(N^*(\mu))}e^{-\lambda\tilde{\tau}(N^*(\mu))}.\end{aligned} \tag{6.20}$$

Let $\lambda \in \mathbb{C}$. One can see that $\tilde{\Delta}(\mu\lambda, \mu) = \mu\Delta(\lambda, \mu)$ for all $\mu \in [0, \overline{\mu})$. Then, for $\mu \in (0, \overline{\mu})$, $\lambda$ is an eigenvalue associated with (6.20) if and only if $\lambda/\mu$ is an eigenvalue associated with (6.5). Thus, it is straightforward that (6.20) has a unique pair of simple conjugate purely imaginary eigenvalues for $\mu = \mu_c$, which satisfy (6.17), since these properties hold for the characteristic equation (6.5). Then, from [26], a Hopf bifurcation occurs at $N^*$ when $\mu = \mu_c$. This concludes the proof. □

*Remark* 2. The asymptotic stability of the positive steady state of (3.7) has been analyzed with respect to the parameter $\mu$. One may notice that it can, however, be investigated with respect to every parameter in the model. The role of each parameter on the stability of the positive steady state is numerically determined in the next section, which is devoted to numerical simulations of solutions of (3.7).

**7. Numerical simulations.** Inspired by Mackey [43], Pujo-Menjouet and Mackey [53], and Adimy, Crauste, and Ruan [5], we take $\beta$ as a Hill function, given by (2.2). The following values for the parameters are chosen according to [43, 52, 53]:

$$\delta = 0.05 \text{ day}^{-1}, \quad \gamma = 0.2 \text{ day}^{-1}, \quad \beta_0 = 1.77 \text{ day}^{-1}, \quad \text{and} \quad r = 3. \tag{7.1}$$

The value of $\theta$ is set to $\theta = 1$ cell.g$^{-1}$, which is not relevant for a quantitative analysis, but does not modify the qualitative behavior of solutions of (3.7).

The delay function $\tilde{\tau}$ is chosen as

$$\tilde{\tau}(N) = \tilde{\tau}_0 + (\tilde{\tau}_{\max} - \tilde{\tau}_0)\frac{N}{N + \theta_\tau},$$

with $\tilde{\tau}_{\max} > \tilde{\tau}_0 > 0$ and $\theta_\tau > 0$ (otherwise the delay is constant). Hence $\tilde{\tau}(N)$, and consequently $\tau(N)$, is an increasing bounded positive function. One may note that $\tau_0 = \mu\tilde{\tau}_0$ and $\tau_{\max} = \mu\tilde{\tau}_{\max}$.

We use MATLAB and the solver DDESD [56] for state-dependent delay differential equations to numerically compute the solutions of (3.7).

In a first example, we fix

$$\tilde{\tau}_0 = 0.1 \text{ day}, \quad \tilde{\tau}_{\max} = 1 \text{ day}, \quad \text{and} \quad \theta_\tau = 1 \text{ cell.g}^{-1}. \tag{7.2}$$

With values in (7.1) and (7.2), a unique positive steady state $N^*(\mu)$ of (3.7) exists (condition (4.1) holds true) for $\mu < \overline{\mu}$, where computations give $\overline{\mu} \approx 33$ (see Figure

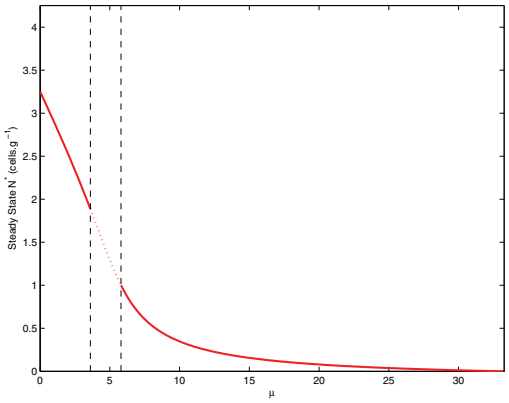


FIG. 7.1. *Positive steady state $N^*(\mu)$ of* (3.7) *for $\mu \in [0, \overline{\mu})$. The solid line corresponds to stable values of the steady state, whereas the dotted lines account for unstable values of $N^*(\mu)$. Parameters are given by* (7.1) *and* (7.2).

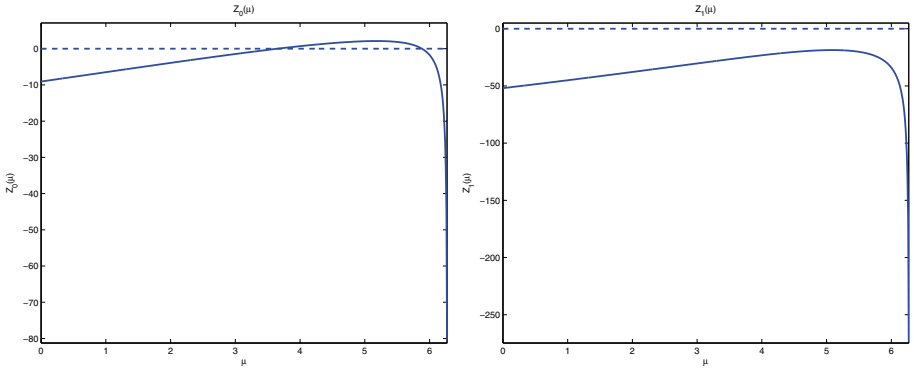


FIG. 7.2. *Functions $Z_k$. Left: Function $Z_0$, which exhibits two positive roots, $\mu_1 = 3.66$ and $\mu_2 = 5.88$. Right: Function $Z_1$, which is negative. Parameters are given by* (7.1) *and* (7.2).

7.1). We also obtain $\mu^* = 6.27$ and the functions $Z_k$ defined in Lemma 6.4. The function $Z_0$ has two roots in $(0, \mu^*)$, $\mu_1 = 3.66$, and $\mu_2 = 5.88$, and the function $Z_1$ has no root. This is displayed in Figure 7.2.

According to the results stated in Theorem 6.6, the positive steady state $N^*$ is asymptotically stable for $\mu < \mu_1$ and $\mu > \mu_2$ and unstable when $\mu \in [\mu_1, \mu_2]$. In this latter case, $N^*$ undergoes a Hopf bifurcation when $\mu = \mu_1$, and the solutions of (3.7) periodically oscillate with a period of about 17 days. This is shown in Figure 7.3. Variations of the delay function $\tilde{\tau}(N(t))$ are also displayed. The same periodic behavior is observed.

The stability and instability areas, delimited by the roots of the $Z_k$ functions, can be computed as functions of a given parameter. For instance, critical values of $\mu$ as functions of $\theta_\tau$ are displayed in Figure 7.4. The stability zone is bounded above by the value $\overline{\mu}$. For $\mu \geq \overline{\mu}$, (3.7) has only one steady state, $N \equiv 0$. The stability area decreases as $\theta_\tau$ increases. When $\theta_\tau$ becomes very large, the instability zone is a strip with rather constant width, and, as $\mu$ increases, one always observes a stability switch (from unstable to stable) before the positive steady state no longer exists, that is, for

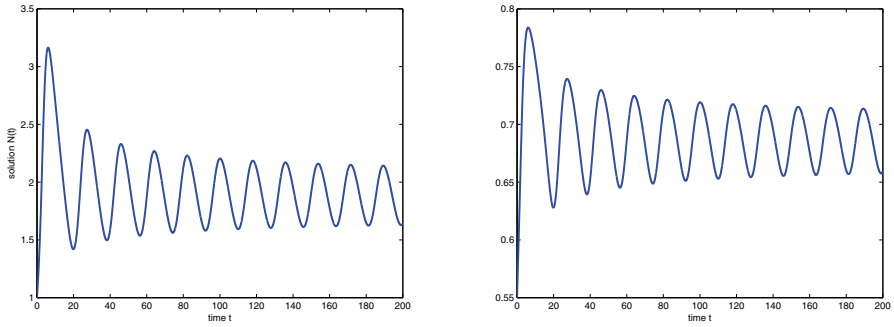


FIG. 7.3. *Left: Periodic solution at the Hopf bifurcation. With parameters given by* (7.1) *and* (7.2)*, the solution of* (3.7) *undergoes a Hopf bifurcation when* $\mu = 3.66$*, so periodic solutions are observed. Right: The corresponding delay function* $\tilde{\tau}(N(t))$*.*

$\mu > \overline{\mu}$ (not shown here). One can also notice that when $\theta_\tau = 0$ a stability switch appears as $\mu$ increases. In this case, the delay is constant, with $\tau(N) = \mu\tilde{\tau}_{\max} = \tau_{\max}$. Hence the instability area appears to be larger when the delay depends on the cell population than in the constant case with a delay $\tau = \tau_{\max}$.

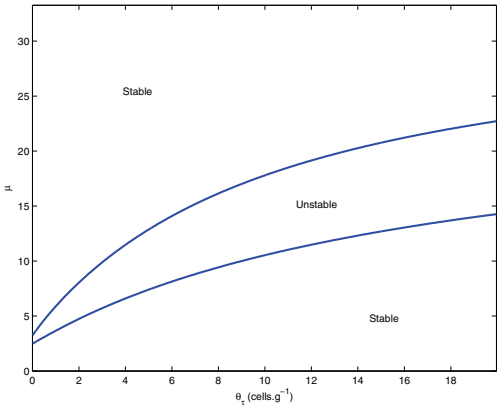


FIG. 7.4. *With parameters given by* (7.1) *and* (7.2)*, except for* $\theta_\tau$ *which varies, the stable and unstable zones in the* $(\theta_\tau, \mu)$*-plane are obtained.*

Critical values of $\mu$, as functions of $\tilde{\tau}_0$ and $\tilde{\tau}_{\max}$, are presented in Figure 7.5. Contrary to $\theta_\tau$, values of $\tilde{\tau}_0$ and $\tilde{\tau}_{\max}$ for which the positive steady state exists are limited: $\tilde{\tau}_0$ must satisfy (4.1) and be less than $\tilde{\tau}_{\max}$. One can observe that instability areas are rather small compared to the stability areas, both in the $(\tilde{\tau}_0, \mu)$-plane and in the $(\tilde{\tau}_{\max}, \mu)$-plane. The dependence of critical values of $\mu$ on $\tilde{\tau}_{\max}$ seems strong: one observes in Figure 7.5 that values of $\mu$ for which stability switch occurs drastically decrease when $\tilde{\tau}_{\max}$ increases. For large values of $\tilde{\tau}_{\max}$, the positive steady state $N^*(\mu)$ is almost always stable. However, for every value of $\tilde{\tau}_0$, $\tilde{\tau}_{\max}$, and $\theta_\tau$ there exist values of $\mu$ for which the steady state is unstable. This is not the case with all parameters, as described hereafter.

In Figure 7.6, critical values of $\mu$ are displayed as functions of $\gamma$ and $r$, defined

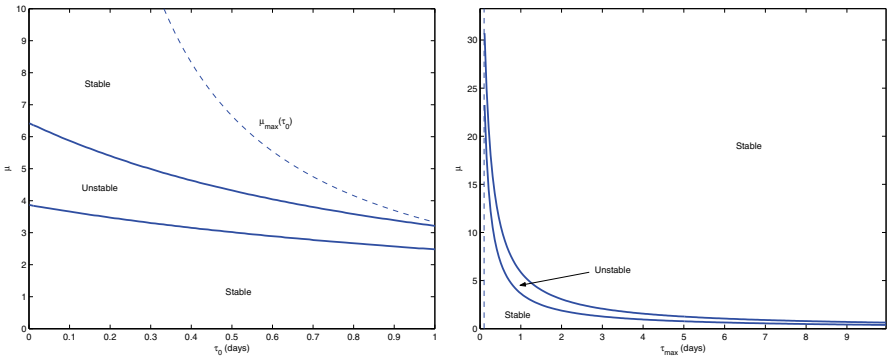


FIG. 7.5. *Left: Critical values of $\mu(\tilde{\tau}_0)$, with $\mu < \overline{\mu}(\tilde{\tau}_0)$, for $\tilde{\tau}_0$ satisfying* (4.1) *and $\tilde{\tau}_0 < \tilde{\tau}_{\max}$. Parameters are given by* (7.1) *and* (7.2)*, except for $\tilde{\tau}_0$ which varies. Right: Critical values of $\mu(\tilde{\tau}_{\max})$ for $\tilde{\tau}_{\max}$ satisfying $\tilde{\tau}_0 < \tilde{\tau}_{\max}$. Parameters are given by* (7.1) *and* (7.2)*, except for $\tilde{\tau}_{\max}$ which varies.*

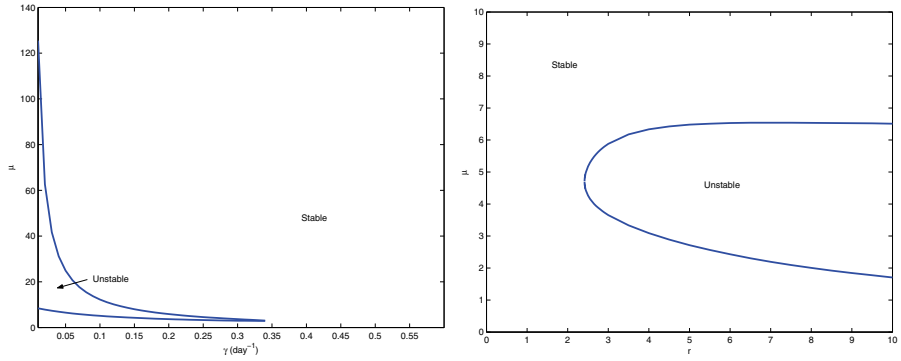


FIG. 7.6. *Left: Critical values of $\mu(\gamma)$, with parameters given by* (7.1) *and* (7.2)*, except for $\gamma$ which varies. Right: Critical values of $\mu(r)$, with parameters given by* (7.1) *and* (7.2)*, except for $r$ which varies.*

in (2.2), respectively. Critical values of $\delta$ (resp., $\beta_0$) are not shown here, yet they are qualitatively similar to the ones obtained for $\gamma$ (resp., $r$). Differences are mentioned in the following discussion.

The instability zone is limited in the $(\gamma, \mu)$- or $(\delta, \mu)$-plane and appears rather small compared to the stability zone. For small values of $\gamma$, close to zero, a wide range of values of $\mu$ induces instability of the solution. The influence of $\gamma$ on the stability of $N^*(\mu)$ seems strong, especially small values of $\gamma$, that is, low apoptosis rates of proliferating cells. High apoptosis rates correspond to a stable steady state.

For small values of $\beta_0$ and $r$ the positive steady state is always stable. As $r$ increases (that is, the sensitivity of the introduction rate becomes more important), the width of the instability area increases. Hence, a large sensitivity $r$ is likely to induce instability. This is not the case with $\beta_0$ (not shown here), whose variations do not increase the instability range.

This numerical study of the stability of the positive steady state $N^*(\mu)$ indicates that three categories of parameters play crucial roles in the stability of the system. First, all parameters related to the delay function $\tilde{\tau}(N)$, that is, $\tilde{\tau}_0$, $\tilde{\tau}_{\max}$, and $\theta_\tau$,

induce, as they increase, stability switches of the positive steady state. For every combination of $(\tilde{\tau}_0, \tilde{\tau}_{\max}, \theta_\tau)$ it is possible to find values of $\mu$ for which the steady state is unstable. This is not surprising, since the delay has been shown, in Theorem 6.6, to lead to instability through the variations of $\mu$. The parameters defining the delay function are consequently expected to modify the stability of the system.

Second, the apoptosis rate $\gamma$ was shown to induce stability switches, particularly for small values. This observation had already been noticed in previous works, with constant delay. See, for instance, Mackey [43], Pujo-Menjouet and Mackey [53], Pujo-Menjouet, Bernard, and Mackey [52], and Adimy and Crauste [3].

Finally, the sensitivity $r$ of the introduction rate $\beta(N)$ was shown to play a significant role in the instability of the positive steady state for large values. This sensitivity is related to the ability of cells to react to stimuli that induce their activation [43]. This indicates that an increase in the ability for a cell to be activated is likely to trigger periodic behaviors.

Instability of the steady state corresponds to oscillating solutions (since solutions are bounded). Hence, it appears relevant to investigate the influence of the parameters involved in the problem on periods and amplitudes of the oscillations observed when the steady state is unstable.

We first investigate the influence of the parameters related to the delay function, that is, $\mu$, $\tilde{\tau}_0$, and $\tilde{\tau}_{\max}$. We fix all the parameters except the one we focus on, which ranges in what we shall call its *instability range*. This is the domain (in what follows, an interval), associated with the fixed parameter values, in which the free parameter can range to ensure instability of the steady state. For instance, when all the parameters are given by (7.1) and (7.2), the instability range of $\mu$ is $[\mu_1, \mu_2]$, with $\mu_1 = 3.66$ and $\mu_2 = 5.88$. For parameters different from $\mu$, the instability range is easily obtained from Figures 7.5 and 7.6 by fixing $\mu$ to a given value (hereafter, $\mu = 4.2$ is used) and determining on the graph the limiting values of the parameter. From Figure 7.6, for instance, the instability range of $\gamma$ is deduced; it is equal to $[0.15, 0.27]$.

In Figure 7.7, periods and amplitudes of the oscillations are displayed when $\tilde{\tau}_0$ varies in its instability range. Variations of $\mu$ and $\tilde{\tau}_{\max}$ are not shown here, yet they are similar.

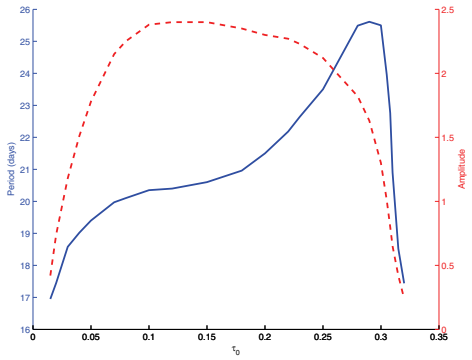


FIG. 7.7. *Periods (solid line) and amplitudes (dashed line) of oscillating solutions, as functions of $\tau_0$. All other parameters are fixed, given by* (7.1) *and* (7.2)*, and $\mu = 4.2$. Scale of the periods is on the left axis; scale of the amplitudes is on the right axis.*

The three parameters have almost the same influence on amplitudes of the os-

cillations, with the same variations. One can consider that amplitudes do not really vary: they quickly reach some plateau, between 2 and 2.5, and finally decrease rapidly before the stability switch. Their influence on the periods of oscillating solutions is more important although limited. Three windows appear when looking at the evolution of periods: a first rapid increase of the periods, then a plateau of about 20–21 days, and then another increase that does not reach high values. Then, even though the influence of the three parameters related to the delay function on the stability of the steady state has been noticed above, their contribution to period and amplitude variations is very limited (especially for amplitude variations).

In Figure 7.8, periods and amplitudes of oscillating solutions are shown as functions of $\gamma$ and $r$. Graphs of periods and amplitudes of oscillating solutions as functions of $\delta$ (resp., $\beta_0$) are not shown here but are similar to the graphs as functions of $\gamma$ (resp., $r$).

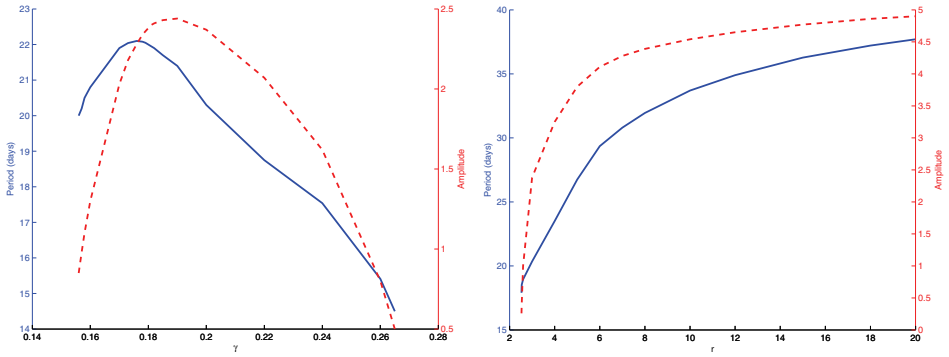


FIG. 7.8. *Periods (solid lines) and amplitudes (dashed lines) of oscillating solutions, as functions of $\gamma$ (left) and $r$ (right). For each figure, all other parameters are fixed, given by* (7.1) *and* (7.2)*, and $\mu = 4.2$. Scale of the periods is on the left axis; scale of the amplitudes is on the right axis.*

Two different types of parameters are identified in Figure 7.8: those that tend to decrease periods and amplitudes of the oscillations, $\gamma$ and $\delta$, and those that increase them, $\beta_0$ and $r$. One has to note that parameters $\beta_0$ and $r$ are not bounded above, their instability ranges are not limited, and they can then increase far from biologically relevant values. However, their positive action on periods and amplitudes are established, and one can easily check that maximal values obtained with other parameters ($\mu$, $\tilde{\tau}_{max}$, $\tilde{\tau}_0$) are quickly overtaken. For instance, periods larger than 25 days are obtained as soon as $r \geq 5$, and amplitudes are larger than 2.5 for $r \geq 3$.

The decreasing action of mortality rates is very significant. Instability usually occurs for small values of mortality rates, and the numerical results in Figure 7.8 clearly show that qualitative properties of oscillating solutions are also strongly affected by variations of mortality rates.

Finally, two categories of parameters emerge: those favoring an increase of periods and amplitudes of oscillating solutions, $\beta_0$ and $r$, and those decreasing both periods and amplitudes, $\gamma$ and $\delta$. The first category of parameters is associated with cell proliferation, whereas the second one is formed with mortality rates. The parameters associated with the delay, that is, $\mu$, $\tilde{\tau}_{\max}$, and $\tilde{\tau}_0$, have limited influence. They have almost no influence on the amplitudes of oscillations, and they act similarly on periods of oscillations.

The influence of the parameters on the stability of the unique positive steady state have already been analyzed by Pujo-Menjouet, Bernard, and Mackey [52] for the discrete model (that is, with $\tau$ constant) with a constant introduction rate $\beta$. They found that $\beta$ and $\tau$ mainly influenced amplitudes of oscillations, and $\delta$ and $\gamma$ influenced periods of oscillations.

Our results, for a different model in which the nature of the delay modifies the roles of the parameters, gives different results. The main difference is that parameters related to the delay have not been found to influence either periods or amplitudes of oscillating solutions. Yet, they were shown to play an important role in the stability of the steady state, which was expected from the nature of the delay.

**Acknowledgment.** The authors are grateful to the anonymous referees for their valuable and helpful comments that improved this manuscript.

REFERENCES

[1] M. Adimy and F. Crauste, *Global stability of a partial differential equation with distributed delay due to cellular replication*, Nonlinear Anal., 54 (2003), pp. 1469–1491.
[2] M. Adimy and F. Crauste, *Existence, positivity and stability for a nonlinear model of cellular proliferation*, Nonlinear Anal. Real World Appl., 6 (2005), pp. 337–366.
[3] M. Adimy and F. Crauste, *Mathematical model of hematopoiesis dynamics with growth factor-dependent apoptosis and proliferation regulations*, Math. Comput. Modelling, 49 (2009), pp. 2128–2137.
[4] M. Adimy, F. Crauste, and L. Pujo-Menjouet, *On the stability of a nonlinear maturity structured model of cellular proliferation*, Discrete Contin. Dyn. Syst., 12 (2005), pp. 501–522.
[5] M. Adimy, F. Crauste, and S. Ruan, *A mathematical study of the hematopoiesis process with applications to chronic myelogenous leukemia*, SIAM J. Appl. Math., 65 (2005), pp. 1328–1352.
[6] M. Adimy, F. Crauste, and S. Ruan, *Stability and Hopf bifurcation in a mathematical model of pluripotent stem cell dynamics*, Nonlinear Anal. Real World Appl., 6 (2005), pp. 651–670.
[7] M. Adimy and L. Pujo-Menjouet, *A singular transport model describing cellular division*, C. R. Acad. Sci. Paris Ser. I Math., 332 (2001), pp. 1071–1076.
[8] M. Adimy and L. Pujo-Menjouet, *A mathematical model describing cellular division with a proliferating phase duration depending on the maturity of cells*, Electron. J. Differential Equations, 107 (2003), pp. 1–14.
[9] W. G. Aiello, H. I. Freedman, and J. Wu, *Analysis of a model representing stage-structured population growth with state-dependent time delay*, SIAM J. Appl. Math., 52 (1992), pp. 855–869.
[10] O. Arino, K. P. Hadeler, and M. L. Hbid, *Existence of periodic solutions for delay differential equations with state dependent delay*, J. Differential Equations, 144 (1998), pp. 263–301.
[11] O. Arino and E. Sanchez, *A saddle point theorem for functional state-dependent delay equations*, Discrete Contin. Dyn. Syst., 12 (2005), pp. 687–722.
[12] T. Alarcon and M. J. Tindall, *Modelling cell growth and its modulation of the G1/S transition*, Bull. Math. Biol., 69 (2007), pp. 197–214.
[13] J. Bélair, *Population models with state-dependent delays*, in Mathematical Population Dynamics (New Brunswick, NJ, 1989), Lecture Notes in Pure and Appl. Math. 131, Dekker, New York, 1991, pp. 165–176.
[14] J. Bélair, M. C. Mackey, and J. M. Mahaffy, *Age-structured and two-delay models for erythropoiesis*, Math. Biosci., 128 (1995), pp. 317–346.
[15] E. Beretta and Y. Kuang, *Geometric stability switch criteria in delay differential systems with delay dependent parameters*, SIAM J. Math. Anal., 33 (2002), pp. 1144–1165.
[16] S. Bernard, J. Belair, and M. C. Mackey, *Sufficient conditions for stability of linear differential equations with distributed delay*, Discrete Contin. Dyn. Syst., 1 (2001), pp. 233–256.
[17] F. J. Burns and I. F. Tannock, *On the existence of a $G_0$ phase in the cell cycle*, Cell. Tissue Kinet., 19 (1970), pp. 321–334.

[18] S. H. Cheshier, S. J. Morrison, X. Liao, and I. L. Weissman, *In vivo proliferation and cell cycle kinetics of long-term self-renewing hematopoietic stem cells*, Proc. Natl. Acad. Sci. USA, 96 (1999), pp. 3120–3125.
[19] K. Cooke and W. Huang, *On the problem of linearization for state-dependent delay differential equations*, Proc. Amer. Math. Soc., 124 (1996), pp. 1417–1426.
[20] F. Crauste, *Global asymptotic stability and Hopf bifurcation for a blood cell production model*, Math. Biosci. Engrg., 3 (2006), pp. 325–346.
[21] F. Crauste, *Delay model of hematopoietic stem cell dynamics: Asymptotic stability and stability switch*, Mathematical Modelling of Natural Phenomena, 4 (2009), pp. 28–47.
[22] F. Crauste, L. Pujo-Menjouet, S. Genieys, C. Molina, and O. Gandrillon, *Adding self-renewal in committed erythroid progenitors improves the biological relevance of a mathematical model of erythropoiesis*, J. Theoret. Biol., 250 (2008), pp. 322–338.
[23] J. Dieudonné, *Foundations of Modern Analysis*, Academic Press, New York, 1960.
[24] R. D. Driver, *Existence theory for a delay-differential system*, Contrib. Differential Equations, 1 (1963), pp. 317–336.
[25] J. Dyson, R. Villella-Bressan, and G. F. Webb, *A singular transport equation modelling a proliferating maturity structured cell population*, Canad. Appl. Math. Quart., 4 (1996), pp. 65–95.
[26] M. Eichmann, *A Local Hopf Bifurcation Theorem for Differential Equations with State-Dependent Delays*, Ph.D. thesis, 2006.
[27] P. Fortin and M. C. Mackey, *Periodic chronic myelogenous leukemia: Spectral analysis of blood cell counts and etiological implications*, Brit. J. Haematol., 104 (1999), pp. 336–345.
[28] H. Fuss, W. Dubitzky, S. Downes, and M. J. Kurth, *Mathematical models of cell cycle regulation*, Brief Bioinform., 6 (2005), pp. 163–177.
[29] J. K. Hale, *Theory of Functional Differential Equations*, Springer-Verlag, Berlin, 1977.
[30] F. Hartung, *Linearized stability in periodic functional differential equations with state-dependent delays*, J. Comput. Appl. Math., 174 (2005), pp. 201–211.
[31] F. Hartung and J. Turi, *Linearized stability in functional differential equations with state-dependent delays*, Discrete Contin. Dynam. Systems, added volume (2001), pp. 416–425.
[32] F. Hartung, T. Krisztin, H. O. Walther, and J. Wu, *Functional differential equations with state-dependent delay: Theory and applications*, in Handbook of Differential Equations: Ordinary Differential Equations Volume 3, A. Canada, P. Drabek, and A. Fonda eds., Elsevier Science B. V., North–Holland, Amsterdam, 2006, pp. 435–545.
[33] C. Haurie, D. C. Dale, and M. C. Mackey, *Cyclical neutropenia and other periodic hematological diseases: A review of mechanisms and mathematical models*, Blood, 92 (1998), pp. 2629–2640.
[34] M. L. Hbid, E. Sanchez, and R. Bravo de la Parra, *State-dependent delays associated to threshold phenomena in structured population dynamics*, Math. Models Methods Appl. Sci., 17 (2007), pp. 877–900.
[35] E. P. Hofer, B. Tibken, and F. Lehn, *Differential equations with state-dependent delays*, in Online Optimization of Large Scale Systems, Springer, Berlin, 2001, pp. 413–432.
[36] E. P. Hofer, B. Tibken, and F. Lehn, *Biomathematical models with state-dependent delays for granulocytopoiesis*, in Online Optimization of Large Scale Systems, Springer, Berlin, 2001, pp. 433–453.
[37] Y. I. Kazmerchuk and J. Wu, *Stochastic state-dependent delay differential equations with applications in finance*, Funct. Differ. Equ., 11 (2004), pp. 77–86.
[38] Y. Kuang, *Delay Differential Equations with Application in Population Dynamics*, Mathematics in Science and Engineering 191, Academic Press, New York, 1993.
[39] Y. Kuang and H. L. Smith, *Slowly oscillating periodic solutions of autonomous state-dependent delay differential equations*, Nonlinear Anal., 19 (1992), pp. 855–872.
[40] L. G. Lajtha, *On DNA labeling in the study of the dynamics of bone marrow cell populations*, in The Kinetics of Cellular Proliferation, F. Stohlman, Jr., ed., Grune and Stratton, New York, 1959, pp. 173–182.
[41] M. Louihi, M. L. Hbid, and O. Arino, *Semigroup properties and the Crandall-Liggett approximation for a class of differential equations with state-dependent delays*, J. Differential Equations, 181 (2002), pp. 1–30.
[42] N. MacDonald, *Time Lags in Biological Models*, Lecture Notes in Biomathematics 27, Springer-Verlag, New York, 1978.
[43] M. C. Mackey, *Unified hypothesis of the origin of aplastic anemia and periodic hematopoiesis*, Blood, 51 (1978), pp. 941–956.

[44] M. C. Mackey, *Dynamic hematological disorders of stem cell origin*, in Biophysical and Biochemical Information Transfer in Recognition, J. G. Vassileva-Popova and E. V. Jensen, eds., Plenum Press, New York, 1979, pp. 941–965.
[45] M. C. Mackey and A. Rey, *Multistability and boundary layer development in a transport equation with retarded arguments*, Canad. Appl. Math. Quart., 1 (1993), pp. 1–21.
[46] M. C. Mackey and R. Rudnicki, *Global stability in a delayed partial differential equation describing cellular replication*, J. Math. Biol., 33 (1994), pp. 89–109.
[47] M. C. Mackey and R. Rudnicki, *A new criterion for the global stability of simultaneous cell replication and maturation processes*, J. Math. Biol., 38 (1999), pp. 195–219.
[48] P. Magal and O. Arino, *Existence of periodic solutions for state dependent delay differential equations*, J. Differential Equations, 165 (2000), pp. 61–95.
[49] J. M. Mahaffy, J. Bélair, and M. C. Mackey, *Hematopoietic model with moving boundary condition and state dependent delay: Applications in erythropoiesis*, J. Theoret. Biol., 190 (1998), pp. 135–146.
[50] J. Mallet-Paret, R. D. Nussbaum, and P. Paraskevopoulos, *Periodic solutions for functional differential equations with multiple state-dependent time lags*, Topol. Methods Nonlinear Anal., 3 (1994), pp. 101–162.
[51] R. Ouifki and M. L. Hbid, *Periodic solutions for a class of functional differential equations with state-dependent delay close to zero*, Math. Models Meth. Appl. Sci., 13 (2003), pp. 807–841.
[52] L. Pujo-Menjouet, S. Bernard, and M. C. Mackey, *Long period oscillations in a $G_0$ model of hematopoietic stem cells*, SIAM J. Appl. Dyn. Syst., 4 (2005), pp. 312–332.
[53] L. Pujo-Menjouet and M. C. Mackey, *Contribution to the study of periodic chronic myelogenous leukemia*, C. R. Biologies, 327 (2004), pp. 235–244.
[54] A. V. Rezounenko and J. Wu, *A non-local PDE model for population dynamics with state-selective delay: Local theory and global attractors*, J. Comput. Appl. Math., 190 (2006), pp. 99–113.
[55] I. Rupes, *Checking cell size in yeast*, Trends Genet., 18 (2002), pp. 479–485.
[56] L. F. Shampine, *Solving ODEs and DDEs with residual control*, Appl. Numer. Math., 52 (2005), pp. 113–127.
[57] H. L. Smith and Y. Kuang, *Periodic solutions of differential delay equations with threshold-type delays*, in Oscillation and Dynamics in Delay Equations, Contemporary Mathematics 129, J. R. Graef and J. K. Hale, eds., AMS, Providence, RI, 1992, pp. 153–176.
[58] J. J. Tyson and B. Novak, *Regulation of the eukaryotic cell cycle: Molecular antagonism, hysteresis, and irreversible transitions*, J. Theoret. Biol., 210 (2001), pp. 249–263.
[59] H. O. Walther, *Stable periodic motion of a system with state-dependent delay*, Differential Integral Equations, 15 (2002), pp. 923–944.
[60] H. O. Walther, *The solution manifold and $C1$-smoothness of solution operators for differential equations with state dependent delay*, J. Differential Equations, 195 (2003), pp. 46–65.
[61] H. O. Walther, *On a model for soft landing with state-dependent delay*, J. Dynam. Differential Equations, 19 (2007), pp. 593–622.
[62] G. F. Webb, *Theory of Nonlinear Age-Dependent Population Dynamics*, Monographs and Textbooks in Pure and Applied Mathematics 89, Marcel Dekker, New York, 1985.

## 5.5 Crauste et al. (2008)

Manuscrit de l'article : [56] F. Crauste, L. Pujo-Menjouet, S. Génieys, C. Molina, O. Gandrillon, *Adding Self-Renewal in Committed Erythroid Progenitors Improves the Biological Importance of a Mathematical Model of Erythropoiesis*, Journal of Theoretical Biology, 250, 322–338 (2008).

Available online at www.sciencedirect.com
ScienceDirect
Journal of Theoretical Biology 250 (2008) 322–338
Journal of Theoretical Biology
www.elsevier.com/locate/yjtbi

# Adding self-renewal in committed erythroid progenitors improves the biological relevance of a mathematical model of erythropoiesis

Fabien Crauste[a,*], Laurent Pujo-Menjouet[a], Stéphane Génieys[a], Clément Molina[b], Olivier Gandrillon[b]

[a]*Université de Lyon, Université Lyon 1, CNRS, UMR 5208, Institut Camille Jordan, Bâtiment du Doyen Jean Braconnier, 43, blvd du 11 novembre 1918, F - 69222 Villeurbanne Cedex, France*
[b]*Equipe "Bases Moléculaires de l'Autorenouvellement et de ses Altérations," Université de Lyon, Université Lyon 1, Lyon, F-69003, France; CNRS, UMR5534, Centre de génétique moléculaire et cellulaire, Villeurbanne, F-69622, France*

Received 7 May 2007; received in revised form 21 September 2007; accepted 28 September 2007
Available online 6 October 2007

**Abstract**

We propose a new mathematical model of erythropoiesis that takes a positive feedback of erythrocytes on progenitor apoptosis into account, and incorporates a negative feedback of erythrocytes on progenitor self-renewal. The resulting model is a system of age-structured equations that reduces to a system of delay differential equations where the delays account for progenitor compartment duration and cell cycle length. We compare this model with experimental data on an induced-anemia in mice that exhibit damped oscillations of the hematocrit before it returns to equilibrium. When we assume no self-renewal of progenitors, we obtain an inaccurate fitting of the model with experimental data. Adding self-renewal in the progenitor compartment gives better approximations, with the main features of experimental data correctly fitted. Our results indicate the importance of progenitor self-renewal in the modelling of erythropoiesis. Moreover, the model makes testable predictions on the lifespan of erythrocytes confronted to a severe anemia, and on the progenitors behavior.


*Keywords:* Stress erythropoiesis; Self-renewal; Severe anemia; Age-structured model; Delay differential equations

## 1. Introduction

Hematopoiesis is the process through which all functional mature blood cells are generated. Homeostasis—that is the regulation of the production of different cell types to maintain stable populations—in the hematopoietic system is required in all vertebrates throughout life and needs a tight and constant regulation of decisions between proliferation, apoptosis and differentiation of hematopoietic cells.

All blood cells originate from hematopoietic stem cells (HSCs) (Weissman, 2000) entering differentiation pathways through successive divisions. Differentiated HSC form burst forming units (BFUs) and colony forming units (CFUs), known as progenitors. These latter can be separated in distinct lineages such as: white cells, platelets, or red blood cells. For example, differentiation of BFU-E and CFU-E can lead to the production of erythrocytes (red blood cells). Finally, after several divisions, progenitors become precursors. These latter go through a finite number of divisions before reaching the bloodstream as mature cells.

Self-renewal (Watt and Hogan, 2000) is the ability of a cell to divide and give two daughter cells that retain the same maturity as the mother cell, while keeping at all time the ability to engage in a differentiation process (i.e. to give two daughter cells, one of which at least being more mature than the mother cell). In the hematopoietic system, self-renewal is generally considered to be a specific property of the HSC (Weissman, 2000). However, neither the daily

*Corresponding author. Tel.: +33 472 448 516; fax: +33 472 431 687.
*E-mail addresses:* crauste@math.univ-lyon1.fr (F. Crauste), pujo@math.univ-lyon1.fr (L. Pujo-Menjouet), genieys@math.univ-lyon1.fr (S. Génieys), clmolina@laposte.net (C. Molina), Gandrillon@cgmc.univ-lyon1.fr (O. Gandrillon).

0022-5193/$ - see front matter © 2007 Elsevier Ltd. All rights reserved.
doi:10.1016/j.jtbi.2007.09.041

generation of $200 \times 10^9$ red blood cells nor stress erythropoiesis (Bauer et al., 1999) can easily be explained by the idea that only HSC can self-renew. Thus the hypothesis that immature progenitors can also self-renew has been proposed and has been supported by experimental evidences (Bauer et al., 1999; Gandrillon et al., 1999; Pain et al., 1991).

We focus our work here on erythropoiesis, the process through which red blood cells are produced. We explore the putative role of self-renewal at the progenitor level, through a mathematical modelling of erythropoiesis that can be confronted with real life data.

Numerous mathematical models of hematopoiesis or hematopoiesis lineages have been proposed (for a recent review, see Roeder, 2006). Among these, let us point out the work of Mackey (1978), who in 1978 published one of the pioneering paper in the field of physiological models for oscillating phenomena within the hematopoietic system. Mackey's model was based on publications by Lajtha (1959) and Burns and Tannock (1970).

Mackey's model has been developed then by many authors, including Mackey and co-workers, to describe differentiation and maturation processes involved in hematopoiesis more precisely. Bernard et al. (2003a, 2004) focused on the white blood cell production to bring an explanation to oscillatory behaviors observed in patients with cyclical neutropenia. Pujo-Menjouet and Mackey (2004) used a similar model to investigate the appearance of oscillations in blood cell counts within patients with chronic myelogenous leukemia. A global model was proposed by Colijn and Mackey (2005a, b), derived by combining sub-models of the various lineages, to explain some cases of periodic hematological diseases (see Haurie et al., 1998, 1999 for a review of periodic hematological diseases). The reader interested in the mathematical modelling of stem cells dynamics applied to blood diseases can consult Adimy and Crauste (2003), Adimy and Pujo-Menjouet (2003), Adimy et al. (2005a, b, 2006b), Mackey and Rudnicki (1994, 1999), Pujo-Menjouet et al. (2005) and the references therein.

In 1995, Bélair et al. (1995) proposed a modification of Mackey's model to consider the influence of growth factors on stem cell differentiation. The authors focused on erythropoiesis and assumed that erythropoietin (EPO)—a growth factor known to play a crucial role in erythropoiesis regulation—acted only on introduction of HSC in cycle. Their model was improved in 1998 by Mahaffy et al. (1998), and recently analyzed in detail by Ackleh et al. (2002, 2006) and Banks et al. (2004). Another erythropoiesis model, inspired by the same article, was introduced in Adimy et al. (2006a). In these works, EPO is the only growth factor supposed to act during erythropoiesis, and its action is always located at the introduction of HSCs in cell cycle. Recently, Adimy and Crauste (2007) considered a modification of the model in Bélair et al. (1995) to take the influence of erythropoietin on HSC apoptosis into account (Koury and Bondurant, 1990), but they only performed a theoretical study of the model.

An important contribution to mathematical modelling of erythropoiesis also appears in the works of Loeffler and his collaborators (Loeffler and Wichmann, 1980; Loeffler et al., 1989; Pantel et al., 1990; Wichmann and Loeffler, 1985; Wichmann et al., 1985, 1989; Wulff et al., 1989), mainly published between 1980 and 1990, but also recently (Roeder and Loeffler, 2002; Roeder, 2006). Throughout a collection of papers, Loeffler et al. investigate mathematical models of erythropoiesis and granulopoiesis, taking into account feedback controls from progenitors at the stem cell level and from mature cells (mainly assimilated to precursors) on progenitors. Their model also consider self-renewal of HSC. This is detailed in Wichmann and Loeffler (1985), where the authors investigated the behavior of this model, and fitted it to various experiments (including irradiations, bleeding, and phenylhydrazine treatments of mice). Application of their model to phenylhydrazine treatments can be compared to the results presented in Section 2, even though our experiments are closer to Wichmann and Loeffler experiments of bleeding on mice. However, all these works were performed, in particular, before the importance of EPO on the regulation of apoptosis was proved (Koury and Bondurant, 1990), and assumptions on erythroid progenitor self-renewal appeared (Bauer et al., 1999; Gandrillon et al., 1999; Pain et al., 1991). Moreover, the dynamics observed by the authors in their series of erythropoiesis–granulopoiesis modelling works is mainly concerned with hematopoietic stem cells properties and their regulation, and this latter problem is still only partially known at the molecular level (Krause, 2002).

In this work, we modify the erythropoiesis part of Colijn and Mackey's 2005a model in order to focus ourselves on the influence of EPO upon progenitor apoptosis (Koury and Bondurant, 1990) and of glucocorticoids upon progenitor self-renewal (Bauer et al., 1999). Indeed, Colijn and Mackey (2005a) only considered feedback of the erythrocyte population on the rate of differentiation of HSCs, and no self-renewal appears elsewhere but in the HSCs compartment. To the best of our knowledge, the latter assumption on the feedback control of erythrocytes on HSCs differentiation is no longer believed to hold amongst biologists (see Krause, 2002). We first present some experimental results that seem to indicate the importance of self-renewal for progenitors. Then, we propose a new model for erythropoiesis, which is an age-structured model, that we reduce to a system of delay differential equations (similarly to what has been done by Bélair et al., 1995). We then analyze this model without taking self-renewal into account, in Section 5, and show that, even though theoretical results display interesting properties, the model does not fit experimental data well. After carrying out numerical simulations on the complete model, we conclude in Section 6 that progenitor self-renewal in erythropoiesis is important, as expected from experimental data. In the last section, a discussion stresses out the limits of this model and rises new questions concerning erythropoiesis modelling.

## 2. Experimental evidence of feedback controls

In order to study the kinetics of erythrocyte populations, we performed a series of experiments (in the Centre de Génétique Moléculaire et Cellulaire Laboratory, O. Gandrillon's team) to measure hematocrit in mice. Hematocrit is a test that measures the volume of red blood cells in a blood sample. It gives a percentage of erythrocyte volume found in the whole blood system. It can be considered that a blood sample is mainly composed with erythrocytes and plasma, since platelets and white cells volumes can be easily neglected. Our approach consisted in destabilizing the steady state hematocrit by creating an anemia, and observing the return to equilibrium.

The hematocrit values were taken from two different batches of adult outbred Hsd-ICR mice. Each batch consisted of six males and six females. One batch was rendered anemic by two intraperitoneal phenylhydrazine injections (60 mg/kg body weight) at 24 h intervals. The control batch was not injected. Blood was collected from the peri-orbital sinus of the mouse directly in microhematocrit tubes at the indicated time intervals (that is daily intervals excluding Sundays for 2 weeks and then at 2–3 days intervals for the rest of the period, for the anemic batch, and at 2–3 days intervals for the control batch). Fig. 1 shows the results of this experiment.

The hematocrit of the control batch stays at its steady value, between 45% and 50% (Panel B), whereas the hematocrit of the injected batch (Panel A) displays very clear features: following the anemia, that makes the hematocrit fall to very low values (about $23 \pm 3\%$), the hematocrit rapidly increases to reach a high value (about $55 \pm 3\%$), and then returns to the equilibrium, but not in a very smooth manner.

In both cases, it seems that the hematocrit oscillates about its steady value. However, the standard deviation lines in the hematocrit of the control batch (Fig. 1B) seem to indicate that what could be thought as oscillations corresponds in fact to perturbations about the mean. For the anemia-induced batch, however, anemia seems to trigger damped oscillations before the hematocrit returns to the equilibrium.

A simple way to determine periodicity in unevenly distributed data samples is to use the Lomb periodogram (Lomb, 1976). If a periodicity exists in a data sample, then it corresponds to a peak in the periodogram curve. We computed the Lomb periodogram for the data in Fig. 1 (data not shown here), and they tend to corroborate the above remark on the damped oscillations. However, since we do not really look for any periodicity in our data, but rather for damped oscillations, the use of the Lomb periodogram can be discussed. One can however keep in mind that the Lomb periodogram confirms that a normal hematocrit does not oscillate.

In the next section, we propose a new model for erythropoiesis, that incorporates nonlinear apoptosis and self-renewal rates of progenitors. This model will be confronted to the above experimental data corresponding to a severe anemia, in order to stress the importance of erythroid progenitors self-renewal in erythropoiesis.

## 3. An age-structured model of erythropoiesis

As described in the introduction, one can basically consider that erythropoiesis involves three types of cell populations. HSCs, considered as the root of the process, progenitors also known as committed stem cells coming from differentiated HSCs, and erythrocytes, or red blood cells, which are the final state of cells in erythropoiesis.

The question of the control of HSC differentiation into given lineages is open (see e.g. Krause, 2002 for a review). It is especially unclear to see whether this cell fate decision is controlled by a purely stochastic mechanism or is the result of environmental cues mediated at least in part through specific receptor ligand interactions. Since this part of the process is mostly unknown, and since we are interested in modelling the erythroid progenitor compartment, we decided not to incorporate the control of HSC

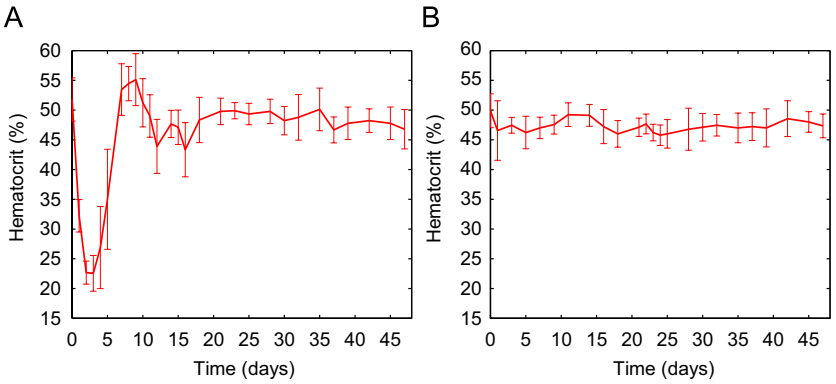


Fig. 1. Hematocrit values from two different batches of adult outbred Hsd-ICR mice, over 48 days. Average hematocrit is represented, with standard deviation lines on either side of the mean. Panel A: Hematocrit of the anemic batch (injected with phenylhydrazine). Panel B: Hematocrit of the control batch (not injected).

differentiation in the model, but to model the flow from HSC into erythroid progenitor as a constant. Hence, in our model, we do not consider the HSC population but rather the influx of HSC becoming progenitors, denoted by $K$.

Then, let us consider three different cell populations, self-renewing progenitors, non-self-renewing progenitors and erythrocytes, with densities respectively denoted by $p_{sr}(t,a)$, $p(t,a)$ and $e(t,a)$. These quantities represent the densities of cell populations formed by progenitors (for $p_{sr}(t,a)$ and $p(t,a)$) or erythrocytes (for $e(t,a)$) with age $a$ at time $t$. For progenitors, age corresponds to the time spent between two successive divisions. It can be noted that all cells age with unitary velocity, that is

$$\frac{\mathrm{d}a}{\mathrm{d}t}=1.$$

Dynamics of these populations are as follows. The progenitor compartment is supplied at a constant rate $K$ with HSCs. Progenitors die by apoptosis with a rate $\beta$ and they self-renew with a rate $\sigma$. We denote by $\tau_c$ the time needed by a progenitor to self-renew, and by $\tau_p$ the progenitor compartment duration, that is the time needed by a progenitor cell to become mature and enter the last part of its differentiation process. Self-renewing progenitors can also die by apoptosis. After maturing and differentiating, progenitors become erythrocytes—we do not explicitly take progenitor differentiation through divisions into account, but we suppose that the cell population entering the erythrocyte compartment corresponds to the progenitors at the end of their compartment (that is when $t=\tau_p$), multiplied by an amplification parameter $A$ which describes the successive divisions of progenitors (about 7–8 divisions). Erythrocytes are assumed to die with a constant rate $\gamma$, equal to 1 over the average lifespan of an erythrocyte. They modulate apoptosis and self-renewal of progenitors through control loops. Erythrocytes are assumed to positively control apoptosis of progenitors, and negatively control their self-renewal. A schematic representation of this model is provided in Fig. 2.

Then, densities $p(t,a)$, $p_{sr}(t,a)$ and $e(t,a)$ satisfy the following evolution equations for $t,a>0$:

$$\frac{\partial p}{\partial t}(t,a)+\frac{\partial p}{\partial a}(t,a)=-\beta p(t,a)-\sigma p(t,a),$$

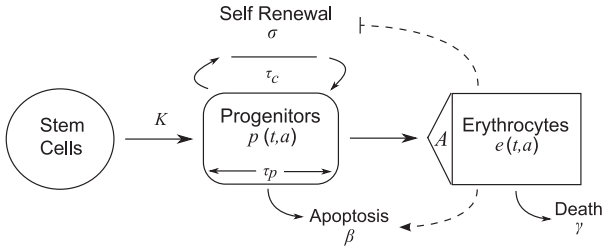


Fig. 2. Schematic representation of the model. Progenitors have an ability to self-renew. A negative feedback of erythrocytes on this self-renewal is incorporated, as well as a positive feedback on progenitor apoptosis. Dashed lines indicate feedback controls.

$$\frac{\partial p_{sr}}{\partial t}(t,a)+\frac{\partial p_{sr}}{\partial a}(t,a)=-\beta p_{sr}(t,a),$$
$$\frac{\partial e}{\partial t}(t,a)+\frac{\partial e}{\partial a}(t,a)=-\gamma e(t,a). \quad (1)$$

This system must be completed by boundary conditions, describing the cell flux between the three compartments (progenitors, self-renewing progenitors and erythrocytes), and initial conditions representing an initial distribution of populations in the system. We do not pay too much attention to initial conditions because our next step will be to reduce system (1) to a delay differential system with different initial conditions.

Boundary conditions for system (1) are given by

$$p(t,0)=K+2p_{sr}(t,\tau_c),$$
$$p_{sr}(t,0)=\int_0^{\tau_p}\sigma p(t,a)\,\mathrm{d}a,$$
$$e(t,0)=Ap(t,\tau_p). \quad (2)$$

The first condition in (2) describes the input of progenitors. Cells entering the progenitor compartment come from HSCs (that is $K$) and from self-renewing progenitors that have completed a cell cycle ($2p_{sr}(t,\tau_c)$). The second equation represents progenitors entering self-renewal. The third equation describes new erythrocytes coming from the progenitor compartment.

We do not impose a maximal age for erythrocytes, but we assume

$$\lim_{a\to+\infty} e(t,a)=0$$

fast enough for the total density of erythrocytes $\int_0^{+\infty} e(t,a)\mathrm{d}a$ to be finite for all time $t$.

We assume that erythrocytes apply a positive feedback on progenitor apoptosis, and a negative feedback on progenitor self-renewal. In fact, progenitor apoptosis is mainly mediated by EPO, whose production is in turn dependent on the number of circulating erythrocytes. We do not want, for the moment, to complicate our erythropoiesis modelling by adding EPO concentration. So we implicitly describe its influence on apoptosis by considering that apoptosis depends on the total number of erythrocytes. In the same way, self-renewal seems to be mainly mediated by glucocorticoids (cortisol), but we suppose that self-renewal depends only on the total number of erythrocytes. That is, we assume

$$\beta=\beta\left(\int_0^{+\infty}e(t,a)\,\mathrm{d}a\right)\quad\text{and}\quad\sigma=\sigma\left(\int_0^{+\infty}e(t,a)\,\mathrm{d}a\right),$$

where $\beta$ is a positive, continuous and increasing function, with

$$\beta(0)=0\quad\text{and}\quad\lim_{E\to+\infty}\beta(E)=\beta_\infty>0,$$

and $\sigma$ a positive, continuous and decreasing function, with

$$\sigma(0)=\sigma_0>0\quad\text{and}\quad\lim_{E\to+\infty}\sigma(E)=0.$$

Under these assumptions, system (1)–(2) is nonlinear, with positive and negative controls. In the next section, we show that this model can be easily reduced to a system of two nonlinear differential equations with delays.

## 4. Reduction to a system of delay differential equations

Let us define the total densities of non-self-renewing progenitors, self-renewing progenitors and erythrocytes at time $t$, denoted by $P(t)$, $P_{sr}(t)$ and $E(t)$, respectively, as

$$P(t)=\int_0^{\tau_p} p(t,a)\,\mathrm{d}a,$$
$$P_{sr}(t)=\int_0^{\tau_c} p_{sr}(t,a)\,\mathrm{d}a \quad \text{and} \quad E(t)=\int_0^{+\infty} e(t,a)\,\mathrm{d}a.$$

Integrating system (1) over the age (between $a=0$ and $a=\tau_p$ for $p(t,a)$, $a=0$ and $a=\tau_c$ for $p_{sr}(t,a)$, and $a=0$ and $a=+\infty$ for $e(t,a)$), one obtains

$$\frac{\mathrm{d}P}{\mathrm{d}t}(t)=-[\beta(E(t))+\sigma(E(t))]P(t)+p(t,0)-p(t,\tau_p),$$
$$\frac{\mathrm{d}P_{sr}}{\mathrm{d}t}(t)=-\beta(E(t))P_{sr}(t)+p_{sr}(t,0)-p_{sr}(t,\tau_c),$$
$$\frac{\mathrm{d}E}{\mathrm{d}t}(t)=-\gamma E(t)+e(t,0),$$

which becomes, using (2),

$$\begin{aligned}\frac{\mathrm{d}P}{\mathrm{d}t}(t)=&-[\beta(E(t))+\sigma(E(t))]P(t)\\&+K+2p_{sr}(t,\tau_c)-p(t,\tau_p),\\\frac{\mathrm{d}P_{sr}}{\mathrm{d}t}(t)=&-\beta(E(t))P_{sr}(t)\\&+\sigma(E(t))P(t)-p_{sr}(t,\tau_c),\\\frac{\mathrm{d}E}{\mathrm{d}t}(t)=&-\gamma E(t)+Ap(t,\tau_p).\end{aligned}\tag{3}$$

One needs to determine $p_{sr}(t,\tau_c)$ and $p(t,\tau_p)$ to obtain a clear expression for system (3). To that aim, we use the method of the characteristics (see Appendix A for details). We thus obtain, for $t>\tau_p+\tau_c$, the reduced model

$$\begin{aligned}\frac{\mathrm{d}P}{\mathrm{d}t}(t)=&-[\beta(E(t))+\sigma(E(t))]P(t)\\&+K+2\sigma(E(t-\tau_c))P(t-\tau_c)\\&\times\exp\left(-\int_{t-\tau_c}^{t}\beta(E(s))\,\mathrm{d}s\right)\\&-\left[K+2\sigma(E(t-\tau_p-\tau_c))P(t-\tau_p-\tau_c)\right.\\&\left.\times\exp\left(-\int_{t-\tau_p-\tau_c}^{t-\tau_p}\beta(E(s))\,\mathrm{d}s\right)\right]\\&\times\exp\left(-\int_{t-\tau_p}^{t}(\beta(E(s))+\sigma(E(s)))\,\mathrm{d}s\right),\end{aligned}$$

$$\begin{aligned}\frac{\mathrm{d}E}{\mathrm{d}t}(t)=&-\gamma E(t)+A\exp\left(-\int_{t-\tau_p}^{t}(\beta(E(s))+\sigma(E(s)))\,\mathrm{d}s\right)\\&\times\left[K+2\sigma(E(t-\tau_p-\tau_c))P(t-\tau_p-\tau_c)\right.\\&\left.\times\exp\left(-\int_{t-\tau_p-\tau_c}^{t-\tau_p}\beta(E(s))\,\mathrm{d}s\right)\right],\end{aligned}\tag{4}$$

where the equation for $P_{sr}$ is omitted since it has no impact on other equations of (4). However, introducing the population of self-renewing progenitors was convenient to obtain system (4) as shown in Appendix A.

Let us briefly explain the role of each term in system (4).

The first equation describes the evolution of the total density of progenitors. The first terms on the right-hand side of the first equation account for cell loss due to apoptosis and cells entering self-renewal. The second term represents the amount of cells entering the progenitor compartment, one part from the HSC compartment and the other one from cells that have completed a cell cycle and re-entered the progenitor compartment (self-renewal), after division (that is why there is a coefficient 2). Finally, the last term is for progenitors that become erythrocytes (one can note that some of these cells directly derive from HSCs that have survived the progenitor compartment).

The second equation determines the evolution of the erythrocyte density. Erythrocytes can only die, with a constant rate $\gamma$, and the second term in the right-hand side of the second equation is for progenitors that enter the erythrocyte compartment, as described above.

In the next sections, we investigate this model, first without self-renewal and then with it. Then we point out the main differences between these two cases.

## 5. Is it necessary to take self-renewal of progenitors into account to reproduce experimental results?

Before investigating the dynamics of system (4) and the consequences of apoptosis and self-renewal, let us first consider the case where progenitors do not self-renew. Then the erythropoiesis process, as described in Fig. 2, becomes simpler as shown in Fig. 3.

In this case, system (4) becomes

$$\frac{\mathrm{d}P}{\mathrm{d}t}(t)=-\beta(E(t))P(t)+K\left[1-\exp\left(-\int_{t-\tau_p}^{t}\beta(E(s))\,\mathrm{d}s\right)\right],\tag{5}$$

$$\frac{\mathrm{d}E}{\mathrm{d}t}(t)=-\gamma E(t)+AK\exp\left(-\int_{t-\tau_p}^{t}\beta(E(s))\,\mathrm{d}s\right).\tag{6}$$

This is an uncoupled system of nonlinear differential equations with a single delay $\tau_p$. The important point is that Eq. (6) does not depend on the progenitor population $P(t)$. Hence, it is sufficient to focus on the dynamics of the

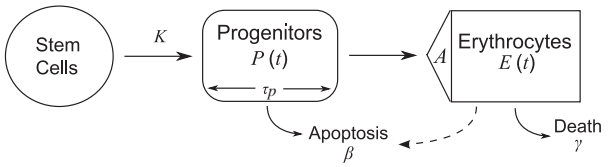


Fig. 3. A schematic representation of erythropoiesis without progenitor self-renewal. We consider two cell populations, progenitors $P(t)$ and erythrocytes $E(t)$. Details of the considered mechanisms describing the dynamics of progenitor and erythrocyte populations are given in Section 3, except that there is no progenitor self-renewal in the present case. Erythrocytes positively control progenitor apoptosis (dashed line).

solutions of Eq. (6). In particular, one only needs to determine a steady state of (6) and its asymptotic behavior to deduce the asymptotic behavior of the entire system (5)–(6).

Even though self-renewal of erythroid progenitors can be considered as the main feature of system (4), it is not the only novelty incorporated in this system. In particular, the feedback control of erythrocytes (via EPO, even in an implicit way) on progenitors apoptosis has never been used in erythropoiesis modelling (the only feedback on apoptosis considered in previous studies used to have an influence on the HSC population, see Adimy and Crauste, 2007), so system (5)–(6) does not reduce to any previously published model of erythropoiesis.

We recall that the apoptosis function $E\mapsto\beta(E)$ is assumed to be increasing with

$$\beta(0)=0 \quad \text{and} \quad \lim_{E\to\infty}\beta(E)=\beta_\infty>0.$$

We first concentrate on the existence of steady states for system (5)–(6). We investigate then the stability of this steady state and we focus on numerical simulations.

### 5.1. Existence of steady states

We recall that $(P^*,E^*)$ is a steady state of system (5)–(6) if $P^*$ and $E^*$ are solutions of (5)–(6) satisfying

$$\frac{\mathrm{d}P^*}{\mathrm{d}t}(t)=\frac{\mathrm{d}E^*}{\mathrm{d}t}(t)=0 \quad \text{for } t>0.$$

Consequently, a steady state of system (5)–(6), also called a stationary solution or equilibrium, is a constant solution of (5)–(6).

Thus, a steady state $(P^*,E^*)$ of system (5)–(6) satisfies

$$\beta(E^*)P^*=K[1-\mathrm{e}^{-\tau_p\beta(E^*)}], \tag{7}$$

$$\gamma E^*=AK\mathrm{e}^{-\tau_p\beta(E^*)}. \tag{8}$$

Eq. (8) gives the existence of a unique $E^*>0$ satisfying (8). Indeed, since $\beta$ is a positive and increasing function, the mapping $z\mapsto AK\mathrm{e}^{-\tau_p\beta(z)}$ is decreasing for $z\geqslant 0$, and ranges from $AK$ to $AK\mathrm{e}^{-\tau_p\beta_\infty}$. The function $z\mapsto\gamma z$ is strictly increasing and ranges from 0 to $+\infty$. Therefore, we deduce the existence of a unique $E^*>0$ verifying (8).

From the expression of $E^*$ one easily deduces $P^*$ using (7), that is

$$P^*=K\frac{1-\mathrm{e}^{-\tau_p\beta(E^*)}}{\beta(E^*)}=\frac{AK-\gamma E^*}{A\beta(E^*)}.$$

Thus we claim the existence of a unique steady state $(P^*,E^*)$ of system (5)–(6) defined by (7)–(8), and satisfying

$$\frac{AK\mathrm{e}^{-\tau_p\beta_\infty}}{\gamma}<E^*<\frac{AK}{\gamma} \quad \text{and} \quad 0<P^*<K\frac{1-\mathrm{e}^{-\tau_p\beta_\infty}}{\beta(AK\mathrm{e}^{-\tau_p\beta_\infty}/\gamma)}. \tag{9}$$

From a biological point of view, the quantity $AK/\gamma$ corresponds to the steady state value of the erythrocyte density in the absence of progenitor apoptosis (it is easily seen from (8) with $\beta=0$), and similarly $AK\mathrm{e}^{-\tau_p\beta_\infty}/\gamma$ corresponds to the steady state value when apoptosis is at its maximum. Thus the above inequality on $E^*$ only gives bounds for $E^*$ that correspond to extreme situations in system (7)–(8), these bounds describing absolutely virtual erythrocyte densities.

### 5.2. Asymptotic stability and existence of periodic solutions

We analyze the asymptotic behavior of the unique steady state of system (5)–(6) by linearizing it about its steady state. Since the behavior of system (5)–(6) is entirely given by the behavior of the solution $E(t)$, we only linearize Eq. (6) about $E^*$.

We set $z(t)=E(t)-E^*$. Then Eq. (6) linearized about $E^*$ is

$$\frac{\mathrm{d}z}{\mathrm{d}t}(t)=-\gamma z(t)-\xi\int_{-\tau_p}^{0}z(t+s)\,\mathrm{d}s, \tag{10}$$

where, from (8),

$$\xi=AK\beta'(E^*)\mathrm{e}^{-\tau_p\beta(E^*)}=\gamma E^*\beta'(E^*)>0. \tag{11}$$

From Eq. (10) we can deduce the characteristic equation of (6), defined by

$$\lambda+\gamma+\xi\int_{-\tau_p}^{0}\mathrm{e}^{\lambda s}\,\mathrm{d}s=0, \quad \lambda\in\mathbb{C}. \tag{12}$$

By studying the complex roots of (12), that are called characteristic roots of (10) or eigenvalues, we can determine whether $E^*$ is asymptotically stable or unstable.

The asymptotic stability of $E^*$ is determined by the sign of the real parts of eigenvalues of (10), that is of roots of (12). If all eigenvalues of (10) have negative real parts, then $E^*$ is locally asymptotically stable. If there exist eigenvalues of (10) with positive real parts, then $E^*$ is unstable. Moreover, the stability of $E^*$ can only be lost if purely imaginary eigenvalues appear.

We first check (see Appendix B for details) that $\lambda=0$ is not an eigenvalue of (10), so the integral in (12) can be computed and (12) is equivalent to

$$\lambda^2+\gamma\lambda+\xi-\xi\mathrm{e}^{-\lambda\tau_p}=0 \quad \text{and} \quad \lambda\neq 0.$$

The study of complex roots of (12) is then equivalent to the study of non-zero complex roots of

$$\lambda^2 + \gamma\lambda + \xi - \xi\,\mathrm{e}^{-\lambda\tau_p} = 0. \tag{13}$$

It is straightforward (see Appendix B) to obtain that all non-zero roots of (13) have negative real parts when $\tau_p = 0$, that is $E^*$ is locally asymptotically stable in this case.

Consequently, we check if there could exist a critical value of $\tau_p > 0$ that destabilizes the steady state $E^*$. Actually, we are going to prove that the steady state may be destabilized through a Hopf bifurcation (see details in Appendix B).

Assuming $\tau_p > 0$, and looking for eigenvalues of the form $\lambda = \mathrm{i}\omega$, with $\omega \in \mathbb{R}$, we first obtain that (10) has no purely imaginary characteristic roots if $2\xi \leqslant \gamma^2$, and so the stability of the steady state $E^*$ cannot be modified. Since it is locally asymptotically stable when $\tau_p = 0$, then it is locally asymptotically stable for $\tau_p \geqslant 0$ under condition $2\xi \leqslant \gamma^2$.

Then, studying the case $2\xi > \gamma^2$, using simple techniques (see, for example, Kuang, 1993) one obtains the existence of simple purely imaginary roots $\pm\mathrm{i}\omega$ of (10), with $\omega = \sqrt{2\xi - \gamma^2}$, for

$$\tau_p = \tau_p^* := \frac{\arccos\left(\dfrac{\gamma^2}{\xi} - 1\right)}{\sqrt{2\xi - \gamma^2}}.$$

Moreover, these characteristic roots satisfy the so-called *transversality condition*, that is real parts of the branch of eigenvalues that passes through $\pm\mathrm{i}\sqrt{2\xi - \gamma^2}$ cross the horizontal axis. This property is necessary to establish the existence of a Hopf bifurcation at the steady state for $\tau_p = \tau_p^*$.

We can then conclude to the following proposition, which summarizes the behavior of the unique steady state of system (5)–(6).

**Proposition 1.** *If $2\xi > \gamma^2$, then for $0 \leqslant \tau_p < \tau_p^*$, the steady state $E^*$ is locally asymptotically stable and, for $\tau_p \geqslant \tau_p^*$ it is unstable. When $\tau_p = \tau_p^*$ a Hopf bifurcation occurs at $E^*$ and periodic solutions appear.*

*If $2\xi \leqslant \gamma^2$, the steady state $E^*$ is locally asymptotically stable for all $\tau_p \geqslant 0$.*

According to the result in Proposition 1, the erythropoiesis process can theoretically lead to the appearance of periodic solutions of the circulating erythrocyte number—through a Hopf bifurcation—and therefore damped oscillations should be observed before the bifurcation, when the steady state is about to be destabilized.

### 5.3. Numerical simulations

We are interested in modelling the rapid recovery of the level of erythrocytes observed after acute anemia (see Section 2). To that aim, we compute the solution $E(t)$ of (6), using the MATLAB solver dde23 which allows the numerical resolution of delay differential equations (Shampine and Thompson, 2001), and we use this solution to draw the hematocrit corresponding to our simulation.

The hematocrit $H(t)$ is defined by

$$H(t) = \frac{vE(t)}{vE(t) + \text{plasma volume}},$$

where $v$ is the considered volume per mass density unit of the erythrocytes. Assuming plasma volume is not modified by our experimental induction of anemia, we relate it to the steady hematocrit, denoted by $H^*$ (with $H^*$ about 45–50%, see Fig. 1), and the steady state $E^*$. Since, at the steady state,

$$H(t) = H^* = \frac{vE^*}{vE^* + \text{plasma volume}},$$

we deduce that

$$\text{plasma volume} = \frac{1 - H^*}{H^*} vE^*.$$

Consequently, in the following, we assume that the hematocrit is given by

$$H(t) = \frac{E(t)}{E(t) + (1 - H^*)E^*/H^*}.$$

Taking the inverse function, we have

$$E(t) = \frac{H(t)}{1 - H(t)} \quad \frac{1 - H^*}{H^*} E^*. \tag{14}$$

We compute $E^*$ from Eq. (6), and $H^*$ from the experimental curve in Fig. 1.

Since $E(t)$ is the solution of a delay differential equation, an initial condition for Eq. (6) must be supplied on the interval $[-\tau_p, 0]$. We consider, as an initial condition for our problem, the function that describes a strong decay of the hematocrit from $H^*$ to $H_{min}$, on the interval $[-\tau_{in}, 0]$ (here, according to Fig. 1, $\tau_{in} = 3$ days). It follows that the initial condition for $H(t)$ in this case is

$$H_0(t) = \begin{cases} H^*, & \text{for } t \in [-\tau_p, -\tau_{in}], \\ \dfrac{H^* - H_{min}}{\tau_{in}^*} t + H_{min}, & \text{for } t \in [-\tau_{in}, 0]. \end{cases}$$

Using (14), we choose as initial condition for Eq. (6)

$$E_0(t) = E^* \frac{1 - H^*}{H^*} \times \frac{H_0(t)}{1 - H_0(t)}, \quad \text{for } t \in [-\tau_p, 0]. \tag{15}$$

Using this initial condition for Eq. (6), we hope to obtain a description of the rapid increase of the hematocrit, with a significant peak and damped oscillations before a steady hematocrit.

In Table 1, values of the parameters used in the simulations are listed. We discuss hereafter these values.

The hematopoietic stem cell influx is known to be, in mammals, about $10^4\,\text{cells}\,(\text{gd})^{-1}$, at maximum. We suppose here that $K = 10^4\,\text{cells}\,(\text{gd})^{-1}$, even if it can be varied between $10^3$ and $10^4\,\text{cells}\,(\text{gd})^{-1}$. The death rate of erythrocytes, estimated by considering that the average

Table 1
Table of parameters

| Parameters | | Values used | Range |
|---|---|---|---|
| $\gamma$ | Erythrocytes mortality rate ($d^{-1}$) | 0.025 | – |
| $A$ | Amplification parameter | $2^8$ | $2^4 - 2^8$ |
| $K$ | HSC population density entering the progenitor compartment per day (cells (gd)$^{-1}$) | $10^4$ | $10^3 - 10^4$ |
| $\tau_p$ | Progenitor compartment duration (days) | 4 | – |
| $\tau_c$ | Self-renewal cycle duration (days) | 1 | – |
| $\beta_\infty$ | Maximum apoptosis rate ($d^{-1}$) | 1 | 0.5 – 1 |
| $\overline{\beta}$ | Threshold value of the apoptosis rate (cells $d^{-1}$) | $10^7$ [a], $10^8$ | $10^7 - 10^9$ |
| $n$ | Sensitivity of the apoptosis rate | 8 | – |
| $\sigma_0$ | Maximum self-renewal rate ($d^{-1}$) | 0.5 | – |
| $\overline{\sigma}$ | Threshold value of the self-renewal rate (cells $d^{-1}$) | $10^9$ | $10^6 - 10^{10}$ |
| $m$ | Sensitivity of the self-renewal rate | 5 | – |

Values of the different parameters involved in system (4) are listed in two columns: in the first one, values used in simulations with and without taking self-renewal into account, and in the second column a range for each parameter, when available.
[a]This value is only used in the absence of self-renewal.

erythrocyte life in mice is 40 days, is taken to be $\gamma = 1/40 = 0.025\,d^{-1}$. The amplification parameter $A$ should correspond to a range of 4–8 divisions, with mortality of some cells. We consider that $A$ varies between $2^4$ and $2^8$, and we usually use the value $A = 2^8$. The progenitor compartment duration $\tau_p$ is chosen by considering that progenitors need about four divisions to differentiate into precursor cells. Therefore we choose $\tau_p =$ 4 days.

The apoptosis rate $\beta(E)$ is chosen as a Michaelis–Menten function,

$$\beta(E) = \beta_\infty \frac{E^n}{E^n + \overline{\beta}^n}.$$

The parameter $n$ describes the sensitivity of the apoptosis rate, $\beta_\infty$ is the maximum apoptosis rate, and $\overline{\beta}$ the value of erythrocyte density for which the apoptosis rate attains half of its maximum.

The shape of the apoptosis rate function can be deduced from Chappell et al. (1997), where the viability dose response of cells to EPO is presented, and Sakata et al. (1985), where the relation between EPO concentration and mature erythrocytes density (via hemoglobin concentration) is described. This led to the Michaelis–Menten function given above to describe the implicit dependence of apoptosis on mature erythrocytes. It can be noted that, to our knowledge, only one work (Adimy and Crauste, 2007) considered an erythropoiesis model with a feedback control of apoptosis, but the feedback function was different, since EPO concentration was explicitly incorporated in the model, which is not the case in the present study.

All the coefficients of the apoptosis function $\beta$ are rather difficult to estimate. Usually, apoptosis in mice varies between 2% and 50%. So we could be tempted to take $\beta_\infty$ equals to 0.5. However, since $\beta_\infty$ represents the maximum apoptosis rate, and since it is a limit value in the function $\beta(E)$, we could also take $\beta_\infty = 1$. It is difficult to choose a good value for $\overline{\beta}$. Since the maximum apoptosis rate is not exactly known, it is not easy to determine the value for which half of this maximum is reached. We decided to fix $\overline{\beta}$ in the range of the erythrocyte density level at equilibrium, that is between $10^7$ and $10^9$ cells $g^{-1}$. In our simulations, we choose $\beta_\infty = 1$, which allows strong cell mortality by apoptosis, and $\overline{\beta} = 10^7$ and $10^8$ cells $g^{-1}$. Finally the value of the sensitivity parameter $n$ has almost no influence, as soon as it is large enough. In the simulations, we choose $n = 8$.

With values indicated in the second column of Table 1, we simulate Eq. (6) and the corresponding hematocrit, for the initial condition given by (15), and for $\overline{\beta} = 10^7$ and $10^8$ cells $g^{-1}$. This is displayed in Fig. 4.

First note that when $\overline{\beta} = 10^8$ cells $g^{-1}$, the simulation gives very bad results, the curve does not fit experimental data at all, although this value of $\overline{\beta}$ would have been close to a realistic value. In fact, from (9) we know that the steady state $E^*$ of the erythrocyte density verifies $E^* < AK/\gamma$. With values in Table 1, the quantity $AK/\gamma$ equals $1.024 \times 10^8$ cells $g^{-1}$. Consequently, the erythrocyte density steady state $E^*$ is almost always strictly less than $\overline{\beta} = 10^8$ cells $g^{-1}$ (in fact as soon as $\tau_p > 0.05$ days, and more precisely for $\tau_p = 4$ days, $E^* = 7.39 \times 10^7$ cells $g^{-1}$), and progenitor apoptosis is thus strictly less than 50%. We are then in the presence of a slow behavior, the hematocrit reaching very slowly and smoothly its equilibrium value.

When $\overline{\beta} = 10^7$ cells $g^{-1}$, it appears that the hematocrit rapidly increases, as observed in experiments, but it does not reach very large values (the observed peak is about 52%, which does not belong to the acceptable range of values, determined by the standard deviation lines), and then the hematocrit smoothly reaches the steady state with no damped oscillations. Moreover, it is noticeable that the simulated peak occurs 6 days after the lowest hematocrit, whereas it occurs after 4–5 days in experiments. One can notice that the steady state of Eq. (6) equals, in this case, $1.03 \times 10^7$ cells $g^{-1}$, which is a rather low value (erythrocyte

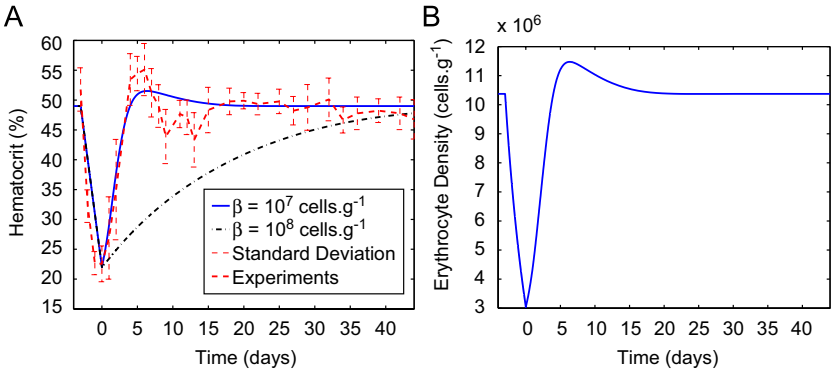


Fig. 4. Evolution of hematocrit over 44 days (Panel A), with values given in Table 1. The solid line corresponds to the simulation of Eq. (6) for $\overline{\beta} = 10^7$ cells g$^{-1}$, the dash-dotted one to the simulation of Eq. (6) for $\overline{\beta} = 10^8$ cells g$^{-1}$, and the dashed one to experimental results (average hematocrit, Fig. 1.A). Panel B: The solution $E(t)$ of Eq. (6) corresponding to the simulated hematocrit represented in A for $\overline{\beta} = 10^7$ cells g$^{-1}$. One can observe that the erythrocyte density converges quickly to the equilibrium $E^* = 1.03 \times 10^7$ cells g$^{-1}$. In both figures, simulations start at time $t = 0$, and initial conditions are drawn for $t<0$, as given in (15).

density in mice is usually considered to range between $10^8$ and $3 \times 10^8$ cells g$^{-1}$). Due to (9) and the above remark, we know that the steady state $E^*$ of the erythrocyte density cannot be very large in this model without self-renewal and, furthermore, with values in Table 1 it is less than $1.024 \times 10^8$ cells g$^{-1}$. Consequently, with this model, the estimated value of the erythrocyte density cannot be really biologically relevant since it will always be strictly less than $10^8$ cells g$^{-1}$.

In Fig. 5, we have shown the solution $E(t)$ of Eq. (6), that is the erythrocyte evolution over time, when the Hopf bifurcation described by Proposition 1 occurs. The steady state is unstable in this case, which means that solutions of (6) oscillate about it. The steady state, at the bifurcation, equals $8.27 \times 10^6$ cells g$^{-1}$, which is still rather low. The erythrocyte density exhibits very long periods, of the order of 26 days.

One can also note that the Hopf bifurcation occurs for a large value of $\tau_p$, so there is no hope to obtain damped oscillations for small—and so biologically relevant—values of $\tau_p$. Thus it appeared to us that using apoptosis control as the only regulator of erythropoiesis results in a modelling unable to reasonably account for reality.

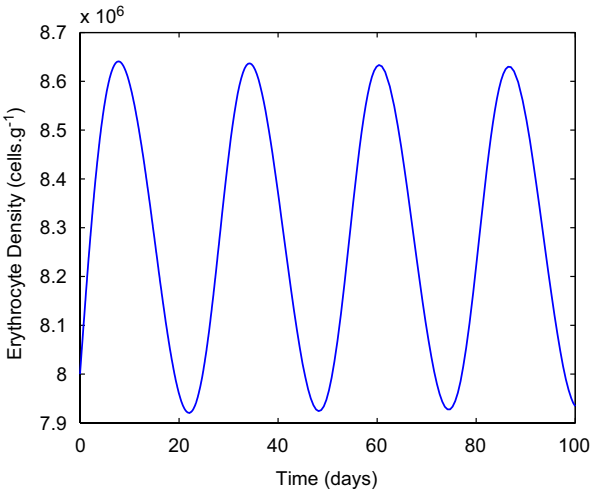


Fig. 5. The solution $E(t)$ of Eq. (6) when the Hopf bifurcation occurs, that is all parameters are given in Table 1 except $\tau_p = 14$ days. The erythrocyte number periodically oscillates with a period of about 26 days.

## 6. Influence of self-renewal

We now return to the analysis of system (4), that is we take progenitor self-renewal in erythropoiesis into consideration. Since glucocorticoids negatively mediate self-renewal, we choose the rate of self-renewal $\sigma$ as a Hill function, that is a smooth decreasing function of the erythrocyte density $E$,

$$\sigma(E) = \sigma_0 \frac{\overline{\sigma}^m}{\overline{\sigma}^m + E^m}, \tag{16}$$

with $\sigma_0 > 0$ the maximum self-renewal rate, $\overline{\sigma} > 0$ the threshold value for which $\sigma$ reaches half of its maximum value, and $m > 0$ the sensitivity of the self-renewal rate.

It can be noticed that no data are available in the literature to determine the shape of the self-renewal function (even though one would like to make this rate directly dependent on glucocorticoid concentrations). Hence, we chose to model it with a Hill function for one main reason. This kind of function is usually used in modelling kinase cascades reactions (Ferrell, 1996,1997), these latter being hidden behind our modelling approach. Hill functions have been used several times to model negative feedbacks at the stem cell level (Mackey, 1978; Pujo-Menjouet and Mackey, 2004). As explained below, coefficients of the self-renewal function (16) are then determined by trying to obtain the best fitting with experimental data.

A theoretical analysis of system (4) would be rather difficult and remains an open question, due to the presence

of multiple delays and nonlinearities. Hence, we focus our study on a numerical analysis of (4), trying to fit the data in Fig. 1.

Our first comment deals with parameters values used in the simulations of Eq. (6). As mentioned in the previous section, in order to finely fit experimental data, we sometimes chose unrealistic values of some parameters for the simulations of the model without self-renewal. For example, the value of $\overline{\beta}$ can be considered too small, when $\overline{\beta} = 10^7$ cells g$^{-1}$, in comparison with the expected value of the erythrocyte steady state $E^*$ (about $10^8$ cells g$^{-1}$). One consequence was then an underestimation of the value of $E^*$ in the model without self-renewal.

Consequently, we try here to adjust values of the parameters to experimentally known data of erythropoiesis. In particular (see Table 1), we only consider $\overline{\beta} = 10^8$ cells g$^{-1}$.

All values we use in numerical simulations of system (4) are listed in Table 1, second column. In particular, we assume progenitors self-renew within one day (so $\tau_c = 1$ day). Values of coefficients that appear in the model without self-renewal are not modified, so we refer the reader to the previous section for our choices. Let us then focus ourselves on the values of the self-renewal rate.

Let us assume a maximum self-renewal rate of about 0.5 d$^{-1}$. This may seem small in comparison with the maximum apoptosis rate. Yet numerical simulations indicate that larger rates lead to overproduction of erythrocytes, self-renewal being more powerful than apoptosis in this case (this is not shown here). To maintain some balance between apoptosis and self-renewal, the value of $\overline{\sigma}$ must be chosen larger than $\overline{\beta}$. Note that this balance seems to be necessary because if one of the two controls was always more important than the other, then this latter would be useless in the model. We have observed in the last section that taking only apoptosis into account as a control for erythropoiesis gave not satisfactory results. The same conclusions occur if self-renewal is the only control. It seems that this condition adjusts, in some sense, the fact that the maximum apoptosis rate $\beta_\infty$ is larger than the maximum self-renewal rate $\sigma_0$. So we choose $\overline{\sigma} = 10^9$ cells g$^{-1}$. The sensitivity $m$ of the self-renewal rate (16) is set to be $m = 5$. Similarly to the sensitivity of the apoptosis rate, it has almost no influence as soon as it is large enough.

Numerical simulations of system (4) with values indicated in Table 1 are displayed in Fig. 6. One can observe that the simulated curve does not exactly fit the experimental curve in Fig. 1A even though it exhibits more interesting features than the simulations in Fig. 4. In particular, there is a rapid increase of the hematocrit, following anemia, that reaches a peak (with a rather overestimated value about 57%, even though it could be acceptable), and then the hematocrit oscillates about the steady hematocrit, with damped oscillations, in contrast to the case without self-renewal where oscillations were not observed. Yet, periods of the oscillations are too large (about 30 days) and do not fit experimental data.

Adding progenitor self-renewal in our erythropoiesis modelling seems to affect the erythrocyte density evolution over time, but not in a sufficiently realistic way: the model does not give a correct answer of the hematocrit to a severe anemia, even though it exhibits interesting properties.

However, when increasing erythrocyte mortality rate $\gamma$, one can obtain a much more realistic simulation (see Fig. 7). The value of $\gamma$ used in previous simulations describes an average lifetime of 40 days in mice. Yet this value must be understood as a normal mortality rate, that is in normal circumstances. Since we simulate a severe anemia, it is not realistic to keep the same value for the mortality of erythrocytes. Indeed, the anemia is obtained by injecting mice with phenylhydrazine and one effect of this substance is to dramatically alter the lifespan of erythrocytes (see Shimada, 1975 for a study on chicken's erythrocytes lifespan under induced anemia). One can see that the simulation of model (4) gives better results when changes in

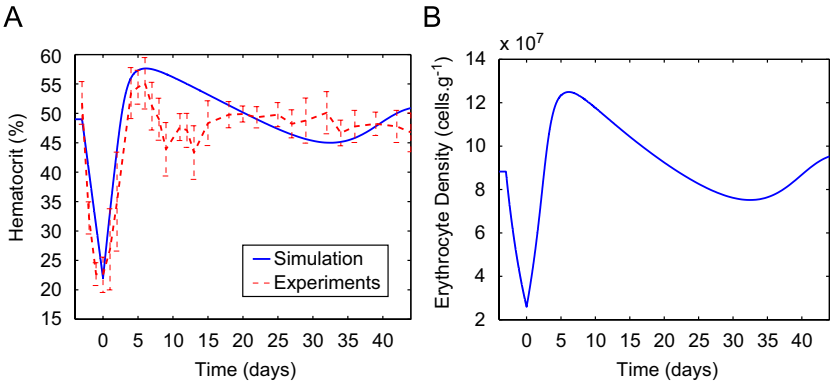


Fig. 6. Evolution of hematocrit over 44 days (Panel A), with values given in Table 1. The solid line corresponds to the simulation of the erythrocyte equation in system (4), and the dashed one to experimental results. Panel B: The solution $E(t)$ of system (4) corresponding to the simulated hematocrit represented in A. One can observe that the erythrocyte density oscillates about its equilibrium $E^* = 8.83 \times 10^7$ cells g$^{-1}$. In both figures, simulations start at time $t = 0$, and initial conditions are drawn for $t < 0$, as given in (15).

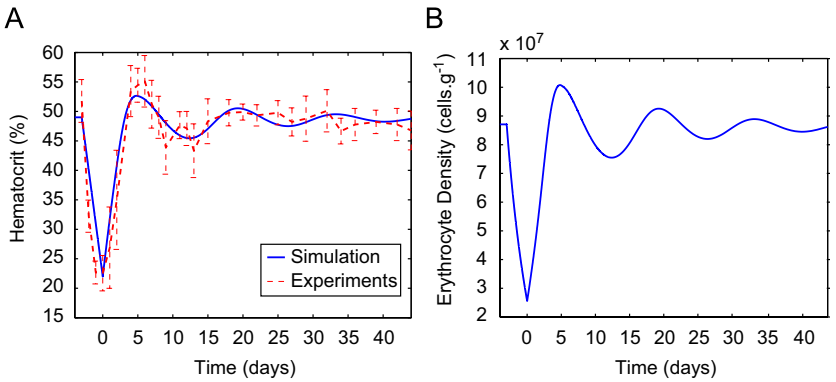


Fig. 7. Evolution of hematocrit over 44 days (Panel A), with values given in Table 1, except $\gamma = 0.15\,\mathrm{d}^{-1}$. The solid line corresponds to the simulation of the erythrocyte equation in system (4), and the dashed one to experimental results (Fig. 1.A). Panel B: The solution $E(t)$ of system (4) corresponding to the simulated hematocrit represented in A. One can observe that the erythrocyte density oscillates about its equilibrium $E^* = 8.7 \times 10^7\,\mathrm{cells\,g}^{-1}$. In both figures, simulations start at time $t = 0$, and initial conditions are drawn for $t < 0$, as given in (15).

erythrocytes mortality are taken into account. Moreover, the steady state value $E^*$ of the erythrocytes is in this case about $8.7 \times 10^7\,\mathrm{cells\,g}^{-1}$, which is a reasonable value.

One may object that the increase of the mortality rate $\gamma$ could allow to obtain better results than the ones presented in Section 5.3 when simulating the model (6). However, and even though simulations are not shown here, this does not improve the model without self-renewal (data not shown). When the threshold value $\overline{\beta}$ equals $10^8\,\mathrm{cells\,g}^{-1}$, simulations do not differ from the one in Fig. 4, and the steady state value $E^*$ is too small, $E^* = 1.7 \times 10^7\,\mathrm{cells\,g}^{-1}$. For $\overline{\beta} = 10^7\,\mathrm{cells\,g}^{-1}$, the simulated curve better fits experimental data (damped oscillations are observed, but with small amplitudes, and the simulated curve does not reach the experimental peak), but values of the erythrocyte density become even less realistic, with a steady state value $E^*$ about $8.3 \times 10^6\,\mathrm{cells\,g}^{-1}$.

One can note that the progenitor dynamics in erythropoiesis process have not really been investigated in this study, mainly because we focused on data related to the hematocrit. However, when simulating the erythrocyte density in system (4), or (5)–(6), one can compute as well the progenitor density. This is done in Fig. 8, for both cases with and without self-renewal. It appears that the equilibrium value of the progenitor density is larger under the action of self-renewal (about $1.1 \times 10^6\,\mathrm{cells\,g}^{-1}$ versus $1.6 \times 10^4\,\mathrm{cells\,g}^{-1}$ when there is no self-renewal), and progenitor population dynamics are more complex in this case, because of the action of a negative and a positive feedback. This might provide a way to further investigate the role of progenitor self-renewal.

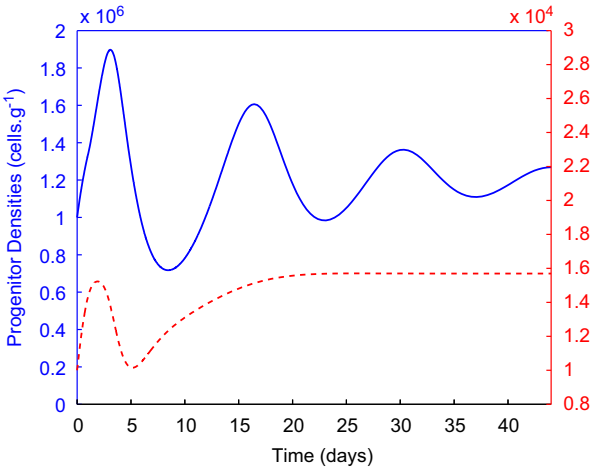


Fig. 8. Progenitors densities. The solid line is the progenitor density associated with the erythrocyte density in Fig. 7.B, that is in the model taking progenitor self-renewal into account, whereas the dashed line describes the evolution of progenitors without self-renewal (this population is associated with the erythrocyte density in Fig. 4.B). The scale of the solid line is set on the left vertical axis, and the scale of the dashed line on the right vertical axis. In particular, the equilibrium value of the progenitor density when self-renewal is incorporated in the model is about $1.1 \times 10^6\,\mathrm{cells\,g}^{-1}$, and about $1.6 \times 10^4\,\mathrm{cells\,g}^{-1}$ when there is no self-renewal.

## 7. Discussion

Based on recent advances in red blood cell research, we proposed a new mathematical model of erythropoiesis that takes into account up-to-date knowledge on red blood cells production—this means inhibition of apoptosis by EPO (Koury and Bondurant, 1990), and existence of erythroid progenitor self-renewal (Bauer et al., 1999; Gandrillon et al., 1999; Pain et al., 1991)—acquired at the cellular and molecular level these last few years.

Although hematopoietic stem cell dynamics are not considered in our study, the model incorporates two feedback loops, a negative glucocorticoid-mediated feedback of erythrocytes on progenitor self-renewal, and a positive EPO-mediated feedback on progenitor apoptosis. Even though this rendered the theoretical analysis of the complete model somewhat difficult, this proved to be

critical for obtaining a model that closely matches experimental data.

Moreover, as similarly done by Loeffler and Wichmann (1980), Wichmann and Loeffler (1985), Wichmann et al. (1985), or by Mackey (1978, 1979, 1997), Pujo-Menjouet and Mackey (2004), the model has been confronted to experimentally-obtained values in a non-equilibrium condition, that is here an experimentally induced severe anemia. We reasoned that our model should be able to model not only steady state but also stress erythropoiesis. This was especially needed since the role of glucocorticoids in mice has precisely been demonstrated to be critical for stress erythropoiesis (Bauer et al., 1999).

Although we could not derive all parameters values from the literature, we nevertheless were very careful to use only values that were within a biologically reasonable range. The fact that some variants of our model produced unreasonable quantitative values was clearly for us the sign that the modelling was not heading in the right direction. We tried to keep the number of parameters as small as possible, so that we could explore their influence on the results of the numerical situations.

Using this modelling strategy we could demonstrate that numerical simulations of the complete model, incorporating both a negative feedback of erythrocytes on progenitor self-renewal and a positive feedback on progenitor apoptosis, exhibited good results, the main characteristics of experimental data being well fitted by the model (see Section 6). These results tend to indicate that a correct modelling of erythropoiesis needs a clear understanding of the feedback mechanisms, in particular those that control progenitor populations (such as self-renewal).

The importance of a dynamically regulated and self-renewing stem cell population in hematopoiesis is self-evident as shown in numerous models, including Loeffler et al. (1989), Wichmann and Loeffler (1985), and Bernard et al. (2004) or Colijn and Mackey (2005a,b). Yet, we decided to deliberately omit this dynamical component in our model, essentially due to our ignorance of the precise molecular controls that could be involved in feedback controls of HSC populations, and of the cells from which the feedback could originate from (erythrocytes, or premature erythrocytes, could control HSC dynamics, among many other controls). On the contrary, molecular process controlling feedbacks on erythroid progenitors are rather well known, and this directed the modelling part of this work, allowing to go deeper in the analysis by investigating these molecular process and their precise roles in erythropoiesis. We are nevertheless aware that the experimental results we obtained might have been correctly modelled by a different model in which the self-renewing ability of hematopoietic stem cells would have been taken into account.

Note that this model makes two testable predictions:

(1) The first deals with the lifespan of mature cells. In order to get a perfect fitting we had to consider that the value of $\gamma$ had to be severely reduced in the wake of phenylhydrazine injection. Since phenylhydrazine dramatically reduces the lifespan of erythrocytes, this might not seem to be far stretched. Nevertheless, this value can return to normal (1/40 per day) only after numerous days to capture the fading oscillations characteristic of our data. It would therefore be of great interest to measure the lifespan of the neosynthesized erythrocytes, after recovery and the following days. A reduction of lifespan can be predicted, since a study in a different species demonstrated that the red cells resulting from phenylhydrazine-induced anemia had a shorter life-span when compared to normal red cells (Berlin and Lotz, 1951, Nagai et al., 1968, 1971, Shimada, 1975, Stohlman, 1961). Such a change in life span could be due to specific membrane properties of the erythrocytes produced during stress erythropoiesis (Walter et al., 1975). In any case, this prediction could be tested in mice.
(2) The second type of predictions that can be made on the basis of our modelling is the behavior of the progenitor populations. Not only the absolute amount but also the oscillating behavior was quite different between the two versions of the model. Measuring the amount of progenitors of phenylhydrazine-treated mice could therefore confirm or not the necessity to incorporate erythroid progenitor self-renewal, and also lead to refinements of this model.

At least four perspectives from the modelling point of view can be drawn. We could first try to see up to which extent we could use the same model with different parameters values for modelling the appearance of erythroleukemia. It has for example been shown that an autocrine EPO production occurred in human erythroleukemia (Mitjavila et al., 1991). In our model this can be modelled quite simply by modifying the value of $\beta$. One could also try to analyze the influence of the self-renewal ability of our cells by modifying the value of $\sigma$. Reducing the amount of progenitors committing in a differentiation process, in order to model for example the effect of v-erbA oncogene on the differentiation process (Gandrillon, 2002), would require modifications of the model.

A second perspective of this work would be to dissect the feedback loops so as to incorporate explicitly important molecules like EPO receptors, signaling molecules and target genes. This would require a specific effort in multi-scale modelling. Thus a richer and more detailed model could be obtained without any loss in our modelling strategy, that is a model in which each parameter has a biological relevance, and in which the effect of each parameter on the blood cell population dynamics can be investigated.

It is obviously tempting to extend the model to more than one hematopoietic lineage. In order to keep the control of the model's behavior, one should start by modelling relatively simple lineage decisions. The lineage

choice between erythrocytic and megakaryocytic fate of a bipotent progenitor, thought to involve cross-antagonism between transcription factors (Starck et al., 2003), could represent an interesting step in this direction.

Finally, our model is a system of age-structured equations, and does not incorporate an explicit maturity-structured variable, that would describe cell differentiation. Hence, differentiation in this model is artificially introduced as an amplification parameter $A$, assumed to incorporate several divisions of progenitors. This leads to a limitation in the model, since progenitor self-renewal and differentiation processes are separated (first progenitor self-renew, and then they differentiate), although this decision is made at the single cell level. A way of considering differentiation explicitly is to add a discrete maturity variable (as it can be found in Adimy et al. (2007) and Bernard et al. (2003b)). This would lead to a system of several differential equations, each of them describing the dynamics of progenitors for a given maturity level. This could also bring more information on the dynamics of erythroid progenitors.

Altogether, our modelling scheme allowed us to design a model that fits experimental data well, allowing to make testable predictions, and that can be extended toward more hematopoietic lineages, in order to model, in the long run, a complete hematopoietic system. The success of our model was strictly dependent upon recent advances in our cellular and molecular understanding of red cell differentiation, and therefore its extension might require new advances, notably in the still open question of the feedback operating at the stem cell level by mature hematopoietic cells.

**Acknowledgements**

Authors are grateful to the anonymous referees for their helpful comments and suggestions that improved the revised version of this work. They also thank Prof. Michael C. Mackey for his comments and suggestions. We would like to thank all members of the BSMC group (http://bsmc.insa-lyon.fr) for stimulating discussions, Emmanuel Risler for his participation in early stages of this project, and Vitaly Volpert for his constant support during the shaping of the model. The work in Olivier Gandrillon's laboratory is supported by the Ligue contre le Cancer (Comité Départemental du Rhône), the UCBL, the CNRS, the Région Rhône Alpes and the Association pour la Recherche contre le Cancer (ARC). We are indebted to Edmund Derrington (CGMC UMR 5534) for his critical and thoughtful reading of the manuscript.

## Appendix A. Method of the characteristics

We develop the method of the characteristics that allows us to express $p_{sr}(t,\tau_c)$ and $p(t,\tau_p)$ in terms of $P$ and $E$, and then to give a clear expression of system (3).

Equations of the characteristics for system (1) are given by

$$\frac{da}{dt}=1,$$

from which we deduce $a(t)=t+a_0$, for $t\geqslant t_0=\max\{0,-a_0\}$. Then, setting

$$x(t)=p_{sr}(t,t+a_0),$$

we obtain from the second equation of (1)

$$\frac{dx}{dt}=-\beta(E(t))x(t).$$

Thus

$$x(t)=x(t_0)\exp\left(-\int_{t_0}^{t}\beta(E(s))\,ds\right).$$

If $t_0=0$, then

$$x(t)=x(0)\exp\left(-\int_{0}^{t}\beta(E(s))\,ds\right),$$

that is

$$p_{sr}(t,a)=p_{sr}(0,a-t)\exp\left(-\int_{0}^{t}\beta(E(s))\,ds\right)$$

if $t<a$,

and if $t_0=-a_0=t-a$, then

$$x(t)=x(t-a)\exp\left(-\int_{t-a}^{t}\beta(E(s))\,ds\right),$$

that is

$$p_{sr}(t,a)=p_{sr}(t-a,0)\exp\left(-\int_{t-a}^{t}\beta(E(s))\,ds\right)$$

if $a<t$.

In particular, we deduce, with (2), that

$$p_{sr}(t,\tau_c)=\sigma(E(t-\tau_c))P(t-\tau_c)\times\exp\left(-\int_{t-\tau_c}^{t}\beta(E(s))\,ds\right)\quad\text{for }\tau_c<t. \tag{A.1}$$

Similarly, we can obtain

$$p(t,a)=\begin{cases}p(t-a,0)\exp\left(-\int_{t-a}^{t}(\beta(E(s))+\sigma(E(s)))\,ds\right) & \text{if } a<t,\\ p(0,a-t)\exp\left(-\int_{0}^{t}(\beta(E(s))+\sigma(E(s)))\,ds\right) & \text{if } t<a,\end{cases}$$

so, from (2), for $a<t$,

$$p(t,a)=[K+2p_{sr}(t-a,\tau_c)]\times\exp\left(-\int_{t-a}^{t}(\beta(E(s))+\sigma(E(s)))\,ds\right).$$

It follows that, for $t>\tau_c$,

$$p(t,\tau_p)=[K+2p_{sr}(t-\tau_p,\tau_c)]\times\exp\left(-\int_{t-\tau_p}^{t}(\beta(E(s))+\sigma(E(s)))\,ds\right),$$

and for $t>\tau_p+\tau_c$, using (A.1) we obtain

$$p(t,\tau_p)=\left[K+2\sigma(E(t-\tau_p-\tau_c))P(t-\tau_p-\tau_c)\times\exp\left(-\int_{t-\tau_p-\tau_c}^{t-\tau_p}\beta(E(s))\,\mathrm{d}s\right)\right]\times\exp\left(-\int_{t-\tau_p}^{t}(\beta(E(s))+\sigma(E(s)))\,\mathrm{d}s\right). \quad (A.2)$$

Hence, with expressions (A.1) and (A.2), we can write system (3), for $t>\tau_p+\tau_c$,

$$\begin{aligned}\frac{\mathrm{d}P}{\mathrm{d}t}(t)=&-[\beta(E(t))+\sigma(E(t))]P(t)\\&+K+2\sigma(E(t-\tau_c))P(t-\tau_c)\\&\times\exp\left(-\int_{t-\tau_c}^{t}\beta(E(s))\,\mathrm{d}s\right)\\&-\left[K+2\sigma(E(t-\tau_p-\tau_c))P(t-\tau_p-\tau_c)\right.\\&\left.\times\exp\left(-\int_{t-\tau_p-\tau_c}^{t-\tau_p}\beta(E(s))\,\mathrm{d}s\right)\right]\\&\times\exp\left(-\int_{t-\tau_p}^{t}(\beta(E(s))+\sigma(E(s)))\,\mathrm{d}s\right),\\\frac{\mathrm{d}P_{sr}}{\mathrm{d}t}(t)=&-\beta(E(t))P_{sr}(t)+\sigma(E(t))P(t),\\&-\sigma(E(t-\tau_c))P(t-\tau_c)\\&\times\exp\left(-\int_{t-\tau_c}^{t}\beta(E(s))\,\mathrm{d}s\right),\\\frac{\mathrm{d}E}{\mathrm{d}t}(t)=&-\gamma E(t)+A\exp\left(-\int_{t-\tau_p}^{t}(\beta(E(s))+\sigma(E(s)))\,\mathrm{d}s\right)\\&+\left[K+2\sigma(E(t-\tau_p-\tau_c))P(t-\tau_p-\tau_c)\right.\\&\left.\times\exp\left(-\int_{t-\tau_p-\tau_c}^{t-\tau_p}\beta(E(s))\,\mathrm{d}s\right)\right]. \quad (A.3)\end{aligned}$$

One can easily check that the first and third equations in (A.3) do not depend on $P_{sr}$, so we omit the second equation in our study, and we focus on system (4).

## Appendix B. Properties of complex eigenvalues

Let us study the existence and properties of purely imaginary roots of Eq. (12), in order to determine the local asymptotic stability of the unique steady state $(P^*,E^*)$ of (5)–(6).

Let first check that $\lambda=0$ is not an eigenvalue of (10). Indeed, if $\lambda=0$ is an eigenvalue of (10), then from (12), we obtain

$$\gamma+\xi\tau_p=0,$$

which is impossible since $\gamma,\xi>0$ and $\tau_p\geqslant 0$.

Consequently, we can compute the integral in (12) and one can see that (12) is equivalent to

$$\lambda^2+\gamma\lambda+\xi-\xi\,\mathrm{e}^{-\lambda\tau_p}=0 \quad \text{and} \quad \lambda\neq 0.$$

Then we focus on the study of complex roots of (13).

### B.1. The case $\tau_p=0$

We first check that all roots of (13) have negative real parts when $\tau_p=0$, that is $E^*$ is locally asymptotically stable in this case.

If $\tau_p=0$, Eq. (13) reduces to

$$\lambda^2+\gamma\lambda=0,$$

that is

$$\lambda(\lambda+\gamma)=0.$$

Since $\lambda=0$ is not a characteristic root of (10), we deduce that $\lambda=-\gamma<0$ is the only characteristic root, and since it is negative, we conclude to the local asymptotic stability of $E^*$ when $\tau_p=0$.

### B.2. Existence of purely imaginary eigenvalues

Assume $\tau_p>0$, and search for eigenvalues $\lambda=\mathrm{i}\omega$, with $\omega\in\mathbb{R}$. Then separating real and imaginary parts in (13), we obtain

$$\cos(\omega\tau_p)=1-\frac{\omega^2}{\xi}, \quad (B.1)$$

$$\sin(\omega\tau_p)=-\frac{\gamma}{\xi}\omega. \quad (B.2)$$

First note that if $\omega$ satisfies (B.1)–(B.2), then so does $-\omega$. Moreover, since $\lambda=0$ is not an eigenvalue of (10), we only focus on the existence of $\omega>0$ satisfying (B.1)–(B.2).

By summing the squares of both sides of (B.1)–(B.2), we obtain

$$\frac{\omega^2}{\xi^2}[\omega^2+\gamma^2-2\xi]=0.$$

Since we look for solutions $\omega>0$, this is equivalent to

$$\omega^2=2\xi-\gamma^2.$$

If $2\xi\leqslant\gamma^2$, then (10) has no purely imaginary characteristic roots, and so the stability of the steady state $E^*$ cannot change. Since it is locally asymptotically stable when $\tau_p=0$, then it is locally asymptotically stable for $\tau_p\geqslant 0$ under condition $2\xi\leqslant\gamma^2$.

Now, let study the case $2\xi>\gamma^2$. From (11), this condition is equivalent to

$$E^*\beta'(E^*)>\frac{\gamma}{2}.$$

Under this condition, if (10) has purely imaginary roots $\pm\mathrm{i}\omega$, then $\omega=\sqrt{2\xi-\gamma^2}$. Therefore, from (B.1),

we deduce that

$$\cos\left(\tau_p\sqrt{2\xi-\gamma^2}\right)=\frac{\gamma^2}{\xi}-1,$$

that is

$$\tau_p=\frac{\arccos\left(\dfrac{\gamma^2}{\xi}-1\right)}{\sqrt{2\xi-\gamma^2}}.$$

Consequently, for $\tau_p=\tau_p^*:=\arccos(\gamma^2/\xi-1)/\sqrt{2\xi-\gamma^2}$, (10) has purely imaginary roots $\pm i\omega$, with $\omega=\sqrt{2\xi-\gamma^2}$.

### *B.3. Properties of purely imaginary roots*

Let us show that purely imaginary roots $\pm i\omega^*:=\pm i\sqrt{2\xi-\gamma^2}$ of (10) that exist when $\tau_p=\tau_p^*$ are simple and satisfy the so-called *transversality condition*, that is

$$\frac{d\mathrm{Re}(\lambda(\tau_p^*))}{d\tau_p}>0.$$

Let consider a branch of eigenvalues $\lambda(\tau_p)$ of (13) such that

$$\lambda(\tau_p^*)=i\omega^*.$$

Then, from (13), it follows that

$$\lambda(\tau_p)^2+\gamma\lambda(\tau_p)+\xi-\xi e^{-\lambda(\tau_p)\tau_p}=0.$$

By differentiating the above equation with respect to $\tau_p$, we obtain

$$[2\lambda(\tau_p)+\gamma+\xi\tau_p e^{-\lambda(\tau_p)\tau_p}]\frac{d\lambda}{d\tau_p}(\tau_p)+\xi\lambda(\tau_p)e^{-\lambda(\tau_p)\tau_p}=0. \tag{B.3}$$

By contradiction, assume $d\lambda(\tau_p^*)/d\tau_p=0$. Then from (B.3)

$$\xi i\omega^* e^{-i\omega^*\tau_p^*}=0,$$

that is, since $\xi>0$,

$$\omega^*\cos(\omega^*\tau_p^*)=0 \quad \text{and} \quad \omega^*\sin(\omega^*\tau_p^*)=0.$$

Since $\omega^*>0$, we deduce

$$\cos(\omega^*\tau_p^*)=0 \quad \text{and} \quad \sin(\omega^*\tau_p^*)=0,$$

which is equivalent, from (B.1)–(B.2), to

$$(\omega^*)^2=\xi>0 \quad \text{and} \quad \omega^*=0,$$

which is impossible. We conclude that $d\lambda(\tau_p^*)/d\tau_p\neq 0$ and $\pm i\omega^*$ are simple eigenvalues.

Moreover, from (13) and (B.3),

$$\begin{aligned}\left(\frac{d\lambda}{d\tau_p}(\tau_p^*)\right)^{-1}&=\frac{2\lambda(\tau_p^*)+\gamma+\xi\tau_p^* e^{-\lambda(\tau_p^*)\tau_p^*}}{-\xi\lambda(\tau_p^*)e^{-\lambda(\tau_p^*)\tau_p^*}}\\&=\frac{2\lambda(\tau_p^*)+\gamma}{-\xi\lambda(\tau_p^*)e^{-\lambda(\tau_p^*)\tau_p^*}}-\frac{\tau_p^*}{\lambda(\tau_p^*)}\\&=\frac{2i\omega^*+\gamma}{-i\omega^*[(i\omega^*)^2+\gamma(i\omega^*)+\xi]}-\frac{\tau_p^*}{i\omega^*}\\&=\frac{2i\omega^*+\gamma}{-i\omega^*[\xi-(\omega^*)^2+i\gamma\omega^*]}+i\frac{\tau_p^*}{\omega^*}.\end{aligned}$$

We deduce

$$\begin{aligned}&\left(\frac{d\lambda}{d\tau_p}(\tau_p^*)\right)^{-1}\\&=\frac{2i\omega^*+\gamma}{\gamma(\omega^*)^2+i\omega^*[(\omega^*)^2-\xi]}+i\frac{\tau_p^*}{\omega^*}\\&=\frac{\gamma^2(\omega^*)^2-2(\omega^*)^2[\xi-(\omega^*)^2]+i\gamma\omega^*[\xi+2\omega^*-(\omega^*)^2]}{\gamma^2(\omega^*)^4+(\omega^*)^2[(\omega^*)^2-\xi]^2}\\&\quad+i\frac{\tau_p^*}{\omega^*}.\end{aligned}$$

Consequently

$$\begin{aligned}\mathrm{Re}\left(\frac{d\lambda}{d\tau_p}(\tau_p^*)\right)^{-1}&=\frac{\gamma^2(\omega^*)^2-2(\omega^*)^2[\xi-(\omega^*)^2]}{\gamma^2(\omega^*)^4+(\omega^*)^2[(\omega^*)^2-\xi]^2}\\&=\frac{\gamma^2-2\xi+2(\omega^*)^2}{\gamma^2(\omega^*)^2+[(\omega^*)^2-\xi]^2}\\&=\frac{\gamma^2-2\xi+2(2\xi-\gamma^2)}{\gamma^2(2\xi-\gamma^2)+[2\xi-\gamma^2-\xi]^2}\\&=\frac{2\xi-\gamma^2}{\xi^2}.\end{aligned}$$

We conclude that

$$\mathrm{Re}\left(\frac{d\lambda}{d\tau_p}(\tau_p^*)\right)^{-1}=\frac{2\xi-\gamma^2}{\xi^2}>0.$$

## References


Ackleh, A.S., Banks, H.T., Deng, K., 2002. A finite difference approximation for a coupled system of nonlinear size-structured population. Nonlinear Anal. 50, 727–748.

Ackleh, A.S., Deng, K., Ito, K., Thibodeaux, J., 2006. A structured erythropoiesis model with nonlinear cell maturation velocity and hormone decay rate. Math. Biosci. 204, 21–48.

Adimy, M., Crauste, F., 2003. Global stability of a partial differential equation with distributed delay due to cellular replication. Nonlinear Anal. 54 (8), 1469–1491.

Adimy, M., Crauste, F., 2007. Modelling and asymptotic stability of a growth factor-dependent stem cells dynamics model with distributed delay. Discrete Continuous Dynamical Syst. Ser. B 8 (1), 19–38.

Adimy, M., Crauste, F., Pujo-Menjouet, L., 2005a. On the stability of a maturity structured model of cellular proliferation. Discrete Continuous Dynamical Syst. Ser. A 12 (3), 501–522.

Adimy, M., Crauste, F., Ruan, S., 2005b. A mathematical study of the hematopoiesis process with applications to chronic myelogenous leukemia. SIAM J. Appl. Math. 65 (4), 1328–1352.

Adimy, M., Crauste, F., Ruan, S., 2006a. Modelling hematopoiesis mediated by growth factors with applications to periodic hematological diseases. Bull. Math. Biol. 68 (8), 2321–2351.

Adimy, M., Crauste, F., Ruan, S., 2006b. Periodic oscillations in leukopoiesis models with two delays. J. Theor. Biol. 242, 288–299.

Adimy, M., Crauste, F., El Abdllaoui, A., 2007. Asymptotic behavior of a discrete maturity structured system of hematopoietic stem cells dynamics with several delays. Math. Modelling Nat. Phenom. 1 (2).

Adimy, M., Pujo-Menjouet, L., 2003. Asymptotic behaviour of a singular transport equation modelling cell division. Discrete Continuous Dynamical Syst. Ser. B 3, 439–456.

Banks, H.T., Cole, C.E., Schlosser, P.M., Hien, T., 2004. Modelling and optimal regulation of erythropoiesis subject to benzene intoxication. Math. Biol. Eng. 1 (1), 15–48.

Bauer, A., Tronche, F., Wessely, O., Kellendonk, C., Reichardt, H.M., Steinlein, P., Schutz, G., Beug, H., 1999. The glucocorticoid receptor is required for stress erythropoiesis. Genes Dev. 13, 2996–3002.

Bélair, J., Mackey, M.C., Mahaffy, J.M., 1995. Age-structured and two-delay models for erythropoiesis. Math. Biosci. 128, 317–346.

Berlin, N.I., Lotz, C., 1951. Life span of the red blood cell of the rat following acute hemorrhage. Proc. Soc. Exp. Biol. Med. 78, 788.

Bernard, S., Bélair, J., Mackey, M.C., 2003a. Oscillations in cyclical neutropenia: new evidence based on mathematical modeling. J. Theor. Biol. 223, 283–298.

Bernard, S., Pujo-Menjouet, L., Mackey, M.C., 2003b. Analysis of cell kinetics using a cell division marker: mathematical modeling of experimental data. Biophys. J. 84, 3414–3424.

Bernard, S., Bélair, J., Mackey, M.C., 2004. Bifurcations in a white-blood-cell production model. C.R. Biol. 327, 201–210.

Burns, F.J., Tannock, I.F., 1970. On the existence of a $G_0$ phase in the cell cycle. Cell Tissue Kinet. 19, 321–334.

Chappell, D., Tilbrook, P.A., Bittorf, T., Colley, S.M., Meyer, G.T., Klinken, S.P., 1997. Prevention of apoptosis in J2E erythroid cells by erythropoietin: involvement of JAK2 but not MAP kinases. Cell Death Differ. 4, 105–113.

Colijn, C., Mackey, M.C., 2005a. A mathematical model of hematopoiesis—I. Periodic chronic myelogenous leukemia. J. Theor. Biol. 237, 117–132.

Colijn, C., Mackey, M.C., 2005b. A mathematical model of hematopoiesis—II. Cyclical neutropenia. J. Theor. Biol. 237, 133–146.

Ferrell, J.E., 1996. Tripping the switch fantastic: how a protein kinase cascade can convert graded inputs into switch-like outputs. Trends Biochem. Sci. 21 (12), 460–466.

Ferrell, J.E., 1997. How responses get more switch-like as you move down a protein kinase cascade. Trends Biochem. Sci. 22 (8), 288–289.

Gandrillon, O., 2002. The v-erbA oncogene. Assessing its differentiation-blocking ability using normal chicken erythrocytic progenitor cells. Methods Mol. Biol. 202, 91–107.

Gandrillon, O., Schmidt, U., Beug, H., Samarut, J., 1999. TGF-beta cooperates with TGF-alpha to induce the self-renewal of normal erythrocytic progenitors: evidence for an autocrine mechanism. EMBO J. 18, 2764–2781.

Haurie, C., Dale, D.C., Mackey, M.C., 1998. Cyclical neutropenia and other periodic hematological diseases: a review of mechanisms and mathematical models. Blood 92, 2629–2640.

Haurie, C., Dale, D.C., Mackey, M.C., 1999. Occurrence of periodic oscillations in the differential blood counts of congenital, idiopathic and cyclical neutropenic patients before and during treatment with G-CSF. Exp. Hematol. 27, 401–409.

Koury, M.J., Bondurant, M.C., 1990. Erythropoietin retards DNA breakdown and prevents programmed death in erythroid progenitor cells. Science 248, 378–381.

Krause, D.S., 2002. Regulation of hematopoietic stem cell fate. Oncogene 21, 3262–3269.

Kuang, Y., 1993. Delay differential equations with applications in population dynamics. Mathematics in Science and Engineering, vol. 191. Academic Press, New York.

Lajtha, L.G., 1959. On DNA labeling in the study of the dynamics of bone marrow cell populations. In: Stohlman, Jr., F. (Ed.), The Kinetics of Cellular Proliferation. Grune and Stratton. New York, pp. 173–182.

Loeffler, M., Wichmann, H.E., 1980. A comprehensive mathematical model of stem cell proliferation which reproduces most of the published experimental results. Cell Tissue Kinet. 13, 543–561.

Loeffler, M., Pantel, K., Wulff, H., Wichmann, H.E., 1989. A mathematical model of erythropoiesis in mice and rats. Part 1. Structure of the model. Cell Tissue Kinet. 22, 13–30.

Lomb, N.R., 1976. Least-squares frequency analysis of unequally spaced data. Astrophys. Space Sci. 39, 447–462.

Mackey, M.C., 1978. Unified hypothesis of the origin of aplastic anaemia and periodic hematopoïesis. Blood 51, 941–956.

Mackey, M.C., 1979. Dynamic hematological disorders of stem cell origin. In: Vassileva-Popova, G., Jensen, E.V. (Eds.), Biophysical and Biochemical Information Transfer in Recognition. Plenum Press, New York, pp. 373–409.

Mackey, M.C., 1997. Mathematical models of hematopoietic cell replication and control. In: Othmer, H.G., Adler, F.R., Lewis, M.A., Dallon, J.C. (Eds.), The Art of Mathematical Modelling: Case Studies in Ecology, Physiology and Biofluids. Prentice-Hall, Englewood Cliffs, NJ, pp. 149–178.

Mackey, M.C., Rudnicki, R., 1994. Global stability in a delayed partial differential equation describing cellular replication. J. Math. Biol. 33, 89–109.

Mackey, M.C., Rudnicki, R., 1999. A new criterion for the global stability of simultaneous cell replication and maturation processes. J. Math. Biol. 38, 195–219.

Mahaffy, J.M., Belair, J., Mackey, M.C., 1998. Hematopoietic model with moving boundary condition and state dependent delay: applications in erythropoiesis. J. Theor. Biol. 190, 135–146.

Mitjavila, M.T., Le Couedic, J.P., Casadevall, N., Navarro, S., Villeval, J.L., Dubart, A., Vainchenker, W., 1991. Autocrine stimulation by erythropoietin and autonomous growth of human erythroid leukemic cells in vitro. J. Clin. Invest. 88 (3), 789–797.

Nagai, K., Oue, K., Kawagoe, H., 1968. Studies on the short-lived reticulocytes by use of the in vitro labeling method. Acta. haematol. Jpn 31, 967.

Nagai, K., Ishizu, K., Kakishita, E., 1971. Studies on the erythroblast dynamics based on the production of fetal hemoglobin. Acta Haematol. Jpn. 34.

Pain, B., Woods, C.M., Saez, J., Flickinger, T., Raines, M., Kung, H.J., Peyrol, S., Moscovici, C., Moscovici, G., Jurdic, P., Lazarides, E., Samarut, J., 1991. EGF-R as a hemopoietic growth factor receptor: the c-erbB product is present in normal chicken erythrocytic progenitor cells and controls their self-renewal. Cell 65, 37–46.

Pantel, K., Loeffler, M., Bungart, B., Wichmann, H.E., 1990. A mathematical model of erythropoiesis in mice and rats. Part 4. Differences between bone marrow and spleen. Cell Tissue Kinet. 23, 283–297.

Pujo-Menjouet, L., Bernard, S., Mackey, M.C., 2005. Long period oscillations in a $G_0$ model of hematopoietic stem cells. SIAM J. Appl. Dynamical Syst. 4 (2), 312–332.

Pujo-Menjouet, L., Mackey, M.C., 2004. Contribution to the study of periodic chronic myelogenous leukemia. C.R. Biol. 327, 235–244.

Roeder, I., 2006. Quantitative stem cell biology: computational studies in the hematopoietic system. Curr. Opinion Hematol. 13, 222–228.

Roeder, I., Loeffler, M., 2002. A novel dynamic model of hematopoietic stem cell organization based on the concept of within-tissue plasticity. Exp. Hematol. 30, 853–861.

Sakata, S., Enoki, Y., Tomita, S., Kohzuki, H., 1985. In vitro erythropoietin assay based on erythroid colony formation in fetal mouse liver cell culture. Br. J. Haematol. 61 (2), 293–302.

Shampine, L.F., Thompson, S., 2001. Solving DDEs in MATLAB. Appl. Numer. Math. 37, 441–458. doi:10.1016/S0168-9274(00)00055-6. ⟨http://www.radford.edu/thompson/webddes/⟩.

Shimada, A., 1975. The maturation of reticulocytes. II Life-span of red cells originating from stress reticulocytes. Acta Med. Okayama 29 (4), 283–289.

Starck, J., Cohet, N., Gonnet, C., Sarrazin, S., Doubeikovskaia, Z., Doubeikovski, A., Verger, A., Duterque-Coquillaud, M., Morle, F., 2003. Functional cross-antagonism between transcription factors FLI-1 and EKLF. Mol. Cell Biol. 23 (4), 1390–1402.

Stohlman, F., 1961. Humoral regulation of erythropoiesis. VII. Shortened survival of erythrocytes by erythropoietin or severe anemia. Proc. Soc. Exp. Biol. Med. 107, 884.

Walter, H., Krob, E.J., Ascher, G.S., 1975. Abnormal membrane surface properties during maturation of rat reticulocytes elicited by bleeding as measured by partition in two-polymer aqueous phases. Br. J. Haematol. 31 (2), 149–157.

Watt, F.M., Hogan, B.L., 2000. Out of Eden: stem cells and their niches. Science 287, 1427–1430.

Weissman, I.L., 2000. Stem cells: units of development, units of regeneration, and units in evolution. Cell 100, 157–168.

Wichman, H.E., Loeffler, M., 1985. Mathematical Modeling of Cell Proliferation. CRC Press, Boca Raton, FL.

Wichmann, H.E., Loeffler, M., Schmitz, S., 1985. A concept of hemopoietic regulation and its biomathematical realisation. Blood Cells 14, 411–429.

Wichmann, H.E., Loeffler, M., Pantel, K., Wulff, H., 1989. A mathematical model of erythropoiesis in mice and rats. Part 2. Stimulated erythropoiesis. Cell Tissue Kinet. 22, 31–49.

Wulff, H., Wichmann, H.E., Loeffler, M., Pantel, K., 1989. A mathematical model of erythropoiesis in mice and rats. Part 3. Suppressed erythropoiesis. Cell Tissue Kinet. 22, 51–61.

## 5.6 Crauste et al. (2010)

Manuscrit de l'article : [55] F. Crauste, I. Demin, O. Gandrillon, V. Volpert, *Mathematical study of feedback control roles and relevance in stress erythropoiesis*, Journal of Theoretical Biology, 263 (3), 303–316 (2010).

Journal of Theoretical Biology 263 (2010) 303–316

Contents lists available at ScienceDirect

Journal of Theoretical Biology

journal homepage: www.elsevier.com/locate/yjtbi

# Mathematical study of feedback control roles and relevance in stress erythropoiesis

Fabien Crauste [a], Ivan Demin [a,*], Olivier Gandrillon [b,c,d], Vitaly Volpert [a]

[a] Université de Lyon, Université Lyon 1, CNRS, UMR 5208, Institut Camille Jordan, Batiment du Doyen Jean Braconnier, 43, blvd du 11 novembre 1918, F - 69222 Villeurbanne Cedex, France
[b] Equipe "Bases Moléculaires de l'Autorenouvellement et de ses Altérations" Université de Lyon, Lyon, F-69003, France
[c] Université Lyon 1, Lyon, F-69003, France
[d] CNRS, UMR5534, Centre de génétique moléculaire et cellulaire, Villeurbanne, F-69622, France

ARTICLE INFO

*Article history:*
Received 30 June 2009
Received in revised form
26 November 2009
Accepted 23 December 2009
Available online 4 January 2010

*Keywords:*
Anaemia
Intracellular regulatory network
Growth factor
Bistability

ABSTRACT

This work is devoted to mathematical modelling of erythropoiesis. We propose a new multi-scale model, in which we bring together erythroid progenitor dynamics and intracellular regulatory network that determines erythroid cell fate. All erythroid progenitors are divided into several sub-populations according to their maturity. Two intracellular proteins, Erk and Fas, are supposed to be determinant for regulation of self-renewal, differentiation and apoptosis. We consider two growth factors, erythropoietin and glucocorticoids, and describe their dynamics. Several feedback controls are introduced in the model. We carry out computer simulations of anaemia and compare the obtained results with available experimental data on induced anaemia in mice. The main objective of this work is to evaluate the roles of the feedback controls in order to provide more insights into the regulation of erythropoiesis. Feedback by Epo on apoptosis is shown to be determinant in the early stages of the response to anaemia, whereas regulation through intracellular regulatory network, based on Erk and Fas, appears to operate on a long-term scale.



## 1. Introduction

All blood cells can be divided into three categories, red blood cells, white blood cells and platelets. Red blood cells (RBCs) are produced during a complex process called erythropoiesis, which is a part of haematopoiesis (production of blood). It involves haematopoietic stem cells, at the root of blood cell production, able to create all haematopoietic lineages (Weissman, 2000), first lymphoid and myeloid lineages, then, within the myeloid branch, different lineages and in particular erythroid lineage, the origin of red blood cells. Haematopoietic stem cells differentiate into immature erythroid cells, called erythroid progenitors, which are undifferentiated cells committed to erythroid lineage. Then, through maturation and differentiation stages, erythroid progenitors become reticulocytes, which are almost mature red blood cells. These latter end their maturation to become red blood cells and enter blood stream, where they transport oxygen to tissues.

Erythropoiesis consists in a series of cell divisions through which erythroid cells acquire differentiation markers. This process allows the production of sufficient amount of erythrocytes to transport oxygen to organs. Erythropoiesis can sometimes exhibit disorders, such as excessive proliferation of immature cells, as observed in acute leukaemias (Kowal-Vern et al., 2000; Mazzella et al., 2000). Such disorders can be caused by alteration of intracellular regulatory networks, which control cell fate (e.g. Madan et al., 2003), that is self-renewal (the ability to produce daughter cells of the same maturity), differentiation (the ability to produce more mature daughter cells) or apoptosis (programmed cell death). By maturity here we understand an accumulation of differentiation markers (like haemoglobin, for example). Hence, the regulation of erythropoiesis depends on a precise control of cell fate by means of intracellular proteins and growth factors.

One of the most studied growth factors, playing an important role in erythropoiesis regulation, is erythropoietin (Epo), a glucoprotein released by the kidney in response to hypoxia, that is a lack of oxygen in tissues. Glucocorticoids (GCs) are lipophilic hormones involved in the regulation of various physiological responses, and in particular in stress erythropoiesis. They are known to favour cell proliferation (Liapi and Chrousos, 1992). Growth factors operate by activating membrane receptors on cell surface to trigger intracellular protein activation.

Recently, Rubiolo et al. (2006) proposed a description of the regulatory network that controls erythroid progenitor fate: some

* Corresponding author. Tel.: +33 472 432 765; fax: +33 472 431 687.
*E-mail addresses:* crauste@math.univ-lyon1.fr (F. Crauste), demin@math.univ-lyon1.fr (I. Demin), gandrillon@cgmc.univ-lyon1.fr (O. Gandrillon), volpert@math.univ-lyon1.fr (V. Volpert).

0022-5193/$ - see front matter © 2010 Elsevier Ltd. All rights reserved.
doi:10.1016/j.jtbi.2009.12.026

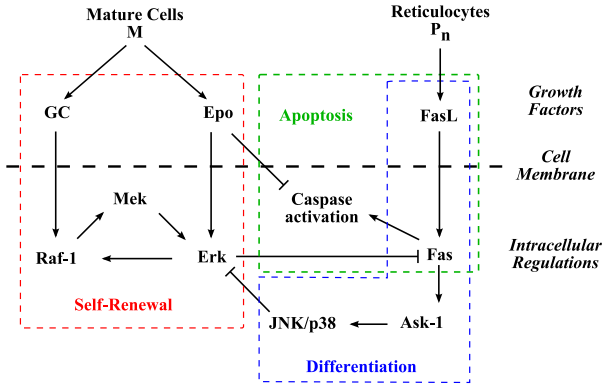


**Fig. 1.** Summary of intracellular protein interactions that determine erythroid progenitor fate, partially adapted from Rubiolo et al. (2006).

proteins are involved in a self-renewal loop, others in a differentiation/apoptosis loop, see Fig. 1. The first loop self-activates and inhibits the second one, whereas the second loop can inhibit the first one and, depending on Epo levels, induce either erythroid progenitor differentiation or apoptosis. Self-renewal loop relies on proteins of the MAPK family, the other loop is mainly controlled by Fas, a protein of the tumour-necrosis factor family.

Pioneering models of erythropoiesis regulation were proposed by Wichmann and Loeffler (1985), who modelled the dynamics of haematopoietic stem cells, erythroid progenitors and erythroid precursors (reticulocytes). They considered feedback controls from reticulocytes on progenitors and from progenitors on stem cells, they confronted their models with experimental data on stress erythropoiesis (bleeding, irradiation) and fitted model parameters. Later Wulff et al. (1989) and Wichmann et al. (1989) improved Wichmann and Loeffler's models. Bélair et al. (1995) proposed a model of erythropoiesis, partially based on previous works by Mackey (1978, 1979) and Mackey and Rudnicki (1994) on haematopoietic stem cell dynamics. In Bélair et al. (1995) the authors proposed an age-structured model describing erythroid cell dynamics, including an explicit control of differentiation by erythropoietin. This model was then improved by Mahaffy et al. (1998). Other works inspired by Bélair et al. (1995) proposed mathematical models of erythropoiesis (Ackleh et al., 2004, 2006; Banks et al., 2004). The erythropoietin-mediated inhibition of apoptosis has been considered in Adimy and Crauste (2007). The authors focused on the appearance of periodic haematological diseases, such as periodic chronic myeloid leukaemia (Fortin and Mackey, 1999). Recently we proposed an age-structured model of erythropoiesis taking into account feedback controls on progenitor self-renewal and apoptosis (Crauste et al., 2008). We confronted the model with experimental data on anaemia induced by phenylhydrazine injections and concluded the relevance of erythroid progenitor self-renewal for the response to stress.

Modelling of regulatory networks, involved in cell decision, has been the subject of recent analysis of lineage specification. Erythrocytes and platelets have one myeloid progenitor in common, known as megakaryocytic-erythroid progenitor (MEP). As a result of competition between two proteins, PU.1 and GATA-1, the MEP differentiates either into an erythroid progenitor or into a megakaryocytic progenitor. This choice has been studied by Roeder and Glauche (2006) and Huang et al. (2007). In both studies, models proposed by the authors demonstrated a bistable behaviour. This idea has been further developed in Chickarmane et al. (2009).

The main objective of this work is to develop a model of erythropoiesis which would allow evaluating the roles of different feedback controls in regulation of erythropoiesis in stress situations. We bring together interactions at the cell population level, growth factor actions and regulation of cell fate by intracellular proteins. From Rubiolo et al. (2006) we identify key proteins involved in the regulation of self-renewal, differentiation and apoptosis, and describe interactions between them. The resulting system is coupled with a model of erythroid cell dynamics. This latter, inspired by Demin et al. (2010), describes cell dynamics using self-renewal, differentiation and apoptosis rates of erythroid progenitors. The rates are determined by intracellular proteins, whereas growth factors and reticulocyte count control evolution of the intracellular proteins. Erythrocyte count, in turn, is responsible for growth factor production. The resulting model is confronted with experimental data on a severe anaemia, which allows determining the roles of the different feedback controls and their relative influences on regulation of stress erythropoiesis. We introduce the following feedback controls: in stress situations Epo inhibits apoptosis independently of intracellular regulatory network based on Erk and Fas (Gregory et al., 1999; Spivak et al., 1991), Epo and GCs promote Erk activation (Rubiolo et al., 2006; Sui et al., 1998), reticulocytes upregulate Fas (De Maria et al., 1999).

The work is organised as follows. In Section 2, we describe intracellular regulatory mechanisms, using available biological information. The resulting model is a nonlinear system of ordinary differential equations. This system describes the dynamics of two key proteins for cell fate regulation, Erk and Fas. We investigate the bistable behaviour of this system in order to explain the choice between cell self-renewal and differentiation or apoptosis. In Section 3 we present erythroid progenitor dynamics and dynamics of growth factors. We consider several sub-populations of erythroid cells according to their maturity. Two main growth factors involved in erythropoiesis regulation are considered: Epo and GCs. We obtain the complete model in Section 4. This multi-scale model is composed with $3(n+1)$ equations, where $n$ is the number of erythroid progenitor sub-populations. Existence of steady states and their stability are briefly discussed in Section 4.2. In Section 6 we present simulations of anaemia and investigate the roles of different feedback functions for the regulation of erythropoiesis. The simulations are confronted with experimental data on anaemia, induced by injection of phenylhydrazine (Cherukuri et al., 2004). Roles of feedback controls by Epo on apoptosis rate, independently of the considered intracellular network, and by the intracellular regulatory network on cell fate are evaluated. Results show that both controls are important for the response, yet they do not operate at the same time and appear to have specific roles. We conclude with a discussion and present possible research directions indicated by this model.

## 2. Intracellular regulatory network

In a recent paper Rubiolo et al. (2006) investigated the differentiation process of erythroid progenitors. In particular, they identified key proteins involved in self-renewal and differentiation/apoptosis, see Fig. 1. Differentiation and apoptosis appear to be controlled by the same proteins. In fact, different proteins are involved both in cell differentiation and cell apoptosis, however, depending on external conditions, cells undergo either differentiation or apoptosis. For example, Epo has been shown to inhibit erythroid progenitor apoptosis (Koury and Bondurant, 1990). Hence, when Epo levels are low, erythroid

progenitors preferentially die by apoptosis, whereas with high Epo levels they differentiate.

Rubiolo et al. (2006) showed that self-renewal was controlled by the self-activated cascade Raf-1–Mek–Erk, whereas differentiation was controlled by the cascade Fas–Ask-1–Jnk/p38, Fas triggering also cell apoptosis. This latter protein cascade is inhibited by the former, and vice versa. Hence, erythroid progenitor self-renewal and differentiation/apoptosis processes are controlled by two inhibitor loops, one being self-activating. Two proteins are of particular interest: Erk and Fas. The former is the cornerstone of the inhibition of differentiation and apoptosis. Erk (Extracellular signal-Regulated Kinase) is a member of the MAPK family, also known as the classical MAP kinase, it regulates cell proliferation and differentiation. Fas belongs to the tumour necrosis factor family (TNF), it induces cell apoptosis. We focus our attention on the interaction between these two proteins, that are key regulators of erythroid progenitor fate.

As mentioned in Fig. 1, external signals activate intracellular proteins. Epo is known to have the dual action of being both a mitogen and a survival factor (Spivak et al., 1991). The molecular mechanisms involved have been clarified (for a review, see Sawyer and Jacobs-Helber, 2000): Epo prevents apoptosis of erythroid progenitors through Stat5/GATA-1/Bcl-xL pathway (Gregory et al., 1999), that is largely independent of the Erk pathway (Chappell et al., 1997; Nagata et al., 1998; Sui et al., 2000). Self-renewal promoting activity of Epo, on the contrary, seems to rely mainly on the activation of the Erk kinase (Rubiolo et al., 2006; Sui et al., 1998). We therefore decided to integrate separately these two aspects of Epo action in the model: prevention of apoptosis is modelled as a direct mechanism, i.e. the molecular players are not explicitly taken into account. This feedback is assumed to be independent of the intracellular regulatory network based on Erk and Fas interactions. This is introduced in Section 4.1, Eq. (12). On the contrary, self-renewal is modelled as an Erk-dependent mechanism, which is introduced below in this section. GCs are involved in regulation of stress erythropoiesis (Bauer et al., 1999; Gandrillon et al., 1999). They activate self-renewing loop by increasing the level of Raf-1 expression.

One source term of activation appears in Fig. 1 concerning the differentiation/apoptosis part. Fas-ligand, denoted by FasL, a membrane protein, activates the transmembrane protein Fas. De Maria et al. (1999) suggested the existence of a negative regulatory feedback between mature and immature erythroid progenitors, in which mature cells exert a cytotoxic effect on immature cells. Mature erythroid progenitors, called reticulocytes, express FasL, which stimulates activation of Fas in immature erythroid progenitors. Sensitivity to FasL decreases with cell maturation. Other external factors, such as c-Kit, the protein associated with the stem cell factor (SCF) (Munugalavadla and Kapur, 2005), proteins from the JAK family (Vainchenker et al., 2008), etc., regulate the levels of activated intracellular proteins. Yet, we cannot take all these proteins into account, and we focus, in the following, on Epo, GCs, and FasL.

Focusing on Erk and Fas and interactions between them, we will state a system of ODEs, which represents the intracellular regulatory network shown in Fig. 1. Denote by $E$ and $F$ the expressions of Erk and Fas, respectively. The following system describes how they evolve in time:

$$\begin{cases} \dfrac{dE}{dt} = (\alpha+\beta E^k)(E_0\text{-}E) - aE - bEF, \\ \dfrac{dF}{dt} = \gamma(F_0\text{-}F) - cEF - dF. \end{cases} \tag{1}$$

Let us explain how this system is obtained. Consider first activation of Erk and Fas. As discussed above, Erk activation is due to Epo. From the scheme we can see that GCs also activate Erk through kinase cascade Raf-1–Mek–Erk. This activation is described by term $\alpha = \alpha(Epo, GC)$. Moreover, Erk self-activates, which is described by term $\beta E^k$ with some positive constant $k > 0$. When more Erk is activated, less Erk receptors remain free and, thus, activation rate saturates. This gives the following overall term for Erk activation, $(\alpha+\beta E^k)(E_0\text{-}E)$ with threshold value of Erk expression $E_0$, which cannot be overpassed. In similar way we describe FasL related activation of Fas by term $\gamma(FasL)(F_0\text{-}F)$. Fas inhibits Erk through Fas–Ask1–JNK/p38 kinase cascade. The rate of the inhibition is thus proportional to Erk and Fas. We describe this inhibition by term $-bEF$ in equation for Erk (by term $-cEF$ in equation for Fas since the inhibition process consumes Fas). Finally, we add an elimination term for both Erk and Fas, and obtain System (1), that describes the intracellular regulatory network shown in Fig. 1. It should be noted that this system is well-posed in the sense that Erk and Fas expressions cannot become negative and are bounded.

To find steady states of System (1), we must solve

$$\frac{dE}{dt} = 0 \quad \text{and} \quad \frac{dF}{dt} = 0,$$

that is

$$F = \frac{(\alpha+\beta E^k)(E_0\text{-}E)}{bE} - \frac{a}{b} \quad \text{and} \quad F = \frac{\gamma F_0}{cE+d+\gamma}. \tag{2}$$

Depending on the parameter values, (2) can have one to three solutions. Indeed, denote by $\xi$ and $\chi$ the following functions:

$$\xi(E) = \frac{(\alpha+\beta E^k)(E_0\text{-}E)}{bE} - \frac{a}{b} \quad \text{and} \quad \chi(E) = \frac{\gamma F_0}{cE+d+\gamma}. \tag{3}$$

Then one easily obtains that $\chi$ is a bounded positive decreasing function, mapping the interval $[0, E_0]$ into $[\gamma F_0/(cE_0+d+\gamma), \gamma F_0/(d+\gamma)]$. The function $\xi$ satisfies

$$\lim_{E\to 0} \xi(E) = +\infty \quad \text{and} \quad \xi(E_0) = -\frac{a}{b} < 0.$$

Consequently, System (1) has at least one steady state.

The analysis of the variations of function $\xi$, easy though tedious, shows that for some values of the parameters $\xi$ is decreasing, hence System (1) has only one steady state. For other parameter values, however, $\xi$ is not monotonous and up to three

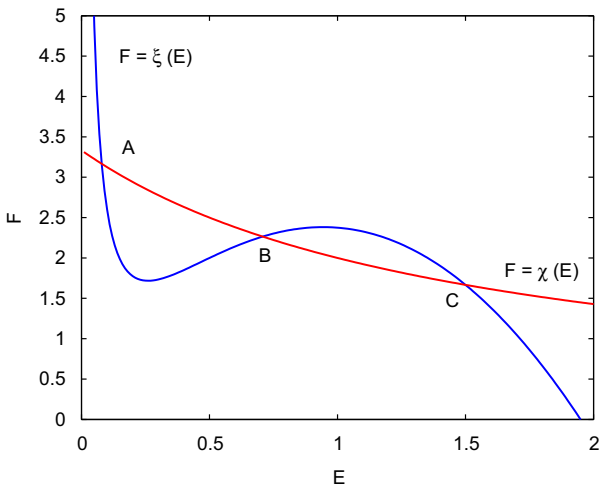


**Fig. 2.** Curves defined by (3). Three intersection points determine steady states of System (1). Two of them, A and C, are stable. Parameters used are given in Section 5.2 when dealing with numerical simulations of the complete multi-scale model.

steady states may exist. In particular, to obtain existence of three steady states it is necessary that $k>1$.

The case of three steady states is shown in Fig. 2. The points $A$ and $C$ are stable nodes, the point $B$ is a saddle. The point $A$ corresponds to high levels of activated Fas and low levels of activated Erk, whereas the point $C$ corresponds to low levels of activated Fas and high levels of activated Erk. Hence, the point $A$ is associated with erythroid progenitor differentiation or apoptosis, the point $C$ with erythroid progenitor self-renewal.

If $\alpha$ and $\gamma$ are not constant but dynamically depend on growth factors, then, during a response to a stress, values of $\alpha$ and $\gamma$ can be such that temporarily the number of steady states of System (1) goes from three to only one, and all cells, then, undergo either self-renewal or differentiation/apoptosis.

In the next section we discuss erythroid progenitor dynamics. The resulting model is coupled to System (1) in Section 4.

## 3. Erythroid progenitor dynamics

Since erythroid cell sensitivity to external signals strongly depends on the maturity, we consider several erythroid progenitor differentiation stages, called sub-populations, characterised by their maturity. We suppose there are $n$ erythroid progenitor sub-populations, with $n>1$ fixed. Let us denote by $P_i$, $i=1,\dots,n$, the number of progenitors in the $i$-th sub-population per μ l of blood, and by $s_i$, $d_i$ and $a_i$ their rates of self-renewal, differentiation and apoptosis, respectively. For the sake of simplicity we consider only symmetric cell division. Considering asymmetric cell division would modify expressions for self-renewal and differentiation rates but the model would remain similar. Then, progenitor self-renewal produces two daughter cells with the same maturity as the mother cell, thus, the two cells belong to the same sub-population. Differentiation produces two cells, which are more mature, and then belong to the next sub-population, see Fig. 3. Dynamics of erythroid progenitors are described by the following system of differential equations (Demin et al., 2010):

$$\frac{dP_1}{dt}=HSC+s_1P_1-d_1P_1-a_1P_1, \tag{4}$$

where $HSC$ accounts for the cell influx from the stem cell compartment, and for $i=2,\dots,n$,

$$\frac{dP_i}{dt}=2d_{i-1}P_{i-1}+s_iP_i-d_iP_i-a_iP_i. \tag{5}$$

Moreover, we denote by $M$ the number of erythrocytes per μl of blood, which satisfies

$$\frac{dM}{dt}=d_nP_n-\delta M, \tag{6}$$

where $\delta$ is the natural mortality rate of erythrocytes.

The term red blood cell (RBC) refers to an erythroid cell which circulates in the blood flow and carries oxygen to tissues. It can be an erythrocyte or a reticulocyte. During normal erythropoiesis very few reticulocytes circulate in the blood. For this reason and since we do not consider spatial aspects of erythropoiesis that could allow distinguishing between circulating reticulocytes and reticulocytes in the bone marrow, we assume that RBC count equals erythrocyte count. RBC count is determinant for the release of various growth factors in the blood stream. For instance, due to a lack of oxygen, kidneys release Epo. RBCs also induce the release of glucocorticoids in stress situations (Bauer et al., 1999). Denote by $Epo$ and $GC$ the blood levels of erythropoietin and glucocorticoids, respectively. They are supposed to satisfy ordinary differential equations (Bélair et al., 1995; Mahaffy et al., 1998),

$$\frac{dEpo}{dt}=f_{Epo}(M)-k_{Epo}Epo, \tag{7}$$

$$\frac{dGC}{dt}=f_{GC}(M)-k_{GC}GC, \tag{8}$$

where $k_{Epo}$ and $k_{GC}$ are degradation constants, and $f_{Epo}$ and $f_{GC}$ are production terms. They depend on the number of erythrocytes, and are supposed to be positive, bounded, decreasing functions, since the more erythrocytes the lower erythropoietin and glucocorticoid levels.

In the next section we couple intracellular protein dynamics with cell population dynamics, and obtain a multi-scale model of erythropoiesis.

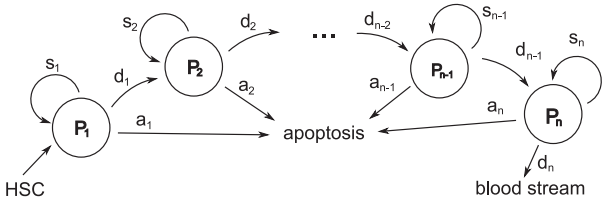


**Fig. 3.** Differentiation scheme of erythroid progenitors. $P_i$, $i=1,\dots,n$, denotes the number of progenitors in the $i$-th sub-population per μ l of blood, and by $s_i$, $d_i$ and $a_i$ their rates of self-renewal, differentiation and apoptosis, respectively.

## 4. Model of erythropoiesis

### 4.1. Coupling the two scales

To simplify the modelling, we neglect variations in cell cycle durations, so cell cycle lengths are supposed to be constant, equal to $T_c$. Each cell cycle ends up with either self-renewal, differentiation or apoptosis. Then, on every time unit

$$s_i+d_i+a_i=\frac{1}{T_c}.$$

Since erythroid progenitors perform one cell cycle in about 24 h (Crauste et al., 2008), and the time unit considered in this paper is also 24 h, we suppose $T_c=1$ and the above equality becomes

$$s_i+d_i+a_i=1. \tag{9}$$

Let us specify how these rates are defined. This is used later in this section and in Section 5.3. Denote by $p_s$ the probability of self-renewal provided that the cell does not undergo apoptosis. Then the probability of differentiation $p_d$, provided that the cell does not undergo apoptosis, is $p_d=1-p_s$. Since cell cycle time is fixed and equals one time unit, we can then write $s$ and $d$ (subscripts are deliberately omitted) as

$$s=(1-a)p_s,\quad d=(1-a)(1-p_s). \tag{10}$$

The term $1-a$ accounts for the rate of survival to apoptosis. Consequently, $s$ denotes the overall self-renewal rate, which is in fact expressed by the probability of self-renewal of non-apoptotic cells $p_s$ multiplied by the rate of survival $1-a$. The same holds for the differentiation rate.

As described in Section 2, self-renewal, differentiation and apoptosis rates depend on one hand on the intracellular protein regulatory network inherent to each erythroid progenitor, and on another hand apoptosis is inhibited by Epo.

Proteins Erk and Fas have been previously identified as the main regulators of erythroid progenitor fate, see Section 2. Erk induces self-renewal, and inhibits differentiation and apoptosis, whereas Fas inhibits self-renewal and induces differentiation or apoptosis, depending on Epo blood concentration. Concentrations of Erk and Fas, denoted by $E$ and $F$, satisfy System (1), where constants $\alpha$ and $\gamma$ account for external sources of Erk and Fas

activators, respectively. As mentioned in Section 2, the source of Erk activator consists mainly in erythropoietin and glucocorticoids. Hence, we assume $\alpha$ is an increasing function of *Epo* and *GC*,

$$\alpha = \alpha(Epo, GC).$$

Parameter $\gamma$ stands for activation of Fas by FasL, which is expressed on surface of reticulocytes. Hence, we assume $\gamma$ depends on $P_n$, which correspond to reticulocytes, and the sensitivity of $\gamma$ to $P_n$ decreases with maturity level $i$, so that

$$\gamma = \gamma_i(P_n),$$

and $\gamma_i$ is a positive, bounded and increasing function.

Finally, before stating the system verified by concentrations $E$ and $F$, let us present the last assumption. As explained in the previous section, quantities of Erk and Fas are supposed to have maximum values, denoted by $E_0$ and $F_0$, respectively. Usually, exact quantities of Erk and Fas in erythroid cells cannot be measured, rather relative levels of activated Erk and Fas are provided. Hence, in order to render this model more comprehensible, we normalise activated Erk and Fas quantities, denoting by $E$ and $F$ the ratios $E/E_0$ and $F/F_0$. This guarantees the variables $E$ and $F$ to be between 0 and 1. Thus, $E_i$ and $F_i$, the levels of activated Erk and Fas in the $i$-th progenitor sub-populations, satisfy the following system, obtained from (1):

$$\begin{cases} \dfrac{dE_i}{dt} = (\alpha(Epo, GC) + \beta E_i^k)(1\text{-}E_i) - aE_i - bE_iF_i, \\ \dfrac{dF_i}{dt} = \gamma_i(P_n)(1\text{-}F_i) - cE_iF_i - dF_i, \end{cases} \tag{11}$$

where $\beta$, $a$, $b$, $c$ and $d$, respectively. stand for $\beta E_0^k$, $aE_0$, $bE_0F_0$, $cE_0F_0$ and $dF_0$. Note that all cells of a sub-population are assumed to express the same levels of activated Erk and Fas. This is a strong hypothesis, because in reality, different progenitors with the same maturity express different levels of Erk and Fas indicating stochasticity in protein expression. This stochasticity certainly plays an important role in erythropoiesis, yet in this model we do not take it into account.

One may observe the complexity of erythropoiesis through the model we propose. Erythroid progenitors and erythrocytes contribute to the control of growth factor concentrations in blood, which in turn regulate intracellular mechanisms of cell fate (self-renewal, differentiation, apoptosis). We complete the model of erythropoiesis by specifying how intracellular regulatory mechanisms influence erythroid progenitor fate.

As described in Section 2, self-renewal, differentiation and apoptosis rates depend on levels of activated Erk and Fas, denoted by $E_i$ and $F_i$, the subscript $i$ referring to a given sub-population. Moreover, apoptosis rate is also inhibited by Epo independently of the intracellular network based on Erk and Fas. Hence, functions $s_i$, $d_i$ and $a_i$ are defined as

$$s_i = s(E_i, F_i), \quad d_i = d(E_i, F_i), \quad a_i = a(E_i, F_i) f_{aEpo}(Epo), \tag{12}$$

where functions $s$, $d$ and $a$ define self-renewal, differentiation, and apoptosis rates, respectively, for given Erk and Fas levels. The function $f_{aEpo}$ describes a direct mechanism of apoptosis inhibition by Epo, which is independent of the intracellular regulatory network. It is assumed to be bounded, positive and decreasing.

Dynamics of erythroid progenitors, described by Eqs. (4) and (5), are then coupled to protein levels (11) through erythrocyte dynamics in (6), growth factor concentration evolution in (7)–(8), and self-renewal, differentiation and apoptosis rates definitions in (9) and (12). This set of equations forms the multi-scale model of erythropoiesis we study below.

### 4.2. Existence of steady states

We investigate the existence of steady states for the system formed with (4)–(9), (11) and (12). It should be noted that existence of such solutions is not straightforward. Indeed, denote by $P_i^*$ the steady state values of (4)–(5), $M^*$ the steady state value of (6), $Epo^*$ and $GC^*$ the steady state values of (7)–(8), and $E_i^*$ and $F_i^*$ the steady state values of (11). We also introduce the notations

$$s_i^* = s(E_i^*, F_i^*), \quad d_i^* = d(E_i^*, F_i^*), \quad a_i^* = a(E_i^*, F_i^*) f_{aEpo}(Epo^*).$$

Then, $P_i^*$, $i = 1, \ldots, n$, exist if and only if

$$\begin{cases} (d_1^* + a_1^* \text{-} s_1^*) P_1^* = HSC, \\ (d_i^* + a_i^* \text{-} s_i^*) P_i^* = 2 d_{i-1}^* P_{i-1}^*, \quad i = 2, \ldots, n. \end{cases}$$

Hence, using (9), $P_i^*$ exists for $i = 1, \ldots, n$ provided that

$$s_i^* < \tfrac{1}{2},$$

and $P_i^*$ is given by

$$P_1^* = \frac{HSC}{1\text{-}2s_1^*}, \quad P_i^* = \frac{2d_{i-1}^*}{1\text{-}2s_i^*} P_{i-1}^*, \quad i = 2, \ldots, n.$$

Then, $M^*$, $Epo^*$ and $GC^*$ are uniquely defined by

$$M^* = \frac{d_n^*}{\delta} P_n^*, \quad Epo^* = \frac{f_{Epo}(M^*)}{k_{Epo}}, \quad GC^* = \frac{f_{GC}(M^*)}{k_{GC}}.$$

Yet, implicitly, all the above steady state values, and in particular $P_n^*$, $Epo^*$ and $GC^*$, are functions of $E_i^*$ and $F_i^*$, for $i = 1, \ldots, n$, through the steady state values of the different rates $s_i^*$, $d_i^*$ and $a_i^*$. Since $E_i^*$ and $F_i^*$ are solutions of system

$$\begin{cases} (\alpha(Epo^*, GC^*) + \beta (E_i^*)^k)(1\text{-}E_i^*) - aE_i^* - bE_i^*F_i^* = 0, \\ \gamma_i(P_n^*)(1\text{-}F_i^*) - cE_i^*F_i^* - dF_i^* = 0, \end{cases}$$

which has been shown to have 1–3 solutions when $\alpha$ and $\gamma$ are constant (see Section 2), it follows that determining steady states for the full model is equivalent to solving a system in the form

$$\begin{cases} E_i^* = \phi_i(E_1^*, \ldots, E_n^*, F_1^*, \ldots, F_n^*), \\ F_i^* = \psi_i(E_1^*, \ldots, E_n^*, F_1^*, \ldots, F_n^*), \end{cases}$$

for all $i = 1, \ldots, n$. Functions $\phi_i$ and $\psi_i$ are some unknown functions. In a general case such a system cannot be solved.

For the sake of simplicity, suppose $\alpha$ is given by

$$\alpha(Epo, GC) = \alpha_0 + f(Epo) + g(GC),$$

where $\alpha_0 > 0$ accounts for Erk activation when erythropoietin and glucocorticoids are low. Since erythropoietin and glucocorticoids are not the only activators of Erk, this assumption is biologically relevant. Functions $f$ and $g$ are bounded nonnegative increasing functions, for instance, Hill functions, with $f(0) = g(0) = 0$. Similarly, suppose $\gamma_i$ is given by

$$\gamma_i(P_n) = \gamma_0 + \mu_i \overline{\gamma}(P_n),$$

where $\gamma_0$ is a constant source of Fas activation independent of mature progenitor cell production of Fas ligand, and $\mu_i$ is a parameter accounting for sensitivity of Fas activation to cell maturity. The function $\overline{\gamma}$ is assumed to be nonnegative, bounded and increasing, with $\overline{\gamma}(0) = 0$ and $\gamma(P_n) \leq 1$.

With these assumptions, we can apply the Implicit Function Theorem to find steady states of the full model. Suppose that in the steady state, values of $Epo^*$ and $GC^*$ are such that $f(Epo^*) + g(GC^*)$ is very small, close to zero. Moreover, $\mu_i$ are supposed to be small parameters.

We first note that the following system:

$$\begin{cases} (\alpha_0 + \beta (E_i^*)^k)(1\text{-}E_i^*) - aE_i^* - bE_i^*F_i^* = 0, \\ \gamma_0(1\text{-}F_i^*) - cE_i^*F_i^* - dF_i^* = 0, \end{cases} \tag{13}$$

has 1–3 solutions, depending on the values of $\alpha_0$ and $\gamma_0$. This has been obtained in Section 2, for $\alpha=\alpha_0$ and $\gamma=\gamma_0$, see System (2). Denote by $(E^{*,0},F^{*,0})$ one of these potential solutions. Then for every pair $(E^{*,0},F^{*,0})$, there exists a unique value of $s_i^*$, $d_i^*$ and $a_i^*$, and consequently of $P_i^*$, $i=1,\dots,n$, $M^*$, $Epo^*$ and $GC^*$.

As $\mu_i$ increases away from zero, the Implicit Function Theorem gives the existence of steady states for the full model. These steady states are small perturbations of the above-mentioned steady states, based on $(E^{*,0},F^{*,0})$. Hence, stability does not change, and steady states of the full system are stable (respectively, unstable) if steady states of (4)–(9), (12) and (13) are stable (respectively, unstable). And (13) has up to two stable steady states for all $i=1,\dots,n$.

We can then state that full system formed with (4)–(9), (11) and (12) has up to $2^n$ stable steady states. This number may appear large, yet it does not take into account biological constraints. An interested reader can find a detailed analysis of a similar system in Demin et al. (2010).

During the process of maturation, erythroid progenitors lose their ability to self-renew (Dazy et al., 2003), thus immature cells are more inclined to self-renewal and mature ones are more inclined to differentiation. Hence, among all possible stable steady states only those, characterised by a certain integer $j$, $1\leq j\leq n$, such that cells in the first $j$ sub-populations (corresponding to variables $P_1$ to $P_j$) preferentially self-renew (let us call them self-renewing sub-populations), and cells in the last $n$-$j$ sub-populations (corresponding to variables $P_{j+1}$ to $P_n$) preferentially differentiate (let us call them differentiating sub-populations), are biologically reasonable. It reduces the number of biologically meaningful stable steady states to $n$. Moreover, it seems natural to expect that in normal erythropoiesis the number of mature cells is larger than the number of immature cells, so we impose the conditions $P_i^*<P_{i+1}^*$, which are equivalent to

$$\frac{2d_i^*}{1\text{-}2s_{i+1}^*}>1,\quad i=1,\dots,n\text{-}1.$$

Thus the multi-scale model formed with (4)–(9), (11) and (12) has, generally speaking, several (from 1 up to $n$) stable steady states, which satisfy the biological constraints discussed above.

The next two sections are devoted to parameter values estimations and to numerical simulations of the system obtained above. We focus our attention, in particular, on anaemia situations.

## 5. Parameter values

A typical situation of stress erythropoiesis is anaemia: a lack of red blood cells, or haemoglobin. It can be either induced, for instance by killing erythrocytes, which can be obtained for instance with phenylhydrazine, or by bleeding, or disease-related. A lot of haematological diseases are characterised by or associated with severe anaemia, such as aplastic anaemia or some leukaemias.

The nature of the induced anaemia can be very different, according to the method used to urge it. Finch et al. (1959) noticed that the way haematocrit evolves following the anaemia induction, and in particular the speed of the return to the equilibrium, strongly depends on its strength. In other words, the more red blood cells are removed from the body, the stronger response to anaemia is. Results of experiments on mice with phenylhydrazine-induced anaemia obtained in Cherukuri et al. (2004) are presented in Fig. 4. One can observe that, following the anaemia, the erythrocyte count quickly increases and, although still not at its equilibrium, decreases once again on day 11 before finally reaching normal values from day 18 up to the end of

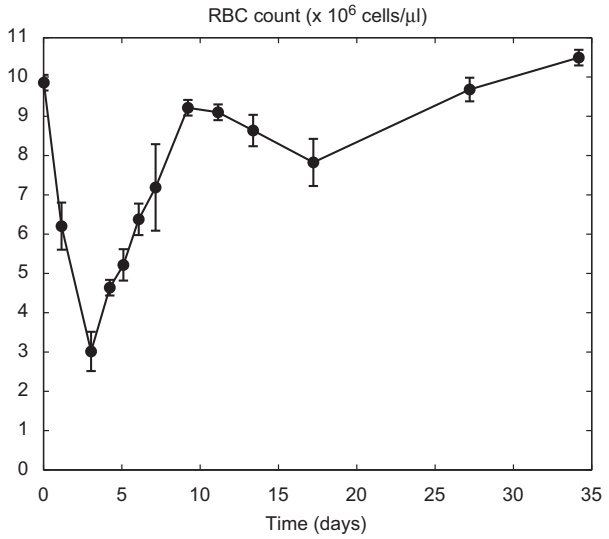


**Fig. 4.** Phenylhydrazine-induced anaemia in mice, adapted from Cherukuri et al. (2004). Two injections (60 mg/kg) are administered intraperitoneally at days 0 and 1. Mean values among six mice are presented with error bars. Initial value of red blood cell count (before starting the experiment) is about $10^7$ cells $\mu l^{-1}$.

experiments. This surprising decrease (days 11–18) will be investigated in Section 6: we will look for feedback controls responsible for it.

We consider the model of erythropoiesis that consists of Eqs. (4)–(6) describing immature and mature blood cell dynamics, Eqs. (7)–(8) describing growth factors dynamics, and Eq. (11) accounting for intracellular regulatory mechanisms.

We determine functions and parameter values of the model. Some parameters are rather easily accessible, whereas other parameters and most feedback functions are usually unavailable. We distinguish between these two kinds of values.

### 5.1. Estimations based on existing data

Among easily accessible parameter values, the mortality rate of erythrocytes ($\delta$ in Eq. (9)) is the first for which a value can be assigned. Since erythrocyte average lifespan in mice equals 40 days, we chose $\delta=1/40\,d^{-1}$.

Let now focus on growth factor dynamics system (7)–(8). In mice the half-life of erythropoietin is about 180 min (Piroso et al., 1991). The half-life of glucocorticoids ranges in a wide interval, yet 90 min can be considered as reasonable for short-term glucocorticoids (Liapi and Chrousos, 1992) (that is glucocorticoids acting for a short time), like cortisol, which are likely to be involved in stress erythropoiesis (Bauer et al., 1999). Using the definition of half-life, we compute degradation constants: consider a substance that degrades with constant rate $v$, then its dynamics can be described by the equation

$$\frac{dx}{dt}=-vx,$$

whose solution is $x(t)=x_0e^{-vt}$. The half-life is the time $T_{1/2}$ such that

$$x(T_{1/2})=\frac{x_0}{2},$$

which gives $v=\ln(2)/T_{1/2}$. Using the above estimations for the half-life of erythropoietin and glucocorticoids, we obtain the

**Table 1**
Values of the parameters used to numerically compute erythrocyte count and growth factor levels.

| Parameter | | Value | Unit |
|---|---|---|---|
| $\delta$ | Mortality rate of erythrocytes | 0.025 | $d^{-1}$ |
| $k_{Epo}$ | Degradation rate of Epo | 5.55 | $d^{-1}$ |
| $k_{GC}$ | Degradation rate of GC | 11.1 | $d^{-1}$ |
| $f^0_{Epo}$ | Maximum value of $f_{Epo}$ | 7130 | mU $\mu l^{-1}$ |
| $\theta_{Epo}$ | Threshold value of $f_{Epo}$ | $4.63 \times 10^6$ | cells $\mu l^{-1}$ |
| $q_E$ | Sensitivity of $f_{Epo}$ | 7 | NU |
| $f^0_{GC}$ | Maximum value of $f_{GC}$ | 2930 | mU $\mu l^{-1}$ |
| $\theta_{GC}$ | Threshold value of $f_{GC}$ | $7.69 \times 10^6$ | cells $\mu l^{-1}$ |
| $q_G$ | Sensitivity of $f_{GC}$ | 6 | NU |

NU means "no unit is relevant".

following values for the degradation constants:

$$k_{Epo} = 5.55\,d^{-1}, \quad k_{GC} = 11.1\,d^{-1}.$$

The functions $f_{Epo}$ and $f_{GC}$ in (7) and (8), accounting for growth factor production terms, are supposed to be Hill functions (Bélair et al., 1995; Mahaffy et al., 1998),

$$f_{Epo}(M) = f^0_{Epo}\frac{\theta^{q_E}_{Epo}}{\theta^{q_E}_{Epo}+M^{q_E}}, \quad f_{GC}(M) = f^0_{GC}\frac{\theta^{q_G}_{GC}}{\theta^{q_G}_{GC}+M^{q_G}}.$$

During anaemia Epo blood concentrations increase by 2–3 orders (Ridley et al., 1994). To our knowledge, variations of glucocorticoids are less important, but exact values are not available. We then chose parameters of functions $f_{Epo}(M)$ and $f_{GC}(M)$ that allowed us to obtain such variations of Epo and GCs in anaemia simulations we carried out. All these parameters are listed in Table 1.

As obtained in Section 4.2, the model we consider has from 1 up to $n$ stable steady states. Not all steady states are biologically meaningful and one of these numerous steady states can be selected by taking into consideration a realistic proportion between the daily influx of haematopoietic stem cells (input of the model) and erythrocyte count in mice (output of the model). From Crauste et al. (2008), the ratio $M^*/HSC$ between normal erythrocyte count and HSC daily influx can be estimated in the order of $10^5$. The number of self-renewing sub-populations (see discussion at the end of Section 4.2) allows to select the appropriate steady state. We carried out several simulations with different numbers of self-renewal-inclined sub-populations and we obtained a correct ratio $M^*/HSC$ for $n = 8$ and the case of four immature preferentially self-renewing sub-populations, and consequently four mature differentiation-inclined sub-populations.

### 5.2. Intracellular regulatory network

Let first focus on the part of the intracellular regulatory system (11) independent of feedback functions. Variables $E$ and $F$ are dimensionless and the parameter values we use are deduced from numerical simulations since no data are available in the literature. They are

$$k = 2, \quad \beta = 40\,d^{-1}, \quad a = 2\,d^{-1},$$

$$b = 40\,d^{-1}, \quad c = 10\,d^{-1}, \quad d = 2.5\,d^{-1}. \tag{14}$$

With these values, the intracellular regulatory network may have three steady states for given $\alpha$ and $\gamma$ (Fig. 2), two steady states being stable.

As mentioned in previous sections, System (11), describing intracellular regulatory network, in which $\alpha$ stands for Erk activation by Epo and GCs, and $\gamma$ stands for Fas activation by FasL, can have either one or two stable steady states. Thus, primordially bistable system can temporarily lose its bistability when values of parameters $\alpha$ and $\gamma$ change, like in stress situations. For the parameters of the intracellular regulatory network mentioned in (14), we found numerically the set of $(\alpha, \gamma)$ values, for which System (11) has a bistable behaviour (domain $D_1$ in Fig. 5).

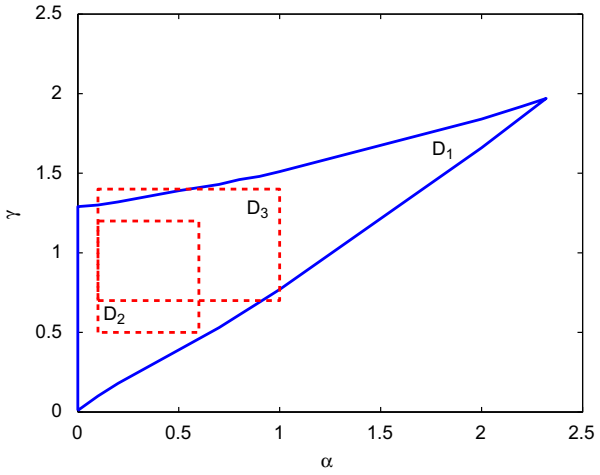


**Fig. 5.** Intracellular system (11) has a bistable behaviour for $(\alpha, \gamma)$ inside $D_1$. Two examples of $(\alpha, \gamma)$ variations are tested numerically, domains $D_2$ and $D_3$, when bistability can be temporarily lost.

After determining system parameters (see below), we numerically tested two cases: first when intracellular regulatory network always keeps a bistable behaviour during anaemia, independently of the values of $\alpha$ and $\gamma$, and second when for some extreme values of $\alpha$ and $\gamma$ the bistability is temporarily lost and the intracellular regulatory network has only one stable steady state. The first case corresponds to variations of $\alpha$ and $\gamma$ in the rectangular domain $D_2$ in Fig. 5 that is entirely inside the bistability area. The second case corresponds, for instance (this is what was tested), to variations of $\alpha$ and $\gamma$ in the domain $D_3$ that partially exits $D_1$. If a system trajectory goes through these out-of-$D_1$ parts of $D_3$, then the bistability of System (11) is lost for the corresponding values of $(\alpha, \gamma)$. We investigated the consequences of these two distinct situations on the response to anaemia.

In the second case the response of the system was stronger but qualitatively the same as the one obtained in the first case. We tried to increase out-of-$D_1$ parts of domain $D_3$ through which the trajectory goes and we obtained that beyond certain thresholds (i.e. if the trajectory stays long enough outside the domain $D_1$), the solution could not come back to its initial state, the solution changed an attractor and went definitely to another steady state, or in other words, the system switched to single stable steady state regimen. The system would then lose its biological meaning (the balance between self-renewal and differentiation would be broken) and consequently we decided to focus only on the first case ($\alpha$ and $\gamma$ range in $D_2$) and we present numerical simulations only for this case.

Let now concentrate ourselves on the choice of functions $\alpha$ and $\gamma$.

For the sake of simplicity, we supposed that FasL exerts the same feedback control on Fas activation for all progenitor sub-populations, which implies that $\gamma_i(P_n)$ in (11) is independent of $i$: $\gamma_i(P_n) = \gamma(P_n)$ for all $i = 1, \ldots, n$.

The system trajectory represented on $(\alpha, \gamma)-$plane stays inside domain $D_2$ during erythrocyte recovery. The domain $D_2$ is characterised by $\alpha \in [0.1, 0.6]$, $\gamma \in [0.5, 1.2]$, see Fig. 5. Recall

**Table 2**
Parameters of the intracellular regulatory network, functions $\alpha(Epo, GC) = \alpha_0 + f(Epo) + g(GC)$ and $\gamma(P_n)$, defined in (15) and (16).

| Parameter | | Value | Unit |
|---|---|---|---|
| $k$ | Sensitivity of Erk self-activation | 2 | NU |
| $\beta$ | Rate of Erk self-activation | 40 | $d^{-1}$ |
| $a$ | Erk degradation rate | 2 | $d^{-1}$ |
| $b$ | Suppression of Erk expression rate | 40 | $d^{-1}$ |
| $c$ | Suppression of Fas expression rate | 10 | $d^{-1}$ |
| $d$ | Fas degradation rate | 2.5 | $d^{-1}$ |
| $\alpha_0$ | Constant Erk activation rate | 0.1 | $d^{-1}$ |
| $f_{max}$ | Maximum value of $f(Epo)$ | 0.25 | $d^{-1}$ |
| $q_f$ | Sensitivity of $f(Epo)$ | 6 | NU |
| $\theta_f$ | Threshold value of $f(Epo)$ | 100 | mU $\mu l^{-1}$ |
| $g_{max}$ | Maximum value of $g(GC)$ | 0.25 | $d^{-1}$ |
| $q_g$ | Sensitivity of $g(GC)$ | 2 | NU |
| $\theta_g$ | Threshold value of $g(GC)$ | 49.4 | mU $\mu l^{-1}$ |
| $\gamma_{min}$ | Minimum value of $\gamma(P_n)$ | 0.5 | $d^{-1}$ |
| $\gamma_{max}$ | Maximum value of $\gamma(P_n)$ | 1.2 | $d^{-1}$ |
| $q_\gamma$ | Sensitivity of $\gamma(P_n)$ | 3 | NU |
| $\theta_\gamma$ | Threshold value of $\gamma(P_n)$ | $1.14 \times 10^6$ | cells $\mu l^{-1}$ |

NU means "no unit is relevant".

that $\alpha = \alpha(Epo, GC)$ and $\gamma = \gamma(P_n)$. We suppose $\alpha(Epo, GC) = \alpha_0 + f(Epo) + g(GC)$, where $\alpha_0$ is constant and $f(Epo)$, $g(GC)$ are Hill functions,

$$f(Epo) = f_{max}\frac{Epo^{q_f}}{\theta_f^{q_f} + Epo^{q_f}}, \quad g(GC) = g_{max}\frac{GC^{q_g}}{\theta_g^{q_g} + GC^{q_g}}. \tag{15}$$

Function $\gamma(P_n)$ is supposed to be a Hill function, given by

$$\gamma(P_n) = \gamma_{min} + (\gamma_{max} - \gamma_{min})\frac{P_n^{q_\gamma}}{\theta_\gamma^{q_\gamma} + P_n^{q_\gamma}}. \tag{16}$$

No information could allow us to determine the shape of such functions. The choice of Hill functions lies on the interest of these functions in describing kinase cascades and, more generally, biological phenomena with saturation effects. Parameter values of functions $\alpha(Epo, GC)$ and $\gamma(P_n)$ are given in Table 2. They were deduced from numerical simulations.

### 5.3. Self-renewal, differentiation and apoptosis rates

From Eqs. (9), (10) and (12), self-renewal, differentiation and apoptosis rates are given, for $i = 1, \ldots, n$, by

$$\begin{cases} s_i = (1 - a_i)\, p_s(E_i, F_i), \\ d_i = 1 - s_i - a_i, \\ a_i = a(E_i, F_i) f_{aEpo}(Epo). \end{cases} \tag{17}$$

The dependence upon Erk and Fas is defined through function $p_s(E, F)$, which describes how the probability of self-renewal depends upon Erk and Fas, and function $a(E, F)$, which describes how apoptosis rate depends on Erk and Fas. The direct action of Epo on apoptosis rate is determined by $f_{aEpo}(Epo)$. Hence, the three functions $p_s$, $a$ and $f_{aEpo}$ entirely determine the three rates.

The function $f_{aEpo}$ is supposed to be decreasing and bounded. In order to describe the effect of large Epo variations (quick changes from 5 to 1000 mU $\mu l^{-1}$), we chose a Hill function of the logarithm of Epo, given by,

$$f_{aEpo}(Epo) = 0.2 + \frac{0.73 \times 1.1^{9.2}}{1.1^{9.2} + (\log_{10}(Epo))^{9.2}}, \tag{18}$$

the parameters being dimensionless, except the threshold value 1.1, which is expressed in mU $\mu l^{-1}$. Parameters have been chosen so that $f_{aEpo}(Epo)$ in the steady state $Epo^*$ equals 0.9 and numerical simulations fit correctly experimental data from Fig. 4.

For the sake of simplicity, we supposed functions $p_s(E, F)$ and $a(E, F)$ to be functions of one variable, $p_s(E, F) = p_s(E\text{-}F)$ and $a(E, F) = a(F\text{-}E)$. The function $p_s$ is supposed to take larger values when Erk levels are high, whereas the value of $a$ is more important when Fas levels are high. Consequently, both functions are supposed to be increasing. Moreover, they are positive and we assumed the following form:

$$z(x) = z_{min} + \frac{(z_{max} - z_{min})(x+1)^{n_z}}{\theta_z^{n_z} + (x+1)^{n_z}}, \quad x \in [-1, 1].$$

Before giving values of the parameters $z_{min}$, $z_{max}$, $n_z$ and $\theta_z$ associated with functions $p_s$ and $a$, let us illustrate how the roles of Erk and Fas are investigated through these functions.

Let us recall that we assumed functions $\gamma_i$ do not depend on the index $i$. Hence, from (11) it follows that all sub-populations have the same steady state values $(E^*, F^*)$, which do not depend on $i$. Moreover, by assuming that $\alpha$ and $\gamma$ evolve in the restricted domain $D_2$, we ensure the existence of two stable steady states for System (11), one in which Erk levels are higher than Fas levels, and the other one with higher Fas levels. These two steady states $(E^*, F^*)$ provide two distinct values of the variable $F^*\text{-}E^*$, one positive and one negative. The positive value is associated with cell differentiation, whereas the negative one corresponds to cell self-renewal. Hence, the positive value of $F^*\text{-}E^*$ characterises differentiation-inclined erythroid progenitors, that is mature cells, and the negative one self-renewal-inclined erythroid progenitors, that is immature cells.

During anaemia, concentrations of Erk and Fas vary, therefore values of $F\text{-}E$ vary as well. Carrying out simulations, however, we observed that variations of $F\text{-}E$ were limited to neighbourhoods of the two stationary points $F^*\text{-}E^*$, and did not range in the whole interval [-1, 1]. This means that variations of functions $p_s(E\text{-}F)$ and $a(F\text{-}E)$ are only relevant on these neighbourhoods of $F^*\text{-}E^*$. Consequently, in order to determine the roles of Erk and Fas on the response to anaemia, we considered three cases describing three different ways of acting on self-renewal, differentiation and apoptosis rates, based on variations of $p_s$ and $a$ in the neighbourhoods of the steady state values.

In the first case $p_s(E\text{-}F)$ and $a(F\text{-}E)$ vary slightly on both neighbourhoods of the steady states. In the second case $p_s(E\text{-}F)$ (respectively, $a(F\text{-}E)$) varies a lot near the steady state corresponding to Erk prevalence, i.e. $F^*\text{-}E^* < 0$ (respectively, Fas prevalence, i.e. $F^*\text{-}E^* > 0$), and is almost constant near the other steady state. Biologically it can be interpreted as follows: in critical situations Erk and Fas importantly modify the progenitor self-renewal rate of immature but not of mature cells, and apoptosis rate is strongly modified in mature cells but not in immature ones. The third case is opposite to the second one. It should be noted that the assumption on the three rates that confines them in the interval [0,1], limits maximum values of functions $p_s$ and $a$, so the fourth possible case, when the functions vary a lot on both neighbourhoods is ineligible. Simulations indicated that the response obtained in the first case is weak, that is the system takes more time to come back to the equilibrium. Second case seemed to us biologically more realistic than the third one, hence we chose to use only the second case for the numerical simulations. Nevertheless, it can be noted that the simulation of the third case showed a weaker response, i.e. slower erythrocyte count dynamics, though the rates displayed different dynamics.

In order to obtain a good fit of experimental data, functions $p_s(E\text{-}F)$ and $a(F\text{-}E)$ used for the simulations are

$$p_s(x) = 0.1 + \frac{1.2 \times x^{40}}{1.7^{40} + x^{40}}, \quad a(x) = 0.12 + \frac{1.02 \times x^{40}}{1.5^{40} + x^{40}}.$$

**Table 3**
Steady state values of the main variables of the system.

| Steady states | | Value | Units |
|---|---|---|---|
| Erythrocyte count | $M^*$ | $10^7$ | cells $\mu l^{-1}$ |
| Reticulocyte count | $P_8^*$ | $4.75 \times 10^5$ | cells $\mu l^{-1}$ |
| Erythropoietin level | $Epo^*$ | 5.7 | mU $\mu l^{-1}$ |
| Glucocorticoids level | $GC^*$ | 44.6 | mU $\mu l^{-1}$ |
| Fas–Erk level for immature cells | $F^*$-$E^*$ | $-0.66$ | NU |
| Fas–Erk level for mature cells | $F^*$-$E^*$ | 0.48 | NU |
| Activation rate of Erk $\alpha(Epo^*, GC^*)$ | $\alpha^*$ | 0.21 | $d^{-1}$ |
| Activation rate of Fas $\gamma(P_n^*)$ | $\gamma^*$ | 0.55 | $d^{-1}$ |
| Self-renewal rate of immature cells | $s^*$ | 0.44 | $d^{-1}$ |
| Self-renewal rate of mature cells | $s^*$ | 0.06 | $d^{-1}$ |
| Differentiation rate of immature cells | $d^*$ | 0.45 | $d^{-1}$ |
| Differentiation rate of mature cells | $d^*$ | 0.53 | $d^{-1}$ |
| Apoptosis rate of immature cells | $a^*$ | 0.11 | $d^{-1}$ |
| Apoptosis rate of mature cells | $a^*$ | 0.41 | $d^{-1}$ |

Units of 0.12 and 1.02 for function $a$ are $d^{-1}$, other parameters are dimensionless values.

### 5.4. Steady state values

Since we are going to confront the simulation results with experimental data presented in Fig. 4, we tried to get equilibrium value of erythrocyte count $M^* = 10^7$ cells $\mu l^{-1}$. This implied $HSC = 80$ cells $\mu l^{-1}$ $d^{-1}$. As initial condition for the number of erythrocytes we took 30% of its equilibrium value, which corresponds to the anaemia presented in Fig. 4 (see value of RBC count on day 3). Equilibrium values are taken as initial conditions for all other system variables. Steady state values of the main system components, obtained through the simulation, are presented in Table 3.

As shown in Table 3, in normal erythropoiesis reticulocyte count is 20-fold smaller than erythrocyte count. Progenitor sub-populations $P_1, \ldots, P_7$ are much smaller than $P_8$ (not shown here). The model predicts that 44% of immature progenitors self-renew per day (only 6% of mature progenitors per day), which allows the conclusion that mature progenitors mainly lost their ability to self-renew. Apoptosis rate is high in mature cells (41% $d^{-1}$), whereas it is only 11% $d^{-1}$ in immature cells. About 53% of mature and 45% of immature progenitors differentiate per day, providing that the differentiation remains important in all erythroid cells. Thus, in normal erythropoiesis, immature progenitor sub-populations are characterised by weak apoptosis and comparable self-renewal and differentiation rates. Mature progenitors, however, preferentially differentiate with high apoptosis.

The next section is devoted to numerical simulations of phenylhydrazine-induced anaemia.

## 6. Simulation of phenylhydrazine-induced anaemia and comparison with experimental data

Using parameter values obtained in the previous section, we numerically computed solutions of system formed with Eqs. (4)–(8) and (11), for an anaemia-induced situation: it is assumed that at the beginning of the numerical computations (day 0) the erythrocyte count is lower than its equilibrium value (30% of its equilibrium) due to previous phenylhydrazine injections. Simulations were carried out using MATLAB and results are presented in Figs. 6–10.

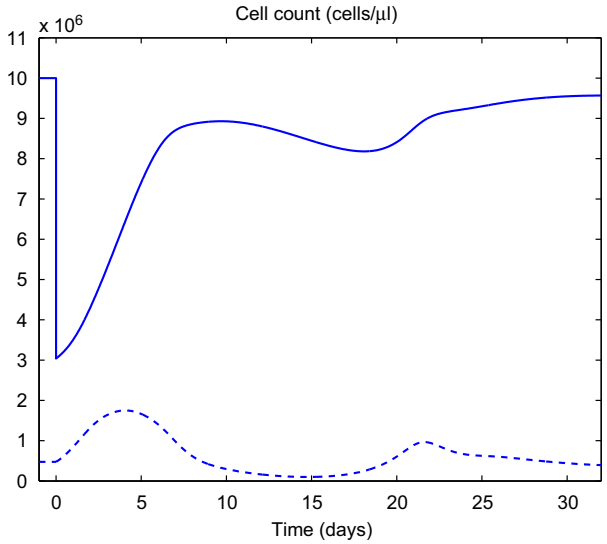


**Fig. 6.** Anaemia simulation. Erythrocyte and reticulocyte count dynamics. Solid curve represents erythrocyte count, dash curve represents reticulocytes. Equilibrium value of erythrocyte count used in the simulation is $M^* = 10^7$ cells $\mu l^{-1}$.

First, dynamics of main variables of the system and of some relevant rates are illustrated: erythrocyte and reticulocyte counts in Fig. 6, erythropoietin and glucocorticoid levels in Fig. 7, Erk and Fas levels in Fig. 8, self-renewal, differentiation and apoptosis rates in Fig. 9. Explanations on the dynamics of the system are proposed. Then results are confronted to experimental data from Fig. 4 in Fig. 10.

All simulations start at day zero. For the sake of clarity, equilibrium values are shown on days -1 to 0.

### 6.1. Erythrocyte and reticulocyte counts

Erythrocyte count (solid line) and reticulocyte count (dash line) dynamics are presented in Fig. 6.

Following the anaemia, erythrocyte count quickly increases and reaches a maximum value (lower than the equilibrium value) after 7 days, then stays there up to day 10. Afterwards, erythrocyte count slowly decreases (days 10–17). Quick increase is observed between days 17 and 21, followed by a gradual return to the equilibrium. Although erythrocyte count globally increases between days 0 and 30, it should be noted that 30 days after anaemia the erythrocyte count is still below its equilibrium value.

At day 0, the reticulocyte count increases to reach a maximum value that equals approximately fourfold of its equilibrium value on day 4, then comes back to its steady state and keeps on decreasing. On day 17, when erythrocyte count is decreasing, the number of reticulocyte increases once again, though less importantly this time.

The first increase of reticulocyte count (up to day 4) is due to a strong increase of mature progenitor differentiation, see Fig. 9 B. Explanations on the behaviour of erythrocyte and reticulocyte counts on day 17 are, however, less straightforward and will be given later in Section 6.5, when confronting the results with experimental data.

### 6.2. Growth factors dynamics

In Fig. 7, erythropoietin and glucocorticoid dynamics are shown. Growth factor levels are strongly perturbed (large

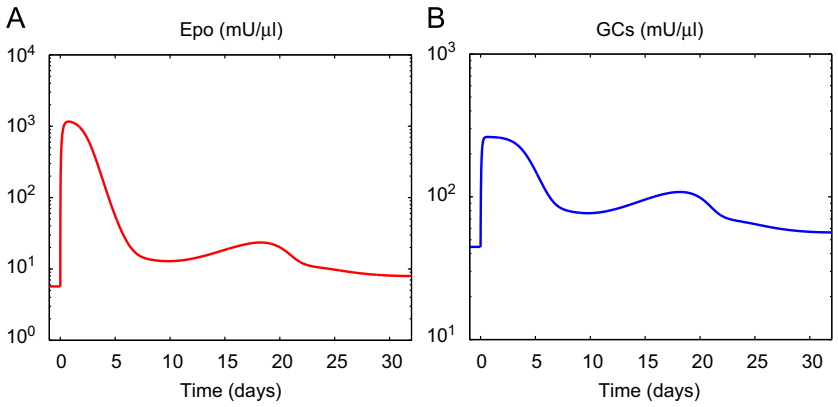


**Fig. 7.** Anaemia simulation. Dynamics of growth factors, shown on logarithmic scale.

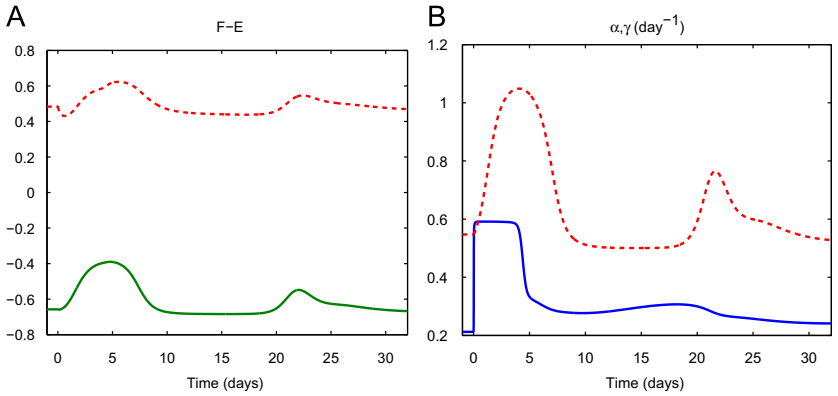


**Fig. 8.** Anaemia simulation. Panel A: dynamics of $F$-$E$ for self-renewing (green solid curve) and differentiating (red dash curve) sub-populations. Panel B: dynamics of $\alpha(Epo, GC)$ (blue solid curve) and $\gamma(P_n)$ (red dash curve).

increase) during the first five days following the anaemia, this perturbation being characterised by a sharp increase of both concentrations on day 1, when the organism lacks erythrocytes. Then values of Epo and GCs levels smoothly return to their equilibria, with small perturbations, in particular they both increase once again on day 17, due to the fall in erythrocyte count (Fig. 6).

As it will be noted in the following sections, two different actions of Epo and GCs appear in the response to anaemia. First, in the early stages of the response to anaemia (between days 0 and 5) mainly Epo inhibits apoptosis (Fig. 9), leading to high proliferation of immature progenitors. Second, from day 6 up to the end of the response, Epo and GCs levels are closer to their equilibrium values and they regulate erythropoiesis mainly through Erk–Fas regulation (Fig. 8).

### 6.3. Erk and Fas levels

Dynamics of variable $F$-$E$ and feedback controls expressed by $\alpha$ and $\gamma$ are presented in Fig. 8. Values of $F$-$E$ in all mature (respectively, in all immature) sub-populations are similar because the feedback by FasL has been supposed to be the same on all cells (see Section 5.2).

On the first day following anaemia the quantity $F$-$E$ decreases. This is more clearly observed for mature cells (red dash curve), yet it also occurs for immature cells (green solid curve). This is due to high values of $\alpha$ (Panel B), the feedback function controlling Erk production. Then, $F$-$E$ increases and reaches its extreme values after 5–6 days following anaemia induction. As one can observe on Panel A, between days 9 and 19 the difference $F$-$E$ has values below its equilibria, which is due to the regulation through $\alpha$ and $\gamma$.

Production of Erk, the feedback control expressed by $\alpha$, is at its maximum during the first four days, while $\gamma$ (production of Fas) is increasing. Then, $\alpha$ sharply decreases almost down to its equilibrium, while $\gamma$ decreases smoothly and reaches its minimum value, where it stays from day 10 up to day 18. On day 18, a new increase of $\gamma$ is observed, due to the increase of the reticulocyte count (Fig. 6). Two different behaviours are observed in $\alpha$ and $\gamma$ dynamics: fast changes ($\alpha$ on days 1 and 4) and modest variations ($\gamma$ between days 1 and 8, and days 18 and 25). Fast changes of $\alpha$ are directly due to sharp Epo and GCs dynamics (see Fig. 7), while modest $\gamma$ dynamics is due to modest evolution of reticulocyte count (see Fig. 6).

### 6.4. Self-renewal, differentiation and apoptosis rates

Self-renewal, differentiation and apoptosis rates are presented in Fig. 9. The three rates exhibit important fluctuations. Their dynamics for immature and mature cell populations are different.

Self-renewal rate varies a lot for all cells. At first sight, it seems not to be the case for mature cells, yet self-renewal equilibrium

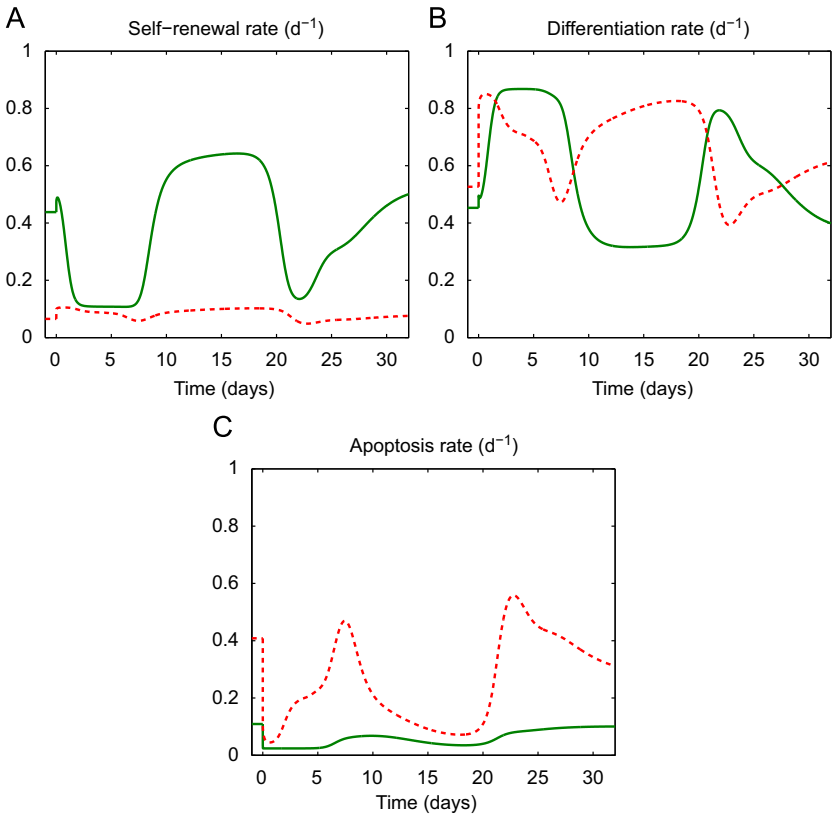


**Fig. 9.** Anaemia simulation. Self-renewal, differentiation and apoptosis rates of immature self-renewing (green solid curve) and mature differentiating (red dash curve) sub-populations.

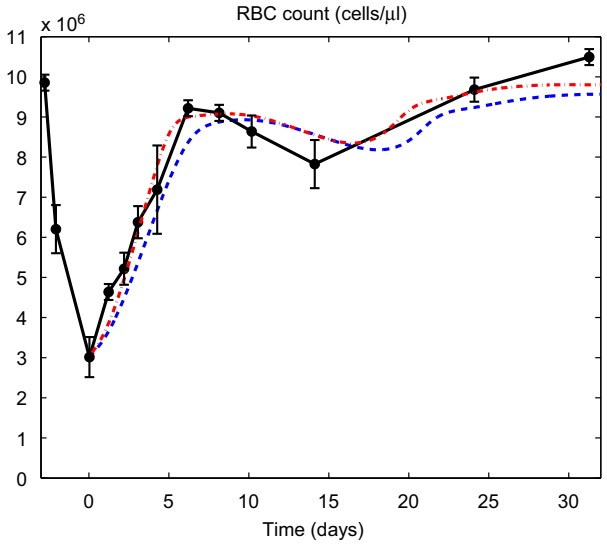


**Fig. 10.** Anaemia simulations. Erythrocyte count dynamics obtained by Cherukuri et al. (2004) in experiments on induced anaemia in mice (black circled solid line), obtained in simulations carried out with $\delta = 1/40\,\mathrm{d}^{-1}$ (blue dash curve) and with $\delta = 1/30\,\mathrm{d}^{-1}$ (red dash-dot curve).

value is small and the variations represent a twofold increase of the equilibrium value. Such important variations are also observed for the two other rates. Moreover, two different types of changes in values of the rates appear in Fig. 9. First, sharp variations appear between days 0 and 1: they are strong, for instance, for mature sub-populations (red dash curves in Fig. 9). Then, after day 1, variations are more gradual, sometimes with large amplitudes.

Taking into account the nature of the feedback controls, we conclude that sudden sharp variations in the three rates right after the induction of anaemia are due to direct inhibition of apoptosis by Epo, independently of the intracellular network based on Erk and Fas, and gradual variations that occur later (after day 2) are due to Erk and Fas regulation. During the first six days these gradual variations are observed for the self-renewal rate (Panel A) and the differentiation rate (Panel B) of immature cells. During days 6–32, the three rates keep on varying gradually, which is due to Erk and Fas variations. These fluctuations are important, suggesting a strong dependence of the rates on Erk and Fas (which at the same time vary modestly), and last longtime (40–45 days, not shown here). These conclusions must, however, be completed by the fact that the influence of Epo on apoptosis rate is observed as long as its levels are not back to equilibrium value, especially for immature self-renewing sub-populations (Fig. 9 C).

It should be noted as well that differentiation in our model is a choice by default, i.e. a cell that is protected against apoptosis and which does not self-renew differentiates.

### 6.5. Confrontation to experimental data

Simulation results and experimental data are presented in Fig. 10. The blue dash curve represents the simulation discussed

above (Fig. 6), the black solid line represents the outcome of experiments by Cherukuri et al. (2004) (Fig. 4).

Let focus on the simulated blue dash curve. First, from days 0 to 7, the computed erythrocyte count increases as fast as observed in the experiments, with only one day delay. From day 10, simulated erythrocyte count decreases in spite of its low value (lower than equilibrium). Similar phenomenon is observed in the experiments (black solid line) from days 8 to 15. The cause of such a decrease in cell numbers although the erythrocyte count is still lower than normal is investigated in the following.

In Fig. 6, reticulocyte count starts decreasing at day 4. Fig. 9 shows that during first four days apoptosis rate is below its equilibrium for mature cells, whereas both self-renewal and differentiation rates are above their equilibrium values. This results in an increase of the number of mature progenitors (not shown here). However, for immature cells the picture is a bit different, self-renewal rate increases a little bit on the first day and then decreases a lot due to high $F$-$E$ values (Fig. 8 A), differentiation rate is higher than at equilibrium, apoptosis rate is lower than at equilibrium. This results in a decrease of the number of immature progenitors (not shown here). Hence, on day 4 the system starts lacking immature cells to maintain the increase of mature progenitors that triggers a decrease of the latter and, thus, of reticulocytes. Apoptosis of mature progenitors is high during days 6–8 (Fig. 9 C), whereas differentiation rate is low (Panel B) and self-renewal is about its steady state (Panel A). This makes reticulocyte count decrease even faster (Fig. 6), go below its equilibrium on day 8, where it stays up to day 19. This, in turn, decreases the supply of mature erythrocytes that results in the reduction of erythrocyte count observed between days 10 and 18. Thus, our model suggests that this decrease of erythrocyte count is a consequence of low self-renewal rate of immature cells during first seven days and of the high apoptosis of mature cells during days 6–8. This, in turn, is due to a high value of $F$-$E$ (Fig. 8 A) and not to Epo control of apoptosis, which is below its equilibrium during these days and should, in contrary, decrease apoptosis rate (Fig. 11). Consequently, this decrease (days 10–18) of the erythrocyte count can be explained by Erk–Fas regulation. It can be compared to the quick increase of erythrocyte count following the anaemia, which is clearly due to an inhibition of progenitor apoptosis by Epo, independently of Erk–Fas regulation.

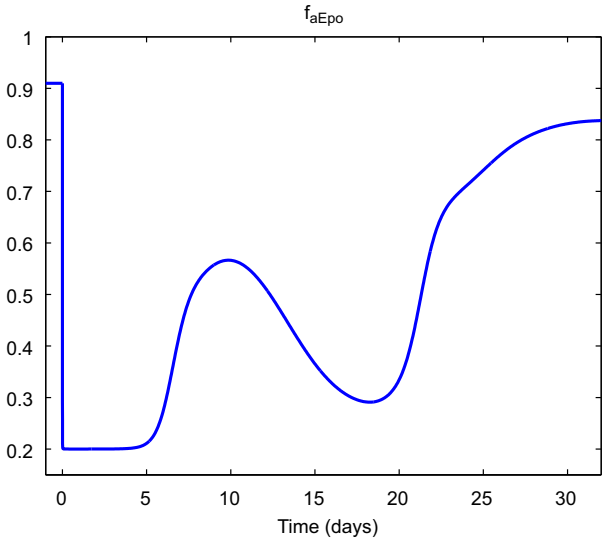


**Fig. 11.** Anaemia simulation. Function $f_{aEpo}(Epo)$.

The above analysis enlightens two different and clear mechanisms of erythropoiesis regulation: first, inhibition of apoptosis by Epo in the early stages of the response to anaemia, and second, a more moderate regulation on the long-term of erythroid progenitor self-renewal, differentiation and apoptosis based on intracellular regulation (Erk and Fas).

Although close to experimental data, the simulated erythrocyte count (blue dash curve) does not appear to be the best fit to the data. Focusing on the nature of the anaemia, that is the consequences of phenylhydrazine use, we can obtain better results.

Phenylhydrazine is known to damage cell membrane, which results in reduced lifetime of erythrocytes following the injections. We tested this assumption with our model, assuming a mortality rate of erythrocytes $\delta = 1/30\,\mathrm{d}^{-1}$, which means the average lifetime of an erythrocyte is reduced to 30 days under the action of phenylhydrazine. Red dash-dot curve in Fig. 10 represents erythrocyte count in this case. It provides a better fit of the data, with a stronger slope on the first days (days 1–5), a smaller undershoot afterward and a faster return to the equilibrium. It should be noted that the current modification of the value of $\delta$ does not alter the above analysis and conclusions, it only allows a better fit of the data. For both simulations presented in Fig. 10, one feature of experimental curve is, however, not well approached: the undershoot in both simulations (observed around day 18) is slower, occurs later and is also smaller than the one obtained in the experiments (observed around day 14).

We confronted our model with other experimental data on phenylhydrazine-induced anaemia, presented in Crauste et al. (2008). In these experiments, haematocrit values were measured during 45 days after anaemia induction. The model used in this work does not a priori provide haematocrit, but only erythrocyte count. Haematocrit $H(t)$ is defined by

$$H(t) = \frac{vM(t)}{vM(t) + \text{Plasma volume}},$$

where $vM(t)$ represents the volume of erythrocytes in the blood. In Crauste et al. (2008) we assumed that the plasma volume was not modified during the experiments and considering normal haematocrit $H^*$ (assumed to equal 50%) and erythrocyte count $M^*$ we obtained

$$H^* = \frac{vM^*}{vM^* + \text{Plasma volume}},$$

which provides

$$\text{Plasma volume} = \frac{1\text{-}H^*}{H^*} vM^*.$$

Consequently, haematocrit can be deduced from the erythrocyte count,

$$H(t) = \frac{M(t)}{M(t) + (1\text{-}H^*)M^*/H^*}.$$

This is displayed in Fig. 12.

To obtain an overshoot on day 5 as presented in Fig. 12, it was necessary to modify functions $f_{aEpo}(Epo), p_s(E\text{-}F)$ and $a(F\text{-}E)$. In particular, the minimum value of $f_{aEpo}$ has been dropped from 0.2 down to 0.1, see (18), functions $p_s(E\text{-}F)$ and $a(F\text{-}E)$ have been modified to have smaller variations on the relevant intervals of $F$-$E$. One can observe that experimental results are properly reproduced by the model, although the decrease following the peak in haematocrit values is slower in the model. Erythrocyte lifespan must be reduced from 40 days to 15 days to obtain these results, similarly to what has been done in Crauste et al. (2008).

Hence, this model is able to reproduce features of a simpler model, and also leads to more insights into regulatory mechanisms of erythropoiesis.

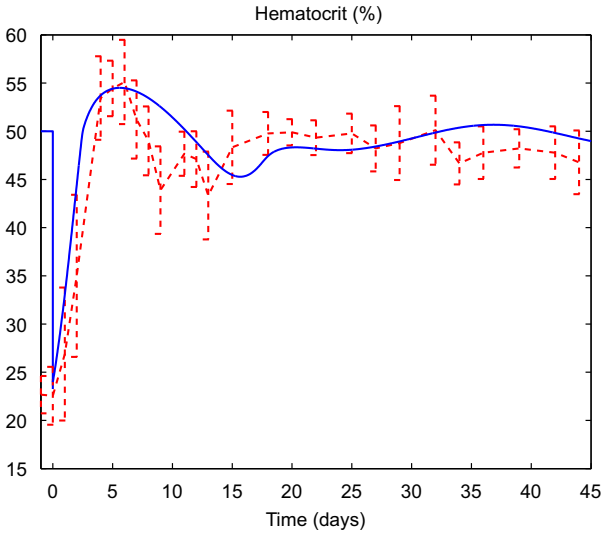


**Fig. 12.** Anaemia simulation. Haematocrit dynamics. Blue solid line represents simulation results, red dash line represents results of experiments on induced anaemia in mice obtained in Crauste et al. (2008). Normal haematocrit is assumed to equal 50%, lifetime of erythrocytes is 15 days.

## 7. Discussion

We built up a new multi-scale mathematical model of erythropoiesis taking into account several biological aspects known up to now. In particular, we considered an intracellular network regulating cell fate, based on two proteins: Erk and Fas. These proteins, together with growth factors (erythropoietin and glucocorticoids), act on cell proliferation, and in turn the number of erythroid progenitor and of erythrocytes controls the production of growth factors and the activation of intracellular proteins. Erythropoietin was also supposed to directly inhibit progenitor apoptosis, and to contribute to intracellular proteins activation.

The resulting mathematical model was briefly analysed and numerically simulated. We focused on simulations of phenylhydrazine-induced anaemia for which parameter values were estimated. Outputs of the model were confronted with experimental data. Although most parameter values were determined through numerical simulations (due to a lack of information in the literature), we then identified two different roles of the feedback controls in response to anaemia: feedback by Epo on apoptosis (inhibition), independently of the intracellular network based on Erk and Fas, was found to be determinant in the early stage of the response, to quickly increase the number of erythrocytes, whereas feedback control through the intracellular regulatory network, introduced in Section 2, was more important later in the response, when the erythrocyte count almost reached its equilibrium value, to regulate on a long-term the response to the stress. This explained, in particular, a surprising fall in erythrocyte count although normal erythrocyte count was still not reached in Cherukuri et al. (2004) data (Fig. 4). It must be noted, however, that Epo has a permanent influence on progenitor apoptosis.

Apart from the study of feedback functions roles and relevance, the model brought some additional features. One deals with the apoptosis rate. The simulation provided that the apoptosis rate in mature sub-populations at the equilibrium (normal erythropoiesis) equals $a^* = 0.41\ \mathrm{d}^{-1}$. Thus, the model suggests that in normal erythropoiesis between 40% and 50% of mature erythroid progenitors undergo apoptosis daily. Such a prediction of the model could be experimentally tested. The model also shows that in stress situations, like anaemia, the organism reacts by temporarily suppressing apoptosis that allows fast recovery of erythrocytes (Fig. 9).

Regarding the model of erythropoiesis, some assumptions deserve to be commented.

All the simulations were performed under the assumption that cell cycle durations were constant, equal to one day. Although there is no evidence that cell cycles vary during response to a stress, nor that such variations could be important, this assumption appears restrictive. In particular, it is responsible in part for the delay observed in the first days of the response for the increase of the erythrocyte count. Hence, considering that cell cycles can be shortened during stress erythropoiesis could enhance the results of the proposed model, by allowing a better fit to the data, and consequently more relevance of the predicted parameters. Nevertheless, the variations of cell cycle durations could not be, to our knowledge, fitted on experimental data and would be decided in a more ad hoc way.

An other point that could potentially lead to a better model concerns the variability in Erk and Fas concentrations within a sub-population of progenitors with the same maturity. In this work we assumed that all erythroid progenitors with the same maturity had similar concentrations of Erk and Fas. Thus, our model does not take into account stochasticity in these expressions, which can play an important role in the regulation of erythropoiesis. One appropriate approach taking into account stochasticity is the individual-based modelling. This considers each cell as an independent element of the whole system and, thus, every cell can have its own properties and protein concentrations.

Let us finally comment on erythropoietin regulation. It is known that Epo levels rise due to the lack of haemoglobin. In this work we did not consider haemoglobin and we assumed that erythrocyte count alters Epo levels (thus implicitly supposing that erythrocyte count and haemoglobin are linearly dependent). Nevertheless, as shown in Cherukuri et al. (2004), there is no linear dependence between haemoglobin and erythrocyte (or red blood cell) count during anaemia. This point can be relevant for the modelling of the response to anaemia. Another point is that no information is currently available about how sensitivity to Epo evolves with maturation. These aspects of Epo regulation should be investigated to improve erythropoiesis modelling.

## Acknowledgements

We would like to thank Samuel Bernard, Stéphane Génieys and Laurent Pujo-Menjouet for useful remarks that allowed to improve the model presented in this paper. We would like to express our gratitude to Dr. Mark Koury for discussions and for the experiments he implemented.

## References

Ackleh, A.S., Deng, K., Cole, C.E., Tran, H.T., 2004. Existence-uniqueness and monotone approximation for an erythropoiesis age-structured model. J. Math. Anal. Appl. 289, 530–544.

Ackleh, A.S., Deng, K., Ito, K., Thibodeaux, J., 2006. A structured erythropoiesis model with nonlinear cell maturation velocity and hormone decay rate. Math. Biosci. 204, 21–48, doi: 10.1016/j.mbs.2006.08.004.

Adimy, M., Crauste, F., 2007. Modelling and asymptotic stability of a growth factor-dependent stem cells dynamics model with distributed delay. Discret. Cont. Dyn. Syst. Ser. B 8 (1), 19–38.

Banks, H.T., Cole, C.E., Schlosser, P.M., Hien, T., 2004. Modelling and optimal regulation of erythropoiesis subject to benzene intoxication. Math. Biosci. Eng. 1 (1), 15–48.

Bauer, A., Tronche, F., Wessely, O., Kellendonk, C., Reichardt, H.M., Steinlein, P., Schutz, G., Beug, H., 1999. The glucocorticoid receptor is required for stress erythropoiesis. Genes Dev. 13, 2996–3002.

Bélair, J., Mackey, M.C., Mahaffy, J.M., 1995. Age-structured and two-delay models for erythropoiesis. Math. Biosci. 128, 317–346, doi: 10.1016/0025-5564(94)00078-E.

Chappell, D., Tilbrook, P.A., Bittorf, T., Colley, S.M., Meyer, G.T., Klinken, S.P., 1997. Prevention of apoptosis in J2E erythroid cells by erythropoietin: involvement of JAK2 but not MAP kinases. Cell Death Differ. 4, 105–113.

Cherukuri, S., Tripoulas, N.A., Nurko, S., Fox, P.L., 2004. Anemia and impaired stress-induced erythropoiesis in aceruloplasminemic mice. Blood Cells Molecules Dis. 33, 346–355.

Chickarmane, V., Enver, T., Peterson, C., 2009. Computational modeling of the hematopoietic erythroid-myeloid switch reveals insights into cooperativity. PLoS Comput. Biol. 5 doi:10.1371/journal.pcbi.1000268.

Crauste, F., Pujo-Menjouet, L., Génieys, S., Molina, C., Gandrillon, O., 2008. Adding self-renewal in committed erythroid progenitors improves the biological relevance of a mathematical model of erythropoiesis. J. Theor. Biol. 250, 322–338, doi: 10.1016/j.jtbi.2007.09.041.

Dazy, S., Damiola, F., Parisey, N., Beug, H., Gandrillon, O., 2003. The MEK-1/ERKs signalling pathway is differentially involved in the self-renewal of early and late avian erythroid progenitor cells. Oncogene 22, 9205–9216.

De Maria, R., Testa, U., Luchetti, L., Zeuner, A., Stassi, G., Pelosi, E., Riccioni, R., Felli, N., Samoggia, P., Peschle, C., 1999. Apoptotic role of Fas/Fas ligand system in the regulation of erythropoiesis. Blood 93, 796–803.

Demin, I., Crauste, F., Gandrillon, O., Volpert, V., 2010. A multi-scale model of erythropoiesis. J. Biol. Dyn. 4, 59–70.

Finch, C.A., Hanson, M.L., Donohue, D.M., 1959. Kinetics of erythropoiesis. A comparison of response to anemia induced by phenylhydrazine and by blood loss. Am. J. Physiol. 197, 761–764.

Fortin, P., Mackey, M.C., 1999. Periodic chronic myelogenous leukemia: spectral analysis of blood cell counts and aetiological implications. Br. J. Haematol. 104, 336–345.

Gandrillon, O., Schmidt, U., Beug, H., Samarut, J., 1999. TGF-beta cooperates with TGF-alpha to induce the self-renewal of normal erythrocytic progenitors: evidence for an autocrine mechanism. Embo J. 18, 2764–2781.

Gregory, T., Yu, C., Ma, A., Orkin, S.H., Blobel, G.A., Weiss, M.J., 1999. GATA-1 and erythropoietin cooperate to promote erythroid cell survival by regulating bcl-xL expression. Blood 94, 87–96.

Huang, S., Guo, Y.-P., May, G., Enver, T., 2007. Bifurcation dynamics in lineage-commitment in bipotent progenitor cells. Dev. Biol. 305, 695–713.

Koury, M.J., Bondurant, M.C., 1990. Erythropoietin retards DNA breakdown and prevents programmed death in erythroid progenitor cells. Science 248, 378–381.

Kowal-Vern, A., Mazzella, F.M., Cotelingam, J.D., Shrit, M.A., Rector, J.T., Schumacher, H.R., 2000. Diagnosis and characterization of acute erythroleukemia subsets by determining the percentages of myeloblasts and proerythroblasts in 69 cases. Am. J. Hematol. 65, 5–13.

Liapi, C., Chrousos, G.P, 1992. In: Yaffe, S.J., Aranda, J.V. (Eds.), Pediatric Pharmacology. second ed. W.B. Saunders Company, Philadelphia, pp. 466–475 (Chapter 41).

Mackey, M.C., 1978. Unified hypothesis of the origin of aplastic anaemia and periodic hematopoiesis. Blood 51, 941–956.

Mackey, M.C., 1979. Dynamic hematological disorders of stem cell origin. In: Vassileva-Popova, G., Jensen, E.V. (Eds.), Biophysical and Biochemical Information Transfer in Recognition. Plenum Press, New York, pp. 373–409.

Mackey, M.C., Rudnicki, R., 1994. Global stability in a delayed partial differential equation describing cellular replication. J. Math. Biol. 33, 89–109.

Madan, A., Lin, C., Wang, Z., Curtin, P.T., 2003. Autocrine stimulation by erythropoietin in transgenic mice results in erythroid proliferation without neoplastic transformation. Blood Cells Molecules Dis. 30, 82–89.

Mahaffy, J.M., Belair, J., Mackey, M.C., 1998. Hematopoietic model with moving boundary condition and state dependent delay: applications in erythropoiesis. J. Theor. Biol. 190, 135–146, doi: 10.1006/jtbi.1997.0537.

Mazzella, F.M., Alvares, C., Kowal-Vern, A., Schumacher, H.R., 2000. The acute erythroleukemias. Clin. Lab. Med. 20, 119–137.

Munugalavadla, V., Kapur, R., 2005. Role of c-Kit and erythropoietin receptor in erythropoiesis. Crit. Rev. Oncol./Hematol. 54, 63–75.

Nagata, Y., Takahashi, N., Davis, R.J., Todokoro, K., 1998. Activation of p38 MAP kinase and JNK but not ERK is required for erythropoietin-induced erythroid differentiation. Blood 92, 1859–1869.

Piroso, E., Erslev, A.J., Flaharty, K.K., Caro, J., 1991. Erythropoietin life span in rats with hypoplastic and hyperplastic bone marrows. Am. J. Hematol. 36, 105–110.

Ridley, D.M., Dawkins, F., Perlin, E., 1994. Erythropoietin: a review. J. Natl. Med. Assoc. 86, 129–135.

Roeder, I., Glauche, I., 2006. Towards an understanding of lineage specification in hematopoietic stem cells: a mathematical model for the interaction of transcription factors GATA-1 and PU.1. J. Theor. Biol. 241, 852–865, doi: 10.1016/j.jtbi.2006.01.021.

Rubiolo, C., Piazzolla, D., Meissl, K., Beug, H., Huber, J.C., Kolbus, A., Baccarini, M., 2006. A balance between Raf-1 and Fas expression sets the pace of erythroid differentiation. Blood 108, 152–159.

Sawyer, S.T., Jacobs-Helber, S.M., 2000. Unraveling distinct intracellular signals that promote survival and proliferation: study of erythropoietin, stem cell factor, and constitutive signaling in leukemic cells. J. Hematother. Stem Cell Res. 9, 21–29.

Spivak, J.L., Pham, T., Isaacs, M., Hankins, W.D., 1991. Erythropoietin is both a mitogen and a survival factor. Blood 77, 1228–1233.

Sui, X., Krantz, S.B., You, M., Zhao, Z.J., 1998. Synergistic activation of MAP kinase (ERK1/2) by erythropoietin and stem cell factor is essential for expanded erythropoiesis. Blood 92, 1142–1149.

Sui, X., Krantz, S.B., Zhao, Z.J., 2000. Stem cell factor and erythropoietin inhibit apoptosis of human erythroid progenitor cells through different signalling pathways. Br. J. Haematol. 110, 63–70.

Vainchenker, W., Dusa, A., Constantinescu, S.N., 2008. JAKs in pathologies: role of Janus kinases in hematopoietic malignancies and immunodeficiencies. Semin. Cell Dev. Biol. 19, 385–393.

Weissman, I.L., 2000. Stem cells: units of development, units of regeneration, and units in evolution. Cell 100, 157–168, doi: 10.1016/S0092-8674(00)81692-X.

Wichmann, H.E., Loeffler, M., 1985. Mathematical Modeling of Cell Proliferation. CRC, Boca Raton, FL.

Wichmann, H.E., Loeffler, M., Pantel, K., Wulff, H., 1989. A mathematical model of erythropoiesis in mice and rats. Part 2. Stimulated erythropoiesis. Cell Tissue Kinet. 22, 31–49.

Wulff, H., Wichmann, H.E., Loeffler, M., Pantel, K., 1989. A mathematical model of erythropoiesis in mice and rats. Part 3. Suppressed erythropoiesis. Cell Tissue Kinet. 22, 51–61.

## 5.7 Fisher et al. (2012)

Manuscrit de l'article : [69] S. Fischer, P. Kurbatova, N. Bessonov, O. Gandrillon, V. Volpert, F. Crauste, *Modelling erythroblastic islands : using a hybrid model to assess the function of central macrophage*, Journal of Theoretical Biology, 298, 92–106 (2012).

Journal of Theoretical Biology 298 (2012) 92–106

Contents lists available at SciVerse ScienceDirect

Journal of Theoretical Biology

journal homepage: www.elsevier.com/locate/yjtbi

# Modeling erythroblastic islands: Using a hybrid model to assess the function of central macrophage

S. Fischer [a], P. Kurbatova [b,c], N. Bessonov [d], O. Gandrillon [c,e], V. Volpert [b,c], F. Crauste [b,c,*]

[a] Université de Lyon, CNRS, INRIA, INSA-Lyon, LIRIS Combining, UMR 5205, F-69621, France
[b] Université de Lyon, Université Lyon 1, CNRS UMR 5208, Institut Camille Jordan, 43 blvd du 11 novembre 1918, F-69622 Villeurbanne-Cedex, France
[c] INRIA Team Dracula, INRIA Grenoble Rhône-Alpes Center, France
[d] Institute of Mechanical Engineering Problems, 199178 Saint Petersburg, Russia
[e] Université de Lyon, Université Lyon 1, CNRS UMR 5534, Centre de Génétique et de Physiologie Moléculaire et Cellulaire, F-69622 Villeurbanne-Cedex, France

ARTICLE INFO

*Article history:*
Received 14 June 2011
Received in revised form
10 November 2011
Accepted 3 January 2012
Available online 11 January 2012

*Keywords:*
Hybrid model
Erythropoiesis
Erythroblastic island
Macrophage

ABSTRACT

The production and regulation of red blood cells, erythropoiesis, occurs in the bone marrow where erythroid cells proliferate and differentiate within particular structures, called erythroblastic islands. A typical structure of these islands consists of a macrophage (white cell) surrounded by immature erythroid cells (progenitors), with more mature cells on the periphery of the island, ready to leave the bone marrow and enter the bloodstream. A hybrid model, coupling a continuous model (ordinary differential equations) describing intracellular regulation through competition of two key proteins, to a discrete spatial model describing cell–cell interactions, with growth factor diffusion in the medium described by a continuous model (partial differential equations), is proposed to investigate the role of the central macrophage in normal erythropoiesis. Intracellular competition of the two proteins leads the erythroid cell to either proliferation, differentiation, or death by apoptosis. This approach allows considering spatial aspects of erythropoiesis, involved for instance in the occurrence of cellular interactions or the access to external factors, as well as dynamics of intracellular and extracellular scales of this complex cellular process, accounting for stochasticity in cell cycle durations and orientation of the mitotic spindle. The analysis of the model shows a strong effect of the central macrophage on the stability of an erythroblastic island, when assuming the macrophage releases pro-survival cytokines. Even though it is not clear whether or not erythroblastic island stability must be required, investigation of the model concludes that stability improves responsiveness of the model, hence stressing out the potential relevance of the central macrophage in normal erythropoiesis.



## 1. Introduction

Hematopoiesis, the process of production and regulation of all blood cell types, has been the topic of modeling works for decades. Dynamics of hematopoietic stem cells have been described by Mackey's early works (Mackey, 1978, 1979), and later developed by Mackey and co-authors (Mackey and Rudnicki, 1994, 1999) as well as Loeffler and co-workers (Roeder, 2006; Wichman and Loeffler, 1985; Wichmann et al., 1985). The white blood cell production process has been modeled in order to illustrate some pathological cases, such as effects of radiations (Wichman and Loeffler, 1985; Wichmann et al., 1985), and brought some information on hematological diseases, mainly leukemia (Bernard et al., 2004; Colijn and Mackey, 2005; Foo et al., 2009; Michor et al., 2005; Michor, 2007, 2008; Scholz et al., 2005) and cyclical neutropenia (Bernard et al., 2003; Colijn and Mackey, 2005; Haurie et al., 1998). The platelet production process attracted less attention through years (Eller et al., 1987; Wichmann et al., 1979), with however some modeling effort in the 2000's (Apostu and Mackey, 2008; Santillan et al., 2000; Scholz et al., 2010). The red blood cell production process (erythropoiesis) has recently been the focus of modeling in hematopoiesis. Early works by Wichmann et al. (1989), Wulff et al. (1989), Bélair et al. (1995), and Mahaffy et al. (1998), on the regulation of cell population kinetics (mainly erythroid progenitors and mature red blood cells) have been completed by recent works (Ackleh et al., 2006; Adimy et al., 2006; Banks et al., 2004). Particular attention was paid to the relevance of erythroid progenitor self-renewal in response to stress and considering multiscale approaches (Bessonov et al., in press, 2010; Crauste et al., 2008, 2010), that is including both cell population kinetics andintracellular regulatory networks dynamics in the models, in order to give insight in the mechanisms involved in erythropoiesis. A case study of erythropoiesis is anemia (Savill et al., 2009), which allows observing the

* Corresponding author at: Université de Lyon, Université Lyon 1, CNRS UMR 5208, Institut Camille Jordan, 43 blvd du 11 novembre 1918, F-69622 Villeurbanne-Cedex, France. Tel.: +33 472 448 516; fax: +33 472 431 687.
*E-mail address:* crauste@math.univ-lyon1.fr (F. Crauste).

0022-5193/$ - see front matter © 2012 Elsevier Ltd. All rights reserved.
doi:10.1016/j.jtbi.2012.01.002

system in a stress situation that can be easily induced (at least in mice). A model of all hematopoietic cell lineages has been proposed by Colijn and Mackey (2005), including dynamics of hematopoietic stem cells and white cell, red blood cell and platelet lineages.

Other modeling approaches, developed by Veng-Pedersen and co-workers (Chapel et al., 2000; Freise et al., 2008; Veng-Pedersen et al., 2002; Woo et al., 2006, 2008), focused on pharmacodynamics/pharmacokinetics (PK/PD) models of erythropoiesis. Such approaches are usually centered on parameter estimation and model fitting to data using statistical approaches. Nevertheless, none of the previously mentioned approaches did consider spatial aspects of hematopoiesis. Models describe cell population kinetics, either in the bone marrow or the spleen (where cell production and maturation occurs) or in the bloodstream (where differentiated and mature cells ultimately end up). Consequently, cellular regulation by cell–cell interaction was not considered in these models.

We focus here on erythropoiesis modeling. Erythropoiesis consists in the differentiation and maturation of very immature blood cells, called progenitors, produced by differentiation of hematopoietic stem cells in the bone marrow. These erythroid progenitors differentiate through successive divisions and under the action of external signals into more and more mature cells, up to a stage called reticulocytes, which are almost differentiated red blood cells. After nuclei ejection, reticulocytes enter the bloodstream and finish their differentiation process to become erythrocytes (mature red blood cells). At every step of this differentiation process, erythroid cells can die by apoptosis (programmed cell death), and erythroid progenitors have been shown to be able to self-renew under stress conditions (Bauer et al., 1999; Gandrillon, 2002; Gandrillon et al., 1999; Pain et al., 1991). Moreover, cell fate is partially controlled by external feedback controls. For instance, death by apoptosis has been proved to be mainly negatively regulated by erythropoietin (Epo), a growth factor released by the kidneys when the organism lacks red blood cells (Koury and Bondurant, 1990). Self-renewal is induced by glucocorticoids (Bauer et al., 1999; Gandrillon, 2002; Gandrillon et al., 1999; Pain et al., 1991), but also by Epo (Rubiolo et al., 2006; Spivak et al., 1991) and some intracellular autocrine loops (Gandrillon et al., 1999; Sawyer and Jacobs-Helber, 2000).

In addition to intracellular regulation of cell fate and feedback induced either by mature red blood cells or reticulocytes on erythroid progenitors, an important aspect of erythropoiesis lays in the structure of the bone marrow. Erythroid progenitors are indeed produced in specific micro-environments, called niches (Tsiftsoglou et al., 2009), where erythroblastic islands develop. An erythroblastic island consists of a central macrophage surrounded by erythroid progenitors (Chasis and Mohandas, 2008). The macrophage appears to act on surrounding cells, by affecting their proliferation and differentiation programs. For years, however, erythropoiesis has been studied under the influence of erythropoietin, which may induce differentiation and proliferation in vitro without the presence of the macrophage. Hence, the roles of the macrophage and the erythroblastic island have been more or less neglected. Consequently, spatial aspects of erythropoiesis (and hematopoiesis, in general) have usually not been considered when modeling cell population evolution or hematological disease appearance and treatment.

We propose a new multiscale model for cell proliferation (Bessonov et al., in press, 2010), applied to erythropoiesis in the bone marrow, based on hybrid modeling. This approach, taking into account both interactions at the cell population level and regulation at the intracellular level, allows to study cell proliferation at different scales and to account for spatial interactions. Moreover, the 'hybrid' modeling consists in considering a continuous model at the intracellular scale (that is, deterministic or stochastic differential equations), where protein competition occurs, and a discrete model to describe cell evolution (every cell is a single object evolving off-lattice and interacting with surrounding cells and the medium), hence allowing to consider small population effects as well as random effects. Hybrid multiscale models have been recently developed and used mainly, but not exclusively, to model solid tumor growth (Alarcon, 2009; Hoehme and Drasdo, 2010; Jeon et al., 2010; Osborne et al., 2010; Patel et al., 2001; Ramis-Conde et al., 2009; Salazar-Ciudad and Jernvall, 2010; Spencer et al., 2006).

In this hybrid model, cells can either self-renew, differentiate or die by apoptosis, depending on the state of the environment and the state of the cell itself. A global feedback control mediated by the population of mature red blood cells (through erythropoietin release) is supposed to positively influence erythroid progenitor proliferation (Rubiolo et al., 2006; Spivak et al., 1991) and inhibit their death by apoptosis (Koury and Bondurant, 1990). A local feedback control, mediated by reticulocytes, is supposed to induce both differentiation and death by apoptosis (De Maria et al., 1999). Global and local feedback controls act by directly modifying the activity of intracellular proteins. A set of two proteins, Erk and Fas, has been shown (Rubiolo et al., 2006) to be involved in an antagonist loop where Erk, from the MAPK family, inhibits Fas (a TNF family member) and self-activates. High levels of Erk induce cell proliferation depending on Epo levels, whereas Fas inhibits Erk and induces apoptosis and differentiation. Competition between these two proteins is considered here in order to determine cell fate.

The motivation to develop and analyze such a hybrid model (which, even in a rather simple form, is a complex model) is to be able to investigate both intracellular and extracellular regulation of erythropoiesis by taking into account the spatial structure of erythroblastic islands, in order to determine the influence of specific spatial structures on erythropoiesis. To our knowledge, this is the first attempt to model erythropoiesis by taking these aspects into account. In this work, we focus in particular on the question of the role of the macrophage located at the heart of the island, and the respective positioning of immature cells (located nearby the macrophage) and the more mature cells at the periphery. This question arises from the fact, as mentioned above, that due to the strong potential of Epo to induce differentiation and proliferation in vitro in the absence of macrophages, this organization has not been really investigated up to now, but only hypothesized (De Maria et al., 1999). We then consider different modeling situations, with and without macrophage at the center of the island, and analyze actions of the feedback controls, especially regarding the feedback of the macrophage on erythroid cell proliferation and differentiation. The 'classical' structure of the erythroblastic island, with the macrophage at the center and immature erythroid cells surrounding it, will be shown to make the hybrid model stable (so the island can be sustained for an unlimited number of cell cycles) and robust to perturbations due to global and local feedback controls, enlightening a crucial role of the macrophage in vivo erythropoiesis. This result, although qualitatively analyzed in this work, can enable quantitative predictions regarding in vivo regulation of erythropoiesis, for instance when confronted to a severe anemia (Crauste et al., 2008, 2010; Savill et al., 2009). Such predictions, however, are not made in this work which focuses on the study of the role of the macrophage within the erythroblastic island.

The next section is devoted to the presentation of the multiscale hybrid model. First, we focus on the intracellular scale, detailing regulatory networks considered in this work, described by nonlinear ordinary differential equations, and investigating their properties, in particular regarding the existence and stability of steady states associated to cell self-renewal, differentiation and death by apoptosis. Second, we concentrate on the extracellular

scale, which consists of erythroid cell populations, possibly a macrophage, bone marrow medium, and is described by a computational model. Interactions between cells and with the surrounding medium are presented. Finally, we justify the coupling of both scales, through global and local feedback controls, and we discuss parameters of the model. In Section 3 we present the analysis of the hybrid model. This analysis consists of two parts: first, we consider an erythroblastic island without a macrophage in its center, and investigate the stability of the island and the roles of feedback controls in the stability. Next we study an island consisting of immature erythroid cells surrounding a macrophage, and the roles of feedback controls in its stability. This analysis stresses out the central role of the macrophage in the stability of the erythroblastic island, and consequently the relevance of considering spatial aspects when modeling erythropoiesis.

## 2. Model

We introduce, in this section, the hybrid model for erythropoiesis used later for in silico experiments. It consists in the coupling of two models, with different space and time scales. The first model describes intracellular dynamics, represented by regulatory networks based on specific protein competition. This intracellular dynamical level is modeled with a continuous approach, namely ordinary differential equations. The second model is at cell population level, where discrete cells and events are computed, so that stochasticity due to random events (cell cycle duration, orientation of the mitotic spindle at division) and small population effects plays an important role. Extracellular regulation by growth factors is partially due to continuous models (partial differential equations). Such discrete-continuous models are usually called hybrid models (Bessonov et al., 2010; Hoehme and Drasdo, 2010; Osborne et al., 2010; Patel et al., 2001; Ramis-Conde et al., 2009; Salazar-Ciudad and Jernvall, 2010; Spencer et al., 2006). We hereafter present how the model is defined at each scale and how the different levels interact.

### 2.1. Intracellular scale: mathematical model

Although all identified proteins playing a role in erythropoiesis cannot reasonably be considered at this stage, a system of ordinary differential equations is introduced to describe competition between two key proteins, Erk and Fas (De Maria et al., 1999; Rubiolo et al., 2006), whose levels of expression lead either to cell self-renewal, differentiation, or death by apoptosis. This competition is driven by protein-related mechanisms and external factors concentrations. The objective is to get intracellular dynamics able to generate three distinct erythroid progenitor behaviors (self-renewal, differentiation, apoptosis) depending on the values of external parameters and of the inner dynamics of the system. In order to define such a framework, existence of steady states, stability, and roles of feedback controls are investigated.

#### 2.1.1. ODE system

Precise intracellular regulatory mechanisms involved in erythroid progenitor cell fate are largely unknown. Based on the current knowledge, we decided to focus on a simplified regulatory network based on two proteins, Erk and Fas, responsible for cell self-renewal and proliferation, and cell differentiation and apoptosis respectively (Crauste et al., 2008; Dazy et al., 2003; Demin et al., 2010; De Maria et al., 1999; Rubiolo et al., 2006). These proteins are antagonists: they inhibit each other's expression. They are also subject to external regulation, through feedback loops.

On the one hand, reticulocytes (differentiated erythroid cells) produce Fas-ligand which is fixed to their exterior cell membrane. Fas-ligand activates Fas, which induces erythroid progenitor differentiation and apoptosis (Rubiolo et al., 2006). On the other hand, the quantity of erythrocytes in bloodstream determines the release of erythropoietin and other growth factors. Erythropoietin is known to inhibit erythroid progenitor apoptosis (Koury and Bondurant, 1990) and to stimulate immature erythroid progenitor self-renewal (Rubiolo et al., 2006; Spivak et al., 1991). Other growth factors, like glucocorticoids (Bauer et al., 1999; Gandrillon, 2002; Gandrillon et al., 1999; Pain et al., 1991), also increase erythroid progenitor self-renewal by activating Erk. Yet, we only focus here on the action of erythropoietin. The only other growth factors we consider are the ones released by the macrophage, within the erythroblastic island. They are pro-survival factors (Rhodes et al., 2008) performing a local feedback control.

The simplified system of Erk–Fas interactions considered as the main regulatory network for erythroid progenitor fate is then (Crauste et al., 2010)

$$\frac{dE}{dt} = (\alpha(Epo,GF)+\beta E^k)(1-E)-aE-bEF, \tag{1}$$

$$\frac{dF}{dt} = \gamma(F_L)(1-F)-cEF-dF, \tag{2}$$

where $E$ and $F$ denote intracellular normalized levels of Erk and Fas. Eq. (1) describes how Erk level evolves by activation through growth factors (function $\alpha$ of erythropoietin, denoted by *Epo*, and macrophage-emitted growth factors, denoted by *GF*) and self-activation (parameters $\beta$ and $k$). In the meantime, Erk is linearly degraded with a rate $a$ and is inhibited by Fas with a rate $bF$.

Eq. (2) is very similar, except there is no proof for Fas self-activation. Fas is however activitated by Fas-ligand, denoted by $F_L$, through the function $\gamma(F_L)$, it is degraded with a rate $d$ and inhibited by Erk with a rate $cE$.

In order to explore the parameter space efficiently and determine the possible behaviors of the cell, it is relevant to study the mathematical interpretation of parameters.

#### 2.1.2. Brief analysis: existence and stability of steady states

For fixed values of *Epo*, *GF* and $F_L$, (1) and (2) is a closed system of ordinary differential equations. In order to analyze the impact of each parameter on the system's behavior, we can derive analytical forms of the null-clines associated with each equation. The null-cline $f$ associated with Eq. (1) is

$$f(E) = \frac{1}{b}\left(\frac{\alpha}{E}-\beta E^{k-1}(1-E)-(a+\alpha)\right). \tag{3}$$

The null-cline $g$ associated with Eq. (2) is

$$g(E) = \frac{\frac{\gamma}{c}}{\frac{\gamma+d}{c}+E}. \tag{4}$$

The shape of the null-clines depends only on 4 and 2 parameters respectively ($\alpha/b$, $\beta/b$, $k$ and $a/b$ for $f$, $\gamma/c$ and $d/c$ for $g$), the 2 remaining parameters ($b$ and $c$, related to cross-inhibition) only affecting the absolute and relative speeds of the dynamics along each dimension. The existence of steady states, defined as intersections of the two null-clines, thus only depends on the former 6 parameters.

Let us stress out that $\alpha$ represents the influence of external factors (erythropoietin, growth factors) on Erk activation, $\beta$ is related to Erk self-activation, and $\gamma$ describes the influence of Fas-ligand on Fas activation.

By noticing that $f$ is the sum of three components, the impact of each parameter can easily be observed. The same can be done for $g$. Fig. 1 shows that the variations of the null-clines are quite constrained, with a central role of $\alpha$ and $\beta$ for $f$ and $\gamma$ for $g$.

One may note that the effect of $k$ is not shown, since $k=2$ in all experiments. It is however noticeable that increasing $k$ simply decreases the maximum value of the polynomial part of $f$ toward 0 while increasing the value for which it is reached toward 1.

Simple considerations show that the null-clines can only cross in the $[0,1]\times[0,1]$ domain. Furthermore, they intersect at least once, so there is at least one steady state, and there can be only up to three steady states. When there is only one steady state, it is stable. When there are three steady states, the central point is unstable and the two surrounding points are stable (Crauste et al., 2010). The case with two steady states is singular hence not really relevant.

Thus, the system exists in two configurations that we will call monostable (one stable state) and bistable (two stable states). The next step is to determine how the system can go from one state to the other one. Thanks to Fig. 2, two kinds of bifurcations can be imagined to achieve this goal.

Let us first start with the case where $\beta$ is large compared to $\alpha$, that is Erk self-activation rate is stronger than external activators (Epo for instance). In this case, $f$ has two local extrema (Fig. 2A). If $\gamma$, which is associated with Fas-ligand, varies then a double saddle-point bifurcation (or fold bifurcation) occurs. For low and high values of Fas-ligand (that is low and high values of $\gamma$, respectively), there is only one stable steady state, whereas for medium values of Fas ligand two stable points coexist, a separatrix determining the attractive domain of each point (Fig. 2B).

Now consider the case where $\alpha$ is large compared to $\beta$. Then $f$ becomes strictly decreasing and, if $\alpha$ is sufficiently large, there will be only one steady state for every value of $\gamma$. The system is thus strictly monostable (Fig. 2C).

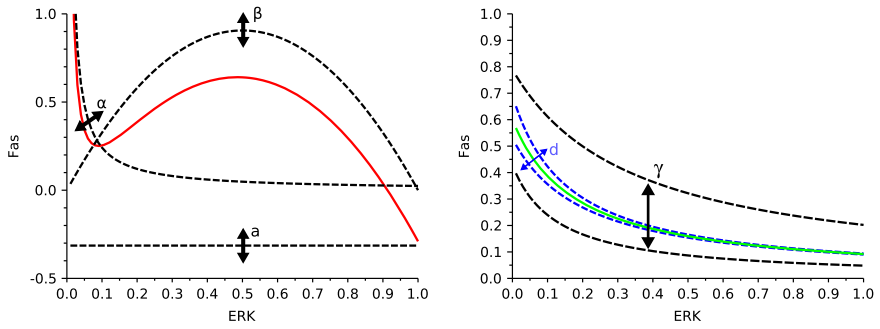


**Fig. 1.** Null-clines $f$ and $g$ defined in (3) and (4). Left panel: the $f$ null-cline (solid red line) and the impact of parameters of Eq. (1). Right panel: the $g$ null-cline (solid green line) and the impact of parameters of Eq. (2). (For interpretation of the references to color in this figure legend, the reader is referred to the web version of this article.)

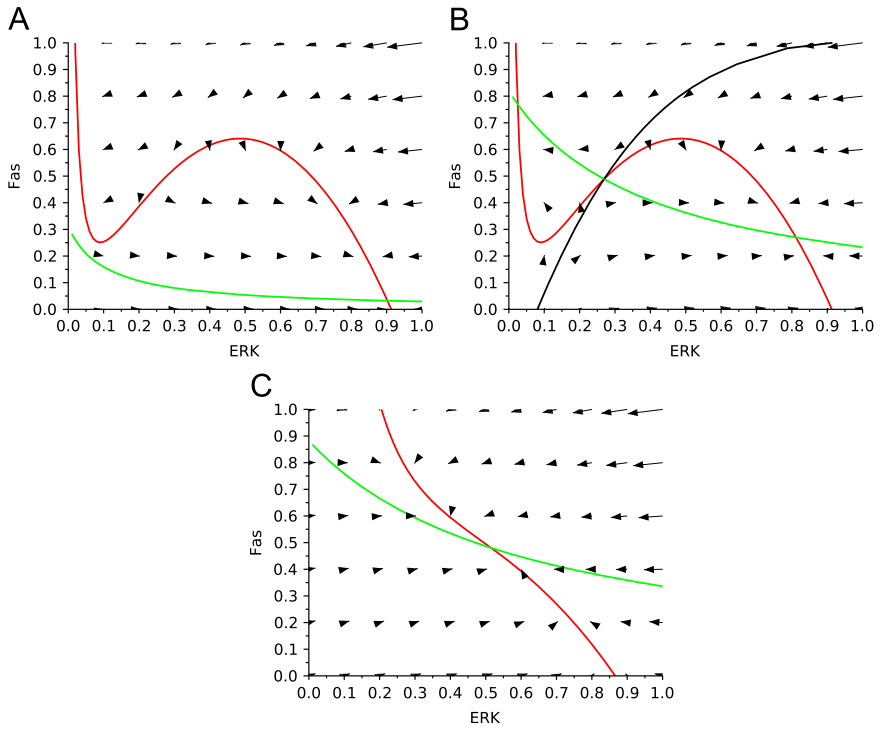


**Fig. 2.** Three possible and characteristic configurations of the system (3) and (4). The red line represents the $f$ null-cline, the green line the $g$ null-cline. Arrows indicate directions of the solutions of system (1) and (2) in the (Erk,Fas) phase plane. A: low value of $\alpha$, low value of $\gamma$. B: low value of $\alpha$, medium value of $\gamma$ (the black curve is the separatrix). C: high value of $\alpha$ compared to $\beta$. (For interpretation of the references to color in this figure legend, the reader is referred to the web version of this article.)

In conclusion, the system (3) and (4) exists in two different configurations: when $\alpha$ is low it is locally bistable, depending on the value of $\gamma$, and when $\alpha$ is high, it is strictly monostable. A kind of fork bifurcation occurs when $\alpha$ increases (approximately around $\alpha=\beta/27$, but exact value depends on other parameters).

### 2.1.3. Dynamics of the ODE system

System (1) and (2) must be able to divide the erythroid progenitor cell population into three different types: self-renewing, apoptotic and differentiating cells. Differentiation corresponds to low values of Fas and Erk at the end of the cycle, apoptosis to high values of Fas, and self-renewal to high values of Erk and reasonable values of Fas (Crauste et al., 2010; Rubiolo et al., 2006).

A simple idea to achieve such a behavior is to introduce two threshold values. The first one, $F_{cr}$, induces apoptosis when reached. The second one, $E_{cr}$, determines the choice between self-renewal and differentiation for cells reaching the end of their cycle. So the phase plane of system (1) and (2) can be divided in three parts: cells having low Erk and Fas values differentiate at the end of their cycle, cells having Erk values greater than $E_{cr}$ self-renew at the end of their cycle, and cells reaching Fas values greater than $F_{cr}$ die immediately by apoptosis.

In order to get three robust cell subpopulations, it is necessary to determine how to correctly place these thresholds. Therefore, cases where the system is either strictly monostable or locally bistable have to be considered.

Let us focus on the dynamics of system (1) and (2) for a fixed value of $\alpha$. One may note that, since the feedback control mediated by Epo is global and acts similarly on each cell, then in the absence of a macrophage emitting growth factors (that is $GF=0$), $\alpha$ has an identical value for all cells. On the contrary, $\gamma$ represents a feedback control by a local factor (Fas-ligand emitted by reticulocytes and acting at short-range, see Section 2.2) so all cell positions on the phase-plane will depend on their own exposition to Fas-ligand.

If the system is strictly monostable, then, independently from its starting position in the $(E,F)$-plane, a cell will converge toward a unique stable state, located on the $f$ null-cline and defined only by its exposition to Fas-ligand (the value of $\gamma$). So, at steady-state, if cells are exposed to a continuum of Fas-ligand values, they will be continuously located along the $f$ null-cline, and their level of Erk will not change: there is no real subpopulation. It is thus quite inefficient to work at steady-state (lack of robustness) to get three subpopulations corresponding to the three possible cell fates in the monostable case.

On the contrary, if the system is locally bistable, cells will still be asymptotically located along the $f$ null-cline, yet a part of it is unstable (roughly speaking the ascending part, see Fig. 1) so cells will be separated into two subpopulations. In this case, the starting point is important: depending on its position, a cell will converge either toward the upper or the lower stable branch of $f$.

Based on these observations, we considered two different initial conditions and dynamics to get the three expected cell subpopulations.

In a first scenario, called the 'out of equilibrium' case, all cells are arbitrarily put at the origin (that is $E=0$ and $F=0$) at the beginning of their cycle (see Fig. 3, left) and, before they have reached a steady-state, they are forced to take a decision based on Erk and Fas levels. This is based on the idea that, if working at steady-state does not allow to obtain distinct subpopulations, then working out of steady-state may be relevant.

When the system is strictly monostable, this solution is nevertheless not satisfactory (no subpopulation appears because cells remain very close to each other). When the system is locally bistable, cells will converge either toward the lower stable branch or the upper stable branch of the $f$ null-cline. It is possible to find a value of Fas-ligand so that the separatrix cuts the origin, hence defining a clear threshold between the two steady states. Even if there is still a continuum of cells on the phase plane for continuous values of exposition to Fas-ligand, two denser groups appear. In fact, cells exposed to high Fas-ligand values quickly converge toward the top, cells exposed to low Fas-ligand values converge toward the bottom-right and those exposed to medium values remain trapped near the origin in a 'slow' zone around the separatrix. The latter cells keep low Erk and Fas values, so by introducing the thresholds, three subpopulations are easily obtained (Fig. 4).

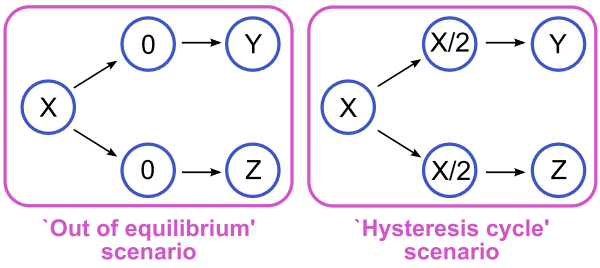


**Fig. 3.** Schematic representation of the two scenarii considered for distribution of Erk and Fas quantities at cell division. The left panel illustrates the 'out of equilibrium' case, the right panel the 'hysteresis cycle' case. In the 'out of equilibrium' scenario a cell with a level $X=(E,F)$ of Erk and Fas at mitosis gives birth to two daughter cells with no Erk and no Fas ($(E,F)=(0,0)$). These cells will in turn reach different levels of Erk and Fas at the end of their own cell cycles (provided that they do not die), denoted by $Y$ and $Z$. In the 'hysteresis cycle' scenario, a cell with a level $X=(E,F)$ of Erk and Fas produces two daughter cells with levels $X/2=(E/2,F/2)$ which will reach a priori different levels of Erk and Fas at the end of their own cell cycle, due to stochasticity and response to signaling.

The second scenario is based on the idea that working at steady-state is more robust. When the system is locally bistable, one can notice that cells on the lower stable branch are those which will self-renew (high values of Erk, reasonable values of Fas). If quantities of Erk and Fas are equally divided between the two daughter cells at birth, those exposed to medium values of Fas-ligand will appear near the separatrix and be divided between the upper branch (differentiation/apoptosis) and the lower branch (self-renewal). We thus have a system where cells rapidly take the decision between self-renewal or differentiation/apoptosis. Once the decision is made, cells are trapped on a hysteresis cycle controlled by Fas-ligand, so the decision is hardly reversible. Fas values have to become very high in order to go from the lower branch to the upper branch and conversely, very low in the opposite direction (Fig. 5).

For this solution, called 'hysteresis cycle' case, introducing thresholds in order to determine cell fate is quite simple. The Erk threshold can be situated anywhere between the two branches and the Fas threshold somewhere on the upper branch, cutting into two the cell populations on this branch and so easily controlling the differentiation/apoptosis ratio.

The 'out of equilibrium' and the 'hysteresis cycle' scenarii are schematically described in Fig. 3.

### 2.1.4. Feedback control role

A key point in system (1) and (2) is how it reacts to feedback controls. The analysis performed in the previous subsections dealt with the influence of each parameter on the system dynamics, mainly parameters related to feedback controls ($\alpha$ and $\gamma$). Let us now study how parameters are affected by feedback controls. Erythropoietin (through function $\alpha$) is expected to decrease apoptosis and enhance self-renewal/differentiation.

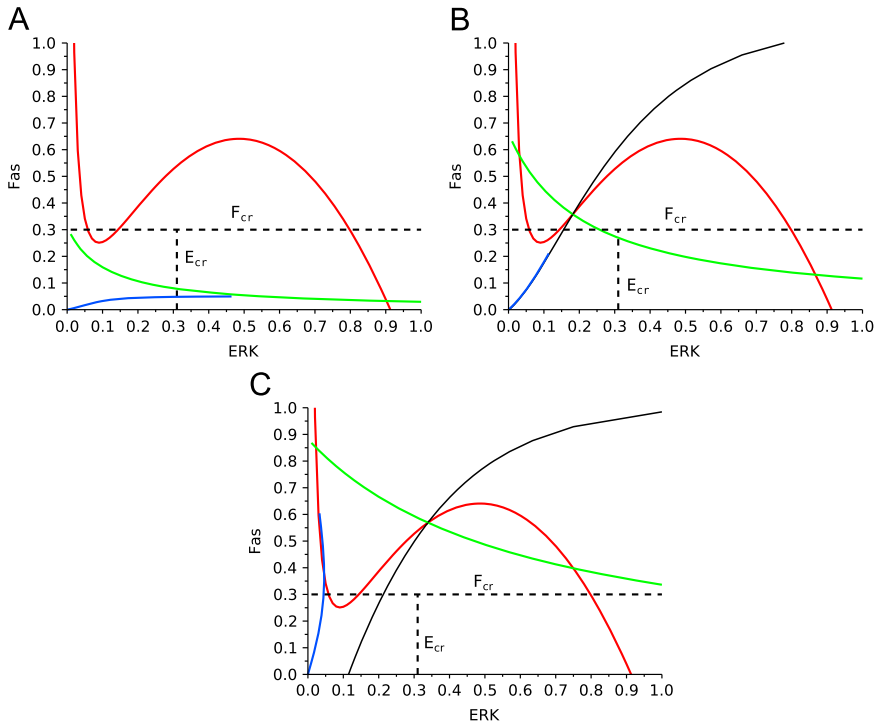


**Fig. 4.** Illustration of the 'out of equilibrium' hypothesis. All daughter cells are initially placed at the origin of the (Erk,Fas) plane and, depending on the external Fas-ligand value, try to escape the default differentiation zone (bottom left area) into apoptosis (above the dashed $F_{cr}$ line) or self-renewal zone (bottom right area) before the end of their cycle. Trajectories from the origin are illustrated by the solid blue curve. A: low exposure to Fas-ligand leads to self-renewal. B: medium exposure to Fas-ligand leads to differentiation. C: high exposure to Fas-ligand leads to apoptosis. (For interpretation of the references to color in this figure legend, the reader is referred to the web version of this article.)

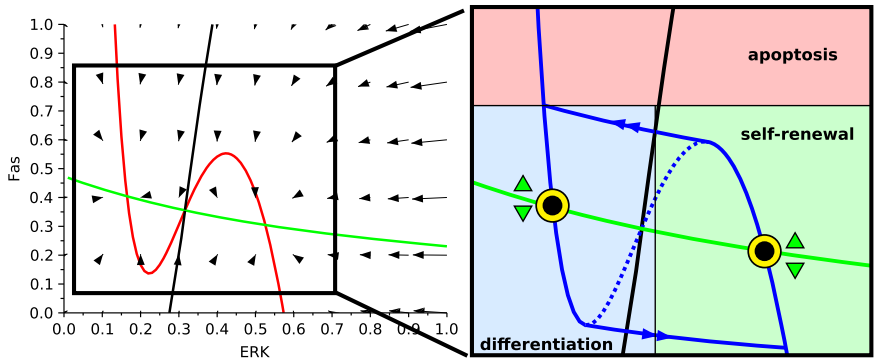


**Fig. 5.** The 'hysteresis cycle' scenario. Daughter cells initially inherit half of their mother's protein level, 'choose' one of the stable branches depending on their exposition to Fas-ligand, and then move on these branches which form an hysteresis cycle, making the decision hardly reversible. Shown with yellow circles are the two possible positions for newborn cells exposed to exactly the same value of Fas-ligand on the hysteresis cycle. One can see how the initial choice is important: cells whose mother had low Fas values will be located on the lower branch, those whose mother had sufficiently high Fas values will switch to the upper branch. (For interpretation of the references to color in this figure legend, the reader is referred to the web version of this article.)

We also know that, at a smaller space scale, Fas-ligand induces apoptosis (through function $\gamma$) and other growth factors, on the opposite, stimulate self-renewal (through the function $\alpha$). In order to validate these dynamics, the effect of each factor must be checked in both cases, the 'out of equilibrium' and the 'hysteresis cycle' scenarii.

The control exerted by Fas-ligand, which increases the value of Fas reached at steady-state, has already been largely discussed. Simply by existence of the threshold $F_{cr}$, Fas-ligand plays the expected role. Fas-ligand is linked to the parameter $\gamma$, which is actually a function of $F_L$.

Epo is known to have a direct action on apoptosis (Koury and Bondurant, 1990), independent of Erk pathway (Chappell et al., 1997; Nagata et al., 1998; Sui et al., 2000). Therefore, a simple idea is to increase $F_{cr}$ with the level of Epo. This clearly reduces apoptosis in favor of differentiation and self-renewal. However, it is also known that Epo, and other growth factors, activate Erk (Jelkmann, 2004; Secchiero et al., 2004). So erythropoietin and growth factors are supposed to influence the variations of $\alpha$.

The value of $\alpha$ controls the monostable/bistable bifurcation (Fig. 1). When the system is locally bistable, $\alpha$ mainly controls the

value of the local minimum of the $f$ null-cline. In the case of the 'out of equilibrium' scenario, $\alpha$ changes the position of the separatrix and of the upper steady states, so when $\alpha$ is increased the separatrix cuts the origin for a higher value of $\gamma(F_L)$ and cells tend to be displaced toward steady-states with lower values of Fas and higher values of Erk. In the case of the 'hysteresis cycle' scenario, increasing the local minimum of $f$ reduces the size of the cycle. Cells located on the upper stable branch instantly 'fall' on the lower stable branch, so self-renewal is immediately enhanced and differentiation reduced.

The effect of $\alpha$ is not the same in both dynamics, but finally it is clearly possible to decrease apoptosis in favor of self-renewal/differentiation and the trends for each protein is roughly what is expected biologically. However, it is still necessary to study whether the feedback is as efficient as observed experimentally, when the intracellular scale is coupled to the extracellular one (see Section 3).

### 2.2. Extracellular scale

In the previous section, we focused on the intracellular scale of the hybrid model, based on a system of ordinary differential equations describing the competition between two key proteins, Erk and Fas. Concentrations of Erk and Fas induce either cell self-renewal, or differentiation, or death by apoptosis. We now focus on an other layer of the hybrid model, the discrete part, which describes how cells interact and how they influence intracellular parameters which depend on extracellular molecules.

In order to describe the evolution of an erythroid cell population, we chose to use an individual-based model. All cells and their interactions are then numerically computed. The objective being to represent erythroblastic islands, which have a limited size, such an approach takes automatically into account small population effects as well as random effects (direction of division, cell cycle length).

A population of cells is numerically simulated in a 2D rectangular computational domain. Each cell is a discrete object, an elastic ball, considered to be circular and composed of two parts: a compressible part at the border and an incompressible part at the center. All newborn cells have the same radius $r_0$ and linearly increase in size until the end of their cycle, when they reach twice the initial radius. When a cell divides, it gives birth to two small cells side by side, the direction of division being randomly chosen. The cell cycle duration is itself variable. From a biological point of view, cell cycle proceeds through $G_0/G_1$, $S$, $G_2$ and $M$ phases. Duration of the first $G_0/G_1$ phase and transitions between phases are controlled by various intracellular and extracellular mechanisms, inducing stochasticity in cell cycle durations (Golubev, 2010; Rew et al., 1991). We assumed the duration of $G_0/G_1$ phase is a random variable with a uniform distribution in some given interval, other phase durations were supposed to be constant.

Under the assumption of small deformations, the force acting between cells can be expressed as a function of the distance between their centers. The force between two particles with centers at $x_i$ and $x_j$ is given by a function $D(d_{ij})$ of the distance $d_{ij}$ between the centers. This function is zero if the distance is greater than the sum of their radii. To describe the motion of a particle, one should determine the forces acting on it by all other particles and possibly by the surrounding medium. The motion of each cell is then described by the displacement of its center by Newton's second law

$$m\ddot{x}+\mu m\dot{x}-\sum_{j\neq i}D(d_{ij})=0, \tag{5}$$

where $m$ is the mass of the particle, the second term in the left-hand side describes the friction by the surrounding medium, the third term is the potential force between cells. The force between two spherical particles is considered in the form

$$D(d_{ij})=\begin{cases} K\dfrac{d_0-d_{ij}}{d_{ij}-d_0+2H_1}, & d_{ij}<d_0,\\ 0, & d_{ij}\geq d_0, \end{cases} \tag{6}$$

where $d_0$ is the sum of cell radii, $K$ is a positive parameter, and $H_1$ accounts for the compressible part of each cell. The force between the particles tends to infinity when $d_{ij}$ decreases to $d_0-2H_1$. On the other hand, this force equals zero if $d_{ij}\geq d_0$.

Three different cell types are computed in this model. It may be noted that all differentiation stages of erythroid progenitors are not described, although the modeling framework allows to do so. However, it would add complexity to this first model as well as difficulties to estimate parameter values. We only decided to focus on the erythroid lineage and consequently did not incorporate neither the hematopoietic stem cell compartment nor its differentiation flux into erythroid progenitors. Hereafter, we specify the characteristics of each cell type considered.

First, erythroblasts, which are immature erythroid cells, also known as erythroid progenitors. They follow the growth rules explained above and their fate is determined as described in Section 2.1. They either self-renew and give two cells of the same type, or differentiate and give two differentiated cells (reticulocytes), or die by apoptosis, depending on their exposition to growth factors and Fas-ligand. It is noticeable that no asymmetric division is considered in this model.

Second, reticulocytes. From a biological point of view, reticulocytes are almost mature red blood cells that leave the bone marrow and enter the bloodstream after ejecting their nuclei. In this individual-based model, they are differentiated cells which stay in the bone marrow a little while after being produced, and leave the bone marrow (computational domain) after a time equal to one cell cycle duration. Contrary to erythroblasts, reticulocytes do not have a choice to make, they only express Fas-ligand, thus influencing the development of surrounding erythroblasts.

Third, macrophages. They are big white blood cells located at the center of erythroblastic islands. They certainly have an active role in the development of blood cells surrounding them (Chasis and Mohandas, 2008). In this model, they express growth factors, driving nearby erythroblasts toward differentiation and self-renewal.

Macrophages express growth factors that are supposed to diffuse in their neighborhood. Reticulocytes express Fas-ligand on their surfaces which do not diffuse in a real bone marrow, yet the expression of Fas-ligand is modeled by short-diffusion. This allows considering some phenomena that are not taken into account in the hybrid model: for instance, there are normally several maturing erythroid subpopulations which increasingly express Fas-ligand, creating a gradient of exposition. Moreover, cells are not circular in reality and this short-range diffusion compensates their inexact representation. Both Fas-ligand ($F_L$) and growth factor ($GF$) concentration evolutions are described with the following reaction–diffusion equations:

$$\frac{\partial F_L}{\partial t}=D_{F_L}\Delta F_L+W_{F_L}-\sigma_{F_L}F_L, \tag{7}$$

$$\frac{\partial GF}{\partial t}=D_{GF}\Delta GF+W_{GF}-\sigma_{GF}GF, \tag{8}$$

where $W_{F_L}=k_{F_L}C_{ret}$ is a source term depending on the number of reticulocytes ($C_{ret}$ denotes the relative volume of reticulocytes in the computational domain) and $W_{GF}$ is a constant source term for growth factor (released by the macrophage) concentration, $\sigma_{F_L}$ and $\sigma_{GF}$ are degradation rates, and $D_{F_L}$ and $D_{GF}$ are diffusion rates.

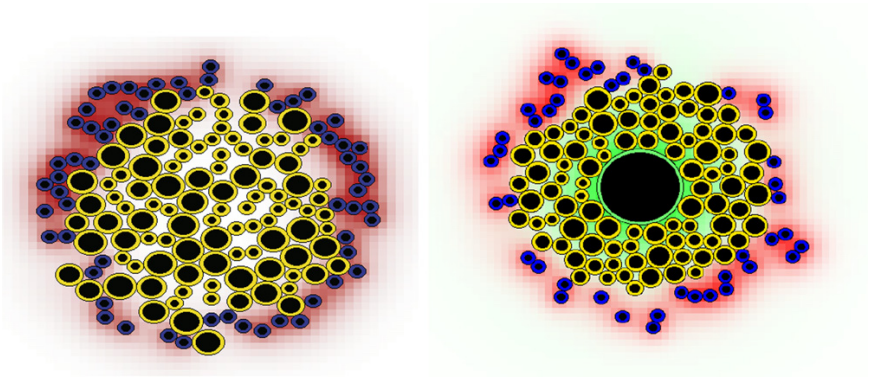

**Fig. 6.** Screenshots of erythroblastic islands with and without macrophage. The green cell is a macrophage, yellow cells are immature cells (erythroblasts) and blue cells are differentiated cells (reticulocytes). The green substance is secreted by the macrophage (growth factors) and the red substance by reticulocytes (Fas-ligand). In each cell, the black area represents the incompressible part of the cell. (For interpretation of the references to color in this figure legend, the reader is referred to the web version of this article.)

If the diffusion coefficient $D_{F_L}$ is sufficiently small, then Fas-ligand is concentrated in a small vicinity of reticulocytes. In this case, Fas-ligand influences erythroid progenitors when they are sufficiently close to reticulocytes. This is the short-diffusion illustrated in this work.

Fig. 6 shows an example of erythroblastic islands in the hybrid model. The big green cell in the center is a macrophage, the green substance surrounding it is the above mentioned growth factors released by the macrophage. At the border, blue cells are reticulocytes emitting Fas-ligand (whose concentration is represented in red). Between them are the erythroblasts, growing in size until they die or divide into two new cells, depending on how they were influenced by the two diffusing proteins.

The feedback control mediated by Epo depends on the number of circulating red blood cells (since Epo is released by the kidneys as a reaction to hypoxia). We chose not to introduce Epo concentration in the model, but rather we considered a fourth cell type, erythrocytes, which is not made explicit (as explained hereafter): the less erythrocytes, the less apoptosis of immature progenitors. Biologically, erythrocytes are mature reticulocytes, circulating in blood and transporting oxygen to the organs. In the model, erythrocytes are reticulocytes that have spent a time equal to one cell cycle in the computational domain and then left it. Hence, erythrocytes are only counted as cells outside the domain (they are not represented on the computational domain) which act, through feedback loops, on the fate of immature cells within the domain. We will assimilate erythrocytes and red blood cells (RBC) in the following, by considering that RBCs are only erythrocytes (in reality, some reticulocytes usually manage to leave the bone marrow and enter the bloodstream where they end their maturation, so they are also red blood cells). Erythrocytes will be supposed to survive (arbitrarily) during a time corresponding to three cell cycle durations (although RBCs do not cycle). This is short, since in mice RBCs have a lifespan of 40 days, yet it allows performing a first feedback test and it can be changed when comparing the model to experimental data.

### 2.3. Coupling both scales

Now that both modeling scales have been described and a general picture of the model is accessible, we detail how the two scales are linked together. At the highest level, there is a small erythroblastic island formed with two populations of developing red blood cells and, optionally, a central macrophage. The island has a particular topology: the macrophage is at the center, differentiated cells (reticulocytes) at the border and immature cells in between. Both macrophage and differentiated cells emit growth factors continuously controlling intracellular protein concentrations: immature cells at the center are rather exposed to growth factors produced by the macrophage whereas those at the border are rather exposed to Fas-ligand. In addition, immature cells are subject to a feedback control mediated by mature red blood cells circulating in the bloodstream, representing the action of erythropoietin. Concentration of Epo in the computational domain is supposed to be uniform, so all cells are similarly influenced by Epo (yet other more sophisticated choices are possible).

Erythroid progenitors are then exposed to a continuum of erythropoietin *Epo*, growth factors *GF* and Fas-ligand $F_L$. Regarding the intracellular scale, this means that $\alpha$ and $\gamma$ take continuous values (see (1) and (2)). Let us remind that high values of $\alpha$ drive erythroblasts to self-renewal, high values of $\gamma$ to death, and intermediate values to differentiation. Hence, the cell population scale influences the intracellular scale through Epo, growth factors and Fas-ligand concentrations, that is through functions $\alpha$ and $\gamma$ and the critical value $F_{cr}$ of Fas concentration (Epo increases $F_{cr}$ in order to inhibit cell apoptosis).

When there is no macrophage, there is only one value of $\alpha$ for all erythroblasts (this value depends on the concentration of Epo which is related to the number of erythrocytes, and is supposed to be the same for all immature cells), so cells are simply situated along a unique $f$ null-cline. How the value of $\gamma$ determines cell's choice in this case has then been investigated in Section 2.1.4, and scenarii have been proposed to define an appropriate framework.

As just mentioned, Epo-mediated feedback control simply corrects the critical value for apoptosis $F_{cr}$ and values of $\alpha$ uniformly, so its impact can be easily understood individually by referring to the analysis in Section 2.1.4. However, in order to compute this feedback control, the number of erythrocytes in blood circulation must be estimated. This is performed from the reticulocyte population as mentioned at the end of the previous section.

## 3. Results: stability of erythroblastic island and function of central macrophage

The hybrid model has been presented in details in the previous section. The applicability of such a modeling will be investigated in this part. To do so, one must question the reasons that led to propose this model. As mentioned in the Introduction section, the aim is to be able to investigate both intracellular and extracellular

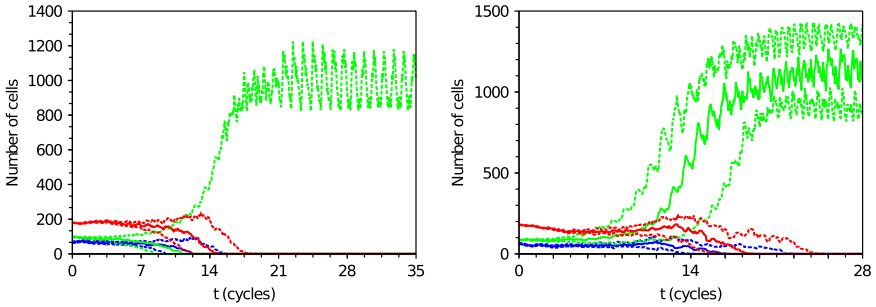


**Fig. 7.** Illustration of the fate of the most stable erythroblastic islands in the absence of macrophage. Results were obtained out of equilibrium (left) and using the hysteresis cycle (right). Green lines represent the number of erythroblasts, blue lines reticulocytes, red lines estimation of circulating red blood cells produced by the island (thick lines are medians, thin lines quartiles over 40 simulations). Observed saturation is only due to space limitation. (For interpretation of the references to color in this figure legend, the reader is referred to the web version of this article.)

regulation of erythropoiesis by taking into account the spatial structure of erythroblastic islands, in order to determine the influence of specific spatial structures on erythropoiesis. First, one should ask: what is the expected behavior of an erythroblastic island? Is this structure expected to be long-lasting? Does talking about 'stable' islands make sense? Or are erythroblastic islands temporary structures unable to resist to external perturbations?

We assumed erythroblastic islands were likely to be stable, meaning that the number of cells in the island should stay almost constant for a certain time when not facing a perturbation. Indeed, one can expect that, in order to be biologically responsive, an island survives for several cell cycles. Consequently, we also assumed that the island should be able to react to changes in the feedback variables values and tested its robustness to feedback controls. Finally, we investigated the behavior of an erythroblastic island under the previously mentioned assumptions of the 'out of equilibrium' and the 'hysteresis cycle' scenarii.

Our objective, in this section, is then to find conditions (parameter values, that are discussed in Appendix A) for the system leading to stable erythroblastic islands, reacting sensibly to global feedback variables and proving to be robust to parameter values variations. This is investigated from a theoretical point of view, and qualitative results are obtained, which represent a first step in the analysis of hybrid models for erythropoiesis. Simple numerical stability and qualitative feedback tests were performed to check whether the presence of the macrophage in the center of the island was necessary to fulfill this objective.

### 3.1. Erythroblastic island without macrophage

Consider an island initially composed of 98 erythroid progenitors and 64 reticulocytes surrounding them. Parameters are carefully chosen to optimize stability and response to feedback (see Appendix A for a discussion on the range of possible parameters).

#### 3.1.1. Stability analysis

In order to determine whether the erythroblastic island can be stable or not, a wide range of parameters has been tested for the two possible dynamics, that is either 'out of equilibrium' or with the 'hysteresis cycle'. At first, the best results (that is providing the longest periods of stability) for both scenarii look like quite similar (Fig. 7). In both cases, the island remains approximately stable during 10 cycles but, due to stochastic variations (cell cycle duration, orientation of the mitotic spindle at division, small size populations), it suddenly dies out or excessively proliferates (it must be noticed that saturation is only due to space limitations). Two questions arise from this fact: why does the system behave this way and is it still biologically relevant? Clearly, extinction of erythroblastic islands can be biologically justified (if one assumes that erythroblastic islands are not stable structures), whereas excessive proliferation is not suitable, at least in vivo.

Let us focus first on the mechanisms leading to an island's stability. When numerically simulating the model, during each cycle there is a turnover of reticulocytes, in order to replace those which entered bloodstream. These reticulocytes then induce apoptosis and differentiation in the erythroblast population. Within this population, in order to remain stable, the proportion of self-renewing erythroblasts has to be constant. From a geometrical point of view, self-renewing erythroblasts are located at the center of the erythroblastic island, differentiating and dying erythroblasts at the border (Fig. 6). When a random variation occurs in the size of the island, the amount of the differentiating and dying cells varies like the perimeter of the circle (occupied by reticulocytes which act at constant range), while the amount of self-renewing cells varies like the area of the circle. As a result, the ratio 'differentiating and dying cells' over 'self-renewing cells' does not remain constant. When it derives too far from the initial value, one subpopulation rapidly overgrows the other.

It appears then that it is impossible to find parameter values for which an island would remain at steady-state on a long term, and consequently stability of an erythroblastic island is not expected in the absence of a macrophage in its center.

When looking more precisely at the results in Fig. 7, one may observe differences between the 'out of equilibrium' and the 'hysteresis cycle' scenarii, the latter scenario providing slightly better stability results (Fig. 7 right), that is the islands survive longer. Moreover, variations of distribution of cell cycle lengths were found to introduce a bias in numerical experiments when the 'out of equilibrium' scenario was considered. Indeed, when cells are placed at the origin at the beginning of their cycle, they all start in the differentiating area. When their cell cycle length is short, they do not have enough time to escape this area and differentiate. When cell cycle duration is long, they cannot differentiate. Consequently, some cell fates are only decided because of cell cycle length, independently of the position in the erythroblastic island, and the island structure is quickly lost. On the other hand, the dynamics at equilibrium ('hysteresis cycle') is very robust when cell cycle lengths distribution vary.

In conclusion, since cell cycle length variation may be large (Golubev, 2010; Rew et al., 1991), it was decided to abandon this 'out of equilibrium' dynamics and to perform further tests with the dynamics using the 'hysteresis cycle' (Fig. 3, right panel).

*3.1.2. Feedback relevance and relation to stability*

The above-described hybrid system should be clearly influenced by feedback control loops, as expected biologically, and, besides, feedback loops may play a role in the stabilization of erythroblastic islands.

As mentioned in Section 2.1, different feedback controls are considered in this model: a local control through Fas-ligand, activating Fas and influencing erythroblast differentiation and death by apoptosis; two global feedback controls by erythropoietin, one activating Erk through the function $\alpha$, the second one varying the critical value of Fas, namely $F_{cr}$, inducing apoptosis. We focus here on the global feedback control mediated by Epo, which acts identically on all erythroblasts.

It is known that increasing Epo levels in the bloodstream, and consequently in the bone marrow, increases Erk activity (Rubiolo et al., 2006; Sui et al., 2000) and decreases erythroblast apoptosis rate (Koury and Bondurant, 1990). Hence, an increase of Epo levels induces an increase in the values of both $\alpha$ and $F_{cr}$. The exact influence of Epo on these two quantities is however not known. Therefore, we began by simply monitoring the behavior of one island under constant values of these two parameters around the default value (Fig. 8). This, of course, does not mimic the dynamics of the whole hybrid model, since the feedback control loop is not closed, however it gives a good indication of the model's behavior when reacting to different values of the feedback control variables.

By comparing the proportions of different erythroblast subpopulations (self-renewing, differentiating and apoptotic populations) during the first five cycles, it appeared that an increase of $F_{cr}$ (that is, an increase of Epo levels) decreases apoptosis and self-renewal in favor of differentiation. For low values of $F_{cr}$, there is no differentiation (erythroblasts at the center of the island survive, others die), so the island proliferates by the absence of death factors. For higher values, effect on self-renewal can be tuned by modifying parameters controlling the hysteresis cycle. At some point the self-renewing population is not affected anymore and there is simply a transfer from the apoptotic subpopulation to the differentiating subpopulation (the differentiation part of the differentiation/apoptosis branch increases).

Increasing $\alpha$, on the contrary, mainly acts on the self-renewing population. An increase of $\alpha$ sends all cells on the self-renewing branch of the hysteresis cycle and differentiation/apoptosis disappears. Reducing $\alpha$ increases the size of the apoptosis/differentiation branch. For a constant value of $F_{cr}$, only the differentiation part of this branch is increased. One thus observes a transfer from the self-renewing branch to the differentiation part of the other branch.

In conclusion, the system's response is qualitatively what is expected: Epo mainly decreases apoptosis in favor of differentiation and stimulates self-renewal. However, the statistics computed above only indicate trends and it is important to see how islands actually react to this feedback.

The next step is then to explicitly include feedback loops in the system's equations to see whether the response is qualitatively correct or not, and to possibly obtain stability of the erythroblastic island for durations longer than in Fig. 7. We assumed a linear variation of both $\alpha$ and $F_{cr}$ with deficiency of red blood cells (RBC), hence implicitly describing the dependency on Epo. Denoting by $N_{RBC}$ the number of circulating red blood cells, and since a decrease of RBC count induces an increase in Epo levels, one gets

$$\alpha := \alpha(N_{RBC}) = \alpha_0 + k_\alpha(N_{target} - N_{RBC}), \tag{9}$$

$$F_{cr} := F_{cr}(N_{RBC}) = F_0 + k_F(N_{target} - N_{RBC}). \tag{10}$$

We remind that $N_{RBC}$ is estimated by the number of reticulocytes which have left the bone marrow and are supposed to survive during a time equivalent to three cell cycles. $N_{target}$ is the number of RBCs in circulation during a typical run before proliferation/extinction of the island. Parameters $\alpha_0$ and $F_0$ are 'typical' values of $\alpha$ and $F_{cr}$ (as given in Appendix A). Parameters $k_\alpha$ and $k_F$ are to be estimated.

It must be mentioned that, from a biological point of view, one would expect the functions $\alpha$ and $F_{cr}$ to saturate for low and high values of $N_{RBC}$. Yet, the linear shapes we chose represent good approximations when the number of red blood cells is not too far away from the target (for instance, in normal erythropoiesis).

Functions $\alpha$ and $F_{cr}$ in (9) and (10) were used together with the previous initial conditions (hysteresis cycle case), and it was impossible to achieve periods of stability longer than previously mentioned when varying the values of $k_\alpha$ and $k_F$ (data not shown). To be more precise, it was possible with strong feedback controls to stop proliferation, instead the island systematically died out. Other tests, based on simulations of a constant number of red blood cells ($N_{RBC}$), showed that the effect of feedback controls was not fast enough to deal with the quick proliferation and extinction of erythroblastic islands. The island still lived around 10–15 cycles and, when it began to expand or die out, feedback response came too late or was too strong to bring it back to its ideal size. Therefore, what was observed was only the usual destabilization of the island, feedback being only able to turn proliferation into extinction after some cycles. This highlights the relevance of introducing spatial aspects in the model. As discussed above, the growth of the island occurs on a shorter time scale than feedback controls acting on the island, thus reducing their efficiency.

As a result, it is very difficult to test feedback reliably on unstable islands. However, the study showed that global feedback loops are inefficient when it comes to controlling local structures, since proliferation or extinction events occur quickly in the model.

Let us briefly comment on the absence of stability for an erythroblastic island which does not contain a macrophage. It is not clear that the lack of stability implies that results are

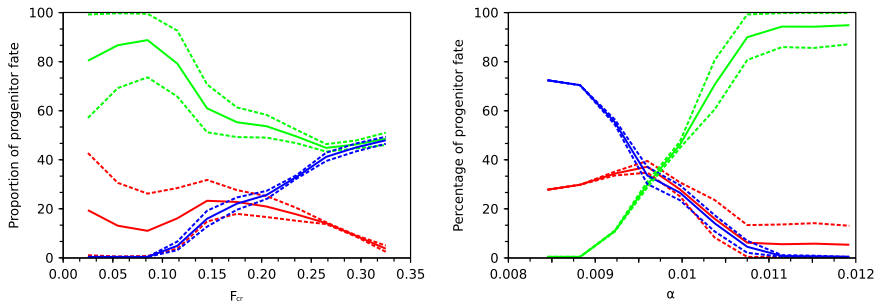


**Fig. 8.** Effect of feedback controls on progenitor subpopulations in the absence of macrophage in the island. Each curve represents the percentage (means $\pm$ standard deviation) of self-renewing (green), differentiating (blue) or apoptotic (red) erythroblasts during the first five cell cycles, as a function of $F_{cr}$ (left panel) and $\alpha$ (right panel). (For interpretation of the references to color in this figure legend, the reader is referred to the web version of this article.)

biologically irrelevant. The fact that islands die in this model is not really surprising since, biologically, there might be a turnover of these structures and erythroid progenitors permanently arise from the differentiation of hematopoietic stem cells, which has been neglected here. Also, proliferation is not as dramatic as it might seem. First, it is possible to turn it down by varying parameters (but sacrificing instead the average lifetime of an island) and also proliferation may not be that simple in a realistic environment. Indeed, there is no obstacle in the computational domain and some particular geometries could clearly reduce variations in the proportion of self-renewing cells. Another point is that when several islands are side-by-side, proliferating islands will collide and be in contact with more reticulocytes than before, which may block their growth (data not shown). Nevertheless, unstable islands revealed hard to control and stability of islands should be expected, as previously mentioned.

In the next section, we consider the addition of a macrophage in the center of the island on the stability of the island and the relevance of feedback controls.

### 3.2. Island with macrophage

In this case, an erythroblastic island is initially composed of one macrophage, 80 erythroid progenitors and 64 reticulocytes (see Fig. 6, right). As done in the previous section, stability of the island and influences of feedback controls are investigated.

In addition to feedback controls exerted, in the previous section, on erythroblast dynamics by Epo and Fas-ligand, the macrophage in the center of the island is supposed to release growth factors, whose concentration is denoted by *GF*, which positively act on Erk activation. A number of proteins associated with the proliferation of erythroid progenitors and that could fulfill such a function have been described. This includes Stem Cell factor (SCF), the c-kit ligand, Ephrin-2, the EphB4 ligand, and BMP4, a member of the TGF$\beta$ family (Rhodes et al., 2008 and references therein). All those growth factors are assumed to diffuse around the macrophage as developed in Section 2.2 (Eq. (8)). They trigger erythroblast self-renewal through the function $\alpha$: the more growth factors, the higher $\alpha$. Function $\alpha$ now becomes

$$\alpha := \alpha(N_{RBC}, GF) = \alpha_0 + k_\alpha(N_{target} - N_{RBC}) + k_{GF}GF. \quad (11)$$

Meaning of parameters $\alpha_0$, $k_\alpha$ and $N_{target}$ is identical to the ones defined for (9). Values are also the same, except for $\alpha_0$ that had to be decreased to compensate the addition of the term $k_{GF}GF$. Parameter $k_{GF}$ was set accordingly (influence of these parameters are discussed below). Default values are $\alpha_0 = 0\ \mathrm{h}^{-1}$ and $k_{GF} = 3\ \mathrm{h}^{-1}\ \mathrm{molecule}^{-1}$.

#### 3.2.1. Stability analysis

Stability of the hybrid system is first investigated without considering global feedback controls (that is, $k_\alpha = 0$ in (11) and $k_F = 0$ in (10)). Results are illustrated in Fig. 9.

For a large range of parameter values, the system quickly converges toward a steady-state. The number of self-renewing and differentiating cells (and thus circulating RBC) can be precisely controlled by parameter values, as will be detailed in the next subsection. There is a first phase where the size of subpopulations oscillates (because of lack or abundance of death factors) yet steady-state is always quickly reached (within a few cycles), even though inherent stochastic oscillations are always present.

The macrophage completely controls the island stability. If $\alpha_0$ is sufficiently low, a cell will not be able to self-renew without external growth factors. Therefore, the default behavior of an isolated cell is differentiation. On the other hand, a cell in contact with the macrophage will be exposed to a very high concentration of growth factors and will always self-renew, since it is generally not exposed to death factors. In the vicinity of the macrophage, there is a competition between growth factors and death factors, which will eventually determine the size of the island. If $\alpha_0$ or $k_{GF}$ gets higher, growth factors will reach further erythroblasts, thus the size of the final island will increase.

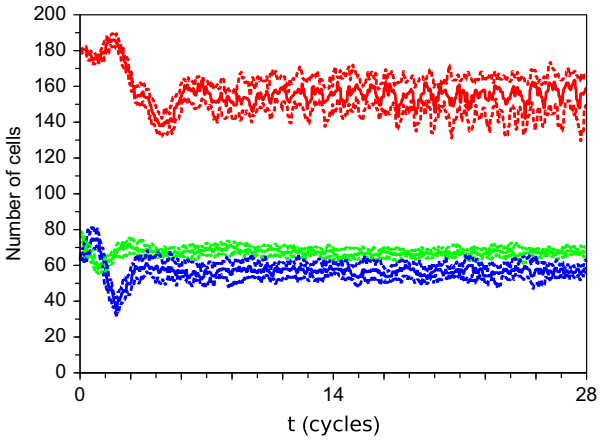


**Fig. 9.** Number of erythroid cells in the presence of a macrophage in the center of the island. Results were obtained using the hysteresis cycle. Green lines represent the number of erythroblasts, blue lines reticulocytes, red lines estimation of circulating red blood cells produced by the island (thick lines are medians, thin lines quartiles over 40 simulations). After addition of a macrophage, islands automatically stabilize for previously chosen parameters. (For interpretation of the references to color in this figure legend, the reader is referred to the web version of this article.)

#### 3.2.2. Feedback relevance and relation to stability

Now that erythroblastic islands are stable, due to the presence of the macrophage, it is not necessary to be limited to a period of five cycles to compare the subpopulations of the island, as was done in the previous case (Section 3.1.2). Rather, it becomes relevant to see how the size of the island and the production of RBC could evolve on a long term.

Similarly to what has been done in the previous case, we once again simulated the expected consequences (in terms of steady state value) of feedback control variations by running simulations under constant values of $\alpha$ and $F_{cr}$. Results are shown in Fig. 10.

When $F_{cr}$ increases, both the number of reticulocytes and RBC increases, as the differentiation part of the differentiation/apoptosis branch increases. For high values of $F_{cr}$, there is no apoptosis anymore. The number of erythroid progenitors seems to be rather independent of the value of $F_{cr}$.

When $\alpha$ increases, which can be seen as an increase of the ground level of global 'surviving factors' (here Epo and macrophage-emitted growth factors), the size of the island increases mainly due to the increase of the self-renewing population. As a result, reticulocytes, situated all around the island, also increase in number, as does the amount of RBC. However, for very high values of $\alpha$, surviving signals are so strong that almost all erythroblasts self-renew (the macrophage has no effect anymore) and the island is made only of proliferating cells, reticulocyte and RBC counts vanish. Such high values of $\alpha$ may only be reached in extreme stress situations and mainly create a pool of cells which may afterwards differentiate and substantially increase the number of RBC at once (but this implies that another mechanism has to lower the value of $\alpha$ at some point). In any case, these values of $\alpha$ may be avoided by adding a saturation effect on the feedback loop.

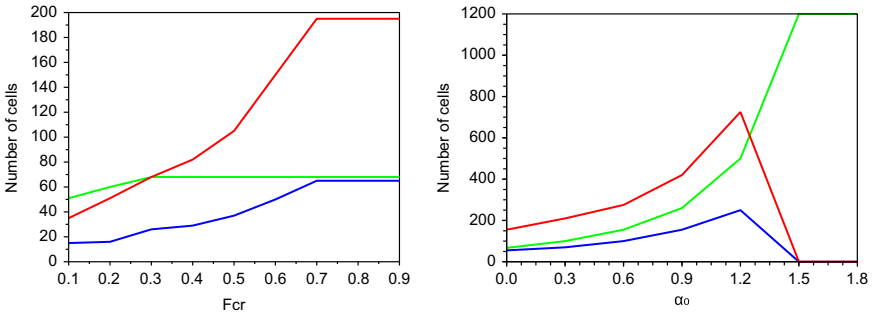


**Fig. 10.** Impact of feedback controls on steady-state values when the erythroblastic island contains a macrophage. Left panel: influence of $F_{cr}$ variations; right panel: influence of $\alpha$ variations. Green lines represent erythroblast counts, blue lines reticulocyte counts and red lines RBC counts. (For interpretation of the references to color in this figure legend, the reader is referred to the web version of this article.)

In each case, a substantial increase of RBC production (about 3-fold and 4-fold respectively) is observed. As the two mechanisms are largely independent, they can be combined and thus the overall production rate can be greatly increased, in magnitudes comparable to what can be observed biologically (Chasis and Mohandas, 2008; Rhodes et al., 2008; Socolovsky, 2007). This seems to indicate that the reaction of the system with macrophage to feedback controls is more efficient, relevant and easy to observe compared to the case without macrophage, again in good agreement with biological evidences (Rhodes et al., 2008).

## 4. Discussion

We proposed a new model for erythropoiesis modeling based on the coupling of two relevant scales, the intracellular scale consisting of protein regulatory networks and the extracellular scale focusing on cell movement and interactions as well as growth factor distribution in the medium. Description of the competition between two proteins within erythroid progenitors has been performed with continuous models (ordinary differential equations) whereas cells have been studied as discrete objects on an off-lattice model, so the whole system can be named 'hybrid model', for it consists in the coupling of continuous and discrete systems. Applied to normal erythropoiesis in the bone marrow, in particular to the regulation of erythroblastic islands, the model suggests an important role of macrophages in the stability of islands. In the absence of macrophages, erythroblastic islands very quickly lose their stability, meaning they either die out or abnormally proliferate (with overproduction of erythroid progenitors). They survive only for the equivalent of about 10 cell cycles. On the contrary, when the erythroblastic island is built around a central macrophage, assumed to release growth factors sustaining erythroid progenitor survival and proliferation (like SCF, Ephrin-2 or BMP-4 Rhodes et al., 2008), then the island is a very robust structure, able to continuously produce erythrocytes while keeping a steady structure (that is an almost constant ratio of reticulocytes over progenitors).

Our modeling approach therefore clearly predicts that the presence of a centrally located macrophage is critical for steady state erythropoiesis. Although the role for macrophage has been demonstrated for stress erythropoiesis (Sadahira et al., 2000), a current formal demonstration for the role of bone marrow macrophages in steady state erythropoiesis is still lacking. The most straightforward way to demonstrate it would be to induce a macrophage-specific expression of a suicide gene, and demonstrate that the in vivo ablation of marrow macrophages would have an effect on steady state erythropoiesis. For this a macrophage-specific promoter driving the expression of an rtTA protein, that could be induced by Dox ingestion to bind to a T3REG promoter driving the expression of a suicide gene would be the right way to go.

This control of the production of differentiated red blood cells by the macrophage at the level of the erythroblastic island may first appear in contradiction with usual knowledge of erythropoiesis. It is indeed well known that during a response to a stress, erythropoiesis is a very intense process, large amounts of cells being produced in a short time, so the whole process is expected to possess the ability to overcome its usual production, in particular the ratio of reticulocytes over progenitors should not stay constant. The hypothesis we propose is that the macrophage, inside the erythroblastic island, controls the explosiveness of erythropoiesis and that, contrary to other hematopoietic lineages (white cells, platelets), this control is necessary because stress erythropoiesis must deal with very large amounts of cells and otherwise the stability of the process could be lost. It is moreover noticeable that getting more stability with the central macrophage does not decrease responsiveness of the model. For instance, the island reacts to perturbations simulating anemia (sudden loss of mature red blood cells), returning quickly to 'normal' values of the different erythroid populations, progenitors, reticulocytes and erythrocytes (Bessonov et al., in preparation). Hence the gain of stability is not compensated by a loss in the system's reactivity.

Some comments may however be made on the behavior of an island without macrophage in its center. Although it is clear that this system cannot lead to a stable island, it is nevertheless possible to hypothesize that such a stability is not necessary. For instance, if islands are put side-by-side, proliferation is made difficult (islands cannot expand due to confinement) and extinction can be compensated by the birth of new islands. Moreover, other assumptions, based on a better knowledge of erythroblastic islands, could lead to more stability (geometry of bone marrow and islands, etc.), even though all scenarii cannot and were not tested. However, the lack of stability makes it hard to have a clear view on how feedback controls act on one single island, and as far as we know of, studying erythropoiesis models (or hematopoiesis models, in a wide sense) without considering feedback controls does not make sense. Hence, searching for island stability appeared relevant in this study. At a global scale, it is still possible that island stability is not necessary and can be compensated by proliferation and extinction. When looking at one single island however, the fact that feedback controls do not work correctly on an unstable island is somewhat compelling.

Stability of the erythroblastic island including a central macrophage was obtained by considering two scenarii (see Fig. 3) for the distribution of Erk and Fas quantities in daughter cells, following mitosis and the division of the mother cell. In the first one, initial values of Erk and Fas in newborn cells were set to zero,

and cell fate was decided depending on the evolution of concentrations through the cell cycle duration (this is the 'out of equilibrium' assumption). This scenario was shown to lead to results strongly dependent on the cell cycle length. The second scenario, called the 'hysteresis cycle' case, which is more biologically relevant, consisted in dividing Erk and Fas values of the mother cell at mitosis into two, so both daughter cells are located on a hysteresis cycle in the Erk–Fas plane at birth. Combining the 'hysteresis cycle' scenario with a structure including a local feedback on the island (the macrophage) gave relevant results and appears very promising. Parameter values which were obtained through mathematical analysis appear to be very robust and the system exhibits qualitatively the same behavior for a wide range of parameters. The stability of the island allows a better control of its size and its subpopulations and, as a result, gives much more satisfying results on feedback tests.

Regarding parameter values used to study the model and check different scenarii (with or without macrophage in the center of the island, distribution of initial quantities of Erk and Fas), one must note that most of these values are mainly not accessible through experiments. Some others, such as for instance the time of survival of RBC, are however rather quite arbitrary and not necessarily in agreement with usual knowledge on erythropoiesis. Yet, results show that the behavior may be satisfying from a biological point of view. Since a wide range of parameters is allowed, it is expected that this system can be tuned to fit experimental data and numerically reproduce certain stress behavior, which will be the next step for modeling erythropoiesis.

Feedback functions considered in this study may also be questioned. Indeed, both erythropoietin's influence on erythroid progenitor self-renewal capacity and on apoptosis protection were taken as linear functions of the number of circulating red blood cells. Saturation effects should be envisaged when confronting the model to strong perturbations (for instance, a severe anemia), in order to be closer to the reality where responses of the organism to a loss of red blood cells have shown to be nonlinear (Crauste et al., 2008, 2010). In order to perform tests presented in the current study, in which the focus was on normal erythropoiesis, linear dependencies of the feedback controls on the red blood cell population were nevertheless probably not limiting.

The question of the relevance of the protein regulatory network considered here may also be asked. Erythroid progenitor fate does not depend only on two proteins, Erk and Fas. However, considering a very 'complete' regulatory network, with several proteins, does not appear appropriate, at least in order to perform first tests on the hybrid model. Complexity that would arise from such networks would certainly hide roles and influences of other actors, such as growth factors, cell–cell interaction, feedback controls, etc. The regulatory network could however be improved by considering some key proteins or receptors, such as GATA-1, involved in erythroid progenitor differentiation, or EpoR, the erythropoietin receptor, which plays a crucial role for erythroid progenitor proliferation and inhibition of apoptosis (Aispuru et al., 2008; Socolovsky, 2007).

One last point that has not been developed in this study deals with the geometry of the bone marrow. First, particular geometries, with obstacles or describing the porous aspect of the bone marrow, have not been included in this study. The hybrid model can deal with various geometries, however the choice was made to focus on the behavior of one single erythroblastic island and on feedback controls at global and local scales. Second, the hybrid model was numerically simulated in two dimensions. The case of simulations in three dimensions has not been developed. Qualitatively, such a change is not expected to modify the results, it should nevertheless be tested.

Although several aspects of erythropoiesis have not been considered in this model, we believe the analysis of feedback control role and relevance as well as the investigation of the role of a central macrophage in the center of an erythroblastic island improve previous models of erythropoiesis by providing information on the role of spatial structures (here, the presence of a macrophage and the organization of an erythroblastic island) and on the action of feedback controls (in particular, local feedback controls). It also gives some insight in the way erythroid cell proliferation and differentiation can be controlled, in vitro and in vivo. Further developments are however necessary, and confronting the hybrid model with experimental data on stress situations is a next step to validate this new and certainly promising approach.

## Acknowledgments

Authors thank Prof. Mark Koury and all members of the INRIA Team DRACULA (http://dracula.univ-lyon1.fr) for fruitful discussions. This work has been supported by ANR grant ProCell ANR-09-JCJC-0100-01.

## Appendix A. Parameter estimation

We discuss here the parameter values used when investigating stability of the hybrid model in Section 3. Some parameters are clearly related to the discrete macroscopic model while some others are related to intracellular dynamics.

Choosing individual-based modeling creates many implicit parameters. Most of them can be chosen quite easily (cell radius, parameters of motion, etc.) and are not essential in the results of simulations. However, other parameters clearly change the overall cell behavior and have to be set carefully.

Let first consider parameters associated with extracellular dynamics (mainly growth factor release and action). Exact quantities of Fas-ligand, Epo and growth factors released by the macrophage are not fundamental, because their effect will be normalized at the intracellular scale (intracellular parameters controlling the sensitivity to these molecules). More important are the diffusion coefficients, for both Fas-ligand and growth factors released by the macrophage. These parameters are chosen in order to describe a short range action of Fas-ligand, and to locate growth factors around the macrophage. It is important that the range of diffusion is set according to the size of the cells in order to have a realistic short-diffusion for instance. The distribution of cell cycle lengths is also really important: it changes how the island expands, how cell cycles are locally correlated and plays a role in the fate of immature cells in the 'out of equilibrium' scenario. Parameter values are shown in Table A1.

Intracellular parameters are chosen in order to optimize robustness of the system. It is noticeable that no experimental data is available to set values of these parameters, only the expected behavior is accessible. Parameters $b$ and $c$ of system (1) and (2) control the relative and absolute speeds of the reactions, they are set first. The magnitude of the hysteresis cycle is then tuned by choosing carefully $\alpha/b$ and $\beta/b$ (these ratios control its height, their absolute values its width). Parameter $a$ controls the offset of the cycle and is then set such that the hysteresis cycle is located in the $[0,1]\times[0,1]$ domain. Finally, parameter $d$ value is determined; $d$ mainly controls how a cell goes from a stable branch of the cycle to the other: the higher the value of $d$, the higher the change in Fas quantity.

In Eq. (2), the function $\gamma$ explicitly describes the influence of Fas-ligand. This function has been taken as $\gamma = k_\gamma F_L$, where $k_\gamma$ is the sensitivity of progenitors to Fas-ligand.

**Table A1**
Extracellular parameters ($M$ is an arbitrary mass unit, $L$ an arbitrary length unit).

| Parameter | Value | Unit |
|---|---|---|
| Cell cycle length | 24 | h |
| Cell cycle variations | 4/3 | h |
| $r_0$ | 0.01 | L |
| $m$ | 1 | M |
| $\mu$ | $3\times10^{5}$ | $h^{-1}$ |
| $K$ | $9\times10^{5}$ | $M\,h^{-2}$ |
| $D_{F_L}$ | $3\times10^{-4}$ | $L^2\,h^{-1}$ |
| $k_{F_L}$ | $3\times10^{-3}$ | Molecules $cell^{-1}\,h^{-1}$ |
| $\sigma_{F_L}$ | 0.6 | $h^{-1}$ |
| $D_{GF}$ | $3\times10^{-3}$ | $L^2\,h^{-1}$ |
| $W_{GF}$ | $3\times10^{-2}$ | Molecules $L^{-2}\,h^{-1}$ |
| $\sigma_{GF}$ | 0.3 | $h^{-1}$ |

**Table A2**
Internal parameters when cells begin at the origin ('out of equilibrium' case). *NU* is a normalized quantity unit for the intracellular molecules (maximum possible quantity is 1).

| Parameter | Value | Unit |
|---|---|---|
| $\alpha$ | 0.01 | $h^{-1}$ |
| $\beta$ | 1.5 | $h^{-1}\,NU^{-2}$ |
| $k$ | 2 | – |
| $a$ | 0.12 | $h^{-1}$ |
| $b$ | 0.414 | $h^{-1}\,NU^{-1}$ |
| $k_\gamma$ | 0.009 | $h^{-1}\,NU^{-1}$ molecule$^{-1}$ |
| $c$ | 0.0828 | $h^{-1}\,NU^{-1}$ |
| $d$ | 0.006 | $h^{-1}$ |
| $E_{cr}$ | 0.31 | NU |
| $F_{cr}$ | 0.3 | NU |

Finally, $\alpha$ and $F_{cr}$ also depend on extracellular molecules. However, in what follows we will first consider the case when feedback loops are not included, so $\alpha$ and $F_{cr}$ will be constants first.

When Erk and Fas levels are supposed to be zero when the cell starts its cycle (the 'out of equilibrium' scenario), the speeds of reactions are very important: some cells have to remain trapped near the origin at the end of their cycle in order to observe differentiation. The values of $b$ and $c$ are thus very constrained. The others simply define a large hysteresis cycle which aims at separating the different cell subpopulations as far as possible from each other. See Table A2 for values.

When Erk and Fas values are initially on the hysteresis cycle, then $b$ and $c$ are allowed to vary more largely. It has been decided to put quicker dynamics than in the first case in order to get rapid variations along the cycle. The width of the hysteresis cycle was also reduced, so values for $\alpha$ and $\beta$ are higher. See Table A3 for values.

As discussed above, several other choices are possible. Indeed, the only constraints are on the value of $\beta/\alpha$ (which has to be close to 27) and on the value of $a$. Values of $b$, $c$ and $d$ can then be set in a very wide range without modifying the qualitative behavior of the system (data not shown). More precise values will have to be found when comparing to experimental data.

Finally, an initial size for the island has to be set and the number of islands that will be simulated must be chosen. An initial size of 144 cells with central macrophage or 162 cells without macrophage was chosen, so that initially the island occupies the same space in the computational domain in both cases, and parameters were adjusted to keep the size of the island roughly constant. Therefore, we only simulated one island at the beginning, but once reasonable parameters are found, it is possible to put several islands side-by-side and see how they interact. Preliminary experiments have been performed in this direction (not shown here), see the end of Section 3.1.1.

**Table A3**
Internal parameters when cells are on the hysteresis cycle. *NU* is a normalized quantity unit for the intracellular molecules (maximum possible quantity is 1).

| Parameter | Value | Unit |
|---|---|---|
| $\alpha$ | 1.62 | $h^{-1}$ |
| $\beta$ | 60 | $h^{-1}\,NU^{-1}$ |
| $k$ | 2 | – |
| $a$ | 15.9 | $h^{-1}$ |
| $b$ | 1.8 | $h^{-1}\,NU^{-1}$ |
| $k_\gamma$ | 0.9 | $h^{-1}\,NU^{-2}$ molecule$^{-1}$ |
| $c$ | 3 | $h^{-1}\,NU^{-1}$ |
| $d$ | 1.5 | $h^{-1}$ |
| $E_{cr}$ | 0.3 | NU |
| $F_{cr}$ | 0.6 | NU |

## Appendix B. Supplementary material

Supplementary data associated with this article can be found in the online version of 10.1016/j.jtbi.2012.01.002.

## References

Ackleh, A.S., Deng, K., Ito, K., Thibodeaux, J., 2006. A structured erythropoiesis model with nonlinear cell maturation velocity and hormone decay rate. Math. Bios. 204, 21–48.
Adimy, M., Crauste, F., Ruan, S., 2006. Modelling hematopoiesis mediated by growth factors with applications to periodic hematological diseases. Bull. Math. Biol. 68 (8), 2321–2351.
Aispuru, G.R., Aguirre, M.V., Aquino-Esperanza, J.A., Lettieri, C.N., Juaristi, J.A., Brandan, N.C., 2008. Erythroid expansion and survival in response to acute anemia stress: the role of EPO receptor, GATA-1, Bcl-xL and caspase-3. Cell Biol. Int. 32 (8), 966–978.
Alarcon, T., 2009. Modelling tumour-induced angiogenesis: a review of individual-based models and multiscale approaches. In: Herrero, M.A., Giraldez, F. (Eds.), The Mathematics of Cancer and Developmental Biology. Contemporary Mathematics, vol. 492; 2009, pp. 45–74.
Apostu, R., Mackey, M.C., 2008. Understanding cyclical thrombocytopenia: a mathematical modeling approach. J. Theor. Biol. 251, 297–316.
Banks, H.T., Cole, C.E., Schlosser, P.M., Hien, T., 2004. Modelling and optimal regulation of erythropoiesis subject to benzene intoxication. Math. Biosci. Eng. 1 (1), 15–48.
Bauer, A., Tronche, F., Wessely, O., Kellendonk, C., Reichardt, H.M., Steinlein, P., Schütz, G., Beug, H., 1999. The glucocorticoid receptor is required for stress erythropoiesis. Genes Dev. 13 (22), 2996–3002.
Bélair, J., Mackey, M.C., Mahaffy, J.M., 1995. Age-structured and two-delay models for erythropoiesis. Math. Biosci. 128, 317–346.
Bernard, S., Bélair, J., Mackey, M.C., 2003. Oscillations in cyclical neutropenia: new evidence based on mathematical modeling. J. Theor. Biol. 223, 283–298.
Bernard, S., Bélair, J., Mackey, M.C., 2004. Bifurcations in a white-blood-cell production model. C. R. Biol. 327, 201–210.
Bessonov, N., Eymard, N., Gandrillon, O., Koury, M., Kurbatova, P., Mejia-Pous, C., Volpert, V. The Role of Spatial Organization of Cells in Erythropoiesis, submitted.
Bessonov, N., Crauste, F., Fischer, S., Kurbatova, P., Volpert, V. Application of hybrid models to blood cell production in the bone marrow. Math. Model. Nat. Phenom. 6 (7), 2–12.
Bessonov, N., Kurbatova, P., Volpert, V., 2010. Particle dynamics modeling of cell populations. Math. Model. Nat. Phenom. 5 (7), 42–47.
Chapel, S.H., Veng-Pedersen, P., Schmidt, R.L., Widness, J.A., 2000. A pharmacodynamic analysis of erythropoietin-stimulated reticulocyte response in phlebotomized sheep. J. Pharmacol. Exp. Therapeut. 296, 346–351.
Chappell, D., Tilbrook, P.A., Bittorf, T., Colley, S.M., Meyer, G.T., Klinken, S.P., 1997. Prevention of apoptosis in J2E erythroid cells by erythropoietin: involvement of JAK2 but not MAP kinases. Cell Death Differ. 4, 105–113.
Chasis, J.A., Mohandas, N., 2008. Erythroblastic islands: niches for erythropoiesis. Blood 112 (3), 470–478.
Colijn, C., Mackey, M.C., 2005. A mathematical model of hematopoiesis—I. Periodic chronic myelogenous leukemia. J. Theor. Biol. 237, 117–132.
Colijn, C., Mackey, M.C., 2005. A mathematical model of hematopoiesis—II. Cyclical neutropenia. J. Theor. Biol. 237, 133–146.

Crauste, F., Pujo-Menjouet, L., Génieys, S., Molina, C., Gandrillon, O., 2008. Adding self-renewal in committed erythroid progenitors improves the biological relevance of a mathematical model of erythropoiesis. J. Theor. Biol. 250, 322–338.

Crauste, F., Demin, I., Gandrillon, O., Volpert, V., 2010. Mathematical study of feedback control roles and relevance in stress erythropoiesis. J. Theor. Biol. 263, 303–316.

Dazy, S., Damiola, F., Parisey, N., Beug, H., Gandrillon, O., 2003. The MEK-1/ERKs signaling pathway is differentially involved in the self-renewal of early and late avian erythroid progenitor cells. Oncogene 22, 9205–9216.

Demin, I., Crauste, F., Gandrillon, O., Volpert, V., 2010. A multi-scale model of erythropoiesis. J. Biol. Dyn. 4, 59–70.

De Maria, R., Testa, U., Luchetti, L., Zeuner, A., Stassi, G., Pelosi, E., Riccioni, R., Felli, N., Samoggia, P., Peschle, C., 1999. Apoptotic role of fas/fas ligand system in the regulation of erythropoiesis. Blood 93, 796–803.

Eller, J., Gyori, I., Zollei, M., Krizsa, F., 1987. Modelling thrombopoiesis regulation—I. Model description and simulation results. Comput. Math. Appl. 14, 841–848.

Foo, J., Drummond, M.W., Clarkson, B., Holyoake, T., Michor, F., 2009. Eradication of chronic myeloid leukemia stem cells: a novel mathematical model predicts no therapeutic benefit of adding G-CSF to imatinib. PLoS Comput. Biol. 5 (9), e1000503.

Freise, K.J., Widness, J.A., Schmidt, R.L., Veng-Pedersen, P., 2008. Modeling time variant distributions of cellular lifespans increases in circulating reticulocyte lifespans: following double phlebotomies in sheep. J. Pharmacokinet. Pharmacodyn. 35, 285–323.

Gandrillon, O., 2002. The v-erbA oncogene. Assessing its differentiation-blocking ability using normal chicken erythrocytic progenitor cells. Methods Mol. Biol. 202, 91–107.

Gandrillon, O., Schmidt, U., Beug, H., Samarut, J., 1999. TGF-beta cooperates with TGF-alpha to induce the self-renewal of normal erythrocytic progenitors: evidence for an autocrine mechanism. Embo J. 18, 2764–2781.

Golubev, A., 2010. Random discrete competing events vs. dynamic bistable switches in cell proliferation in differentiation. J. Theor. Biol. 267 (3), 341–354.

Haurie, C., Dale, D.C., Mackey, M.C., 1998. Cyclical neutropenia and other periodic hematological diseases: a review of mechanisms and mathematical models. Blood 92, 2629–2640.

Hoehme, S., Drasdo, D., 2010. A cell-based simulation software for multi-cellular systems. Bioinformatics 26 (20), 2641–2642.

Jelkmann, W., 2004. Molecular biology of erythropoietin. Intern. Med. 43, 649–659.

Jeon, J., Quaranta, V., Cummings, P.T., 2010. An off-lattice hybrid discrete-continuum model of tumor growth and invasion. Biophys. J. 98 (1), 37–47.

Koury, M.J., Bondurant, M.C., 1990. Erythropoietin retards DNA breakdown and prevents programmed death in erythroid progenitor cells. Science 248, 378–381.

Mackey, M.C., 1978. Unified hypothesis of the origin of aplastic anaemia and periodic hematopoïesis. Blood 51, 941–956.

Mackey, M.C., 1979. Dynamic hematological disorders of stem cell origin. In: Vassileva-Popova, G., Jensen, E.V. (Eds.), Biophysical and Biochemical Information Transfer in Recognition. , Plenum Press, New York, pp. 373–409.

Mackey, M.C., Rudnicki, R., 1994. Global stability in a delayed partial differential equation describing cellular replication. J. Math. Biol. 33, 89–109.

Mackey, M.C., Rudnicki, R., 1999. A new criterion for the global stability of simultaneous cell replication and maturation processes. J. Math. Biol. 38, 195–219.

Mahaffy, J.M., Belair, J., Mackey, M.C., 1998. Hematopoietic model with moving boundary condition and state dependent delay: applications in erythropoiesis. J. Theor. Biol. 190, 135–146.

Michor, F., Hughes, T.P., Iwasa, Y., Branford, S., Shah, N.P., Sawyers, C.L., Nowak, M.A., 2005. Dynamics of chronic myeloid leukaemia. Nature 435 (7046), 1267–1270.

Michor, F., 2007. Quantitative approaches to analyzing imatinib-treated chronic myeloid leukemia. Trends Pharmacol. Sci. 28 (5), 197–199.

Michor, F., 2008. Mathematical models of cancer stem cells. J. Clin. Oncol. 26 (17), 1861–2854.

Nagata, Y., Takahashi, N., Davis, R.J., Todokoro, K., 1998. Activation of p38 MAP kinase and JNK but not ERK is required for erythropoietin-induced erythroid differentiation. Blood 92, 1859–1869.

Osborne, J.M., Walter, A., Kershaw, S.K., Mirams, G.R., Fletcher, A.G., Pathmanathan, P., Gavaghan, D., Jensen, O.E., Maini, P.K., Byrne, H.M., 2010. A hybrid approach to multi-scale modeling of cancer. Phil. Trans. R. Soc. A 368, 5013–5028.

Pain, B., Woods, C.M., Saez, J., Flickinger, T., Raines, M., Peyroll, S., Moscovici, C., Moscovici, M.G., Kung, H.J., Jurdic, P., Lazarides, E., Samaru, J., 1991. EGF-R as a hemopoietic growth factor receptor: the c-erbB product is present in normal chicken erythrocytic progenitor cells and controls their self-renewal. Cell 65, 37–46.

Patel, A.A., Gawlinsky, E.T., Lemieux, S.K., Gatenby, R.A., 2001. A cellular automaton model of early tumor growth and invasion: the effects of native tissue vascularity and increased anaerobic tumor metabolism. J. Theor. Biol. 213, 315–331.

Ramis-Conde, I., Chaplain, M.A., Anderson, A.R., Drasdo, D., 2009. Multi-scale modeling of cancer cell intravasation: the role of cadherins in metastasis. Phys. Biol. 6 (1), 016008.

Rew, D.A., Wilson, G.D., Taylor, I., Weaver, P.C., 1991. Proliferation characteristics of human colorectal carcinomas measured in vivo. Br. J. Surg. 78, 60–66.

Rhodes, M.M., Kopsombut, P., Bondurant, M.C., Price, J.O., Koury, M.J., 2008. Adherence to macrophages in erythroblastic islands enhances erythroblast proliferation and increases erythrocyte production by a different mechanism than erythropoietin. Blood 111, 1700–1708.

Roeder, I., 2006. Quantitative stem cell biology: computational studies in the hematopoietic system. Curr. Opin. Hematol. 13, 222–228.

Rubiolo, C., Piazzolla, D., Meissl, K., Beug, H., Huber, J.C., Kolbus, A., Baccarini, M., 2006. A balance between Raf-1 and Fas expression sets the pace of erythroid differentiation. Blood 108, 152–159.

Sadahira, Y., Yasuda, T., Yoshino, T., Manabe, T., Takeishi, T., Kobayashi, Y., Ebe, Y., Naito, M., 2000. Impaired splenic erythropoiesis in phlebotomized mice injected with CL2MDP-liposome: an experimental model for studying the role of stromal macrophages in erythropoiesis. J. Leukoc. Biol. 68, 464–470.

Salazar-Ciudad, I., Jernvall, J., 2010. A computational model of teeth and the developmental origins of morphological variation. Nature 464 (7288), 583–586.

Santillan, M., Mahaffy, J.M., Belair, J., Mackey, M.C., 2000. Regulation of platelet production: the normal response to perturbation and cyclical platelet disease. J. Theor. Biol. 206, 585–603.

Savill, N.J., Chadwick, W., Reece, S.E., 2009. Quantitative analysis of mechanisms that govern red blood cell age structure and dynamics during anaemia. PLoS Comput. Biol. 5 (6), e1000416.

Sawyer, S.T., Jacobs-Helber, S.M., 2000. Unraveling distinct intracellular signals that promote survival and proliferation: study of erythropoietin, stem cell factor, and constitutive signaling in leukemic cells. J. Hematother. Stem Cell Res. 9, 21–29.

Secchiero, P., Melloni, E., Heikinheimo, M., Mannisto, S., Di Pietro, R., Iacone, A., Zauli, G., 2004. TRAIL regulates normal erythroid maturation through an ERK-dependent pathway. Blood 103, 517–522.

Spencer, S.L., Gerety, R.A., Pienta, K.J., Forrest, S., 2006. Modeling somatic evolution in tumorigenesis. PLoS Comput. Biol. 2 (8), e108.

Spivak, J.L., Pham, T., Isaacs, M., Hankins, W.D., 1991. Erythropoietin is both a mitogen and a survival factor. Blood 77, 1228–1233.

Scholz, M., Engel, C., Loeffler, M., 2005. Modelling human granulopoiesis under poly-chemotherapy with G-CSF support. J. Math. Biol. 50 (4), 397–439.

Scholz, M., Gross, A., Loeffler, M., 2010. A biomathematical model of human thrombopoiesis under chemotherapy. J. Theor. Biol. 264 (2), 287–300.

Socolovsky, M., 2007. Molecular insights into stress erythropoiesis. Curr. Opin. Hematol. 14, 215–224.

Sui, X., Krantz, S.B., Zhao, Z.J., 2000. Stem cell factor and erythropoietin inhibit apoptosis of human erythroid progenitor cells through different signalling pathways. Br. J. Haematol. 110, 63–70.

Tsiftsoglou, A.S., Vizirianakis, I.S., Strouboulis, J., 2009. Erythropoiesis: model systems, molecular regulators, and developmental programs. IUBMB Life 61 (8), 800–830.

Veng-Pedersen, P., Chapel, S., Schmidt, R.L., Al-Huniti, N.H., Cook, R.T., Widness, J.A., 2002. An integrated pharmacodynamic analysis of erythropoietin, reticulocyte, and hemoglobin responses in acute anemia. Pharm. Res. 19, 1630–1635.

Wichmann, H.E., Gerhardts, M.D., Spechtmeyer, H., Gross, R., 1979. A mathematical model of thrombopoiesis in rats. Cell Tissue Kinet. 12, 551–567.

Wichman, H.E., Loeffler, M., 1985. Mathematical Modeling of Cell Proliferation. CRC, Boca Raton, FL.

Wichmann, H.E., Loeffler, M., Schmitz, S., 1985. A concept of hemopoietic regulation and its biomathematical realisation. Blood Cells 14, 411–429.

Wichmann, H.E., Loeffler, M., Pantel, K., Wulff, H., 1989. A mathematical model of erythropoiesis in mice and rats. Part 2. Stimulated erythropoiesis. Cell Tissue Kinet. 22, 31–49.

Woo, S., Krzyzanski, W., Jusko, W.J., 2006. Pharmacokinetic and pharmacodynamic modeling of recombinant human erythropoietin after intravenous and subcutaneous administration in rats. J. Pharmacol. Exp. Ther. 319, 1297–1306.

Woo, S., Krzyzanski, W., Jusko, W.J., 2008. Pharmacodynamic model for chemotherapy-induced anemia in rats. Cancer Chemother. Pharmacol. 62, 123–133.

Wulff, H., Wichmann, H.E., Loeffler, M., Pantel, K., 1989. A mathematical model of erythropoiesis in mice and rats. Part 3. Suppressed erythropoiesis. Cell Tissue Kinet. 22, 51–61.

# Bibliographie


[1] Adimy M. et Crauste F., *Global stability of a partial differential equation with distributed delay due to cellular replication*, Nonlinear Anal. **54**, 1469–1491 (2003).

[2] Adimy M. et Crauste F., *Un modèle non-linéaire de prolifération cellulaire : extinction des cellules et invariance*, C. R. Mathematiques **336**, 559–564 (2003).

[3] Adimy M. et Crauste F., *Stability and instability induced by time delay in an erythropoiesis model*, Monografias del Seminario Matematico Garcia de Galdeano **31**, 3–12 (2004).

[4] Adimy M. et Crauste F., *Existence, positivity and stability for a nonlinear model of cellular proliferation*, Nonlinear Analysis : Real World Applications **6 (2)**, 337–366 (2005).

[5] Adimy M. et Crauste F., *Modeling and asymptotic stability of a growth factor-dependent stem cell dynamics model with distributed delay.*, Discrete Contin. Dyn. Syst., Ser. B **8 (1)**, 19–38 (2007).

[6] Adimy M. et Crauste F., *Mathematical model of hematopoiesis dynamics with growth factor-dependent apoptosis and proliferation regulations*, Math. Comput. Modelling **49 (11-12)**, 2128–2137 (2009).

[7] Adimy M., Crauste F. et El Abdllaoui A., *Asymptotic behavior of a discrete maturity structured system of hematopoietic stem cell dynamics with several delays*, Math. Model. Nat. Phenom. **1 (2)**, 1–22 (2006).

[8] Adimy M., Crauste F. et El Abdllaoui A., *Boundedness and Lyapunov Function for a Nonlinear System of Hematopoietic Stem Cell Dynamics*, Comptes Rendus Mathématiques, **348 (7-8)**, 373–377 (2010).

[9] Adimy M., Crauste F., Halanay A., Neamţu M. et Opriş D., *Stability of limit cycles in a pluripotent stem cell dynamics model.*, Chaos Solitons Fractals **27 (4)**, 1091–1107 (2006).

[10] Adimy M., Crauste F., Hbid H. et Qesmi R., *Stability and Hopf bifurcation for a cell population model with state-dependent delay*, SIAM J. Appl. Math, **70 (5)**, 1611–1633 (2010).

[11] Adimy M., Crauste F. et Marquet C., *Asymptotic behavior and stability switch for a mature-immature model of cell differentiation*, Nonlinear Analysis : Real World Applications, **11 (4)**, 2913–2929 (2010).

[12] Adimy M., Crauste F. et Pujo-Menjouet L., *On the stability of a maturity structured model of cellular proliferation*, Discret. Cont. Dyn. Sys. Ser. A **12 (3)**, 501–522 (2005).

[13] Adimy M., Crauste F. et Ruan S., *A mathematical study of the hematopoiesis process with applications to chronic myelogenous leukemia*, SIAM J. Appl. Math. **65 (4)**, 1328–1352 (2005).

[14] Adimy M., Crauste F. et Ruan S., *Stability and Hopf bifurcation in a mathematical model of pluripotent stem cell dynamics*, Nonlinear Analysis : Real World Applications **6 (4)**, 651–670 (2005).

[15] Adimy M., Crauste F. et Ruan S., *Periodic oscillations in leukopoiesis models with two delays*, J. Theoret. Biol. **242 (2)**, 288–299 (2006).

[16] Aiello W., Freedman H. et Wu J., *Analysis of a model representing stage-structured population growth with state-dependent time delay*, SIAM J. Appl. Math. **52 (3)**, 855–869 (1992).

[17] Anderson R.F.V., *Geometric and probabilistic stability criteria for delay systems*, Math. Biosci. **105**, 81–96 (1991).

[18] Anderson R.F.V., *Intrinsic parameters and stability of differential-delay equations*, J. Math. Anal. Appl. **163**, 184–199 (1992).

[19] Angulo O., Crauste F. et Lopez-Marcos J., *A Model of Phenylhydrazine-Induced Anemia in Mice : Investigating the Roles of the Experimental Protocol and of Age-Dependent Feedback Controls*, J. Theor. Biol. (soumis).

[20] Aniţa S., *Analysis and control of age-dependent population dynamics*, *Mathematical Modelling : Theory and Applications*, tome 11, Dordrecht : Kluwer Academic Publishers (2000), x+199 .

[21] Antia R., Bergstrom C., Pilyugin S., Kaech S. et Ahmed R., *Models of CD8+ Responses : 1. What is the Antigen-independent Proliferation Program*, J. Theor. Biol. **221**, 585–598 (2003).

[22] Antia R., Ganusov V. et Ahmed R., *The role of models in understanding CD*$8^+$ *T-cell memory*, Nat. Reviews **5**, 101–111 (2005).

[23] Appay V. et Rowland-Jones S., *Lessons from the study of T-cell differentiation in persistent human virus infection*, Seminars in Immunol. **16**, 205–212 (2004).

[24] Arino O., Hadeler K.P. et Hbid M.L., *Existence of periodic solutions for delay differential equations with state dependent delay*, J. Differential Equations **144 (2)**, 263–301 (1998).

[25] Arino O. et Sánchez E., *A saddle point theorem for functional state-dependent delay differential equations*, Discrete Contin. Dyn. Syst. **12 (4)**, 687–722 (2005).

[26] Atay F., *Delayed feedback control near Hopf bifurcation*, Discrete Contin. Dynam. Systems Ser. S **1 (2)**, 197–205 (2008).

[27] Bauer A., Tronche F., Wessely O., Kellendonk C., Reichardt H., Steinlein P., Schutz G. et Beug H., *The glucocorticoid receptor is required for stress erythropoiesis*, Genes Dev. **13**, 2996–3002 (1999).

[28] Bélair J. et Campbell S.A., *Stability and bifurcations of equilibria in a multiple-delayed differential equation*, SIAM J. Appl. Math. **54 (5)**, 1402–1424 (1994).

[29] Beretta E. et Kuang Y., *Geometric stability switch criteria in delay differential systems with delay dependent parameters*, SIAM J. Math. Anal. **33 (5)**, 1144–1165 (2002).

[30] Berezansky L. et Braverman E., *Stability of linear differential equations with a distributed delay*, Comm. Pure Appl. Math. **10 (5)**, 1361–1375 (2011).

[31] Berezansky L., Braverman E. et Idels L., *Mackey-Glass model of hematopoiesis with non-monotone feedback : stability, oscillation and control*, Appl. Math. Comput. **219 (11)**, 6268–6283 (2013).

[32] Bernard S., *How to Build a Multiscale Model in Biology*, Acta Biotheoretica **61 (3)**, 291–303 (2013).

[33] Bernard S., Belair J. et Mackey M.C., *Sufficient conditions for stability of linear differential equations with distributed delay*, Dis. Cont. Dyn. Sys. Ser. B **1**, 233–256 (2001).

[34] Bernard S., Belair J. et Mackey M.C., *Oscillations in cyclical neutropenia : New evidence based on mathematical modeling*, J. Theor. Biol. **223**, 283–298 (2003).

[35] Bernard S. et Crauste F., *Optimal linear stability condition for scalar differential equations with distributed delay*, Discrete Contin. Dynam. Systems (soumis).

[36] Bessonov N., Crauste F., Fischer S., Kurbatova P. et Volpert V., *Application of Hybrid Models to Blood Cell Production in the Bone Marrow*, Math. Model. Nat. Phenom., **6 (07)**, 2–12 (2011).

[37] Billy F. et Clairambault J., *Designing proliferating cell population models with functional targets for control by anti-cancer drugs*, Discrete Contin. Dyn. Syst. Ser. B **18 (4)**, 865–889 (2013).

[38] Billy F., Ribba B., Saut O., Morre-Trouilhet H., Colin T., Bresch D., Boissel J., Grenier E. et Flandrois J., *A pharmacologically based multiscale mathematical model of angiogenesis and its use in investigating the efficacy of a new cancer treatment strategy*, J Theor Biol **260**, 545–562 (2009).

[39] Boese F.G., *The stability chart for the linearized Cushing equation with a discrete delay and Gamma-distributed delays*, J. Math. Anal. Appl. **140**, 510–536 (1989).

[40] Burns F.J. et Tannock I.F., *On the existence of a $G_0$ phase in the cell cycle*, Cell Tissue Kinet. **19**, 321–334 (1970).

[41] Byrne H. et Drasdo D., *Individual-based and continuum models of growing cell populations : a comparison*, J Math Biol **58**, 657–687 (2009).

[42] Charlesworth B., *Evolution in age-structured populations*, *Cambridge Studies in Mathematical Biology*, tome 1, Cambridge : Cambridge University Press (1980), xiii+300 .

[43] Charlesworth B., *Evolution in age-structured populations*, *Cambridge Studies in Mathematical Biology*, tome 13, 2$^{e}$ édition, Cambridge : Cambridge University Press (1994), xiv+306 .

[44] Chauviere A., Preziosi L. et Verdier C., *Cell mechanics : from single scale-based models to multiscale modeling*, Mathematical and Computational Biology, Chapman and Hall/CRC (2010).

[45] Clairambault J., *Modelling physiological and pharmacological control on cell proliferation to optimise cancer treatments*, Mathematical Modelling of Natural Phenomena **4**, 12–67 (2009).

[46] Clairambault J., *Optimising cancer pharmacotherapeutics using mathematical modelling and a systems biology approach*, Personalized Medicine **8**, 271–286 (2011).

[47] Colijn C. et Mackey M., *A mathematical model of hematopoiesis : Cyclical neutropenia*, J. Theor. Biol. **237**, 133–146 (2005).

[48] Colijn C. et Mackey M., *A mathematical model of hematopoiesis : Periodic chronic myelogenous leukemia*, J. Theor. Biol. **237**, 117–132 (2005).

[49] Cooke K.L. et Grossman Z., *Discrete delay, distributed delay and stability switches*, J. Math. Anal. Appl. **86**, 592–627 (1982).

[50] Cooke K.L. et Huang W.Z., *On the problem of linearization for state-dependent delay differential equations*, Proc. Amer. Math. Soc. **124 (5)**, 1417–1426 (1996).

[51] Crauste F., *Global asymptotic stability and Hopf bifurcation for a blood cell production model.*, Math. Biosci. Eng. **3 (2)**, 325–346 (2006).

[52] Crauste F., *Delay model of hematopoietic stem cell dynamics : asymptotic stability and stability switch*, Math. Model. Nat. Phenom. **4 (2)**, 28–47 (2009).

[53] Crauste F., *Stability and Hopf bifurcation for a first-order linear delay differential equation with distributed delay*, dans *Complex Time Delay Systems (Ed. F. Atay)*, 320, Springer, (2010).

[54] Crauste F., *A review on local asymptotic stability analysis for mathematical models of hematopoiesis with delay and delay-dependent coefficients.*, Ann. Tiberiu Popoviciu Semin. Funct. Equ. Approx. Convexity, **9**, 121–143 (2011).

[55] Crauste F., Demin I., Gandrillon O. et Volpert V., *Mathematical study of feedback control roles and relevance in stress erythropoiesis*, Journal of Theoretical Biology, **263 (3)**, 303–16 (2010).

[56] Crauste F., Pujo-Menjouet L., Génieys S., Molina C. et Gandrillon O., *Adding self-renewal in committed erythroid progenitors improves the biological relevance of a mathematical model of erythropoiesis*, J. Theoret. Biol. **250 (2)**, 322–338 (2008).

[57] Crauste F., Terry E., Le Mercier I., Mafille J., Djebali S., Andrieu T., Mercier B., Kaneko G., Arpin C., Marvel J. et Gandrillon O., *Predicting Pathogen-Specific CD8 T Cell Immune Response from a Modeling Approach* (2014), submitted.

[58] Crauste M.A.F. et El Abdllaoui A., *Discrete-maturity structured model of cell differentiation with applications to acute myelogenous leukimia.*, J. Biol. Syst. **16 (3)**, 395–424 (2008).

[59] Cushing J.M., *An introduction to structured population dynamics*, *CBMS-NSF Regional Conference Series in Applied Mathematics*, tome 71, Philadelphia, PA : Society for Industrial and Applied Mathematics (SIAM) (1998), xiv+193 .

[60] De Boer R., Oprea M., Antia R., Murali-Krishna K., Ahmed R. et Perelson A., *Recruitment Times, Proliferation, and Apoptosis Rates during the CD8 T-Cell Response to Lymphocytic Choriomeningitis Virus*, J. Virol. 10663–10669 (2001).

[61] De Boer R.J. et Perelson A.S., *Quantifying T lymphocyte turnover*, J. Theoret. Biol. **327**, 45–87 (2013).

[62] Deisboeck T. et Stamatakos G., *Multiscale cancer modeling*, Mathematical and Computational Biology, Chapman and Hall/CRC (2010).

[63] Demin I., Crauste F., Gandrillon O. et Volpert V., *A multi-scale model of erythropoiesis*, Journal of Biological Dynamics, **4 (1)**, 59–70 (2010).

[64] Driver R.D., *Existence theory for a delay-differential system*, Contributions to Differential Equations **1**, 317–336 (1963).

[65] Dupuis X., *Optimal Control of Leukemic Cell Population Dynamics*, Mathematical Modelling of Natural Phenomena **9**, 4–26 (2014).

[66] Eichmann M., *A local Hopf Bifurcation Theorem for differential equations with state-dependent delays*, Thèse de doctorat, Justus-Liebig-Universität Giessen (2006).

[67] Eymard N., Bessonov N., Gandrillon O., Koury M. et Volpert V., *The Role of Spatial Organization of Cells in Erythropoiesis*, J. Math. Biol. (2014).

[68] Faria T., *On the study of singularities for a planar system with two delays*, Dyn. Contin. Discrete Impuls. Syst. Ser. A Math. Anal. **10 (1-3)**, 357–371 (2003), second International Conference on Dynamics of Continuous, Discrete and Impulsive Systems (London, ON, 2001).

[69] Fischer S., Kurbatova P., Bessonov N., Gandrillon O., Volpert V. et Crauste F., *Modeling erythroblastic islands : Using a hybrid model to assess the function of central macrophage*, Journal of Theoretical Biology, **298**, 92 – 106 (2012).

[70] Gandrillon O., Schmidt U., Beug H. et Samarut J., *TGF-beta cooperates with TGF-alpha to induce the self-renewal of normal erythrocytic progenitors : evidence for an autocrine mechanism*, Embo. J. **18**, 2764–2781 (1999).

[71] Gopalsamy K., Kulenović M.R.S. et Ladas G., *Oscillations and global attractivity in models of hematopoiesis*, J. Dynam. Differential Equations **2 (2)**, 117–132 (1990).

[72] Halanay A., *Differential Equations ; Stability, Oscillations, Time Lags*, New York : Academic Press (1966).

[73] Hale J.K., *Theory of functionnal differential equations*, New-York : Springer-Verlag (1977).

[74] Hale J.K. et Huang W.Z., *Global geometry of the stable regions for two delay differential equations*, J. Math. Anal. Appl. **178 (2)**, 344–362 (1993).

[75] Hartung F., *Linearized stability in periodic functional differential equations with state-dependent delays*, J. Comput. Appl. Math. **174 (2)**, 201–211 (2005).

[76] Hartung F., Krisztin T., Walther H.O. et Wu J., *Functional differential equations with state-dependent delays : theory and applications*, dans *Handbook of differential equations : ordinary differential equations. Vol. III*, Handb. Differ. Equ., 435–545, Elsevier/North-Holland, Amsterdam (2006).

[77] Hartung F. et Turi J., *Linearized stability in functional differential equations with state-dependent delays*, Discrete Contin. Dynam. Systems **Added Volume**, 416–425 (2001).

[78] Haurie C., Dale D.C. et Mackey M.C., *Cyclical neutropenia and other hematological disorders : A review of mechanisms and mathematical models*, Blood **92 (8)**, 2629–2640 (1998).

[79] Haute Autorité de Santé, *Leucémies aiguës de l'adulte* (2011), Guide Affections de Longue Durées (ALD).

[80] Hayes N.D., *Roots of the transcendental equation associated with a certain differential difference equation*, J. London Math. Soc. **25**, 226–232 (1950).

[81] Hofer E.P., Tibken B. et Lehn F., **Differential equations with state-dependent delays*, dans *Online optimization of large scale systems*, 413–432, Berlin : Springer (2001).

[82] Huang C. et Vandewalle S., *An Analysis of Delay-Dependent Stability for Ordinary and Partial Differential Equations with Fixed and Distributed Delays.*, SIAM J. Sci. Comput. **25 (5)**, 1608–1632 (2004).

[83] Kaech S. et Ahmed R., *Memory CD8+ T cell differentiation : Initial antigen encounter triggers a developmental program in naive cells*, Nat. Immunol. **2**, 415–422 (2001).

[84] Kazmerchuk Y.I. et Wu J.H., *Stochastic state-dependent delay differential equations with applications in finance*, Funct. Differ. Equ. **11 (1-2)**, 77–86 (2004).

[85] Kemp R., Powell T., Dwyer D. et Dutton R., *Cutting Edge : Regulation of CD*$8^+$ *T Cell Effector Population Size*, J. Immunol. **173**, 2923–2927 (2004).

[86] Kim P., Lee P. et Levy D., *Modeling regulation mechanisms in the immune system*, J. Theor. Biol. **246**, 33–69 (2007).

[87] Koury M. et Bondurant M., *Erythropoietin retards DNA breakdown and prevents programmed death in erythroid progenitor cells*, Science **248**, 378–381 (1990).

[88] Kuang Y., *Delay differential equations with applications in population dynamics*, *Mathematics in Science and Engineering*, tome 191, New-York : Academic Press (1993).

[89] Kuang Y., *Nonoccurrence of stability switching in systems of differential equations with distributed delays*, Quart. Appl. Math. **LII (3)**, 569–578 (1994).

[90] Kuang Y. et Smith H.L., *Slowly oscillating periodic solutions of autonomous state-dependent delay equations*, Nonlinear Anal. **19 (9)**, 855–872 (1992).

[91] Kurbatova P., Bernard S., Bessonov N., Crauste F., Demin I., Dumontet C., Fischer S. et Volpert V., *Hybrid Model of Erythropoiesis and Leukemia Treatment with Cytosine Arabinoside*, SIAM J. Appl. Math., **71 (6)**, 2246–2268 (2011).

[92] Louihi M., Hbid M.L. et Arino O., *Semigroup properties and the Crandall Liggett approximation for a class of differential equations with state-dependent delays*, J. Differential Equations **181 (1)**, 1–30 (2002).

[93] Lyons A., Blake S. et Doherty K., *Flow cytometric analysis of cell division by dilution of CFSE and related dyes*, Curr. Protoc. Cytom. **64**, 9.11.1–9.11.12 (2013).

[94] Mackey M.C., *Unified hypothesis of the origin of aplastic anaemia and periodic hematopoiesis*, Blood **51**, 941–956 (1978).

[95] Magal P. et Arino O., *Existence of periodic solutions for a state dependent delay differential equation*, J. Differential Equations **165 (1)**, 61–95 (2000).

[96] Mahaffy J.M., Bélair J. et Mackey M.C., *Hematopoietic model with moving boundary condition and state dependent delay*, J. Theor. Biol. **190**, 135–146 (1998).

[97] Mahaffy J.M., Joiner K.M. et Zak P.J., *A geometric analysis of stability regions for a linear differential equation with two delays*, Internat. J. Bifur. Chaos Appl. Sci. Engrg. **5 (3)**, 779–796 (1995).

[98] Mallet-Paret J., Nussbaum R. et Paraskevopoulos P., *Periodic solutions for functional-differential equations with multiple state-dependent time lags*, Topol. Methods Nonlinear Anal. **3 (1)**, 101–162 (1994).

[99] Niculescu S.I., Morărescu C.I., Michiels W. et Gu K., *Geometric ideas in the stability analysis of delay models in biosciences*, dans *Biology and control theory : current challenges*, *Lecture Notes in Control and Inform. Sci.*, tome 357, 217–259, Springer, Berlin (2007).

[100] Ouifki R. et Hbid M., *Periodic solutions for a class of functional differential equations with state-dependent delay close to zero*, Math. Models. Meth. Appl. Sciences. **13**, 807–841 (2003).

[101] Ozbay H., Bonnet C. et Clairambault J., *Stability analysis of systems with distributed delays and application to hematopoietic cell maturation dynamics*, dans *Decision and Control, 2008. CDC 2008. 47th IEEE Conference on*, 2050–2055, IEEE (2008).

[102] Perthame B., *Transport equations in biology*, Frontiers in Mathematics, Basel : Birkhäuser Verlag (2007), x+198 .

[103] Precup R., Serban M., Trif D. et Cucuianu A., *A Planning Algorithm for Correction Therapies After Allogeneic Stem Cell Transplantation*, Journal of Mathematical Modelling and Algorithms **11 (3)**, 309–323 (2012).

[104] Pujo-Menjouet L., Bernard S. et Mackey M.C., *Long period oscillations in a $G_0$ model of hematopoietic stem cells*, SIAM J. Appl. Dyn. Systems **4 (2)**, 312–332 (2005).

[105] Qu Z., Garfinkel A., Weiss J. et Nivala M., *Multi-scale modeling in biology : how to bridge the gaps between scales ?*, Prog Biophys Mol Biol **107 (1)**, 21–31 (2000).

[106] Ren H., *A necessary and sufficient condition for asymptotic stability of a first order delay equation with two delays*, Ann. Differential Equations **20 (1)**, 59–69 (2004).

[107] Rezounenko A. et Wu J., *A non-local PDE model for population dynamics with state-selective delay : local theory and global attractors*, J. Comput. Appl. Math. **190**, 99–113 (2006).

[108] Rouzine I., Murali-Krishna K. et Ahmed R., *Generals die in friendly fire, or modeling immune response to HIV*, J. Computational and Appl. Math. **184**, 258–274 (2005).

[109] Ruan S. et Wei J., *Periodic solutions of planar systems with two delays*, Proc. Roy. Soc. Edinburgh Sect. A **129 (5)**, 1017–1032 (1999).

[110] Ruan S. et Wei J., *On the zeros of transcendental functions with applications to stability of delay differential equations with two delays*, Dyn. Contin. Discrete Impuls. Syst. Ser. A Math. Anal. **10**, 63–874 (2003).

[111] Sadahira Y., Yasuda T., Yoshino T., Manabe T., Takeishi T., Kobayashi Y., Ebe Y. et Naito M., *Impaired splenic erythropoiesis in phlebotomized mice injected with CL2MDP-liposome : an experimental model for studying the role of stromal macrophages in erythropoiesis*, J. Leukoc. Biol. **68**, 464–470 (2000).

[112] Saker S.H., *Oscillation and global attractivity in a periodic delay hematopoiesis model*, J. Appl. Math. Comput. **13 (1-2)**, 287–300 (2003).

[113] Santillan M., Bélair J., Mahaffy J.M. et Mackey M.C., *Regulation of platelet production : The normal response to perturbation and cyclical platelet disease*, J. Theor. Biol. **206**, 585–603 (2000).

[114] Shampine L.F., *Solving ODEs and DDEs with residual control*, Appl. Numer. Math. **52 (1)**, 113–127 (2005).

[115] Stewart I., *Les mathématiques du vivant*, Flammarion (2013).

[116] Stipdonk M., Lemmens E. et Schoenberger S., *Naive CTLs require a single brief period of antigenic stimulation for clonal expansion and differentiation*, Nat. Immunol. **2**, 423–429 (2001).

[117] Su M., Wladen P., Golan D. et Eisen H., *Cognate peptide-induced destruction of $CD8^+$ cytotoxic T lymphocytes is due to fratricide*, J. Immunol. **151**, 658–667 (1993).

[118] Swat M., Thomas G., Belmonte J., Shirinifard A., Hmeljak D. et Glazier J., *Multi-Scale Modeling of Tissues Using CompuCell3D*, Computational Methods in Cell Biology, Methods in Cell Biology **110**, 325–366 (2012).

[119] Tang X., *Asymptotic Behavior of a Differential Equation with Distributed Delays.*, J. Math. Anal. Appl. **301**, 313–335 (2005).

[120] Terry E., Marvel J., Arpin C., Gandrillon O. et Crauste F., *Mathematical model of the primary CD8 T cell immune response : stability analysis of a nonlinear age-structured system*, J. Math. Biol., **65**, 263–291 (2012).

[121] Walther H., *Stable periodic motion of a system with state-dependent delay*, Differential Integral Equations **15**, 923–944 (2002).

[122] Walther H., *On a model for soft landing with state-dependent delay*, Journal of Dynamics and Differential Equations **19**, 593–622 (2007).

[123] Walther H.O., *The solution manifold and $C^1$-smoothness for differential equations with state-dependent delay*, J. Differential Equations **195 (1)**, 46–65 (2003).

[124] Webb G.F., *Theory of nonlinear age-dependent population dynamics*, *Monographs and Textbooks in Pure and Applied Mathematics*, tome 89, New York : Marcel Dekker Inc. (1985).

[125] Özbay H., Bonnet C., Benjelloun H. et Clairambault J., *Stability analysis of cell dynamics in leukemia*, Mathematical Modelling of Natural Phenomena **7**, 203–234 (2012).

# Équations à Retard et Modèles de Dynamiques de Populations Cellulaires

**Résumé :** A travers deux chapitres, je présente mon activité de recherche depuis 2006, date de mon recrutement au CNRS. Celle-ci a concerné la modélisation et l'étude mathématique de processus biologiques liés à des dynamiques cellulaires et impliquant des régulations des mécanismes considérés. Tant les processus que les mécanismes de régulation font intervenir des échelles physiques et temporelles différentes, et les travaux présentés évoluent de l'étude de problèmes "mono"-échelle à l'étude de problèmes multi-échelles. Bien que les travaux théoriques et les applications en biologie soient présentés séparément, ces aspects sont en pratique traités simultanément la plupart du temps. La présentation a pour but de souligner les apports tant théoriques qu'applicatifs.
Dans le premier chapitre, je présente de façon synthétique les résultats obtenus lors de l'étude qualitative d'équations à retard et d'équations aux dérivées partielles structurées en âge. J'ai étudié la stabilité asymptotique d'équations à retard dans les cas de retards discrets, distribués, et dépendant de l'état, et je présente les résultats les plus marquants dans ces trois cas. La stabilité globale de telles équations est brièvement évoquée.
Dans le deuxième chapitre je présente les applications biologiques qui ont motivé les travaux théoriques du premier chapitre. Je commence par l'étude de la dynamique des cellules souches hématopoétiques, débutée lors de ma thèse et poursuivie pendant quelques années. Je présente ensuite les travaux réalisés sur la modélisation de l'érythropoïèse et de la réponse immunitaire, tous deux réalisés en collaboration avec des collègues biologistes lyonnais. Dans chacun de ces cas, la pertinence des résultats obtenus est présentée en fonction des questions biologiques et des réponses théoriques qui sont apportées.

**Mots clés :** Biomathématiques ; Modèles non-linéaires ; Équations à retard ; Prolifération cellulaire ; Modélisation multi-échelles.

## *Delay Equations and Models of Cell Population Dynamics*

**Abstract :** I pressent my research activity from 2006, when I have been recruited by the CNRS, throughout two chapters. It deals with the modeling and mathematical study of biological processes associated with cell dynamics and involving regulations of the considered mechanisms. The processes as well as the regulatory mechanisms deal with different physical and temporal scales, so the works I present evolve from the study of "mono"-scale problems to multiscale problems. Although theoretical works and applications are presented separately, they are usually dealt with simultaneously. The current presentation aims at stressing both theoretical and applied contributions.
In the first chapter, I present the results obtained while qualitatively studying delay equations and age-structured partial differential equations. I focus on the asymptotic stability analysis of delay equations for discrete, continous distributed, and state-dependent delays, and I present the most relevant results in these three cases. Global stability for such equations is briefly discussed.
In the second chapter, I present biological applications that motivated the theoretical works presented in the first chapter. I begin with the study of hematopoietic stem cell dynamics, a work started during my PhD thesis and carried on for few years. I then move to the presentation of the works on the modeling of erythropoiesis and the immune response, both performed in close collaboration with biologists from Lyon. In both cases, the relevance of the results is presented with respect to biological questions of interest and to theoretical answers that have been brought.

**Keywords :** Biomathematics ; Nonlinear models ; Delay equations ; Cell proliferation ; Multiscale modeling.

**Image en couverture :** Valeurs de l'hématocrite de souris lors d'une réponse à une anémie sévère, d'après Crauste et al. (2008).


UNIVERSITÉ DE LYON